No. FHWA-RD-77-11

W SENSING SYSTEM FOR PRE-EXCAVATION URFACE INVESTIGATION FOR TUNNELS IN ROCK MASSES

Vol. II. Appendixes: Detailed Theoretical, Experimental, and Economic Foundation

August 1976
Final Report

Prepared for
FEDERAL HIGHWAY ADMINISTRATION
Offices of Research & Development
Washington, D. C. 20590

NOTICE

This document is disseminated under the sponsorship of the Department of Transportation in the interest of information exchange. The United States Government assumes no liability for its contents or use thereof.

The contents of this report reflect the views of ENSCO, Incorporated, which is responsible for the facts and the accuracy of the data presented herein. The contents do not necessarily reflect the official views or policy of the Department of Transportation. This report does not constitute a standard, specification, or regulation.

The United States Government does not endorse products or manufacturers. Trade or manufacturers' names appear herein only because they are considered essential to the object of this document.

FHWA DISTRIBUTION NOTICE

A limited number of copies of this report describing research methodology and preliminary findings are being distributed by memorandum to appropriate members of the research community.

Technical Report Documentation Page

1. Report No.	2. Government Accession No.	3. Recipient's Catalog No.
FHWA-RD-77-11		

4. Title and Subtitle
A New Sensing System For Pre-excavation Subsurface Investigation For Tunnels in Rock Masses Volume 2. Appendices: Detailed Theoretical, Experimental and Economic Foundation

5. Report Date
August 1976

6. Performing Organization Code

8. Performing Organization Report No.
1061-TR-3-1

7. Author(s)
L.A. Rubin, J.C. Fowler, J.N. Griffin and W.L. Still

9. Performing Organization Name and Address
ENSCO, Inc.
5408A Port Royal Road
Springfield, Virginia 22151

10. Work Unit No. (TRAIS)

11. Contract or Grant No.
DOT-FH-11-8602

13. Type of Report and Period Covered
Final Report

12. Sponsoring Agency Name and Address
Offices of Research and Development
Federal Highway Administration
U.S. Department of Transportation
Washington, D.C. 20590

14. Sponsoring Agency Code

15. Supplementary Notes
FHWA Contract Manager: Charles H. McGogney, HRS-11

16. Abstract

This report includes a feasibility study and system design for an initial prototype of a sensing system for pre-excavation subsurface investigation for tunnels in rock. Tunnels in rock are very expensive, and costs often rise far above estimates when unforeseen problems are encountered during excavation. New techniques in rapid excavation technology, such as the development of boring machines, have increased the need for improved site investigation. Possibilities for a new sensing system that will provide more complete data on subsurface conditions were investigated. Favorable results obtained from high-resolution geophysical sensing in boreholes have been combined with improvements in drilling of long, horizontal, precise boreholes in order to provide an economical alternative to pilot tunnel for subsurface investigation. Pilot tunnel costs as with all subsurface construction are rising at rates much higher than the economy, thus the use of borehole site investigation has potentially very high benefit/cost characteristics. The prototype system designed is a highly mobile geophysical measurement (data acquisition) system. The system will take electromagnetic radar measurements, pulsed acoustical measurements, and multi-spaced array resistivity measurements. The sensors will be used in traverses along the borehole, and data will be taken and stored on magnetic tape for subsequent reduction and analysis at a computational center. The system could reduce accidents, reduce bid contingencies, and reduce other factors contributing to rapid escalating costs of subsurface excavation. Volume I (FHWA-RD-77-10) describes the feasibility study and system design. Volume II (FHWA-RD-11) is the Appendices A-R.

17. Key Words	18. Distribution Statement
Site Investigation, Sensing of Geology from Pilot Tunnels and Long Horizontal Boreholes, Pre-excavation Mapping of Tunnels, Ground Probing Radar, Acoustic Sensing in Ground	No restrictions. This document is available to the public through the National Technical Information Service, Springfield, Virginia 22161

19. Security Classif. (of this report)	20. Security Classif. (of this page)	21. No. of Pages	22. Price
Unclassified	Unclassified	498	

Form DOT F 1700.7 (8-72) Reproduction of completed page authorized

PREFACE

The work reported herein was conducted under a Contract with the U.S. Department of Transportation, Federal Highway Administration, Office of Research, Structures and Applied Mechanics Division. This research is a part of FHWA Project 5B2, Tunneling Research Project, Site Investigation Subproject. The authors wish to acknowledge the helpful participation in the effort by Mr. Charles H. McGogney, Contract Manager, along with that of Dr. Donald Linger, Program Coordinator, and his predecessor, Dr. Steven I. Majtenyi. These FHWA staff members, along with several others, provided many technical contributions, guidance, encouragement and much understanding to the ENSCO project staff.

A number of persons and organizations outside of ENSCO contributed to this report. These include Dr. Ronald E. Heuer, University of Illinois; Dr. Eugene L. Foster, UTD Corp; Dr. John C. Cook, The Terradar Company; Dr. George V. Keller, Colorado School of Mines; Dr. Thomas E. Owen, Southwest Research Institute; and Mr. Rexford M. Morey, Geophysical Survey Systems, Inc.

The authors wish to thank the many ENSCO people who contributed in one way or another to this project. We thank especially Edward G. Cunney, Senior Civil Engineer, and Jeffrey A. Bloom, Senior Mechanical Engineer for their valuable inputs to the study and this report. The report could not have been produced without the very-much-appreciated skillful efforts of Raymond L. Farmer, Laura J. Money, Clifford C. Reynolds and Charles F. Taylor.

METRIC CONVERSION FACTORS

Approximate Conversions to Metric Measures

Symbol	When You Know	Multiply by	To Find	Symbol
	LENGTH			
in	inches	*2.5	centimeters	cm
ft	feet	30	centimeters	cm
yd	yards	0.9	meters	m
mi	miles	1.6	kilometers	km
	AREA			
in^2	square inches	6.5	square centimeters	cm^2
ft^2	square feet	0.09	square meters	m^2
yd^2	square yards	0.8	square meters	m^2
mi^2	square miles	2.6	square kilometers	km^2
	acres	0.4	hectares	ha
	MASS (weight)			
oz	ounces	28	grams	g
lb	pounds	0.45	kilograms	kg
	short tons (2000 lb)	0.9	tonnes	t
	VOLUME			
tsp	teaspoons	5	milliliters	ml
Tbsp	tablespoons	15	milliliters	ml
fl oz	fluid ounces	30	milliliters	ml
c	cups	0.24	liters	l
pt	pints	0.47	liters	l
qt	quarts	0.95	liters	l
gal	gallons	3.8	liters	l
ft^3	cubic feet	0.03	cubic meters	m^3
yd^3	cubic yards	0.76	cubic meters	m^3
	TEMPERATURE (exact)			
°F	Fahrenheit temperature	5/9 (after subtracting 32)	Celsius temperature	°C

*1 in = 2.54 (exactly). For other exact conversions and more detailed tables, see NBS Misc. Publ. 286, Units of Weights and Measures. Price $2.25, SD Catalog No. C13.10:286.

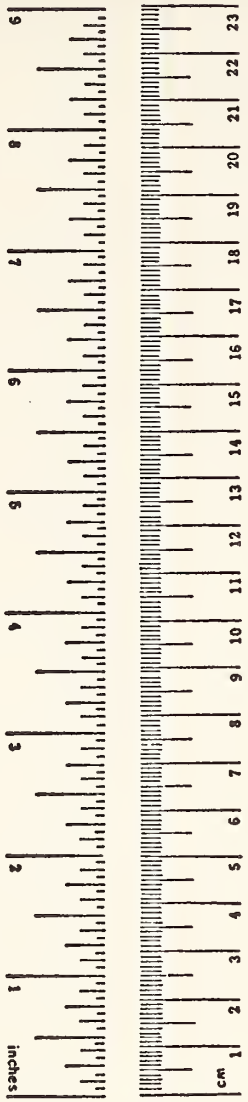

Approximate Conversions from Metric Measures

Symbol	When You Know	Multiply by	To Find	Symbol
	LENGTH			
mm	millimeters	0.04	inches	in
cm	centimeters	0.4	inches	in
m	meters	3.3	feet	ft
m	meters	1.1	yards	yd
km	kilometers	0.6	miles	mi
	AREA			
cm^2	square centimeters	0.16	square inches	in^2
m^2	square meters	1.2	square yards	yd^2
km^2	square kilometers	0.4	square miles	mi^2
ha	hectares (10,000 m^2)	2.5	acres	
	MASS (weight)			
g	grams	0.035	ounces	oz
kg	kilograms	2.2	pounds	lb
t	tonnes (1000 kg)	1.1	short tons	
	VOLUME			
ml	milliliters	0.03	fluid ounces	fl oz
l	liters	2.1	pints	pt
l	liters	1.06	quarts	qt
l	liters	0.26	gallons	gal
m^3	cubic meters	35	cubic feet	ft^3
m^3	cubic meters	1.3	cubic yards	yd^3
	TEMPERATURE (exact)			
°C	Celsius temperature	9/5 (then add 32)	Fahrenheit temperature	°F

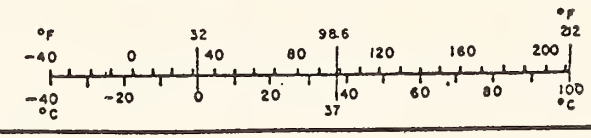

TABLE OF CONTENTS

Volume 1. Feasibility Study and System Design

Volume II - Appendices: Detailed Theoretical, Experimental and Economic Foundation

APPENDIX A

ALTERNATIVES CONSIDERED FOR A FEASIBLE BASELINE SYSTEM (TASK A)

TABLE OF CONTENTS

BACKGROUND STATEMENT

In defining the eventual configuration of the system, all major alternatives were considered. This was a continuing process throughout the program. In all, there were three major iterations of the system which occurred.

- The initial baseline system, presented early in the program. (Task A)
- The baseline system presented at the Preliminary Design Review. (Task B)
- The final system presented in the specifications. (Not published)

This appendix is a compilation of the alternatives considered. It starts with a fairly broad screening of the first iteration, in which some specific selections were made and other alternatives left unresolved.

The second iteration starting with paragraph 3 is fairly specific. The selection of the final configuration was based upon pragmatic risk and economic considerations which modified some of the results of the screening. However, all of its features are covered within the alternatives discussed within this document.

This appendix represents the state of development that existed at the conclusion of Task A, (after four months of the 18 month effort), and is presented for historical perspective and in compliance with contractual requirements. Paragraph 3 and beyond cover the state of development that existed at the end of month nine, (midway in Task B).

ALTERNATIVES CONSIDERED FOR A FEASIBLE BASELINE SYSTEM

ABSTRACT

The purpose of a baseline system is to freeze a total system configuration at a specific point in time. This is essential because at any one time there are a number of disciplinary specialists working on various portions of the system. The baseline system thus becomes the common reference to which all these efforts are equated. The fact that the baseline system presents this frozen instant in time does not imply that it is static. As studies were performed and designs solidified which were improvements on various portions of the baseline system, they were incorporated into the system for its overall improvement. The fact that the baseline does exist insured that these improvements are not incorporated until their total impact on the system had been evaluated.

Rather than presenting the baseline system, this appendix consists of a documentation of the numerous independent studies conducted in the process of defining it. Alternative approaches for all foreseeable problems of mechanizing the system are considered. The appendix provides support for the selection and modification of the baseline system, through two iterations, separated in time by approximately one year.

ALTERNATIVES CONSIDERED FOR A FEASIBLE BASELINE SYSTEM

1. INTRODUCTION

In the process of defining the system, there have been many sequential steps and iterations. Following the initial functional analysis, a baseline system was synthesized which would meet the functional and operational requirements of the system.

The purpose of a baseline system is to freeze a total system configuration at a specific point in time. This is essential because at any one time there are a number of disciplinary specialists working on various portions of the system. The baseline system thus becomes the common reference to which all these efforts are equated. The fact that the baseline system presents this frozen instant in time does not imply that it is static. As studies were performed and designs solidified which were improvements on various portions of the baseline system, they were incorporated into the system for its overall improvement. The fact that the baseline does exist insured that these improvements were not incorporated until their total impact on the system had been evaluated.

The total baseline system consists of the downhole package, the umbilical and the surface support system, the field control center, and the data-to-information conversion center. The downhole package, its function, and its configuration tend to dictate what can be done on the surface. Thus, the engineering problems of defining this package become the pacing items of the development. The surface segments of the system are no less important. The foreseeable engineering problems involved, however, are much more amenable to a variety of

straightforward engineering approaches than those involved in the downhole package. Thus, this study concentrated upon those functions which had to go into the hole, plus the critical in-line processes associated with the data collection.

In defining a feasible baseline system, alternatives were considered in all critical areas. This study outlines the alternative solutions and presents the basis of selection for the system. In many cases, there is little proven advantage of one technique over another and the choice has been subject to change as better information was developed during the design phase.

The method of presentation is as a series of short independent studies. There has been no attempt to make this paper a sequentially cohesive document. Each treatment is intended to present the rationale for a separate technical decision.

Two sequential iterations of the baseline system were constructed; both are presented in this report. The final configuration specified differed from the second iteration by separating the sensing system development from the penetrator development, and initially using the drill rig for propulsion. However, it is anticipated that the system will eventually grow to a configuration closely resembling the second iteration of the baseline system.

2. FIRST BASELINE SYSTEM

The first baseline system was generated early in the program. This portion of the study addresses itself to the alternatives considered in the initial selection.

2.1 PROPULSION SYSTEM

A means of propelling the system in and out of a 10,000 foot (3.0480 km) hole is a stated requirement. The alternatives considered were:

- Push rods or drill rig
- A tracked vehicle with extendable arms to adapt to the borehole size
- A linear hydraulic stepping device operating on the same general principles as the propulsive mechanism of boring machines.

2.1.1 Push-Rods or Drill Rig

Push-rods present a simple, attractive means for propelling packages into horizontal holes. They have the advantage of requiring no active mechanism in the hole for propulsion. Thus, their development cost is nil and within their range of feasibility their reliability is high.

Their range is limited to about 500 feet (152 m) with manual operation. Even with the drill rig as a thrusting device, their practical limit is probably in the order of 1,000 to 2,000 feet (304.8 to 609.6 m).

ENSCO has performed an independent study in this area [ ], considering the buckling of drill string in compression. A major conclusion of this study was that it is doubtful if the hole itself can be drilled beyond 5,000 feet (1.524 km) in hard rock without an in-hole thrusting device. The thrust requirements to propel the sensors into the hole will be much less than those to drill it. This is because the feasible weight and diameter of push-rods for this system will be much less than the corresponding values for drill string.

Even with a full complement of drill string and the massive hydraulic ram to drive it, the upper limit of range would be

less than 10,000 feet (3.0480 km). Thus, except for reduced depth requirements, push-rods were not considered further.

2.1.2 Tracked Vehicle

The concept of a tracked vehicle similar to a tractor has been considered. It suffers two major drawbacks:

- A track can be considered as an elongated wheel.
- A wheel is a poor mechanism of propulsion in a borehole. In order to provide thrust, the surface of the wheel must travel exactly the same distance as the vehicle moves. There can be no slippage at the point of contact. It is mathematically possible for only two points on the surface of the wheel to meet this criteria at any instant in time. All other points on the surface of a wheel of finite width must move with respect to this point of contact and the wall of the borehole. This can be projected to a practical interpretation of the meaning with respect to a tracked vehicle. It implies that, because of the curvature of the borehole, only a very thin section of track can apply traction to the vehicle without slipping.
- A tracked vehicle requires bogey wheels to distribute its footprint pressure evenly. The reliability of these wheels in a borehole environment would be poor.

Assume:

- A 5000-pound (22.24 kN) thrust to pull cable, and penetrate blockages
- 0.25 in. (6.4 mm) effective cross section of track
- A coefficient of friction of 0.75
- A 10 psi (69 kPa) footprint pressure

The reaction force against the borehole must be at least 6667 pounds (29.66 kN). This generates a need for 667 square inches (43.03 cm^2) of effective track area, or 2667 linear inches,

222 feet (67.7 m), of track in contact with the borehole wall, with even pressure applied to all points of contact. The mechanical devices to accomplish this are feasible but expensive. When this operation is envisioned in an abrasive borehole environment, the concept is unattractive.

2.1.3 Hydraulic Thruster

The hydraulic thruster has the same requirement as the wheel. The point of contact against which thrust is applied must be motionless with respect to the wall of the borehole. Unlike the wheel, the thruster does not use rotary motion. It involves an elastomeric locking cell, such as a rubber boot. This is hydraulically expanded against the wall of the borehole so that its entire circumference is in contact.

Assume the same number as the previous example. The hydraulic thruster will also require 6667 pounds (29.66 kN) of reaction force. A 10 psi (69 kPa) footprint pressure will require 667 square inches (43.03 cm^2), or 4.6 square feet (0.427 m^2) of locking surface. A 6-3/4 inch (17.14 cm) borehole has a circumference of 1.77 feet (0.539 m). Thus, a cell need be only 2.62 feet (0.799 m) long to withstand the 5000 pound (22.24 kN) thrust with a 10 psi (69 kPa) footprint pressure. This is an extremely modest requirement. Thus, the thruster concept was selected.

2.1.4 Discussion

Once the thruster was selected, there were additional alternatives to consider. It could be either mechanical or hydraulic. Several mechanical concepts were considered. Their only advantage was that a single mechanical unit would be adjustable to a wide range of borehole sizes. Their disadvantages were in high design and fabrication costs and poor suitability to the abrasive borehole environment.

The hydraulic thruster can be supplied with fluid-filled adapter cells for various borehole sizes. Cells such as this must be

designed to achieve good acoustical contact with the borehole wall anyway. Thus, the cell design concept can be applied to either type of cell, and total design costs are reduced. Since this hydraulic system presents no moving metal parts to the environment, it is not subject to the excessive abrasion of a mechanical device. The hydraulic thruster was selected for the initial design concepts.

2.2 THE PENETRATOR

There is a requirement that the system be able to penetrate blockages in the borehole. The system does not need a true drilling capability. Borehole blockages can take many forms. Thus, various degrees of penetration capability must be considered as alternatives. Four levels of penetration capability were considered.

2.2.1 Full Crushing Capability

This is a capability just short of drilling. It can penetrate any blockage up to and including hard rock fragments just short of the full hole size. It would crush them to less than 1/2 inch (13 mm) in diameter and spread the fragments around and along the hole. This would allow the instrument package which will be designed to pass 1/2 inch (13 mm) fragments, to traverse the hole.

The device would attach directly to the propulsion package, without the intervening instrument package. An initial full traverse of the hole would be made prior to any instrument runs. The device would clean the hole by crushing any rock fragments and spreading them prior to an instrumented run. There is ample precedent for this approach. It is standard logging practice to run a dummy package into a hole prior to logging if there is any question as to the hole's integrity.

Preliminary analysis indicates that this is a quite feasible procedure within the horsepower which can be expected to be available within the hole.

2.2.2 Partial Crushing Capability

Partial crushing capability can be achieved with a device similar to the above. It would go ahead of the instrument package. It would either be battery powered, or some mechanism would have to be designed to pass power through or around the instrument package. This device could be the same device as the full crusher; however, it is doubtful if enough battery power could be carried along to allow it to crush more than a few minor blockages. If the hole had been previously subjected to a cleaning pass, this should be ample.

2.2.3 Spreading Capability

In this concept, there is a long conical nose operating as a reverse auger. It is ahead of the instrument package and rotates as the package is forced into the hole. Since the pitch on the auger is reversed, it tends to keep pushing any debris forward ahead of the normal buildup. The fact that it rotates means that any loose material will spread itself around the hole. The clearance between the auger and the bore hole is such that any debris buildup of less than 1/2 inch (13 mm) will pass through. Anything in excess of this thickness will be pushed forward, and spread still farther. Rock fragments in excess of 1/2 inch (13 mm) would be continuously pushed forward in a tumbling action. The unit would be either battery powered, or extract its rotational power from guide wheels against the borehole wall.

If the blockages are not excessive, this action should be sufficient. If there is much or repeated blockage, the sensing package would be withdrawn and the hole would be cleaned by regular drilling procedures.

2.2.4 Pure Pushing Action

The concept of a pure pushing action by a specially shaped ram was considered. It would be an extremely simple brute force approach. The shape of the ram would be designed to break up blockages and either spread them ahead or push them in front of the package. It was rejected early because of the danger of jamming the package.

2.2.5 Discussion

This is an area which needs more study in the second phase of the program. None of the concepts is entirely satisfactory. The spreading action was selected for the baseline system purely on the basis of current feasibility. It is believed that after additional study some form of penetrator with a crushing action will be selected. However, there are too many unknowns for it to be specified as the initial baseline candidate.

2.3 INTERNAL TELEMETRY LINK

A major feature of the baseline system is that it must have the capability of taking individual sensor packages into the hole without major modifications. This could include such commercially available packages as the Birdwell 3-D Velocity log and standard resistivity tools. It could also include geophysical sensors which are not currently being considered. The penetration and guidance functions have to be in front of the instrument package. These must receive control commands and transmit back, status, and control information.

There is no way to determine in advance if a wire telemetry link passing along the surface of or through the sensor package will affect the operation of the sensors. Thus, there is a probable need to telemeter this data past the sensor package to the telemetry and control subsystem in the aft section of the downhole package.

2.3.1 Alternatives

The only specification needed at this time is that the link must exist, that it must be a two-way communications channel, and it must be wireless.

The candidates considered are:

- Electromagnetic telemetry. Here there are a number of feasible approaches.
- Acoustic telemetry. Although data on specific hardware has not been collected, a simple acoustic link over these distances is well within the state-of-the-art.
- Fiber optics. Although this approach is only wireless in the more restrictive sense of the word, it would be a most attractive method if the data rates were high.
- Pure optic. This differs from the fiber optics only in that it would provide a pure optical path past the sensor package. In some packages, this would be simple, in others more complex. There is no question of its feasibility.

2.3.2 Discussion

There did not seem to be a strong technical reason to select one technique over another, at the time. The determination should be made during the final design.

2.4 SENSOR POWER

There are three alternatives in the methods of supplying power to the sensors.

- They may draw power from the central power supply of the system.
- They can provide their own power in the form of self-contained battery packs.
- They can obtain power from both sources.

2.4.1 Common Power Source

Of the sensors considered, any of the alternatives may be acceptable. Powering a downhole package is a critical process. A single common power supply generates many problems, especially in power radiating sensors such as the acoustic and EM radars. Common grounding and ground loop problems are extremely difficult to resolve because of the long cylindrical packaging configurations which must be used. The problems are compounded by the large dynamic ranges involved between transmitted and received power. A 150 dB dynamic range indicates that within the close confines of a single package received powers of signals are being measured in close proximity to a transmitter with 10^{15} times their power. Common power supplies for transmit and receive equipment are out of the question. Almost the only way this can be accomplished would be to draw power from two separate power supplies to provide isolation.

2.4.2 Battery Supplies

Where self-contained sensor packages are taken into the hole, they will possibly have their own batteries. If this is the case, they will be used. However, high power devices usually are fed through the logging cable. Batteries may be used for receiver supplies, but carrying sufficient batteries to drive a powerful transmitter could be a problem.

2.4.3 Hybrid Power

Should a single power source prove infeasible, the preferred approach would be to include a rechargeable battery supply to power the most sensitive receiving circuits and to draw the main source of power from the power converted so that the main power is supplied from the surface.

The baseline system assumes this approach.

2.5 MODULATION TECHNIQUES

It is premature to specify a specific modulation technique in this analysis. This is a subject that requires considerably more study. Thus, a modulation technique is not specified for the baseline system. However, the technique to be employed impacts on many aspects of other parts of the baseline system. A modulation had to be assumed, and it must be recognized that a change could significantly alter some of the baseline assumptions.

Three approaches have been considered for both the EM and the acoustic radars:

- A pure pulse
- A swept frequency such as "chirp"
- A pseudo-random code.

2.5.1 Pure Pulse Modulation.

The principle advantage of a pure pulse system is simplicity of the circuitry involved. The simplicity extends to include not just the radar package but through the total system, including telemetry, encoding, quick-look display, and eventual computerized processing. The entire concept of data processing assumes that the signal returns from reflected objects are impulse functions, or at least impulse functions whose frequency characteristics are distorted by the target or interaction between targets. Other techniques are simply radiated signals with specified characteristics which by inverse filtering, or deconvolution, can be converted into impulses as an initial step in the data processing phase. The simplicity of the pure pulse transmission is such that there is strong justification for its use.

The major disadvantage of pulse transmission is that most power transducers are peak power limited. A pure pulse is radiated and then no further transmissions can be made until ample time has elapsed for reflected returns to arrive back at the receiver. At this time, another pulse is radiated. Typically, a pulsed radar will operate on a .1 to .5% duty cycle. It is effectively using only a small fraction of the available time.

The systems employed will be pushing their maximum range, and one way to increase both range and resolution is to integrate the returns from a large number of pulses. This implies increased data gathering and data reduction time. It can have a major impact on system operating costs.

2.5.2 Swept Frequency, "Chirp" Modulation

A swept frequency modulation makes use of the fact that the frequency transformation of a pulse is a uniform distribution of all frequencies. The chirp signal transmits a varying frequency, so that in one sweep it transmits cumulatively the same frequency spectrum as the pulse. The signal returns then pass through a deconvolution process in a matched filter which maintains that amplitude of the frequency spectrum, but shifts the phase as a function of frequency in such a manner that the output is an impulse for each reflected signal.

The main advantage of the "chirp" is that it can drive the power transducer at its maximum power, over an extended period of time. Thus, it supplies an average power equivalent to the peak power of the pulse.

When the chirp signal is reconverted to its pulse form, the signal amplitudes emerge as though a pulse many times the true peak power capability of the transducer had been transmitted.

The main disadvantage is that the signal must be processed to be interpreted, even for a quick look. At any instant, the receiver is receiving signals back from a number of targets, each return at a different frequency. Thus, the returns are featureless until processed. A second disadvantage is the impact that this technique places on the dynamic range of the associated telemetry and recording equipment. This can be seen by considering a typical return from two targets, one close in, and one at near maximum range. The close-in target returns will be strong reflections of signals just transmitted while the returns from the distant target will be weak reflections of frequencies transmitted much earlier. A signal shape must be preserved consisting of a wave containing frequencies with power ratios in the order of one million to one hundred million to one.

2.5.3 Pseudo-Random Code Modulation

There are a number of signals which can be radiated, which, on deconvolution, can be converted into a pulse. Deconvolution by itself is not enough. It will produce a pulse of maximum amplitude whenever the returned signal cross correlates with the reference signal. However, it will also produce pulses, but of lesser amplitude whenever partial correlation occurs. It is necessary that a modulation be radiated which has the frequency components to be reconverted into the Dirac delta function, and that the interrelation between various interior portions of the wave shape does not have significant correlation at any other point. In the frequency domain, the swept frequency "chirp" signal has these characteristics.

The pseudo-random code in the time domain can be arranged to accomplish the same features as "chirp". By transmitting selected sequences of positive going and negative going pulses, it is possible to both effectively use the average power characteristics of the chirp and retain the time domain features of a pulse.

Pseudo-random codes have had tremendous emphasis and development effort in the military fields of communication, anti-jamming, and cryptographic techniques. However, the earliest approach used a taped delay line.

A pulse is introduced into a delay line and, as it propagates along the line, trigger pulses are drawn off at equally spaced intervals and coded according to a pseudo-random code as positive or negative pulses. These modulate the transmitter. When this code is received, it is fed into an identical delay line where the tapped outputs are summed, with the negative pulses inverted prior to summing. When all pulses align with their corresponding taps, the output is a pulse amplified by the number of taps involved. Analog delay lines over the delays of interest to seismology have not been too successful. The shorter times of flight required for the acoustic radar system make the concept of analog delay lines more attractive. The extremely short times of flight, a few hundred nano seconds at most, make the implementation of the tapped delay line for EM radar not only simple, but if deconvolution is involved, almost mandatory.

Only a pulse return can be interpreted in field displays. The desirability of having the operator be able to interact with the equipment on the basis of return data is great. Thus, it would be advantageous to be able to use a code such as this. It would enable the transducer to operate on a full average power basis for lengths of time exceeding the actual time of flight. The return signal would pass through an analog delay line with the similar code to reconstruct the entire return into a single pulse for each target. The amplitude of the pulse would be equal to the amplitude of the return from a single pulse times the number of pulses. Of course, the noise would also amplify, but only as the square root of the number of pulses. Thus, the improvement in the signal-to-noise ratio would increase as the square root of the number of pulses in the train.

There are a number of codes which have the characteristic of negligible side lobes (false correlation peaks). The best known are the Barker codes. These code sequences approximate the ideal correlation function. Mathematically they are defined as a finite sequence of pulses of amplitude, a_i where $a_i = \pm 1$. The length of the sequence is B. The Barker code has an autocorrelation function:

$$C = \sum_{i=1}^{B-S} a_i a_{i+s}$$

such that

$C = B$ for $S = 0$ (zero shift)

$|C| \leq 1 \quad 0 \leq S \leq B - 1$ (This defines the side lobes)

$C = 0 \quad S \geq B$

The only known binary codes which satisfy this condition are of lengths 1, 2, 3, 4, 5, 6, 7, 11, and 13. Longer codes have been developed (2) which come close to meeting the Barker criteria. Reference [1] lists codes up to 200 bits in length. Figure 4 illustrates a 24-bit code, its correlation function, and a schematic of delay line decoding. Code lengths giving processing gains in excess of 1000/1 have been used.

2.5.4 Assumed Modulation

Since the pseudo-random code presents the best features of both "chirp" and pulse, and can be decoded downhole to ease design problems in telemetry, display, and recording, it has been selected for the baseline system.

---

[1] Newman, F., and Hofman, L., "New Sequences with Desirable Correlation Properties," NTC Record, p. 277-282, 1971.

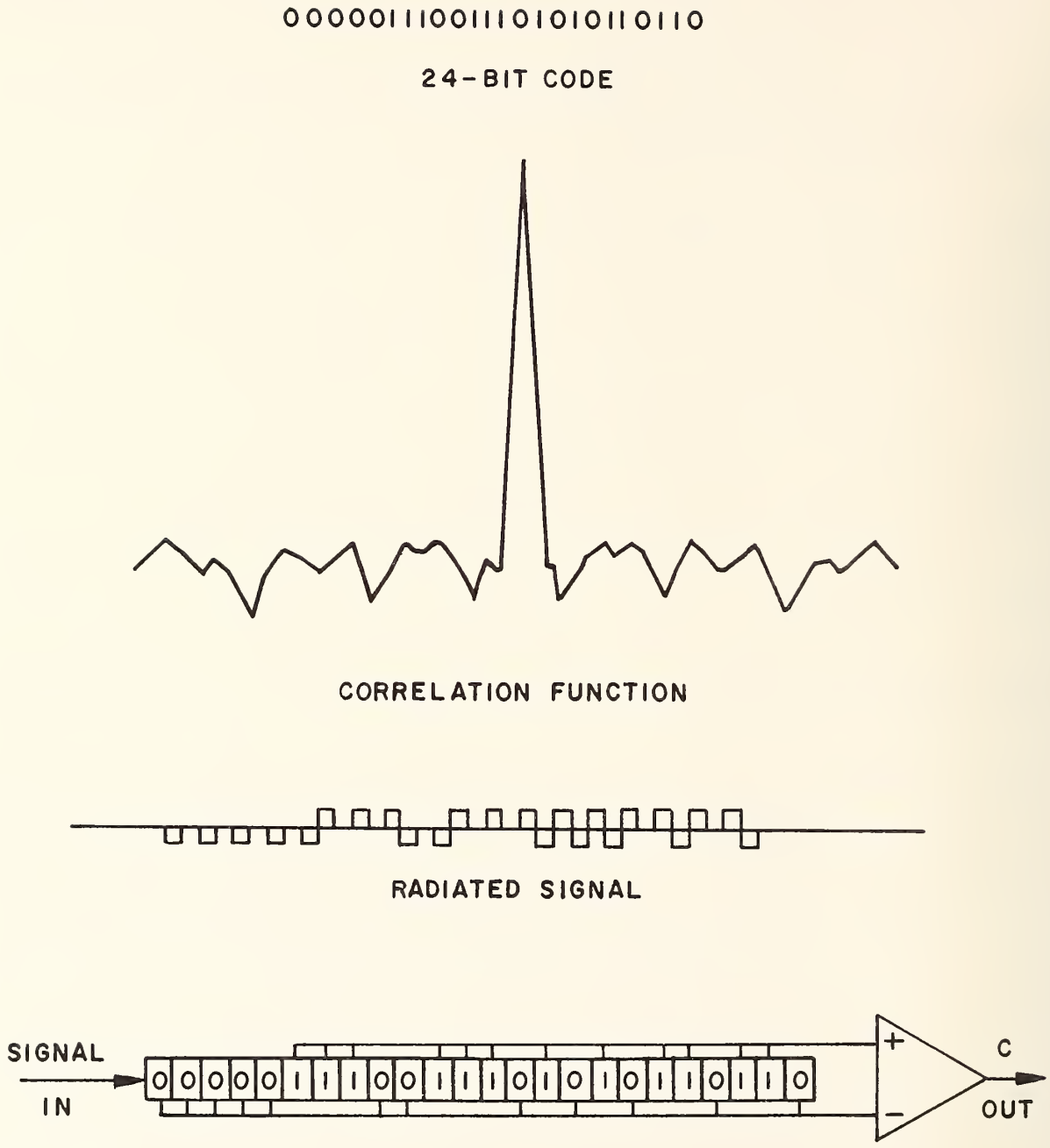

Figure 1. Illustration of pseudo-random code and real-time delay line deconvolution.

2.6 CONTROL OF DYNAMIC RANGE

2.6.1 Introduction

The dynamic range in the signal is the ratio of the maximum value of the strongest return to be measured to the minimum detectable signal. Even without processing, this is in the order of 60 dB. Advanced data processing techniques can add an additional 40 to 60 dB to this value. This creates the requirement that the signal conditioning, transmission, recording, and display might have to handle singals with amplitude ratios as high as one million to one. When all components and operations are considered, this is an impossible task to accomplish in a single step.

Fortunately, the problem can be broken into discrete steps. There are three major contributors to the dynamic range of the signal:

- Spreading Loss which causes the received signal to vary as inverse square of the distance to the target.
- Attenuation Loss which is due to a certain percentage of each cycle of energy which is converted to heat. This will vary as an exponent function of the range to the target.
- Signal Variation due to the reflection and scattering characteristics of the targets themselves.

Although the design is difficult, dynamic ranges of 120 dB can be handled by analog means for every step in the process except the tape recording and the display. Thus it is necessary to either convert to a digital signal or reduce the dynamic range prior to recording and it must be reduced prior to any meaningful analogue display.

The eventual means of reducing the dynamic range requirements of radar time of flight signals is by a process of time varying gain control. Where the amplification applied to the signal increases as a function of the range to the target. This can be done in either an analog or digital manner.

2.6.2 Methods Considered

Three methods were considered for the reduction of dynamic range requirements:

- Pure digital.
- Logarithmic amplification.
- Time-varying automatic gain control.

2 6.2.1 Pure Digital

In seismology it is normal practice to bring the data directly into an analogue to digital converter. This implies that the converter itself must be capable of this dynamic range. Once converted to numbers, there is no problem in manipulating the data in such a manner as to find the range sensitive parameters and to remove them by computation. This leaves only the signals characteristic of the individual target returns for further processing.

The A to D converter will have to work to better than a 20-bit resolution. This is achievable but the equipment is expensive and sensitive to its environment. It also slows the data acquisition, and could create a data rate limited system.

2.6.2.2 Logarithmic Amplifiers

Amplifiers are available which have an amplification proportion to the logorithm of the amplitude of the incomming signal. They are satisfactory for some purposes. If their amplification characteristics are well defined, the signal could be compressed prior to transmission and subsequently be processed by the antilog function of the amplifier to remove the compression and recreate the proper response digitally.

2.6.2.3 Time-Varying A.G.C.

The received signal can be multiplied in an analog function generator, by a function which increases its amplitude with time after the initial pulse transmission. If the amplification is the inverse of the product of the spreading loss and the exponential

attenuation, then only the target signal amplitude remains. Fortunately, both of these loss factors are simple analog simulations. They need only a term defining the wave velocity and the attenuation factor to make a true correction. Even if the gain functions are not well defined, the applied corrections need only be known. Further refinement can be accomplished digitally.

2.6.3 Discussion

If a matched filtering technique such as "chirp" or a pseudo-random code is used, then only the pure digital technique can be employed to reduce dynamic range prior to deconvolution. Both logarithmic amplification and time varying gain are nonlinear processes. When signals are arriving from multiple targets simultaneously, the use of nonlinear processes will produce cross-modulation products which would show up as noise on deconvolution.

One of the deciding factors on selecting the pseudo-random code was that it could be used to decode the spread-spectrum return in the hole. This can be accomplished as part of the receiving process. Thus, deconvolution can take place immediately. This allows the consideration of both the logarithmic amplifiers and the time-varying gain (TVG) circuits.

A major disadvantage of both the logarithmic amplification and the direct A to D conversion is that both need subsequent digital processing before the signal can be meaningfully displayed. This is not the case with the time varying gain (TVG). Thus only the TVG approach allows a display for the Field Test Operator (FTO) prior to recording and digital processing. TVG also reduces the dynamic range and bandwidth requirement on the telemetry link and allows simpler and more reliable equipment. Thus the time varying gain operating on the deconvoluted signal in the downhole package has been selected for the baseline system.

2.7 ELECTRICAL POWER

2.7.1 Introduction

The electrical power for the operation of the Down Hole Package must be transmitted down the umbilical logging cable. The size of this cable, both in weight and volume, will be a critical system parameter. Electrical power can be expected to be in the order of kilowatts. Thus the power must be transmitted down the cable at as high a voltage and as low a current as feasible.

2.7.2 Alternatives

Three methods of power have been considered:

- 60 hz normal power.
- 400 hz aircraft power
- High voltage DC with SCR conversion.

2.7.2.1 60 Hz Normal Power

Presents the advantage of low cost and a large body of commercial equipment and knowledge from which to draw. It has the disadvantage for requiring larger transformers and motors than the higher frequency equipment.

2.7.2.2 400 Hz Aircraft Power

Will be more expensive but due to the progress of aerospace developments, there are compact components available. Its transmission over 10,000 feet with adequate power factors may be a problem.

2.7.2.3 High-Voltage Direct Current

Recent advances in high power capacity silicon controlled rectifiers make the concept of taking 60 hz at the surface, transforming it to a high voltage, and converting it to high voltage direct current for actual transmission. Downhole it would be reconverted to, say 400 hz AC and transformed down to usable voltage levels. This would have the advantage of low loss power

transmission wihtout power factor problems. It would also ease the insulation requirements, as there is no need to insulate for the peak voltage, and transfer power on the basis of rms voltage and power.

2.7.3 Discussion

Pending further study, and better definition of the power requirements, 60 Hz normal power was selected. It was unknown at the time whether either total power availability or component sizes would be limiting factors in design. For this reason, 60 Hz had been tentatively selected as the power source. Although either of the other approaches could be technically superior, there seems little justification in exploiting this superiority at greater expense unless technical consideration indicate it is necessary.

2.8 COOLING

2.8.1 Introduction

In dry holes, cooling could be a problem. A major fraction of the energy transmitted down the hole will be lost in the form of heat. This could occur during the A.C. power conversion cycle, the electrical to hydraulic conversion cycle, or in the actual propulsion itself. This heat must be transferred to the borehole wall and thence to the earth which acts as a heat sink.

2.8.2 Alternatives

The problem of cooling cannot really be attacked until more is known about the amount of heat to be dumped. Three alternatives can be seen but there is insufficient data to specify one above the other. The one which presents the simplest and most reliable system will be selected. The alternatives to be considered are:

- Radiant and Convection Cooling. Here a cooling surface of sufficient area to allow cooling by convection and radiation to the borehole wall would be provided.

- Conductive Cooling. Here an elastomeric cell, possibly serving double duty as one of the locking cells of the propulsion system, would be provided. Hydraulic fluid would serve as the coolant. The cell material would probably be loaded with either lamp black, or metal filling to increase its thermal conductivity. It would be expanded against the wall and cooling would occur by conductive heat transfer.

- Refrigerant Cooling. The refrigerant cooling concept would be similar to either of the other two except that there would be a small aircraft type refrigeration unit which would draw heat from the critical areas. It would discharge it into the intermediate heat sink of either a radiant cooling area or the conduction heat transfer boot. Fluroelastomers are available which will work to 400 degrees Farenheit.

2.8.3 Discussion

It would seem that radiant cooling, if achievable, would be preferred. Even if it added considerable bulk to the downhole package, it probably would be more cost effective than either of the other two. The actual choice will have to await the determination of the amount of heat to be dumped and the heat transfer characteristics of the rock.

2.9 THE LOCATION OF THE ANALOG/DIGITAL INTERFACE

2.9.1 Introduction

All sensors are, by their very nature, analog. The system will use a digital computer for its signal processing. At some point between the sensor and the computer there must be an analogue to digital conversion. Just where this conversion takes place physically can have a major impact on the system design and its operational effectivity. The alternatives considered are:

- Conversion in the Downhole Package
- Conversion in the Field Data Control Center (FDCC)
- Conversion in the Data to Information Conversion (DICC)

2.9.2 Discussion of Alternative Conversion Locations

2.9.2.1 The Downhole Package

There is one school of design philosophy which believes that A to D conversion should take place as early in the sensing stream as possible. This would place the converter directly behind the time-varying gain-control circuits in the downhole package.

The principal advantage of this approach is that once the A to D conversion has taken place, it alleviates many design and operational problems for the rest of the data link.

- Amplification need no longer be linear.
- Analog scale factors need no longer be retained.
- Calibration problems are reduced.
- Maintenance is simplified in that modules can be replaced without realignment, scale factor, and gain adjustment.
- Circuit noise and cross talk between circuits is much less of a problem.

The disadvantages are:

- The digital system requires a great deal more bandwidth than the analog system.
- The data is no better than the stability and drift of the reference voltages used in the conversion.
- Digital equipment can require a higher level of skill and more complex and expensive test equipment than analog equipment.

2.9.2.2 The Field Data Control Center (FDCC)

The location of the analog to digital conversion in the control center has several advantages:

- It alleviates the problem of information bandwidth in the transmission of information up the umbilical logging cable.
- It simplifies the downhole package.
- It is less restrictive as to packaging and environmental restraint.
- Better, more stable voltage control can be assured, thus it can accept a wider dynamic range of signal.
- It allows editing and digital formatting of information, ancillary to the raw data and yet necessary to the effective data conversion process at the DICC.

Its major disadvantages would be:

- Greater susceptibility to noise in the telemetry link up the logging cable.
- It would still require a digital rather than an analog tape recorder.
- It would still require digital maintenance skills in the field.

2.9.2.3 Data-to-Information Conversion Center (DICC)

Location of the A to D interface in the DICC has several advantages:

- It keeps the required digital skills and the analog skills at separate locations.
- It allows a skill level in the field which is probably more available.
- Operationally, analog equipment has been used in the field for years. Although its limitations are recognized, people know how to cope with them.
- It will allow one lower level of design for field equipment, as there is a larger base of field proven equipment from which to draw.
- Field equipment will be simpler.
- Analog tape recorders are in general better suited to the field environment.

The major disadvantages are the inverse of the advantages of either of the previous locations.

The location of the A to D conversion in the Downhole Package is rejected pending the results of studies defining the information bandwidth requirements. It is believed that the limiting factor here will be in the bandwidth available in 10,000 feet (3.3 kM) coaxial cable in the unbilical. It must be remembered that unlike any other sensing system, this system senses in four dimensions rather than three. It must define a point in three dimensional space in terms of the intensity of the reflected signal from that point. This additional degree of freedom will show up in vastly increased data transmission requirements.

There is little choice between the conversion in the field and in the DICC. None of the arguments in favor of one over the other are very strong. In general, the pragmetic considerations favor analog in the field and digital in the computational center. The technical arguments favor conversion in the field.

The analog-to-digital conversion in the computational center was selected for the baseline system on technical considerations. Probably, the deciding factor will be the relative costs between the two approaches. It could easily be that the same argument used in selecting the modular sensor package approach will be valid in this case also. It is better to spend the initial developmental resources on proving the sensors and the basic concepts than in designing and building non-standard intermediate data handling techniques. There is no question of the feasibility of the intermediate digital approach. It is believed the relative costs will govern the final determination.

2.10 FIELD TEST OPERATOR'S DISPLAY

2.10.1 Introduction

The Field Data Control Center is, in effect, the office of the Field Test Operator. In order to define the functions of the Center, it is necessary to evaluate the class of man who can be expected to operate the equipment in the field. It would be

poor system design to specify functions for the FDCC which were beyond the capabilities of the normal operator, it would be even worse to underrate what this man can contribute to the success of the operation.

It may be possible, in later generations of this equipment, to automate the data taking to a point that human judgment is not required in the process. This cannot be assumed in a piece of first-generation equipment. Thus, the problem resolves itself into defining the capabilities of the man, and giving him the data and control functions to vary those test parameters which we cannot define and automate on an apriori basis.

2.10.2 The Field Test Operator (FTO)

In all probability, the FTO will be a paraprofessional, field engineer. He will have at least a high school education, and probably a technical associate (2 year) degree or equivalent technical school, or military technician background. Historically, within his field he will be a professional. After a few months or operational experience, he will know more about the actual operating characteristics of the equipment in the field environment than the engineer who designed it. He will know its strengths, its weaknesses, its failure modes, and the signatures in the data of incipient failures. He will be highly motivated and will take personal pride in delivering good data under adverse conditions. The field environment is unpleasant; men who are not motivated for this type of work don't stay in the field. Above all, the man will be a self-reliant individualist; given the data to aid him, he can make a major contribution.

2.10.3 Functions In Support Of The FTO

The functions which the FTO must perform and must be supported by equipment include:

- Normal operational functions, such as getting the equipment into and out of the hole; getting the vehicle on-site and aligned; routine maintenance and calibration of both the complete sensing system and the surface supporting equipment necessary for the system to function.

- Operation of the sensing equipment. These functions include: planning how he will run his tests, based upon as much apriori information on the hole conditions as possible; controlling the movement in and out of the hole; monitoring the status of the various subsystems involved; evaluating the quality of the data as it emerges prior to recording for subsequent processing at the Data Reduction Center; adjusting gains for best signal returns; selecting among alternatives operating modes and sensors; selecting frequencies.

- Judgment Operations. Aside from the pure mechanics of operating the system, he must exercise judgment. He must know when he is taking good data and how to adjust his equipment to achieve this end. The data taken for advanced signal processing by its nature will be featureless. The FTO will need a real-time pulse, time-of-flight, quick-look display. This implies that either there must be preprocessing of some type at the FDCC or there must be a single pulse mode so that the FTO can adjust his equipment, select the operating mode, and decide upon the quantity of data to be taken for subsequent processing. Under foreseeable conditions, he may need to rerun a specific area, taking and retaking data at several operating modes or frequencies.

2.10.4 Administrative Functions

A critical function of the data taking will be the editing of the data to insure that every thing needed at the DICC is on the tape. This must include:

- All gain settings;
- The operating mode;
- The coordinates within the boreholes;
- Any special calibration data;
- The sensors used;
- Traverse speeds.

Many of these functions can be automated and automatically entered on the basis of switch settings. Others may have to be entered manually by keyboard, or on an ancillary data sheet to accompany the data tape.

2.10.5 The Field Test Operator's Display

There is a firm requirement that the FTO have a quick-look display to enable him to evaluate the functioning of the equipment, and the quality of the data being taken.

The functioning of the equipment can be indicated with a bank of go/no-go lights. Alternatively, the equipment can scan the status of the individual pieces of equipment and merely indicate a fault condition. Which approach is the more cost and operationally effective will depend upon the number of status signals eventually decided upon.

The determination of the quality of the data, and the controls necessary to control the data, is more complex. There are many alternatives involved which must be considered in the details of system design. Only the broadest aspects affecting the feasibility of the alternatives will be considered at this time.

The majority of the signal characteristics will be extracted or enhanced by advanced data processing techniques at the computational center. Thus, the FTO will be unable, in the field, to identify specific features in the data upon which to make his judgment. However, the majority of these features will show up as two-dimensional defraction patterns in the x, y, I, or a ρ, θ, I display. These are two space dimensional displays where the third coordinate is the intensity of the return at any x, y, or ρ, θ, coordinate.

The operator may not know how to interpret these patterns, but he must be able to see them and to make those adjustments which are available to him to enhance them as much as possible. The simplest possible display for the FTO would be an oscilloscope

trace. However, this is a one-dimensional return in space. It does not give him the comparative data from adjoining tracks to make his judgment concerning the quality of the data.

The next step in sophistication of the display is to give him an x,y or polar ρ, θ, chart recorder or facsimile with paper chart recording. This provides him with the opportunity to make adjustments, and reruns of various lengths within the hole to get the best possible data prior to recording on tape for subsequent computerized processing.

The final level in sophistication if simultaneous sensors were to be employed would be to give him a color oscilloscope TV-like display. The electromagnetic radar could be displayed in one color and the acoustic radar in another. He would have the display sweep velocity of each type under his control. This would enable him to match at least selected portions of the display of these two pictures. This would be an excellent tool for an analyst to use in the field. It is doubtful if this degree of sophistication would be warranted for the FTO.

The three display alternatives require increasing degrees of sophistication for their implementation. However, they all require a certain basic amount of preprocessing to make the data interpretable at all.

2.10.6 Common Implementation Problems

Three actions must be taken on the raw data from the receivers before it can be displayed to the FTO.

2.10.6.1 Deconvolution

The data must be converted to a pulse/time-of-flight mode, unless, of course, it is already in that form. Data taken by a swept frequency such as Chirp, or by pseudo-random code for delay-line decoding is featureless until it has passed through a deconvolution or matched filtering process. These techniques increase the power-handling capability of the transmitters by

spreading the signal in time. In this manner they can transmit much higher average power than that produced by a single pulse. Since they do spread the signal in time, at any instant the receiver is receiving different data from different targets simultaneously. Features, both near and far, are smeared together. Thus, they cannot be interpreted until these overlapping data points have been reconverted into the conventional time-of-flight/pulse configuration.

2.10.6.2 Automatic Gain Control (Dynamic Range Correction)

Once having been corrected to a pulse/time-of-flight configuration, the signals need one further operation. The sensors involved have a dynamic range of the order of 120 to 150 dB. This means that the return signals will be varying in the order of 100 dB (100,000/1) within the length of the sample. Even the most sensitive chart recorders cannot hope to meaningfully display this range of signal magnitude in a single sweep setting. The individual sweeps must be multiplied by a time varying gain function so that returns from equal reflectors, at different distances, will be displayed at equal amplitudes. Alternatively, the signal could be passed through a logarithmic amplifier so the log of the signal only is displayed. Both of these alternatives are non-linear operations; thus, they can only be accomplished after deconvolution. To do otherwise would distort the data and cause cross product modulation which would show up as noise, masking the true signal.

2.10.6.3 Sweep Slowing by Data Sampling

The pulsed radar returns occur too rapidly for any of the display techniques to be used without slowing them down. This is accomplished by a sequential sampling process. This is a function which must be performed in the hole prior to any other operation. It must be used whether there is to be a visual display or not. The incorporation of the visual display merely slows down the process without materially changing the circuitry involved.

2.10.7 Discussion of Alternatives

2.10.7.1 The Single Sweep Oscilloscope

The single sweep oscilloscope display involves all of the processes discussed above. The acoustic display trace might not have to be slowed and the degree of slowing would be less than that required for the paper display of the two-dimensional plotters.

2.10.7.2 Two-Dimensional Plotters

The two-dimensional plotters either x, y, or ρ, θ, require the above processes plus the ability to advance the trace on the plotters so that adjacent sweeps are displaced one from the other. They would also require slowing both sweeps to match the plotting velocity of the recorder.

2.10.7.3 Two-Dimensional Oscilloscope Display

The concept of the two-dimensional color oscilloscope requires the same preprocessing as the other displays, except that it does not require any special slowing of the sweep as in the hard copy recorder. In addition to these, however, it needs considerable storage memory. The entire two-dimensional data matrix must be stored and repetitively read from memory. Although the cost and complexity would increase, it could easily pay for itself in data acquisition costs. The color display would allow the FTO to vary both the velocity and attenuation terms in his automatic gain control function to make a best visual fit on the data from the combined acoustic and electromagnetic sensors. He could then better visualize how he should conduct his tests, and set his equipment to obtain the most meaningful data.

2.10.8 Summary

The display for the FTO could cover a wide range of possibilities. It could include:

- Simple go/no-go lights to enable him to evaluate the functional status and control his equipment. These are basic and common to all alternatives.

- An oscilloscope to evaluate the quality of his data on a sweep-by-sweep basis.

- A hard copy printout of a two-dimensional display where traverse along the hole is shown on a sweep-by-sweep basis. This will enable the FTO to evaluate the quality of the data and observe defraction patterns which could be emphasized by proper adjustment of his equipment.

- A color two-dimensional oscilloscope display to give the FTO the same information as the hard copy display. It would also include the superposition of data from various sensors in a form where any variations would become instantaneously obvious. It would provide him much better information on the quality of his data and on the interaction between the responses of various sensors. However, it would also involve considerable increase in the sophistication of the surface equipment.

2.10.9 Conclusions

Each successive alternative presents an increase in the capability for the FTO to perform his critical function of getting the best data possible for future processing. It is believed that the simple go/no-go display and the single oscilloscope sweep are too restrictive. They do not give the FTO sufficient data to effectively function to his full capability.

The hard copy printout seems to be an acceptable alternative by allowing him to identify the defraction patterns which must be enhanced. It thereby gives him the information necessary to plan and conduct his measurements.

The color two-dimensional oscilloscope display would unquestionably further enhance the FTO's capability. However, it is questionable whether he, or even a full professional, would be knowledgeable enough to fully exploit this capability. It has the capability for interactive interpretation in the field. The data base for the whole system, at this time, is insufficient to enable us to intelligently use this capability as a full field tool. This type of interaction could probably better be used at the data reduction center. It will prove of value and eventually may be incorporated in the field. However, it is believed this

would be a second or third generation system before it could be properly exploited.

While all techniques discussed are technically feasible, the hard copy graphic display is recommended as the baseline approach for this system.

3. SECOND ITERATION OF BASELINE SYSTEM

3.1 INTRODUCTION

A second iteration of the baseline system was conducted approximately nine months after the configuration discussed in paragraph 2. An approximately half-scale model of the baseline configuration as we currently visualize it was fabricated. It is an aid to visualization of the three-dimensional packaging problem of the downhole package, and the physical restraints which must be imposed upon the mechanical packaging because of the general borehole configuration. The total assembled model is approximately 25 feet long. This would imply an operational length in the order of 50 feet. The model is broken into four basic packages:

- A penetrator, which contains the required rock crushing and steering functions.
- One of a series of three interchangeable sensor packages, which may be either an acoustic or electromagnetic pulsed radar or a resistivity probe.
- A propulsion package, which moves the system into or out of the hole at a precisely controlled speed.
- An energy conversion package, which transforms the energy transmitted down the umbilical into other energy forms which are more usable in the package itself.

The presentation will discuss these in sequence starting at the nose of the downhole package.

3.2 THE PENETRATION UNIT

Figure 2 shows an exploded view of the penetrator model with all pertinent functions located and labeled. Here again, the discussion will start at the nose of the system. We have a requirement for penetration of the borehole which includes minor rock crushing capability. Although it has not been specifically stated, a steering capability is needed. It is rather obvious from studying the problems of boring a horizontal borehole to the length required by this system, that it will be necessary for these holes to be redirected and diverted a number of times. In the drilling process, this will involve backing the drill and redrilling the hole at some new angle with respect to its current center line. The old hole may or may not be cemented. Thus, it is necessary to incorporate a steering function to insure that the system has the capability to select, on the basis of the driller's log, which hole branch to enter. The steering is more analogous to throwing the switch on a railroad track than to what would normally be considered as steering of a vehicle. The general solution posed for both rock crushing and steering have been incorporated in the model.

A conical crusher is shown in the model in Figure 2. This serves to provide both the steering and the crushing functions. In Figure 2 the crusher is shown with the nose diverted into a steering mode. This is accomplished through a combined universal joint and steering deflection knuckle which allows the crusher to be deflected at a single fixed angle with respect to its own center line. The conical penetrator has a helical row of tungsten carbide crushing buttons, which also serve as a propulsive force to draw the penetrator nose forward independently

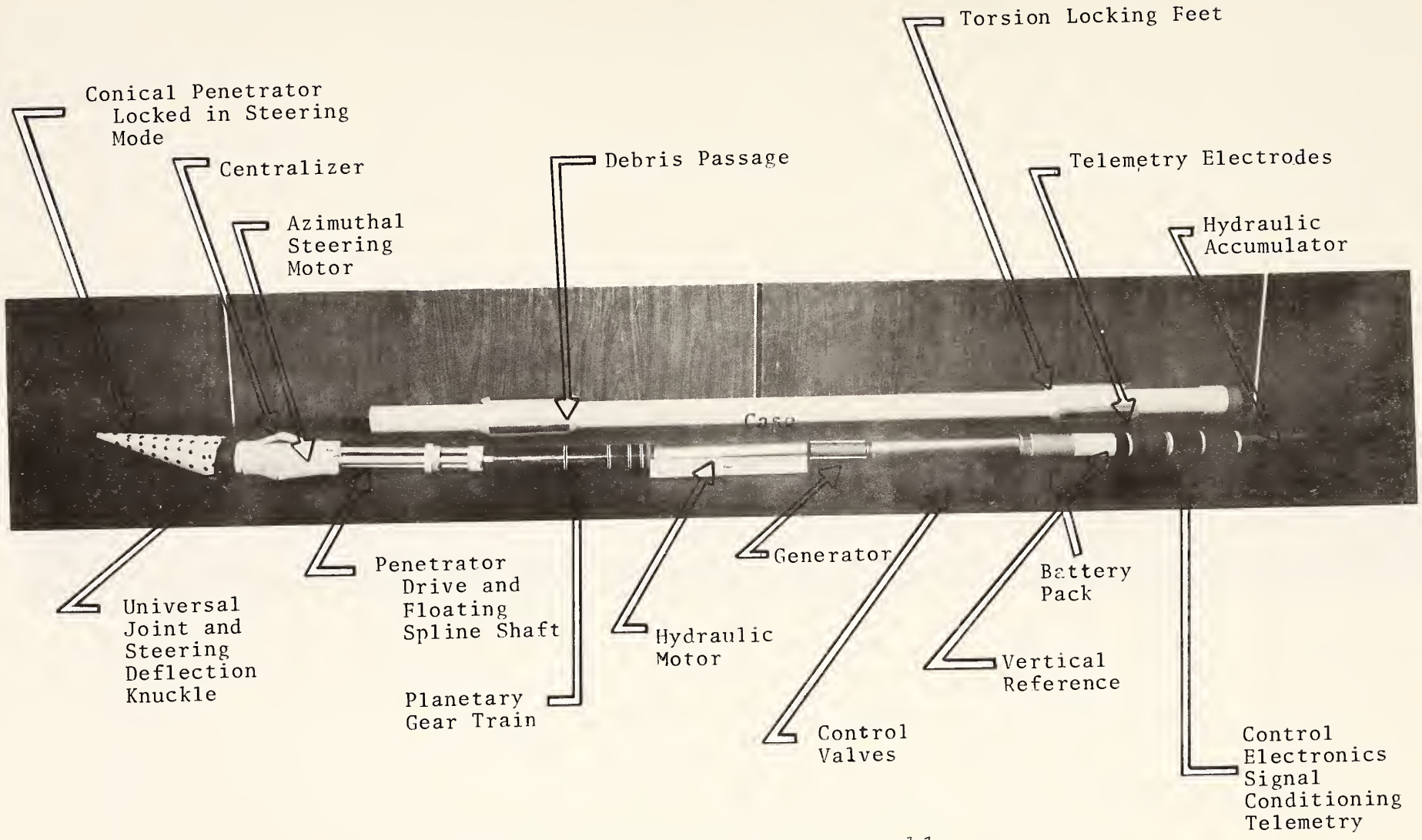

Figure 2. Exploded view of penetrator model.

from the normal movement of the total downhole package. Actual steering is accomplished by an azimuthal steering motor located directly behind the crusher. This has the capability of rotating the plane of deflection of the steering nose through 360°.

In actual practice, the location of a deviated hole and the angle at which it was deviated would be obtained from the driller's log. On approaching this point in the borehole, the nose would be deviated through activation of hydraulic pistons and the plane of deviation rotated azimuthally to that of the deviated hole into which the tool must enter. Figure 3 shows the model being directed into a new hole which is simulated by the cut-out area in the simulated borehole tubing shown in this figure.

At this point in the operation, the nose of the conical penetrator has been deflected through such an angle that the tip of the cone is beyond the point to which it could be deflected in the borehole itself. In this condition, the tool cannot continue down the existing borehole beyond the point of final intersection between this and the deviated hole. The tip of the cone is shown entering the deviated hole. Since the cone is rotating as the tool progresses, the helical threads caused by the crushing buttons tend to pull the tool forward along this new course. The entire penetrator nose is mounted on a sliding spline shaft which provides a capability of independent travel of the nose over a distance greater than the length of the nose cone. Thus, the nose is pulled completely into the new hole before the limits of spline extension are reached, and the tool will continue down this new hole.

In the crushing mode, the face plate, which was deflected to cause the tip of the cone to deviate, is readjusted perpendicular to the axis of the rotation of the nose. The conical penetrator is loosely spring-loaded so that the nose tends to travel down the center of the hole. On encountering debris which generates any appreciable retarding force to the device, a pressure switch

Figure 3. Conical penetrator steered into deviated hole.

will be operated which will cause the nose to start to rotate. Since the cone is only lightly loaded to the center of the hole, the rotation will cause a search pattern to start as the nose is deflected and the cone climbs the debris. The deflection of the nose will continue until the side of the cone opposite the debris is forced against the wall of the borehole as shown in Figure 4. The helically-arranged buttons will pull the cone forward and pull the debris back into the crusher. It can be seen from Figure 4 that the broad section of the cone pressed against the wall of the borehole will absorb the reaction force caused in crushing the debris. Since the nose is spline-mounted, no portion of the crushing force is transferred to the rest of the downhole package. However, a mechanism is needed to absorb the reaction torque produced by the crushing process. This torque is transferred to the borehole walls through the locking feet which are inflatable, elastomeric cells, and are automatically expanded whenever the debris builds up to the point that the crusher starts to rotate. In Figure 4, a rock is shown being drawn in to the crusher with residual crush debris being spread around the borehole. The size of the crusher cone is such that any debris which passes between it and the borehole wall will be sufficiently fine, and well spread around the wall of the borehole, so that the rest of the downhole package can pass through without jamming.

Figure 5 shows the penetrator at the completion of the crushing cycle. The rock shown in Figure 4 has been drawn through the crusher and the penetrator has moved forward as can be seen by the relative positions of the spline shafts in Figures 4 and 5., At this time the cycle is complete, the penetrator nose has recentered itself and, since there is no longer any force applied to it, the drive motor has turned itself off. This deactivates the locking feet, reactivates the normal forward propulsion unit of the downhole package and the unit is ready to proceed forward. Within the case of the penetrator

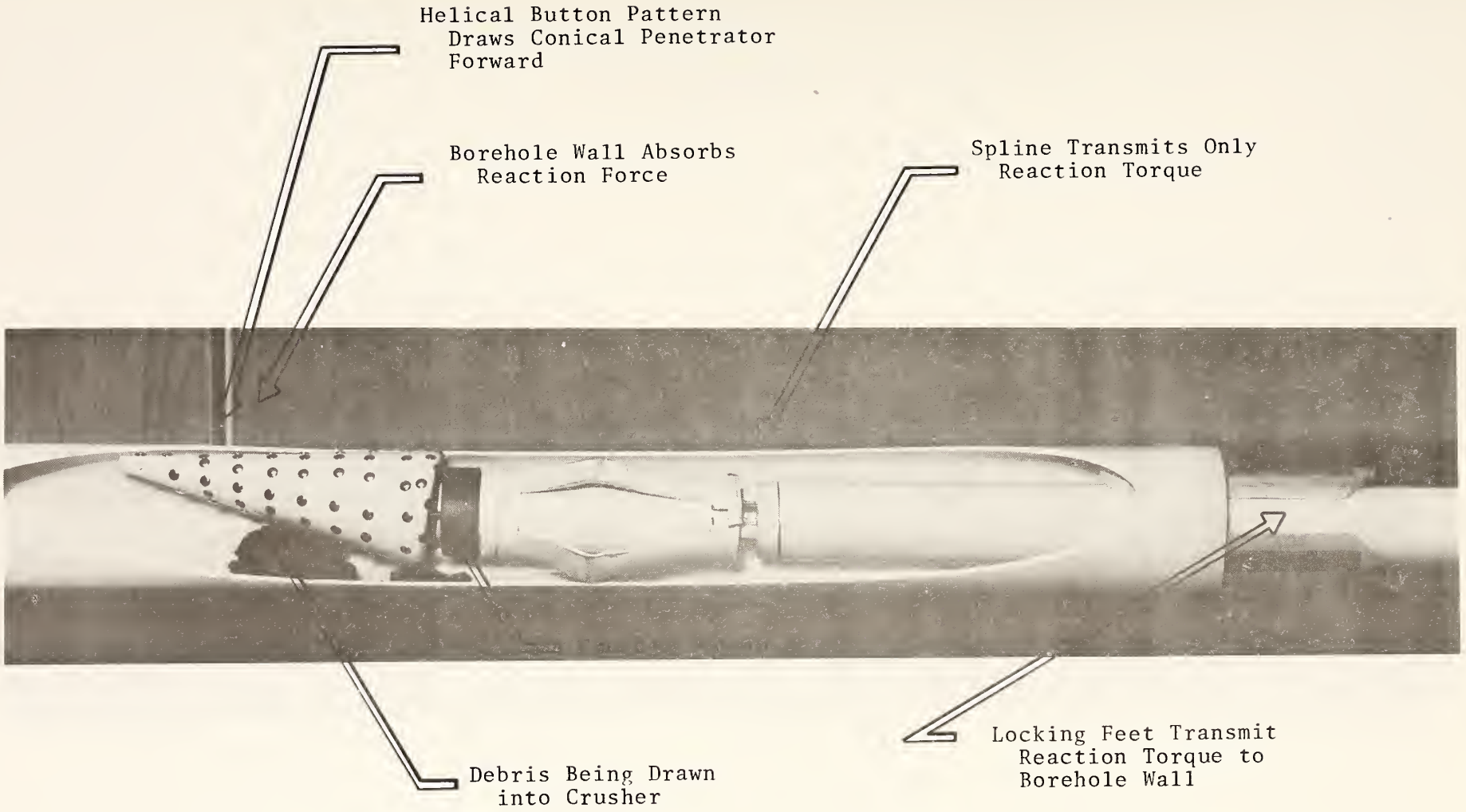

Figure 4. Penetrator crushing debris.

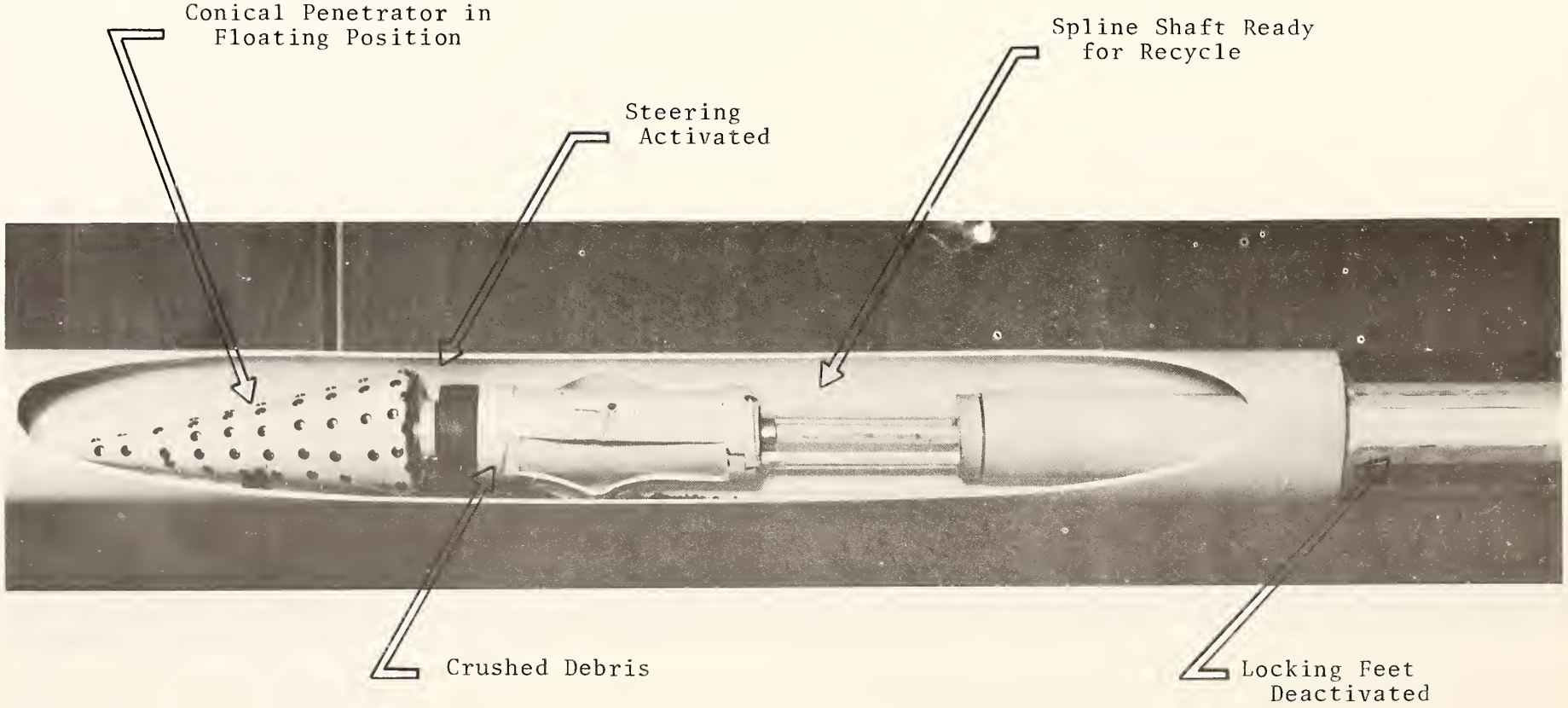

Figure 5. Penetrator at completion of crushing ready for recycling.

unit is the drive for the conical crusher. There has been considerable question as to the amount of power which would be applied to this function. Since the normal forward drive of the propulsion unit must be deactivated during the crushing cycle, the baseline system defines the amount of power used by the crusher as being the same propulsive energy normally used to traverse the package but diverted to the crushing function. The conical crusher must use its power in a low rpm, high-torque mode. However, it must be driven by hydraulic power which in turn must be transferred through the center of the downhole package. Packaging considerations and space limitations dictate that only a limited amount of continuous cross sectional area can be allocated to this energy transfer function. Thus, hydraulic fluid must be transmitted at as high a pressure, and minimum pipe diameter as feasible. This requirement indicates that the hydraulic drive motor will probably be a standard positive displacement unit operating at high rpm and low torque. Thus, the torque speed characteristics of the motor must be matched to those of the crusher through the planetary gear train shown in Figure 2.

There is a question as to whether it will be feasible to pass normal electrical wiring by the antenna of the electromagnetic radar package without destroying the radiation characteristics of this subsystem. Until this question is resolved, the baseline system will be assumed to operate in complete electrical isolation from the rest of the package. This dictates that a short telemetry control link be operated to control the penetrator package and to synchronize it with the propulsion function of the rest of the system. A generator is shown behind the motor in Figure 2 which keeps a battery on charge so that the control electronics and the telemetry system can operate without the need of carrying a completely independent battery system. Behind the generator are the solenoid-operated hydraulic valves which control the action of both the crusher motor and the azimuthal steering motors.

Since the steering action of this package requires the capability to orient the plane of the nose deflection in an azimuthal angle with reference to the vertical, a simple vertical reference package must be included.

The telemetry function is achieved by a low-power, low-frequency system which generates current in the surrounding borehole wall through contacting electrodes which are either embedded in the elastomeric cells of the torsion locking feet. Alternatively, the cells themselves may be made of an electrically conducting elastomeric material. The final unit in the penetrator is a hydraulic accumulator. The crusher will call for high surge power requirements. Thus, in order to keep the pipe size to a minimum, an accumulator is incorporated in the system to provide ample hydraulic flow to handle this transient.

3.3 SENSORS

Figure 6 is a photograph of the half-scale model of the acoustic sensor package. The acoustic sensor was selected for modeling in that it presents the most severe restraints upon the rest of the system. In order to couple acoustic energy into the rock and to receive the signal, some form of mechanical contact with the borehole walls is needed. The acoustic sensors will be encased in fluid-filled elastomeric cells. These will be expanded to make very firm contact with the borehole walls. Possibly several hundred psi of pressure will be required. In order to meet the resolution requirements of the system, these sensors will have to rotate in a scanning mode. Thus, the acoustic locking cells, unlike the locking feet of the penetrator unit, cannot have channels through which debris can pass. This will necessitate that, with each cyclic forward movement of the downhole package between acoustical measurement points, the acoustic locking cells must be deflated to such a point that any debris within the borehole can pass between them and the borehole wall. If it is desired to take acoustic

measurements at frequent intervals, then the inflation and deflation cycle times of these boots could have a significant operational impact. For example, if a 10,000 foot (3.3 kM) were to require acoustical readings every foot, and the inflation/deflation cycle takes only one second, then the survey time for the total borehole would be increased by only two and one-half hours for inflation and deflation alone. There seems to be a requirement for additional trades among acoustic survey requirements, acoustic resolution requirements, the eventual operational procedures, and economics.

The model in Figure 6 shows three sensors required as a minimum. There would be a single acoustic transmitter and two spaced receivers. Two receivers are required so that velocity information concerning the surrounding rock can be acquired without the need of calibrating the shape of the pulse of the acoustic transmitter. In order to calculate the engineering modulii of the rock, it is necessary to know both acoustic compressional and shear-wave velocities. The acoustic sensors would have this capability. The electronics equipment necessary to operate this package is well defined and within the state-of-the-art. There seems to be no engineering problems involved in packaging within the space constraints shown in this model. A possible exception to this would be if it were found that it was necessary to go to some form of very high power acoustic transmitter, such as an oil-filled spark gap. However, acoustical sparkers with peak powers in excess of 25 megawatts have been packaged and are operating in boreholes of diameters smaller than those projected for this system.

Scale models of the resistivity and the electromagnetic radar packages were not built. The resistivity package can be visualized by referring to Figure 2. It would be a package approximately the same size with the same type of locking feet shown on the shell of the penetrator. In these elastomeric cells would be implanted electrodes similar to those shown for the telemetry system. The only difference in appearance between these two packages would be that, where the casing of the

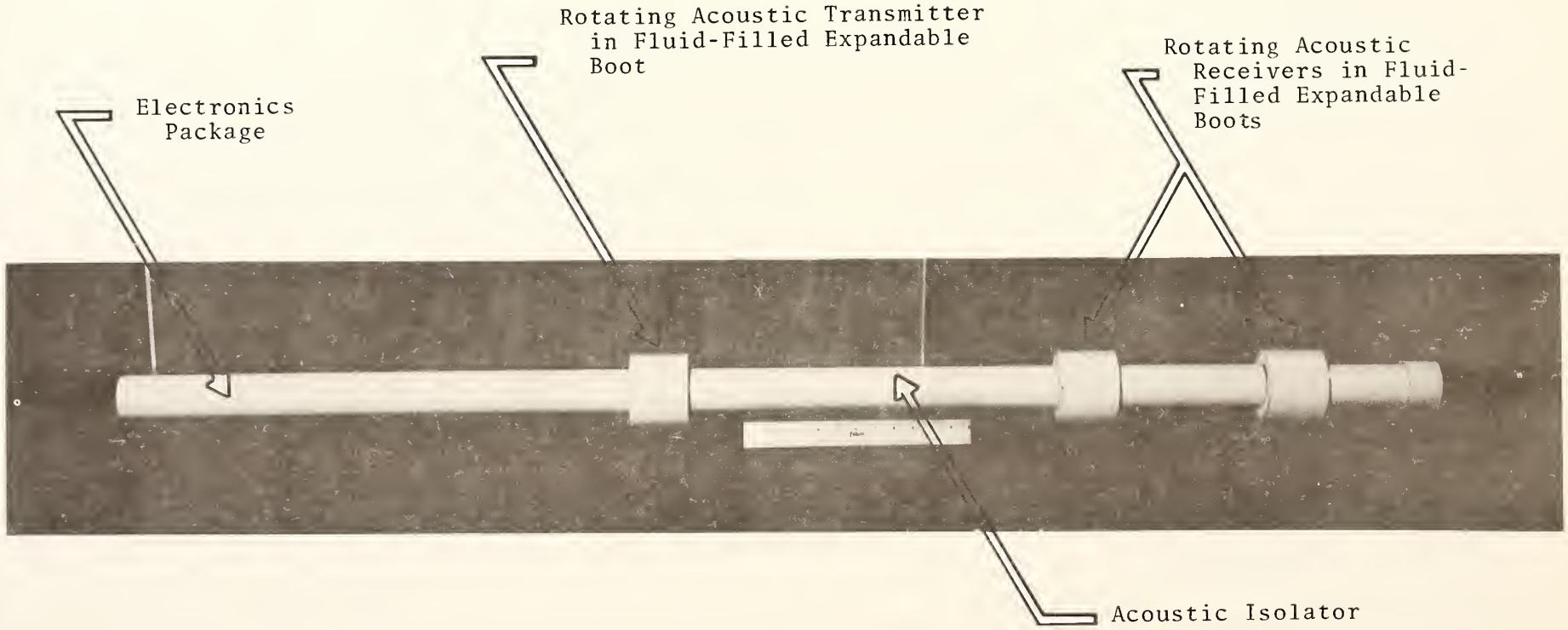

Figure 6. Acoustic sensor package.

penetrator shows only two pairs of feet, the resistivity probe would have sequential sets of feet in order to provide a number of different resistivity electrode baseline links. These locking cells, which would be expanded to make good electrical contact with the borehole walls, would be operated in synchronism with the stepping action of the propulsion unit so that the resistivity probe would provide data samples at frequent intervals, without added operating time impact as that chargeable to the acoustical system.

Although it seems highly probable that the electromagnetic radar package will become the prime sensor of the system, no model was made at this time. Such a model would simply be a straight, featureless section of tubing, as the radar system does not have any requirement to make contact with the borehole walls.

3.4 PROPULSION UNIT

Figure 7 shows a model of the propulsion unit. Actually, this is a picture of a full-scale model of a similar propulsion unit to be constructed on a different program. This particular propulsion unit is designed to go into an NX (3 in/7.6 cm) borehole. As such, it is slightly different in appearance than would be a model designed specifically for this program. However, it is reasonably close to half-scale.

The simplicity of this type of propulsion unit is obvious from Figure 7. It consists of two modular thrust units (a number of these units could vary from one to as many as required to achieve the desired thrust). Each unit consists of two locking cells interconnected and driven by a two-way hydraulic cylinder. The action of the cells is controlled by four-way solenoid operated valves. Two of these valves common to all units are

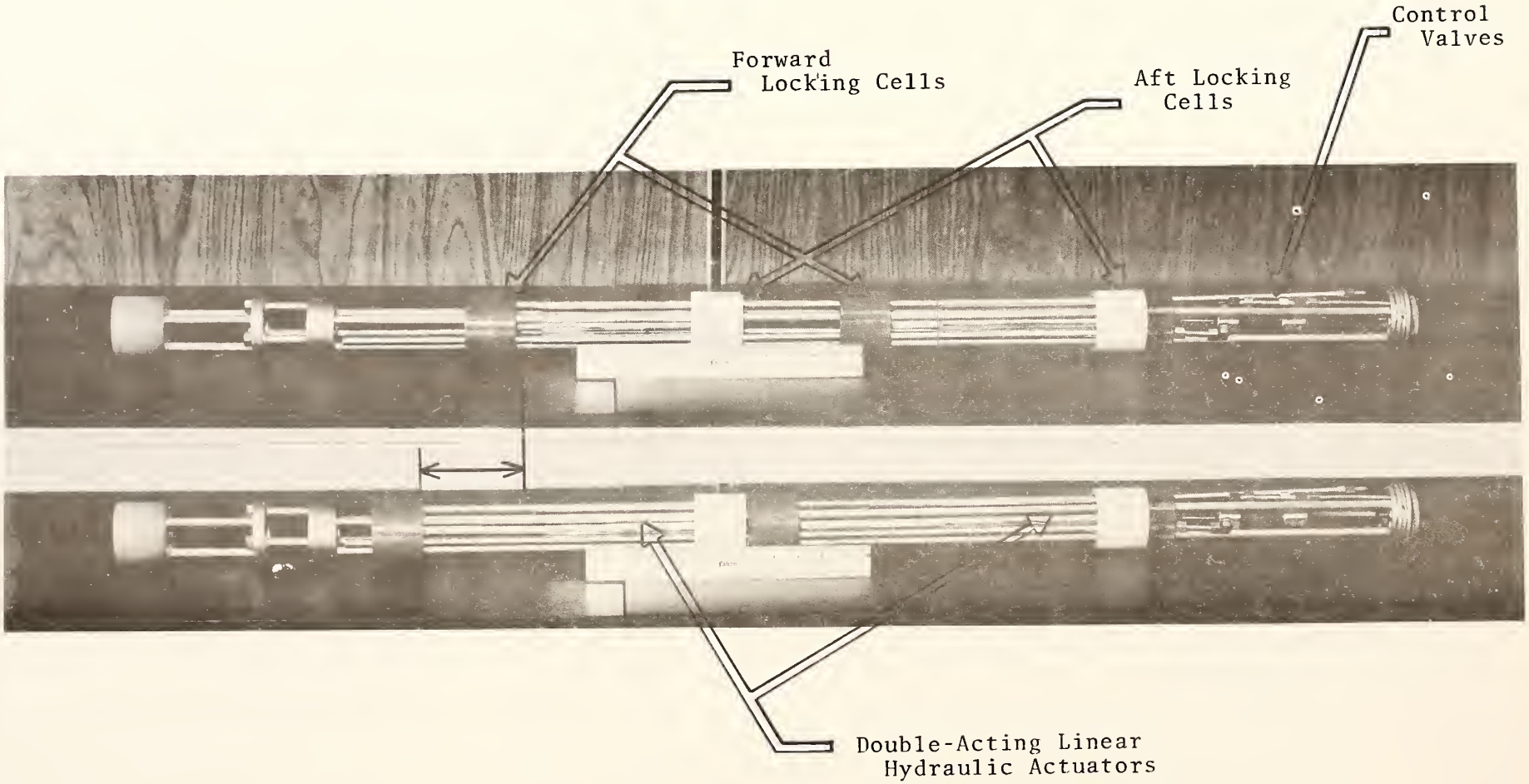

Figure 7. Propulsion unit showing linear displacement of locking cells.

all that are required. This particular unit is designed to operate from 150 psi pneumatic pressure from the surface. As such, it will provide in the order of 300 pounds of forward or reverse thrust.

The system required to drive the downhole package must be capable of operating with static water pressure surrounding as high as 500 psi. Since this pressure acts upon the elastomeric cells, it is necessary that the downhole package be driven by a closed cycle hydraulic system. This system will maintain a static pressure equal to that of the surrounding fluid. Thus, the pressures which it generates will be incremental pressures with respect to the surrounding hydraulic head.

3.5 ENERGY CONVERSION PACKAGE

The power conversion from the form of energy selected to drive the downhole package to hydraulic power takes place in the power conversion and data transmission unit shown in Figure 8. The current baseline system uses electrical power transmitted down the umbilical. This in turn is used to drive a hydraulic pump which transfers fluid from an elastomeric accumulator at the surrounding static pressure and raises it to the added incremental pressure necessary to drive not only the propulsion unit but also the various expandable cells in the acoustic package, resistivity package, and the penetrator, as well as to provide power to the crushing and steering motors of the penetrator unit. Since the elastomeric cells of the locking feet will be operated at a relatively low incremental pressure, and the crusher mechanism must use high pressures, it is highly probable that two closed hydraulic systems will be involved. In the electric-to-hydraulic energy conversion, there will be considerable energy loss due to heat. The available electrical motors for operating in boreholes have a long

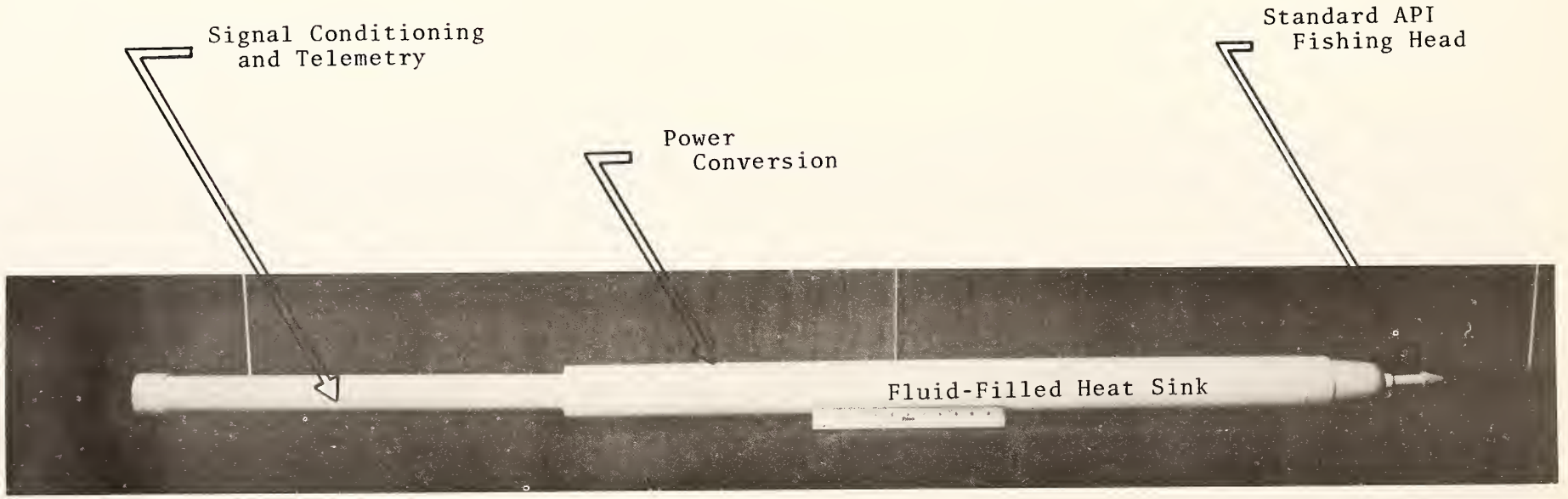

Figure 8. Power conversion and data transmission unit.

slim configuration. Their torque transfer characteristics are fairly poor and the conversion efficiency is low. Thus, it is anticipated that it will be necessary to provide cooling for these motors. This is achieved in the fluid-filled heat sink shown in Figure 8. It is anticipated that the motors and hydraulic conversion units will be immersed in a cooling fluid and that the heat which they generate will be transferred to the metallic skin of the heat sink. From thence, the heat will be dumped into the surrounding rock by normal convection and radiation means. The size of the heat sink will be balanced so that ample heat flow can occur from the energy conversion process into the rock and the components involved will be operated within their ambient operating temperatures. The final functional element in the downhole package consists of signal conditioning and telemetry. There are many techniques and modulation schemes which can be used, and their seems to be little choice of one being preferable to the other for this particular application. Their final definition will await a final design of the system, unless some peculiar characteristic of the downhole package places an unusual or a specific restraint upon this equipment.

3.6 REVIEW

A review of this model indicates that the operational unit would be in the order of 35 to 50 feet even if only one package is carried in the hole at any one time. It is recognized that the downhole package, as a system requirement, must be able to operate in various size boreholes up to and including pilot tunnels. When consideration is taken of all of the features which this downhole package must have which interact with the borehole and whose design and size are dictated by the borehole diameter, the multiple hole size requirement becomes extremely difficult to meet. Reasonable variations in borehole size can be met by changing the locking feet involved in the system.

The crusher can be adjusted to the size of the borehole by considering it as an assembly of conical frustra. It would be adapted to the size of the borehole by removing it from the penetrator and adding the particular frustrum necessary to extend the slope of the cone to meet the borehole dimensions. Thus, although difficult, and operationally cumbersome, the requirement of operating in multiple size boreholes can be met by this system. It would seem to be unreasonable to attempt to expand this philosophy for operation in a pilot tunnel. It is quite possible that the individual sensor packages may be adapted for pilot tunnel operation, however, this in itself becomes a questionable requirement in that the sensors designed for borehole operation would be far from optimum under any conditions when applied in a pilot tunnel.

APPENDIX B

ROCK CHARACTERISTICS OF SIGNIFICANCE IN TUNNELING

TABLE OF CONTENTS

BACKGROUND STATEMENT

The statement of work requires that the new sensing system under this contract deal with "rock characteristics of significance to tunnel designers and contractors."

This appendix was prepared by Dr. Ronald E. Heuer, practicing civil engineer, for ENSCO under a consulting agreement. Additional material was furnished by Mr. Edward Cunney, ENSCO staff civil engineer.

The aim of this work is to bridge the gap between rock anomalies and the physical features which make them "visible" to electrical, acoustic, and electromagnetic sensing signals. The bridge is completed by the next appendix, "Range and Resolution."

It is likely that most readers of this report will not find a need to read this appendix. For those few who are not involved directly in geology or geotechnology, it is recommended reading.

ROCK CHARACTERISTICS OF SIGNIFICANCE IN TUNNELING

ABSTRACT

The costs of tunnel construction are affected greatly by unforeseen problems encountered during rock excavation. All variations in rock characteristics that are uncovered during construction require special investigations. In many cases design changes and unusual construction methods are needed, so that the tunnel excavation can be continued safely and economically. Tunnel lining systems, rock bolt systems, grouting to reduce the inflow of water, pre-reinforcing, and even changes in the shielding at the face of the tunnel cannot be designed for maximum cost-effectiveness until full information is obtained on the rock characteristics in the problem areas.

The most frequent and costly problems in tunneling arise from rock instabilities and hydrologic conditions that are not predicted by investigations in advance of construction of a tunnel. Rock characteristics related to these two major problem areas are discussed in this appendix. These characteristics include rock materials, weathering, boundaries between rock types, discontinuities such as faults and joints, permeability and porosity, ground water, and high stress in the rock. Problems related to high temperatures and gas deposits are also mentioned briefly.

Exploratory sensing systems should provide information on significant rock characteristics that will be sufficient for the accurate prediction of the location, severity, and extent of problem conditions.

ROCK CHARACTERISTICS OF SIGNIFICANCE IN TUNNELING

1. INTRODUCTION

Tunnel construction in rock is costly. A significant portion of the costs, often involving increases far beyond initial estimates, is caused by unforeseen problems encountered during excavation [1]. The most frequent and costly problems occur because of rock instabilities and excessive inflows of water. These and other serious problems are related to the characteristics of the rock itself [2,3,4].

Rock instability generally causes the most serious and common of the unexpected problems encountered in tunneling. This is especially true where the instability is so extreme that the rock will not stand alone. In such cases pre-reinforcement, rock bolts, or costly supports are often needed to prevent the rock from falling. When zones of weak rock are encountered unexpectedly, questions immediately arise as to what degree of inherent stability exists and how long the rock will stand before falling or breaking away. Tunneling operations must be delayed while these questions are being answered; and such operations as scheduling, materials selection, and ordering must be matched to whatever stand-up time is finally determined for the weak rock.

The presence of ground water, especially large volumes of water under high pressure, generally causes the second group of major problems encountered in tunneling through rock. The volume of water may be so great that it floods the tunnel, and water in lesser amounts may wash away materials and quickly reduce the stability of the rock. Unforeseen water inflows may overload the planned pumping facilities and cause

extreme hazards and long delays in the construction of a tunnel. In such cases additional investigations must be made to collect facts, so that the water inflow can be stopped or diverted effectively. Again tunneling operations must be delayed while plans are made and equipment is assembled for such operations as grouting and freezing to reduce the inflow of water, or high-volume pumping to remove it, or the boring of interceptor drains to reduce the head of water and sometimes to let it flow by gravity to ditches and streams.

Many exploratory techniques and much equipment have been developed for investigating the conditions that will be met in tunneling as discussed elsewhere in this report and in other reports [5,6]. However, unexpected variations in conditions continue to be encountered during the excavation of tunnels. As a result, needs have been projected for a new sensing system for pre-excavation subsurface investigation for tunnels in rock, in order to obtain more complete and accurate information and to avoid delays and extra costs.

The new sensing system which is to be used in bore holes and pilot tunnels, must be able to identify and locate rock features or characteristics associated with the most frequent and serious of the unexpected problems that are encountered in tunneling. Accordingly, rock characteristics commonly indicative of unstable rock and excessive water, and other related rock characteristics, and phenomena associated with them are discussed in some detail in this appendix. The characteristics discussed include material properties of the rock itself, the effects of weathering, boundaries between rock types, discontinuities, porosity and permeability, quantity and flow of ground water, and stresses in the rock. In addition, temperature and gas deposits are discussed.

2. ROCK CHARACTERISTICS

2.1 MATERIAL PROPERTIES

Since most rocks are aggregations of several minerals, their properties vary greatly in accordance with the kinds of minerals and their proportions in the rocks, the way the different minerals present are associated, and the size of the mineral grains. The fabric of a rock is determined by the shape and arrangement of its mineral grains. The grain size and fabric of a rock reflect the conditions of heat, pressure, gas content, and rate of cooling under which the rock was formed; or in the case of a sedimentary rock, the sizes and types of materials and pressures under which it was formed. When the shape, arrangement, and size of the mineral grains are all considered together, the effect is called the texture of the rock. Rocks of distinctly different types, such as some of the granites and schists, may be similar in their chemical composition, but very different in texture which is indicative of differences in other physical properties.

The material properties of rock such as its strength and hardness must be determined, so that tunneling operations can be planned to suit exactly the type of rock that is encountered. Most rocks are brittle. Stress concentrations beyond the capacity of the rock can cause local fracturing and lead progressively to failure of an entire tunnel structure. The strength and other mechanical properties of a large mass of rock of any one type may vary greatly from place to place in the mass. The strength characteristics of a rock are difficult to measure in situ, and laboratory measurements do not give the true strength of the rock under the different conditions that exist underground along the line of a proposed tunnel.

The rock material parameters of interest to the geologist and the design engineer include the hardness of the rock, its

compressive strength, tensile strength, shear strength, impact strength, density, moisture content, grain size, fabric, abrasivity, and chemical composition. Changes in the mechanical properties of the rock may occur when a tunnel is opened and air is introduced. Accordingly, the reactions of the uncovered rock to the oxygen and carbon dioxide in the air, and the behavior of the rock when its moisture content is changed are often important. The mechanical properties of the rock not only fix the tunneling methods that should be used and the types of supports that may be needed, but they also indicate many detailed requirements for the drilling or boring equipment that must be met in order to avoid waste of time and energy.

The size and horsepower of the rock boring machines or rock cutting machines, or the specifications for the drills to be used to drill holes for blasting, should be based on detailed knowledge of the mechanical properties of the rock to be excavated from the tunnel. Hardness and abrasivity are particularly significant when considering the advantages of percussive drilling versus rotary drilling. Design, thrust, torque, and speed of rotation of boring machines; type, number, arrangement, and sharpness of cutters; the spacing of grooves to be cut into rock; the type and size of drills and the spacing of blast holes; all should be selected to best suit the mechanical properties of the rock along the line of the tunnel. Changes in any of the tunneling equipment parameters from the optimum for the particular rock that is to be excavated result in higher energy requirements, slower work, and higher costs. Accordingly, the changes in tunneling equipment, preplanned to suit the variations in the rock, should be made quickly when changes are encountered in the properties of the rock that has to be removed.

The size and arrangement of the rock structure, from the grains of its mineral components to its foliation, bedding, joints, and other anisotropies, fix the cleavage planes along which the rock can be broken out with least work in tunneling

operations. These characteristics and the strengths of the mineral components determine the size and shape of the rock fragments that result from cutting or blasting at the face. They also affect the rate of dust production from drilling and cutting and may dictate need for dust collection systems.

The sizes and quantities of rock that are removed at the face of the tunnel, must be considered carefully in planning work procedures, mucking equipment, haulage, tunnel supports, and other elements of tunneling operations. The rock structure, especially the spacing of joints and shear strength along planes of foliation and bedding, also has large effects on the stability of the exposed tunnel walls and roof and the need for rock bolts or supports.

Some rocks such as periodotite swell greatly when the minerals in them combine with water, as do shales that contain large quantities of montmorillonite or other expansive clays. Even small seams of expansive clays can cause serious problems where they prevent adhesion between protective coating and the rock, unless enough clay is removed to leave room for the renewing clay to expand without harming the coating. Some shales shrink and separate along cleavage planes parallel to the bedding when they dry upon exposure to air. Such rocks may weaken a tunnel structure and necessitate special construction items such as tunnel supports, protective coatings for the rocks, and strong seals over seams and minor gouges. In all, potential tunneling problems are so varied that detailed knowledge of the rock characteristics must be combined with knowledge of available equipment and tools well in advance of the actual work, in order to develop plans that will result in safe and economical tunnel construction.

In order to facilitate studies of the stability of the rock surrounding a tunnel opening, the rock is usually classified according to its dominant characteristics. A classification

system that is often used places the rock in classes and subclasses as follows:

1. Competent rock, rock that will sustain an opening without artificial support.

    a. Massive-elastic, homogeneous and isotropic.

    b. Bedded-elastic, homogeneous and isotropic beds with the individual bed thicknesses less than the span of the opening and having little cohesion between the beds.

    c. Massive-plastic, rock that will flow under low stresses.

2. Incompetent rock, rock which requires artificial supports in order to sustain an opening.

The quality of hard rock depends largely on the spacing of joints. If joints are spaced very closely, the rock will not sustain an opening without supports even if the major joints and slip planes are in favorable locations with respect to the line of the tunnel.

Systems for describing the quality of the rock have been developed from the examination of samples obtained by core drilling. A commonly-used system is the Rock Quality Designation (RQD) method [3,7]. In this method, sections of sound rock in the core that are longer than four inches are measured and their total length is compared to the total length of rock pieces recovered in the core. Thus, a core 60 inches long might include 50 inches of rock of which only 40 inches is in sections longer than four inches, with the remaining ten inches of the core consisting of small particles, fines, and voids. The RQD would then be 40/50 or 80% and would be called "good", while the core recovery would be 50/60 or 83%.

Rock quality is described according to its measured RQD as follows:

Rock Quality	RQD
Very Poor	0 to 25%
Poor	25 to 50%
Fair	50 to 75%
Good	75 to 90%
Excellent	90 to 100%

2.2 WEATHERING

Weathering has a great influence on types of material encountered in the tunneling operation. Weathering generally tends to degrade the rock into smaller particles and weaker chemical compounds. Where zones of weathering extend deep into the rock, the nature, intensity, and depth of the weathering determine the quality and extent of much of the inferior material along the line of the tunnel. A tunnel that is excavated mostly through competent rock may also pass through zones of weak rock and even soil [3]. Weathering alters rock materials most extensively at the surface where erosion is a major process; where oxygen, water, and organic acids are abundant; and where temperature changes are wide and rapid. However, weathering may extend to great depths in bands of rock that are fissured or porous.

Mechanical and chemical weathering usually occur simultaneously, and they are so interrelated that is is often difficult to separate the effects of one form of weathering from the other.

Mechanical weathering causes the disintegration of rock. It includes processes such as the freezing of water that wedges rocks apart, and the expansive cracking of rock that occurs when erosion removes the weight of overburden. These processes open the rock to intensified chemical weathering. While they do not occur at great depths, deep cracks and

fractures in the rock open it to chemical weathering. Some mechanical degradation of rock is caused deep underground by movements of the crust and by actions that change the stress in the rock such as the extrusion of materials from below that are forced into openings in the rock, or the removal of a heavy weight of the earth above by erosion. Movements of the crust and changes in stress are accompanied by fracturing of the rock and the grinding and crushing of the rock along faults and slip planes. New surfaces of the rock are then opened to chemical weathering, as water and air penetrate all cracks and crevices.

Chemical weathering causes the decomposition of rock. It rearranges the elements and compounds of the rock into new minerals and generally tends to degrade the rock into small particles, oxides, and clays. However, calcites are also formed that may be deposited to cement and strengthen jointed rock where the flow of water is slow and where evaporation occurs.

The main reactions involved in chemical weathering are oxidation, hydrolysis and carbonation. Organic acids from decomposing leaves and plants, and salts dissolved in water also contribute to weathering reactions. Oxidation and other reactions occur when the rock at the surface is in contact with atmospheric oxygen. However, chemical reactions between dry substances are very slow, and water plays a most important part in chemical weathering as a medium in which other reagents can work. Thus the chemical attack on the rock minerals is often more intense in the moist cracks and crevices than it is on the surfaces of the rock which may be dry much of the time.

Air flows through crevices in rock that are not full of water bringing with it carbon dioxide as well as oxygen. The water itself that percolates into the rock fissures brings some

dissolved oxygen with it to react with the rock. More important, the water contains carbon dioxide absorbed from air and carbon dioxide from decaying vegetation that reacts with the water to form carbonic acid. The carbonic acid in turn reacts with many of the minerals in rocks.

While only a few minerals are soluable in pure water, many others are dissolved by the carbonic acid that is formed when carbon dioxide from the air or from decaying vegetation unites with water. Over long periods of time and at slow rates, water and the chemical compounds it carries make a very effective solvent. Even gold can be found dissolved in sea water. Limestone is particularly susceptible to leaching, since it is easily dissolved by the carbonic acid carried by water. This process leads to the formation of the large cavities and caves found in limestone formations.

Many of the mineral grains scattered through granite and other rock dissolve very slowly, but this action slowly weakens the rock and opens large new surface to chemical weathering. In addition to acting as a medium for other reagents and dissolving some rock minerals, the water itself reacts with some rock minerals to form decomposition products.

Chemical weathering is very intense on grain surfaces, and since most of the reactions involve an increase in volume, the overall swelling of the rock mass that results from chemical weathering causes disintegration of the outer layers of rock; this in turn opens the rock to more intense chemical weathering. In hydration, which occurs when water is placed in intimate contact with lime and some other minerals, molecular water is incorporated into large, complex molecules along with molecules of the lime and other substances, thus rapidly increasing the volume of solid material. In hydrolysis, new chemical compounds are formed when the water molecules react with the mineral molecules. Hydrogen and oxygen atoms of the

water are then locked into new molecules of clay and other solids to increase the total volume of solid material. Since aluminum and other elements that react with water and carbonic acid to form clays are abundant in the rock minerals, clay is generally the most evident product of chemical weathering.

Some common rock minerals that are attacked by chemical weathering and their products are listed as follows:

- Potassium Feldspars: clay, potassium carbonate, colloidal silica, and soluable silica.
- Plagioclase Feldspars: clay, potassium carbonate, sodium carbonate, colloidal silica, and soluable silica.
- Amphibole and Pyroxene: clays usually containing red or yellow iron oxides.
- Muscovite: same compounds as potassium feldspars.
- Quartz: resists weathering; grains of quartz in granites and other rocks that decompose are released as sand.

2.3 BOUNDARIES BETWEEN ROCK TYPES

Rock boundaries indicate the presence of different types of rock for which different tunneling operations and procedures may be needed, and thus are very important in the design and construction of tunnels. It is very advantageous to determine the exact locations of these boundaries where rock conditions change, before they are uncovered by the work at the advancing face of the tunnel. Knowledge of their exact locations permits orderly and effective planning and scheduling of the tunnel excavation. The tools, equipment, and procedures to fit the changed conditions can then be provided at the correct locations and times during the advance of the tunnel, so that costly delays and hazards can be avoided. Rock boundaries often indicate severe changes in the quality of the rock such as zones of gouge or intrusive clay where special construction techniques and extra safety precautions will be needed.

The location and orientation of rock boundaries may be very significant in relation to the centerline and the boundaries of a tunnel. Thus, a gouge zone or a zone of fractured rock lying below the floor of a tunnel would have little importance unless it contained expansive materials or materials that could be squeezed in by pressure, and were thick enough for swelling or heaving to cause problems. On the other hand, a gouge zone intersecting a tunnel high on the wall or in the roof, along a line near parallel to the axis of the tunnel, could have disastrous effects upon the work. The strike and dip of rock layers, joints, and faults, and the locations of anticlines and synclines in the rock formations are important indicators of conditions that must be allowed for in planning and construction.

2.4 DISCONTINUITIES

Discontinuities in rock, especially those at joints and fractures, cause very serious problems in tunneling [2]. All rock masses are jointed or fractured. Joints or cracks develop during the geologic history of rock masses because of high stresses in the heavily-loaded rock and geological actions that change the stresses. In the movements and stress releases that occur, individual joint blocks are formed in arrangements and sizes that are indicative of the type of rock and the pressures under which jointing occurred.

Because of the importance of joints, some of their characteristics and problems associated with them are highlighted below:

- Joints generally occur in sets. There are usually at least three intersecting joints (planes) in a set. The interior of a set is thus a block of rock that is free to break away from the general rock mass. The joint block may have dimensions of tens of feet or an inch. There are usually several joint sets per rock mass.

- Orientation of the joints is an important factor in tunneling [3]. Joints that are parallel, or subparallel, to the tunnel axis are the more critical as the blocks are then more likely to break away or fall into the tunnel. The problem is obviously more serious when the joints are above or along side the tunnel than if below.

- The nature of joint (crack) surfaces and the materials in the joint are important and can vary considerably. For example, joints can be totally tight and clear with smooth plane surfaces; or they may have clay in them; or their surfaces may be irregular and open with water moving through them. Some clay is found in most joints but may be as thin as 0.01" (0.025 cm) or so. Joints with smooth plane surfaces with clay in them are the most critical, as the clay acts as a lubricant which allows the smooth rock to slip relatively easily. The amount, or thickness, of clay in the joints depends on the rock type. Clay is very common in igneous rock masses, such as granite or any type containing feldspars or mica, because the decomposition of such rock results in clay. On the other hand, sandstone, which is fundamentally quartz to start with, does not decompose into clay; so faults in sandstone generally contain little clay. Calcite deposits are common at joints and can seal or strengthen them, possibly to the strength of the original rock.

- The spacing of the joints (referring to the distance between joints in a set as opposed to the width of the crack, or joint) effect the tendency of the joint block to fall, or their stand-up time [2]. The wider the joint spacing the less likely they are to slip. Rock with joint spacings of 2 to 3 feet (0.6 to 0.9 m) or more will usually stand long enough to allow supports to be emplaced. In rock with joint spacings less than about one foot, rock-fall problems are generally encountered. However, problems associated with joint spacings are also a function of the tunnel size. In general, the smaller the tunnel cross section the smaller the critical spacing.

- The general rock quality is an important indicator of problems to be encountered in tunneling, as discussed previously under Material Properties.

- The characteristics of joints, faults, and discontinuities in general can change along the line of discontinuity and a local core sample alone is not necessarily indicative of the surrounding medium [4].

2.5 POROSITY AND PERMEABILITY

The porosity of a subsurface rock mass plus fissures and other voids determine the amount of gas or water that the mass can hold. All rocks have some porosity, but porosity is very low in igneous rocks; and in some igneous rocks, it is less than one percent of the total volume of the rock. Porosity is higher in metamorphic rock, and it is as high as twenty percent in some sedimentary rocks such as open sandstones and conglomerates.

The porosity of the crystalline rocks results mainly from microfractures, although some may be caused by small voids that exist among mineral grains. Even some mineral grains have microcracks that permit the entrance of some moisture. Such cracks are widened by weathering, and additional openings are also formed. The porosity of clastic rocks, formed from weathered materials, depends on the open, intergranular spaces. Generally, the porosity is higher where the grain or particle size is quite uniform, and porosity is low where there is a good gradation of grains and particle sizes. Measurements of porosity can be misleading in the case of some clastic rocks that contain large amounts of expansive clays as water molecules are bonded tightly to the clay particles. Although the porosites may be high, water will not flow through the pores of such rocks even when they are saturated and under differential pressure.

Porosity is affected by the depth of cover over the rock that is being examined. A great weight of overburden compresses the rock and squeezes the pores down to smaller dimensions, so that the voids can hold less water and less water can flow through them. This phenomenon accounts in part for large changes in the rate of inflow of water that may occur during tunnel excavation. A sudden rush of water may develop during the excavation of rock from a tunnel, when cracks are opened, and the rock is suddenly freed to expand towards the center-line of the tunnel. The water compressed within the rock is free to expand also and to move quickly through the enlarged voids in the disturbed layer of rock. Later when drainage and pumping have been removing the inflow of water for some time, the rate of inflow will be determined by the movement of water through rock beyond the disturbed layer, where high pressures continue to affect the porosity of the rock.

The permeability of a subsurface rock mass determines the rate of flow of gas or water through it. Permeability depends mainly on the interconnections of pore space and other voids rather than their volume. Thus, the permeability of the subsurface mass involves not only the porosity of the rocks within it, but also the fissures in the rocks, open joints, the porosity of the gouge materials and other materials that fill zones along faults and major slip planes, and any channels or cavities where soluable materials have been leached out of the rocks.

Coefficients of permeability to water are often estimated from measurements of the flow of ground water from sections of boreholes or pilot tunnels, and the hydraulic gradient is measured directly or calculated from measurements of draw down when the water is pumped from the hole. The values obtained are then used to estimate the inflow of water that can be expected in a tunnel. The simplest and probably most commonly used expression for estimating water inflow is Darcy's equation [5]

$$Q = kAi$$

where Q is the quantity of water flowing

A is the cross sectional area through which the water flows

k is the coefficient of permeability of the material

i is the hydraulic gradient.

2.6 STRESSES

High initial stresses in the rock through which a tunnel is excavated can result in the fracturing of the rock around the tunnel boundaries. The fracturing occurs when the pressures are relieved by the removal of the tunnel rock, and the rock on the boundaries of the tunnel is then free to expand towards the centerline of the tunnel. The fracturing from stress release is increased greatly by the shock waves that accompany blasting during the excavation of tunnels. The fracture zone that develops during the excavation of a tunnel by blasting and machining may extend as far as 10 feet (3.0 m) from the tunnel wall into competent rock [6]. Excavation by boring machines reduces the shock and the resulting fracturing to a minimum.

The large stresses that may lead to fracturing of the rock at tunnel boundaries can be predicted fairly well from laboratory measurements of the rock strength and knowledge of the pressure at tunnel depth. Fortunately serious problems associated with the relief of large stresses in rocks at tunnel boundaries are not common. They occur most often in weak rock at depths of several hundred feet or more, where pressures are very high.

In the course of investigation of geophysical measurements by the U.S. Geological Survey, studies were made of the rock at the boundaries of a pilot tunnel that had been disturbed by cutting and blasting and the removal of material [6]. It was found that the disturbed rock consisted of a layer of fractured rock with two distinct characteristics. The fractured layer varied in thickness from less than 1 to 17 feet (0.3 to 5.2 m),

and it was attributed to blast damage and the inward movement of rock towards the centerline of the tunnel along fracture and fault surfaces in response to changes in stress caused by removal of material from the tunnel. It was characterized by low seismic velocity. In addition, part of this layer of fractured rock varying from less than 1 foot to 10 feet (0.3 to 3.0 m) was found to have relatively low electrical resistivity. This was attributed to the evaporation of moisture from the rock that occurred when it was exposed to air.

The seismic and electrical resistivity measurements that were made were used to obtain the seismic velocity and electrical resistivity of rock behind the disturbed layer at the boundary of the tunnel. The velocity and resistivity were then correlated with construction parameters such as time rate of construction, cost per lineal foot, rock quality, and tunnel support required. The quality of the correlations was very good, and it was found that good predictions could be made of the engineering and economic parameters that must be estimated accurately for cost-effective planning and construction of tunnels.

Surface geophysical measurements were also made, consisting of seismic velocity and electrical resistivity on the surface and in holes drilled along the line of the pilot tunnel. The results indicated that reasonably good predictions of engineering parameters could be made from the data obtained. It became apparent that detailed information and very accurate predictions could be obtained from geophysical logging measurements made in small holes drilled ahead of the working face as tunnel construction progressed. The cost of such work should be small compared to the savings that would be possible in tunnel construction as a result of improvements in the predictions of rock characteristics along the line of the tunnel.

A technique has been developed to reduce the cost of lining tunnels that are built in fairly-competent rock that is under high stress. This technique involves close measurement of rock strength and stresses and careful prediction of how much the rock will move in towards the centerline of the tunnel after material has been excavated. A limited amount of this movement is then permitted to occur before a lining is installed, or a void space is left behind the lining and some movement of the rock into the void space is permitted before the space is grouted. Permitting some inward movement of the rock while a redistribution of loads around the tunnel is occurring, reduces the loads that would otherwise be imposed on the lining and allows the construction of a lighter and less costly lining system.

3. GROUND WATER

Large deposits of water are more likely to occur in limestone and basalt-type rock, as these rocks often have large cavities formed in them and usually water is present in large cavities in rock. When large, water-filled cavities are encountered during tunneling, or when closely-jointed or porous zones connecting water-filled cavities are encountered, flooding may occur at high rates. Flooding at very high rates, such as 10,000 gallons (37.85 kl) per minute, will typically occur only in limestones. The flow of water along joints, fracture zones and other openings in the rock tends to erode such spaces and reduce rock stability. The common occurrence of fracture zones in clusters enlarges the problems associated with flooding and rock instability.

A serious flooding problem occurs when a tunnel penetrates an acquifer where artesian water is trapped between two impervious layers under a high hydrostatic head. However, this condition is easily predicted from normal exploratory investigations, and plans can be developed to intercept the water or to seal off the acquifer before tunneling.

Joints permit the flow of ground water when a tunnel excavation opens a passageway for water that is under pressure. Wide joints and closely spaced joints greatly increase the permeability of the rock mass adjacent to the tunnel and permit a rapid inflow of water. The permeability of the rock and problems caused by water are closely associated. While the initial pressure at which ground water is encountered during a tunneling operation may not be affected greatly by the permeability of the rock mass, the flow rate and the quantity of water that must be drained or pumped related directly to permeability as well as pressure.

4. GAS DEPOSITS AND HIGH TEMPERATURES

4.1 GAS DEPOSITS

Gases are most common in shales and sedimentary rocks, and about 95% of the gases found are methane. Methane gas is very dangerous. Gas explosions continue to cause many deaths in tunnels as well as in coal mines, in spite of good equipment for measuring gas concentrations, good ventilating equipment, and strict enforcement of safety rules. The latest accident reported that involved methane gas was an explosion in a 10-foot-diameter (3.0 m) irrigation tunnel in Yamagata, Japan, that took four lives.

Methane gas is produced by decaying or decayed organic maetriais trapped in the rock during formation. Ventilation is normally used to dilute the gas in mining operations and other tunneling, but gases can pose serious problems. At fast drill rates [100 to 150 ft/day (30.5 to 45.7 m/day)], the gas does not bleed off fast enough to dilute it to a safe level [5]. Gas sensors are being placed on some "moles" that have fast drill rates and improvements in ventilation are being pursued.

4.2 HIGH TEMPERATURES

Temperatures may approach 100°F (37.8°C) or more in rock a few hundred feet below the surface. High temperatures are common in young materials that are still "working". Lava flows and active fault zones in the vicinity are indicative of young materials where high temperatures may be expected. Hot water may be encountered in such formations and can be very troublesome when it flows into a tunnel a high rates and high temperature.

The most dangerous situation exists when high pressures prevent superheated water from turning to steam. Tunneling and other work that opens rocks reduces the large pressures and permits the superheated water to flash and release enormous quantities of steam at high temperatures and high velocities.

5. CONCLUSIONS

The usefulness of information for tunnel planners that may be obtained by remote sensors operated in a horizontal borehole should be related to the relative seriousness and frequency of the problems that otherwise may not be foreseen. Since joint patterns and discontinuities in the rock relate very closely to the two most costly and frequent problems of instability and bad hydrologic conditions, the collection of information on these rock characteristics should be top priority. Accordingly, the priorities for a subsurface sensing system should include:

- The definition of joint patterns to distances of at least 20 feet (6 m) from which the geophysicist can reasonably extrapolate to further distances, and
- The location and identification of major discontinuities such as big fault zones, cavities, and changes in the type of rock mass, to distances as far as they can be identified [5].

The information obtained from remote sensors would be used in conjunction with other data for tunnel planning and construction and should be processed so that it will fit in with the other geophysical data used by the designers.

6. REFERENCES

1. Money, Lloyd J., "Our Last Unexplored Frontier - The Space Beneath Our Feet," Proc. of Conference on Subsurface Exploration for Underground Excavation and Heavy Construction, ASCE, August 1974.

2. Underwood, Lloyd B., "Exploration and Geologic Prediction for Underground Works," Proc. of Conference on Subsurface Exploration for Underground Excavation and Heavy Construction, ASCE, August 1974.

3. Merritt, Andrew H., "Underground Excavation: Geologic Problems and Exploration Methods," Proc. of Conference on Subsurface Exploration for Underground Excavation and Heavy Construction, ASCE, August 1974.

4. Heuer, Ronald E., "Important Ground Parameters in Soft Ground Tunneling," Proc. of Conference on Subsurface Exploration for Underground Excavation and Heavy Construction, ASCE, August, 1974.

5. Ash, J. L., Russell, G. E., and Rommel, R. R., "Improved Subsurface Investigation for Highway Tunnel Design and Construction, Vol. 1, Subsurface System Investigation Planning," Report to the Federal Highway Administration by Fenix and Susson, Inc., Report No. FHWA-RD-74-29, May 1974.

6. Scott, J. H., and Carroll, R.D., "Surface and Underground Geophysical Studies at Straight Creek Tunnel Site, Colorado," Highway Research Record, Number 185.

7. Deere, D. U., A. J. Hendron, Jr., F. D. Patton, and E. J. Cording. "Design of Surface and Near-Surface Construction in Rock." Proceedings of 8th Symposium on Rock Mechanics (1966). AIME, New York. 1967. pp. 237-302.

8. Heuer, Ronald E., (Personal Communications)

APPENDIX C

RANGE AND RESOLUTION

TABLE OF CONTENTS

BACKGROUND STATEMENT

This appendix continues and completes the overall basis for sensing in hard rock, by relating the characteristic of sensor signals to rock and rock anomalies. It is essential to understanding the technique of sensing from boreholes.

PREFACE

This appendix discusses the relations and trade-offs among detection range, resolution, and wavelength that must be considered in designing acoustic and EM probes. Propagation loss for a variety of rock types is considered. Detection of three configurations of a geologic target is considered: (a) an extensive boundary across which the rock changes character, such as a fault (this is referred to as a "first Fresnel Zone" boundary herein); (b) a localized target within a larger body of rock, such as a small cavity; and (c) a thin but extensive layer within a rock body, such as a clay-filled joint.

RANGE AND RESOLUTION ATTAINABLE IN SENSING HARDROCK BY ACOUSTIC AND ELECTROMAGNETIC SIGNALLING FROM BOREHOLES

ABSTRACT

The reliability with which geologic structures can be detected and mapped from a borehole by means of radar-like acoustic and electromagnetic signals depends strongly on the propagation conditions, the size and contrast of the target structures, and the nature of the signals and of the radar system. The range at which targets can be detected can be increased by increasing the signal wavelength, but at the cost of a reduction in resolution. Available data shows that large high-contrast targets in competent rock such as granite can be detected at about 50 meters range, with about .1 meter resolution, by acoustic signals in the 10 KHz band and by EM signals in the 100 MHz band. In incompetent rock such as shale, detection in the same bands is limited to a few meters. Thin targets such as clay-filled joints that are at least 5 mm thick should also be detectable in these frequency bands.

RANGE AND RESOLUTION

1. INTRODUCTION: GENERAL CONSIDERATIONS

In addressing the problem of describing the physical properties of rock surrounding a borehole by means of sonic or electromagnetic probes, consideration must be given to the relationships that exist between the ranges and the resolutions that will be attainable in that environment. Some of the more important relationships are described below, together with guidelines for establishing the necessary trade-offs.

1.1 DETECTION RANGE

Of fundamental importance to the success of the signal probe is its ability to sense signal returns from discontinuities in and host rocks at distances of at least several meters. The distance at which discontinuities can be detected depends on three factors: the strength of the return, the strength and nature of the background noise, and the coherence of the returns as well as the noise over repeated sensings. The signal strengths and background noise determine the signal-to-noise ratio of the returns, which is closely related to the range at which the returns can be detected. The coherence determines the limit to which the range and resolution can be increased by means of array processing techniques.

The return signal-to-noise ratio can be described as the fraction of the radiated signal energy that returns to the receiver from a high-interest "target" scatterer (after undergoing losses due to geometrical spreading and absorption), divided by the noise energy due to reverberation from low interest scatters and due to ambient background noise, all in a specific signal frequency band.

1.2 RANGE RESOLUTION

The limiting accuracy with which the range can be measures will be determined by the effective wavelength of the return signal, whether the range to a scatterer is measured from the transit time of a pulse (as in sounding by impulsive or swept-frequency signals) or from the phase characteristics of an interference pattern (as in holographic methods).

Given good signal coherence and knowledge of the propagation speed, the best range measurement accuracy that is attainable is on the order of a quarter wavelength. To illustrate, assume that the attainment of 50 feet (15 m) penetration requires that the signal's wavelength not be less than 3.28 feet (1 m). Then targets closer together than about .82 feet (.25 m) could not be resolved.

The limit to range resolution imposed by the signal frequency spectrum is an example of the uncertainty principle that governs the precision with which joint measurement of time and frequecy can be made. The principle states that if one wishes to generate a pulse that occupies a small interval at time Δt, one cannot confine it to an interval in frequency narrower than Δf, where $\Delta f \cdot \Delta t \simeq 1$. This applies whether the pulse is generated as a short trainsient or as a correlogram peak resulting from the cross-correlation of two signals longer than Δt.

The accuracy with which the arrival time differences can be measured between returns from closely spaced scatters can be described in terms of one's ability to measure the interference patterns in the composite signal spectrum.

1.3 DIRECTIONAL SENSITIVITY VERSUS ARRAY SIZE AND SIGNAL FREQUENCY

The above considerations also control the directional sensitivity that can be attained by an array of given size. Translated into terms of directional sensitivity, this means that for the array to resolve an angular difference as small as $\Delta\theta$, the signal must contain wavelengths at least as short as

$$\lambda \leq \frac{L\Delta\theta}{\pi}$$

L = array spacing

Thus, to achieve 6° resolution from two sensors 1 foot (0.3 m) apart would require signal frequencies whose wavelengths are of the order of .06M. Considering typical attenuation rates of subsurface material, the prognosis of obtaining substantial angular resolution when operating from a single small borehole is not very good, unless one is willing to use specially designed and costly procedures.

2. PROPAGATION EFFECTS

Here are summarized the effects on propagation loss in various kinds of rock on the effective range and resolution attainable for EM and acoustic signals. The data shown here are abstracted from Appendices D and F of this report.

2.1 DETECTION RANGES FOR EM SIGNALS

Appendix F of this report includes theoretical and empirical data on propagation of EM signals in various kinds of rock. Figure 1 summarizes this data in the form of graphs of the maximum range at which a good reflection could be detected in each of several types of rock. It shows that an EM system with 120 db dynamic range and 100 MHz signals could detect reflections at ranges up to about 328 feet (100 m) in granite, and perhaps 66 feet (20 m) in schist, but only a couple of meters in shale. Resolution attainable should be about one wavelength, which is about a meter at 100 MHz.

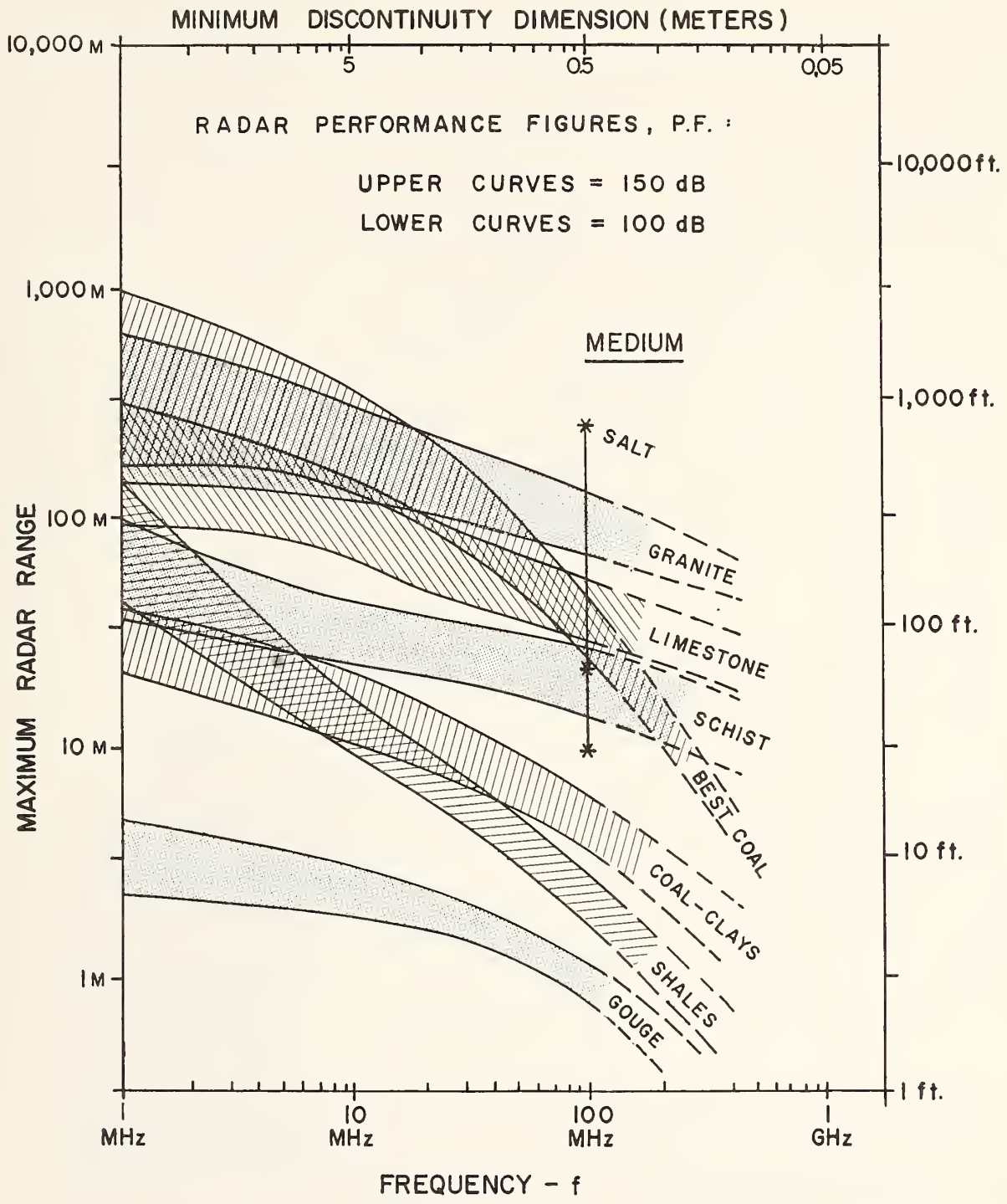

Figure 1. Maximum radar range in typical rock as a function of frequency and radar performance figure.

Figure 1 shows that the maximum range achievable depends strongly on the rock type and the frequency. In all cases, the maximum range decreases with increasing frequency. Greater ranges can be achieved in the harder rock, such as granite and limestone. Shale and gouge, however, because of high moisture content, hence their greater attenuation rate, severely limit the maximum range. Figure 1 shows that maximum ranges of 100 feet (30.5 m) or more are achievable in limestone, granite and some coals at frequencies as high as 100 mHz. For the other coals, schist, shales and gouge materials examined, ranges of 100 feet (30.5 m) do not appear to be achievable even at frequencies as low as 10 mHz. In particular, gouge materials are strongly attenuating and limit the maximum range to a few feet even at frequencies as low as 1 to 10 mHz.

The theoretical performance estimates depicted in Figure 1 provide valuable guidelines in the design of a monocyclic pulse radar for borehole application. The close agreement between the predicted range and measured ranges at 100 mHz tends to confirm the validity, at least qualitatively, of the system parameters and target characteristics employed. Note also that the P.F. of 100 db is achieved with present monocyclic pulse radar systems and, with system improvements the signal integration techniques presently within the state-of-the-art, the P.F. of 150 db is a realistic estimate. (See Appendix F.)

2.2 DETECTION RANGES FOR ACOUSTIC SIGNALS

Appendix D of this report provides theoretical and empirical data on the propagation of acoustic signals in various kinds of rock. Figure 2 summarizes this data in the form of graphs of the maximum range at which a good reflection could be detected in different types of rock.

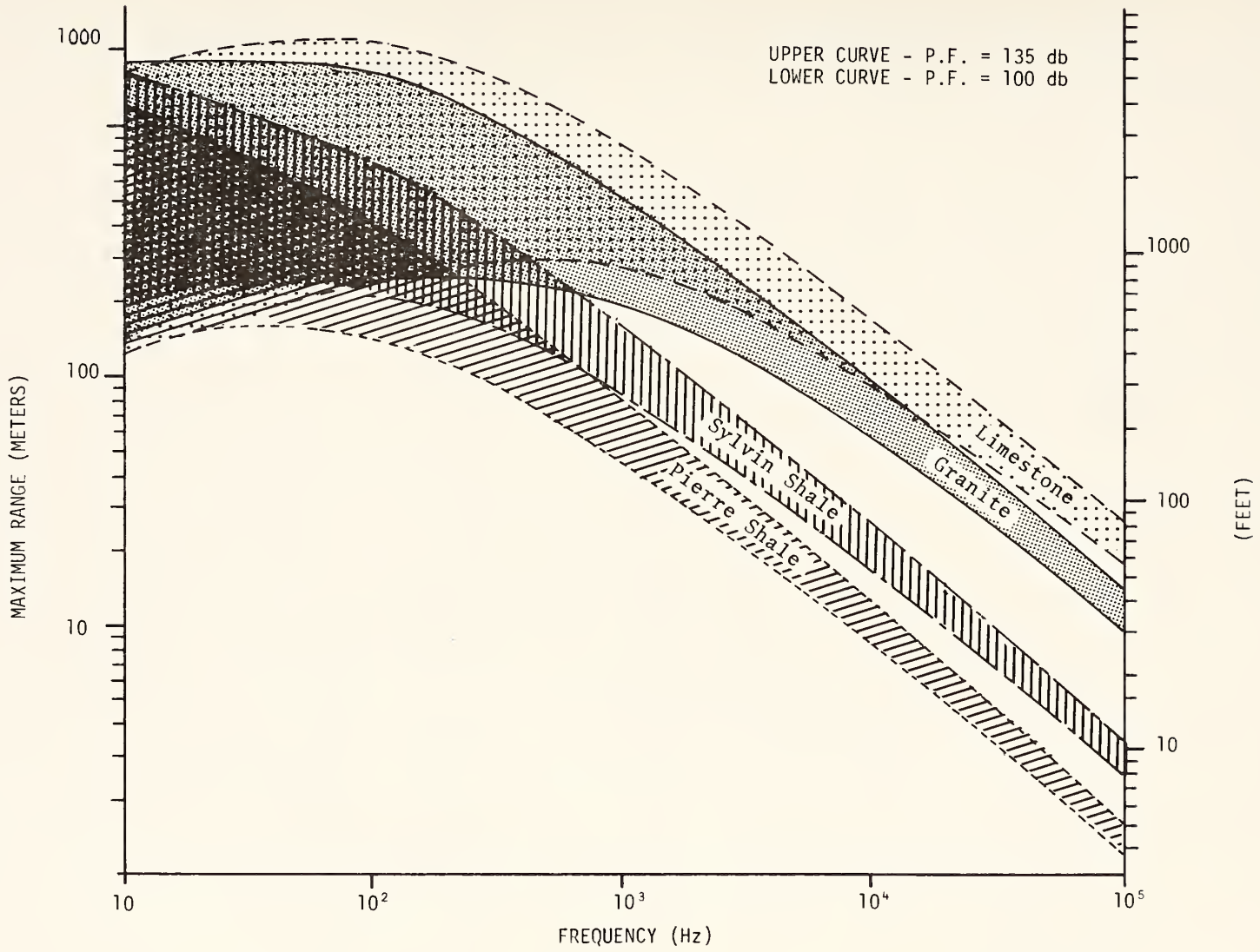

Figure 2. Maximum range for an acoustic radar in typical rock as a function of frequency and radar performance figure.

It can be seen in Figure 2 that with limestone, which has good propagational characteristics for acoustic waves, a range of 100 feet (30.5 m) can be attained at frequencies well above ten kilohertz. This means that in a purely limestone environment the system could achieve fairly high resolutions at the maximum ranges of interest. Thus, small targets could be detected at these ranges. At the other end of the rock spectrum in a lossy medium like shale, the system will be severely limited to frequencies on the order of a kilohertz in order to get a 100-foot (30.5-m) penetration. This would imply that only gross features could be resolved at these distances. The term "hard rock" as used in this procurement to define the medium in which the system must operate must be considered to include this complete spectrum. The medium rock, in general, would not be anticipated to be as bad as shale as far as attenuation characteristics are concerned. However, there will be certain types of decomposed crystalline rock which might easily approximate shale and its properties. Thus, over the range of properties included under the broad generic term of hard rock, a range of 100 feet (30.5 m) can be expected to be attainable. However, resolution can be expected to vary from a few inches to the order of tens of feet, depending upon the material in which the measurements are being made.

3. TARGET SHAPE EFFECTS

The effect of the shape and orientation of geologically interesting targets on their detectability must be considered. These effects are included in portions of Appendices E and F and are summarized below. Three types of target configuration are considered: (a) an extensive interface across which there is a change in rock type, such as a fault, or the boundary of an intrusive body (these are referred to here as a "first Fresnel Zone" boundary; (b) a localized object within a larger body of

rock, such as a cavity or a localized zone weathering; and (c) a thin but extensive layer within a rock body, such as a clay-filled joint.

3.1 FIRST FRESNEL ZONE SCATTERER

The range versus resolution characteristic of a first Fresnel Zone Scatterer is shown in Figure 3. Radars having a dynamic range of 100 dB and 200 dB are considered. Assuming a radar having a 3-foot (1-m) aperture, it shows that:

- There is an optimum range of wavelengths that is dependent on the attenuation characteristics of the medium.
- There is no difficulty in obtaining a 50-foot (15 m) range in all but the most attenuating subsurface media using 100 dB radar.
- For wavelengths shorter than optimum, no great improvement results from increasing the dynamic range of the radar.

3.2 LOCALIZED SCATTERER

Obviously an interface that covers only a small area is more difficult to detect than one that covers a large area. As an example, we take a radar having a 3-foot (1-m) aperture and a scatterer having a cross-section of 10.8 square feet (1.00 sq. m). Again, radar dynamic ranges of 100 dB and 200 dB are chosen. A graphic presentation of the analysis of these conditions is given in Figure 4.

The results demonstrate clearly the optimistic nature of the first Fresnel Zone predictions. As might be expected for the aperture and cross-section chosen, optimal performance, even when attenuation is slight, occurs for a wavelength of 3 feet (1 m). Unlike the first Fresnel Zone case, improvement in radar performance figure is accompanied by substantial improvements in range.

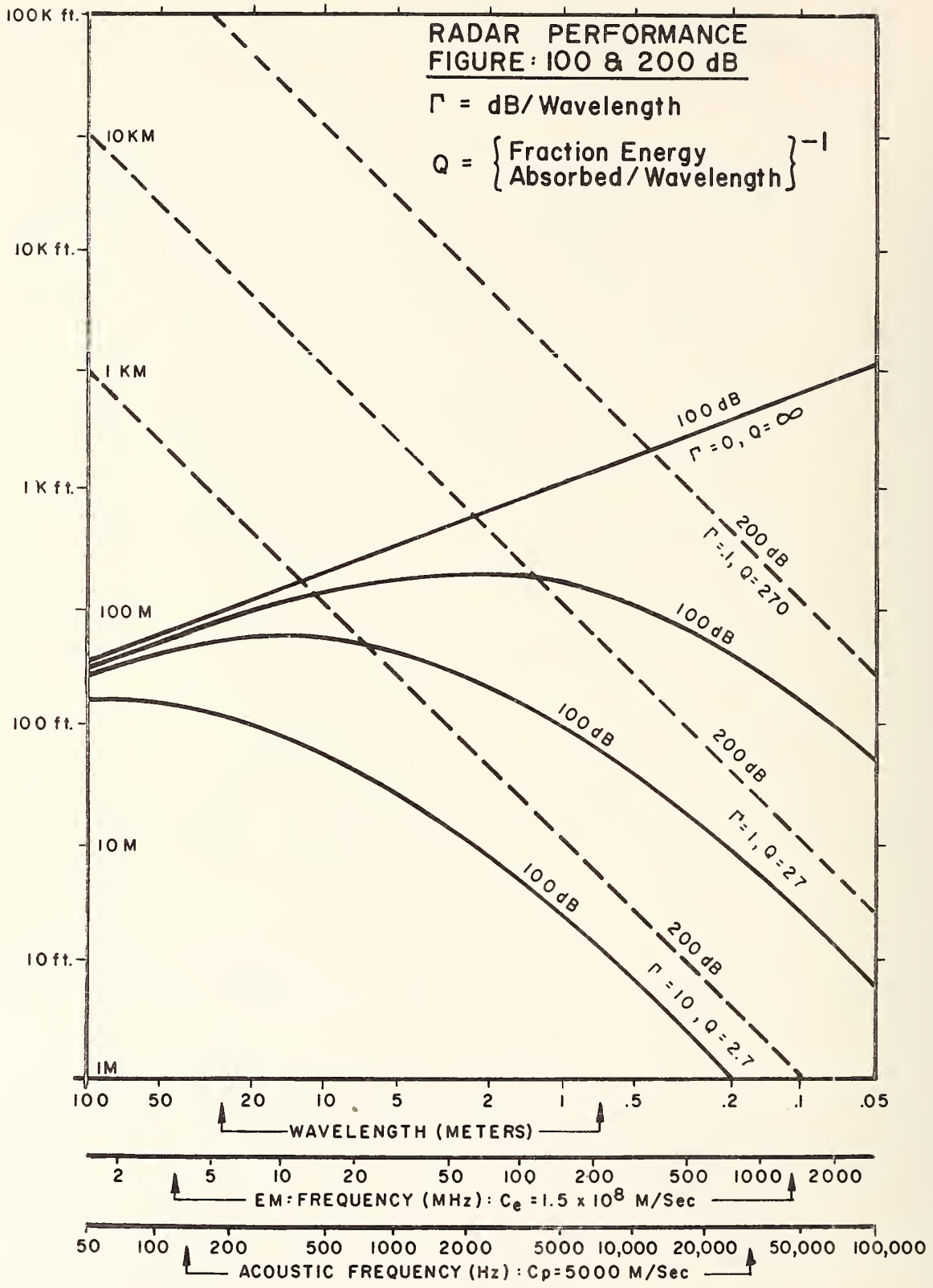

Figure 3. Radar probing distance vs. frequency, Fresnel Zone case.

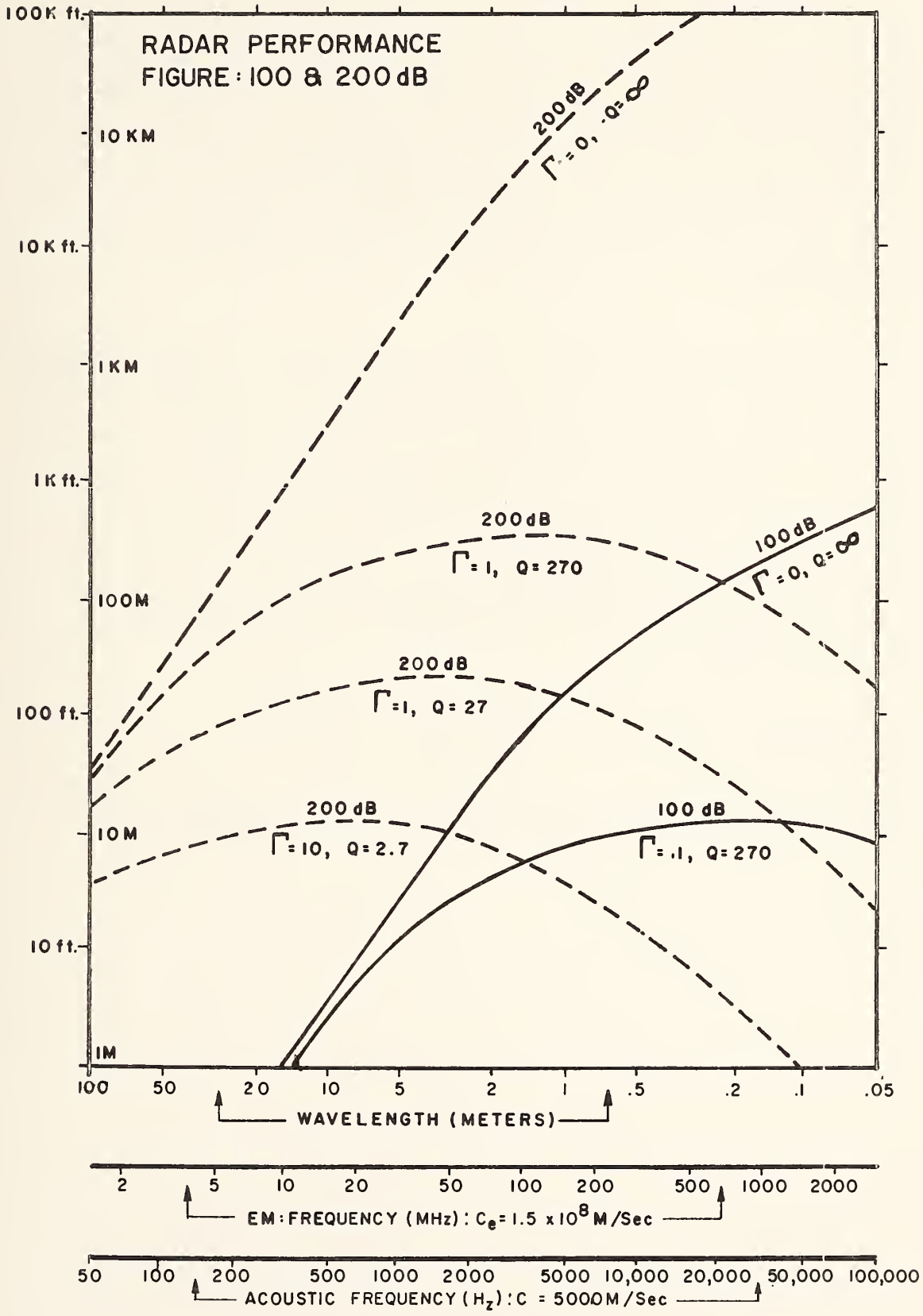

Figure 4. Radar probing distance vs. frequency, 1M² anomaly.

3.3 THIN LAYER

The problem of detecting a thin layer in an otherwise homogeneous rock matrix (such as a clay-filled joint in a granite mass) is somewhat different from that of detecting a boundary between two different rock masses. Widess [1] has shown that the difference in reflection amplitudes between the two cases can be expressed as a function of the ratio of layer thickness to signal wavelength.

The amplitude of a reflection from a thin layer is approximately equal to $4\pi Ad/\lambda$, where d is the thickness of the layer, λ is the predominant signal wavelength in the layer, and A is what the reflection amplitude would be if the layer were infinitely thick. This indicates that thin joints can give fairly substantial reflections: a joint only 1/20 wavelength thick can give a reflection amplitude about 60% as big as a joint many wavelengths thick (assuming the joint is filled with clay or minerals - not air).

4. REFERENCES

1. Widess, M. B., "How Thin is a Thin Bed?", Geophysics, Vol. 38, No. 6, December 1973, page 1176-1180.

APPENDIX D

ACOUSTIC WAVE PROPAGATION IN HARD ROCK

TABLE OF CONTENTS

BACKGROUND STATEMENT

In order to determine the effectiveness of acoustic probing in hard rock, it was first necessary to determine the characteristics of acoustic waves in those rocks of interest.

This appendix starts with the basic physics of wave propagation and ends with curves showing the maximum range for acoustic signals in real rock environments, including the losses associated with the various rock interfaces encountered.

For the reader who is familiar with acoustic wave propagation in near-homogeneous, lossy media, this appendix is not needed. For others, it will be useful in understanding the following appendix, "Acoustic Sensing Subsystem Trade-Offs."

ACOUSTIC WAVE PROPAGATION IN HARD ROCK

ABSTRACT

An acoustic pulse radar is a candidate system for operation within boreholes to investigate rock characteristics of significance to tunneling. The maximum range achievable is of major importance in evaluating the radar performance. The radar range is strongly dependent, among other things, on the attenuation of acoustic waves by the particular rock environment and the frequencies in the transmitted pulse. Published attenuation factors for acoustic waves are employed in the radar range equation, using realistic estimates of acoustic radar and target parameters, to estimate the maximum range as of function of frequency for a pulsed acoustic radar in various types of rock. The results indicate that the maximum range generally decreases with increasing frequency. Frequencies in the range of about 1 kHz to 50 kHz appear to offer the best compromise between maximum range and target resolution in rock environments. A maximum range in excess of 100 ft. (30.5 m) appears to be achievable in granites and limestones at frequencies on the order of 25 kHz, but will be limited to about 32 feet (10 m) or less in shales at 25 kHz. The target is assumed to be a rough surface, oriented normal to the wave front, and at least as large as the first Fresnel zone. This type target is expected to be representative of various rock discontinuities of significance in tunneling such as faults, fracture zones, boundaries between different type rock masses, large water-filled cavities, voids, and the like. System reliability, sources of error, limitations, and general performance of an acoustic pulse radar for detection of rock discontinuities from within a borehole are quite similar to those of an electromagnetic pulse radar. They are not repeated here, but some differences are pointed out.

ACOUSTIC WAVE PROPAGATION IN HARD ROCK

The primary purpose of this appendix is to estimate the maximum range for acoustic pulse radar (also known as echo-ranging systems) for operation in various types of rocks. Some fundamentals of acoustic waves are reviewed and some recent applications of acoustics in borehole investigations of rock characteristics are noted.

In discussing general acoustic wave characteristics, it is assumed that the propagating medium is an unbounded, homogeneous, isotropic and near-elastic (linearity holds but losses are present) solid. Solutions to the acoustic wave equation in such media describe longitudinal waves (also called compressional and primary or P-waves) and transverse waves (also called shear and secondary or S-waves)[1]. All acoustic waves involve the mechanical vibration of particles in the transmission medium. In the P-waves, the direction of particle vibration is longitudinal, or along the axis of wave propagation. In S-waves, the vibrations are transverse to the direction of propagation and involve a shearing action. The S-waves may be resolved into orthogonal components transverse to the direction of propagation and treated separately. The P-waves and S-waves are independent in a homogeneous, isotropic, unbounded medium. Lord Rayleigh showed that in all cases P-waves travel at a faster velocity than S-waves [2]. The attenuation by the medium is expected to be greater for S-waves than for P-waves but the evidence is inconclusive [3]. The attenuation rate in rocks is approximately proportional to the frequency [4].

The attenuation rate of P-waves in a liquid is approximately proportional to the square of frequency [3]. Hence, for fluid saturated rocks, the attenuation rate of P-waves can be expected to

be larger than in dry rock. This may provide a means of estimating the relative water content of different rock masses. Water does not support the propagation of S-waves. This may offer a means of detecting or verifying the presence of large water filled cavities. However, direct reflection from such discontinuities is expected to be the primary method of detection.

In general, a subsurface rock mass will not be homogeneous or isotropic but will contain joints, faults, gouge and fracture zones, boundaries between different rock masses, stratification, voids, water-filled cavities and the like. Acoustic waves will generally be reradiated by scattering, reflection or diffraction by such discontinuities. At such discontinuities, a single incident P- or S-wave will generally give rise to both a transmitted and reflected P- and S-wave and a surface wave [5]. A surface, or Stonely, wave travels along the surface or interface of discontinuities. Their amplitude decreases exponentially with distance from the discontinuity. They may constitute a source of interference but due to their attenuation away from the interface, they are expected to be detected only when an interface is oriented along the borehole and in close proximity to the receiver. Tube waves, which propagate along the cylindrical surface of a borehole, may also be present [1]. They might be effectively ignored for colocated or closely spaced transmitter and receiver by time gating the receiver to be off until they have passed. They can also be used to obtain information about the bulk properties of the rock around the borehole as their velocity depends upon such properties [1].

The primary source of information about the rock discontinuities is expected to come from the reradiation of P-waves and S-waves. The velocity and amplitude variations of the P- and S-waves as a function of motion of acoustic probes along boreholes have been used for determining rock characteristics. Yamshchikov, et al, [6], analyzed the spatial variation of the velocity and amplitude

of P- and S-waves obtained from ultrasonic (35 kHz) soundings between boreholes [apparently at 32.8 feet (10 m) spacing)]. Their results indicate that the coefficient of variation (standard deviation divided by the average) of the velocity is characteristic of the rock inhomogeneity. They found the standard deviation of the S-wave velocity to be larger than for the P-wave velocity in fissured rock with quartz inclusions. Their results also indicated that the amplitude characteristics of the signals are more sensitive to the degree of rock disturbance than is the velocity. An acoustic logging system known as the "3-D" velocity log has been used in numerous borehole logging operations to investigate rock mechanics, fracturing and other rock characteristics [7]. In particular, a reduction in the amplitude of both P- and S-waves across fractures have been observed with the system [8]. The 3-D velocity log employs a pulsed transmitter (pulse width is 22 microseconds and pulse rate is 20 per second) and one or more receiving units in a single borehole [7]. It can also be used in hole-to-hole operations with an expected range of 200 feet (61.0 m) in competent rock [8]. Acoustic waves have been utilized for many years in investigations of seismic phenomena. The potential of acoustic techniques for subsurface investigations of importance in tunneling is recognized. A recent investigation suggested the use of arrays of acoustic sensors for operation in an L-shaped configuration of short boreholes for investigation in advance of tunneling [9]. Acoustic holography, with the system being an integral part of a tunneling machine, for investigating beyond the tunnel face in advance of cutting has also been suggested [10].

The efforts in the area of subsurface investigations in advance of or prior to tunnel excavation with acoustic techniques are apparently still in the research stage. Questions as to data interpretation appear to be common in virtually all subsurface investigations. One of the major problems is extraction of meaningful data in the presence of background acoustic clutter (unwanted

echos) or noise. The use of special types of transmitted waveforms and signal processing techniques may significantly improve the data interpretation [11]. There is still much to be learned, however, and it is not yet clear that an acoustic (or other) technique alone will provide sufficiently complete and reliable information to significantly improve tunnel planning and construction.

Perhaps the simplest, most economic and technically attractive approach to this is associated with the use of an acoustic system in conjunction with others operating from within a single small diameter borehole. This is the subject of the present report. A fundamental consideration in this approach is the range that can be achieved by the acoustic sensors. Attention is now turned to estimating the maximum range of an acoustic radar operating from within a single borehole.

The radar equation is employed in estimating the maximum range. The MKS system of units is used in equations with the equivalent English measure given when numbers result. It is assumed that the transmission medium is an unbounded, homogeneous, isotropic, and near-elastic (linear but lossy) rock environment. System and environmental parameters are based on experimental data where available and necessary engineering estimates are identified and discussed.

Attenuation by the medium must be included in the radar equation. This is developed first.

In the propagation of plane, cylindrical, or spherical waves, the phase and attenuation factors are given by $e^{-\gamma R}$ where R is the range and $\gamma = \alpha + i\beta$ is the wavenumber [1]. The symbols α and β denote the attenuation and phase factors, respectively. They are given by

$$\alpha = \frac{\omega}{2vQ} \text{ nepers/meter} \qquad (1)$$

and

$$\beta = 2\pi/\lambda = 2\pi f/v \text{ radians/meter} \qquad (2)$$

where $\omega = 2\pi f$ is the radian frequency, f is frequency in Hertz, $Q \equiv f/\Delta f$ is a dimensionless quality factor that expresses the sharpness of resonance of the rock medium (Δf is the frequency shift which reduces the peak force amplitude at the resonant frequency at f to $1/\sqrt{2}$ times the peak), v is the phase velocity of the wave where

$$v|_{P\text{-wave}} = c_P = \sqrt{\frac{1}{\rho}(\Gamma + 2\nu)} \tag{3}$$

$$v|_{S\text{-wave}} = c_s = \sqrt{\frac{\nu}{\rho}} \tag{4}$$

where Γ and ν (the shear modules) are Lame' elastic constants in newtons/m^2 and ρ is the density in kg/m^3. The bulk modulus $B = \Gamma + 2/3\nu$ is also used by some authors in expressing the velocity. The power in the wave is proportional to the square of the absolute magnitude of the pressure or displacement wave function [1]. Hence, the phase and attenuation factors for the power are $|e^{-\gamma R}|^2 = |e^{-(\gamma+i\beta)R}|^2 = e^{-2\gamma R}$. It is assumed that the transmitting and receiving transducers are colocated. Thus the range from the target (discontinuity) to the transmitter and receiver is the same.

The radar transmission equation for acoustic waves is analogous to that for electromagnetic waves. It is briefly developed here. The power density at range R in the far field of an isotropic radiator is

$$I_t = \frac{P_t}{4\pi R^2} e^{-\alpha R} \text{ watts/m}^2 \tag{5}$$

where P_t is the peak transmitted power in watts. The far field of a transducer with circular cross section commences at ranges on the order of $R = \pi \ell^2/\lambda$ where ℓ is the radius of the transducer [12]. This is also applicable to the far field of an equivalent antenna in electromagnetic radiation.

If the transmitting transducer has a gain G_t relative to an isotropic radiator, the power density at range R is given by $I_t G_t$. If there is a discontinuity at range R that reradiates energy back to the radar, its radar cross section may be denoted by σ in square meters. The power density of the signal arriving at the receiver is then

$$P_d = \frac{P_t G_t e^{-2\alpha R}}{4\pi R^2} \cdot \frac{\sigma e^{-2\alpha R}}{4\pi R^2} \text{ watts/m}^2 \tag{6}$$

The receiving transducer with an effective aperture area A_e will intercept the power over this area. Hence, the received power is given by $P_r = P_d A_e$, or

$$P_r = \frac{P_t G_t \sigma A_e e^{-4\alpha R}}{(4\pi)^2 R^4} \text{ watts} \tag{7}$$

The gain of the receiver is related to its effective aperture by [13]

$$G_r = 4\pi A_e/\lambda^2 \tag{8}$$

Substituting this into Equation (7) gives

$$P_r = \frac{P_t G_t G_r \sigma \lambda^2 e^{-4\alpha R}}{(4\pi)^3 R^4} \text{ watts.} \tag{9}$$

An equivalent form of Equation (9) is employed by Sigelmann and Reid [13], for example, in obtaining the acoustic backscatter from an ensemble of scatterers. A more useful form of the radar equation for our purposes results by defining the received signal-to-noise power ratio P_r/P_n. P_n is the noise power level of the receiving system or of unwanted external acoustic signals, whichever is greater. The noise power level determines the minimum detectable signal power (i.e., $P_{r_{min}} = P_n$). Writing Equation (9) in terms of the noise power gives

$$\frac{P_r}{P_n} = \frac{P_t G_t G_r \sigma \lambda^2 e^{-4\alpha R}}{P_n (4\pi)^3 R^4} \qquad (10)$$

Note that this equation is identical to the radar equation discussed previously, for the electromagnetic pulse radar.

This should not be surprising because both are a direct consequence of wave propagation described by the same wave equation and propagating in the same medium [5]. Differences emerge when the appropriate constitutive parameters (electrical and elastic) of the medium and different system parameters are employed.

Without loss of generality, it is assumed here that the gain of the transmitting and receiving transducers are equal (i.e., $G_t = G_r = G$). Then, employing the estimate of radar cross section for a rough surface of [14]

$$\sigma = \pi\left(\frac{\lambda R}{2} + \frac{\lambda^2}{16}\right) \simeq \pi\lambda\frac{R}{2}$$

and the total propagation loss T.P.L., or transmission loss, in decibels of

$$\text{T.P.L.} = 10 \log [P_t/P_r],$$

one obtains from Equation (10)

$$\text{T.P.L.} = 10 \log \left[\frac{128\pi^2 R^3}{G^2\lambda^3}\right] + 2RA \qquad (11)$$

where the attenuation factor A db/unit distance = $20\alpha \log e$ neper/unit distance. Note from Equation (1) that the value of α, and hence A, is directly proportional to frequency if Q and v are independent of frequency. This has been found to be the case [1] and it will be convenient to use experimentally determined values of Q and v to define an attenuation factor A = Lf db/m in numerical computations, where L is a constant for the particular rock type.

Cook [14] defines a radar performance figure, also sometimes known as a dynamic range, as P.F. = 10 log (P_t/minimum detectable signal). Using the definition of T.P.L. above, it is easily seen that the P.F. = T.P.L. when the received signal is equal to the minimum detectable signal (i.e., when $P_r = P_n$). From Equation (10), it can be seen that the minimum signal will, other things being equal, determine the maximum range.

Hence, if resonable performance figures and gains can be estimated for an acoustic radar, then Equation (11) can be used to estimate the maximum achievable range as a function of frequency for various rock types for which the attenuation factors and velocity (or λ) are known.

The minimum power density which typical geophones can detect in rock is on the order of 3×10^{-11} to 9×10^{-11} watts/m^2. Based on practical limitations of electrical components for small devices, the peak power transmitted may be on the order of kilowatts to megawatts. For a peak transmitted power of 1 kw, the power density at 1 meter range in a lossless medium is $10^3/4\pi \simeq 79.6$ watts/m^2, and for 1 megawatt peak power, it is 79.6×10^3 watts/m^2. This gives performance figures on the order of $P_t/P_r = 79.6/9 \times 10^{-11} \simeq 8.8 \times 10^{11} \simeq 119$ db to $79.6 \times 10^3/3 \times 10^{-11} = 26.5 \times 10^{14} \simeq 154$ db. Signal enhancement techiques may possibly increase this by 15 db or more. A value of 100 db for the performance figure would seem to be readily achievable while a value of 170 db would appear to be approaching the practicable limit. The maximum range will be computed here for the reasonable performance figures of 100 and 135 db.

Values of the absorption coefficient and velocity for various rocks are tabulated in Table 1 from data given by White [1].

Table 1.

Attenuation Factors and Velocity of Propogation
For Acoustic Waves In Various Types of Rock

Rock Type	α (nepers/ wavelength)	v(m/sec)	A = Lf (db/m)
Granite	0.02	5×10^3	$0.034744fx10^{-3}$
Limestone	0.012	6.1×10^3	$0.017087fx10^{-3}$
Sandstone	0.017	5×10^3	$0.02953fx10^{-3}$
Sylvin Shale	0.045	2.2×10^3	$0.177668fx10^{-3}$
Pierre Shale	0.099	2.2×10^3	$0.39087fx10^{-3}$

It is assumed that the effective area of the apertures of the transducers are $A_e = 1m^2$. Then, using A = Lf, $G = 4\pi A_e/\lambda^2$, and $\lambda = v/f$, Equation (11) may be written in the more convenient form for computations of

$$T.P.L. = 10 \log(8R^3_{max} \frac{v}{f}) + 2R_{max}Lf. \qquad (12)$$

Values of the velocity and attenuation factors for various rock types from Table 1 are used to compute the maximum range as a function of frequency for assumed values of performance figure (or T.P.L.) of 100 dB and 135 dB, and are plotted in Figure 1. Figure 1 shows that the maximum range depends strongly on rock type and frequency. With minor exceptions, the maximum range decreases with increasing frequency. The greater ranges are generally possible in the harder rock, such as granite and limestone. At 5 kHz, the maximum range in granite is indicated to be about 100m (328 ft) to 200 m (656 ft). This corresponds to the maximum range in granite for the electromagnetic radar at about 100 mHz (see Appendix F). Assuming a typical acoustic velocity of $5x10^3$ m/sec, the acoustic wavelength at 5 kHz is about 1 m (3.28 ft). Assuming a minimum detectable target depth

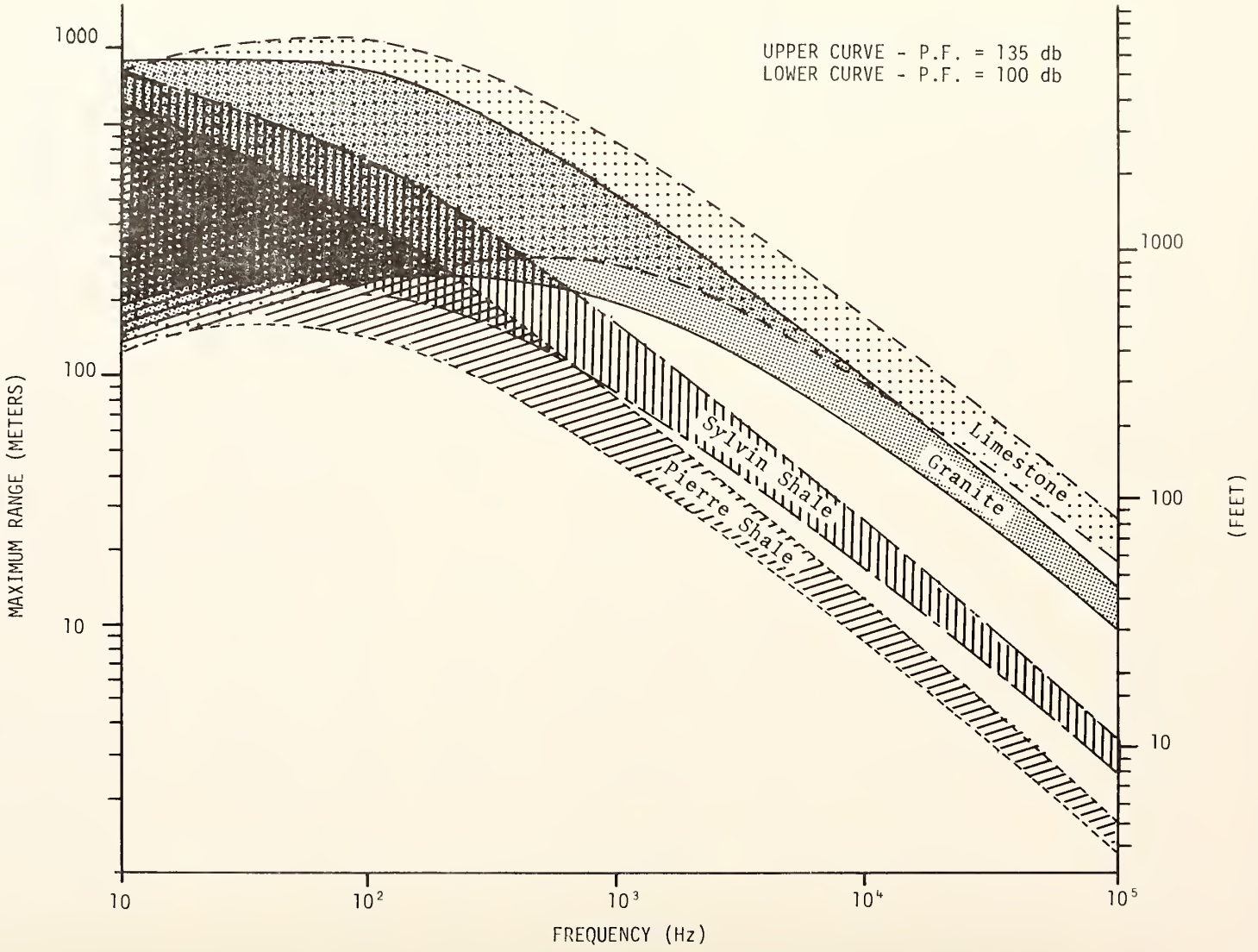

Figure 1. Maximum range for an acoustic radar in typical rock as a function of frequency and radar performance figure.

of $\lambda/4$, this implies that layers some 10 in. (25 cm) thick can be resolved at ranges of some 100 m (328 ft) in granite with an acoustic radar with performance figure of 100 dB. The resolution at a comparable range in granite (assuming $\varepsilon_r \simeq 4$, at 100 mHz) with the electromagnetic radar of P.F. = 100dB is about 15 in (0.38 m) (see Appendix F). This is an interestingly close agreement in the maximum range and resolution of the two types of radar. However, while agreement in trends of theoretical performance of the radar range versus frequency for the two systems can be expected here, it is cautioned that the rock samples used in the acoustic and electromagnetic cases are not the same. Hence, too much emphasis should not be placed on quantitative agreements.

The results in Figure 1 provide performance estimates and guidelines in the design of an acoustic radar. Considerations in the expected performance of an acoustic radar in detecting various types of targets of significance in tunneling, sources of error, reliability and system limitations in general are quite analogous to those for the electromagnetic radar. They are discussed in Appendix F and are not repeated here. However, there is a major difference which should be recognized. This is in the area of the transducers (antennas). Efficient coupling of acoustic energy into the medium requires physical contact between the transducers and the medium. This is done with fluid in present acoustic borehole logging systems. The horizontal boreholes may be essentially dry in the subject applications, however, so the design will have to incorporate a method for making physical contact. This may be achieved in several ways (eg., an inflatable fluid-filled container housing the transducers, mechanical arms to press transducers against the borehole wall, or possibly others). Impedance matching will also be a design requirement. However, impedance matching and efficient coupling of energy into the

medium are necessary in both systems. The major difference is the requirement for physical contact in the acoustic system which is not required in the electromagnetic system. There may be portions of the borehole walls that are fractured or caved out where effective physical contact between the acoustic transducers and the rock medium is not practicable. Such regions can deteriorate the performance of an electromagnetic radar due to mismatch but it is not expected to be as serious as in an acoustic system. However, unless such caved out regions are extensive, the practical limitations may be insignificant. For example, the loss of data over a few feet should not seriously affect the interpretation in mapping a continuous joint or fracture plane running parallel to the borehole. However, the extent of such fractured or caved areas in boreholes and the associated problems that may arise in practical applications are, as with the ultimate evaluation of performance and data interpretation in general, likely areas for experimental investigation.

REFERENCES

1. White, J. E., Seismic Waves: Radiation, Transmission and Attenuation, McGraw-Hill, New York, 1965.

2. Kinsler, Lawrence E., and Austin, R. Frey, Fundamentals of Acoustics, John Wiley & Sons, New York, 1950.

3. Attewell, P. B., and Y. V. Romana, "Wave Attenuation and Internal Friction as Functions of Frequency in Rocks," Geophysics, Vol. XXXI, No. 6, December 1966.

4. Winter, T. G., "A Survey of Sound Propagation in Soils," Acoustic Society of America, 84th Annual Meeting, November 1972.

5. Brekhovskikh, Leonid, M., Waves in Layered Media, Academic Press, New York, 1960.

6. Yamshchikov, V. S., and P. M. Tyutyunnik, and A. V. Blok, "An Experimental Study, Based on Ultrasonic Wave Propagation, of the Spatial Inhomogeneity of the Solid Rock near a Mine Working," Soviet Mining Science, Vol. 10, No. 3, May-June 1974

7. Hamilton, R. G. and J. I. Myung, "Summary of Geophysical Well Lossing," Birdwell Division, Seismograph Service Corp., Tulsa, Oklahoma.

8. Myung, John I., and R. W. Baltosser, "Fracture Evaluation by the Borehole Logging Method," 13th Annual Symp. on Rock Mechanics, U. of Illinois, Urbana, August 1971.

9. Soland, Duane E., Harold M. Mooney, Sudarshen Singh, Duane Tack, and Richard Bell, "Excavation Seismology," First Annual Technical Report, Bureau of Mines Contract No. HO210025, Honeywell, Inc., St. Paul, Minnesota, 1972.

10. Price, T. O., "Acoustical Holography as a Tool for Geologic Prediction," Proc. of Subsurface Exploration for Underground Excavation and Heavy Construction, ASCE, August 1974.

11. Hipkins, D. L., and L. A. Whitney, "Acoustic Techniques Suitable for Use in Soil," Proc. of Subsurface Exploration for Underground Excavation and Heavy Construction, ASCE, August 1974.

12. Huether, Theodor F., and Richard H. Bolt, SONICS, John Wiley & Sons, New York, 1955.

13. Sigelmann, Rubens A., and John M. Reid, "Analysis and Measurement of Ultrasound Backscatter from an Ensemble of Scatterers Excited by Sine-Wave Bursts," J. Acoust. Soc. Am. Vol. 53, No. 5, May 1973.

14. Cook, John C., "Radar Transparencies of Mine and Tunnel Rocks," 44th Int. SEG Meeting, Dallas, Texas, 1974.

APPENDIX E

ACOUSTIC SENSING SUBSYSTEM TRADE-OFFS

TABLE OF CONTENTS

BACKGROUND STATEMENT

Once it was decided that the prototype hard-rock sensing system would require an acoustic sensor, a study was conducted to review the state-of-the-art and, by the process of trade-offs, pick the best candidate.

This appendix covers that system trade-off study in detail and is here presented for the reader who wishes to follow the logic and development. The salient results are included in Volume I, Section 3.1.2.

The work reported herein is largely an extension and coverage of the acoustic probe work performed for the U. S. Bureau of Mines and U. S. Geological Survey by Southwest Research Institute, and in particular has been extracted from their reports [1] [2]. It is published here by special permission with our thanks.

ACOUSTIC SENSING SUBSYSTEM TRADE-OFFS

ABSTRACT

This appendix summarizes the pertinent factors which must be considered in the design of an acoustical sensing subsystem. The critical performance requirements are developed and discussed. Various methods of coupling and acoustical energy into the borehole wall are considered and a preferred approach developed. The possible signal wave shapes are covered and a pulse or pulsed CW source is selected. The natural parameters affecting the required range and resolution of the system dictate that a system will probably have to operate in the range between one kilohertz and 100 kilohertz. This will give a resolution which could vary from as fine as a few inches in good rock to as course as ten feet in rocks with poor propagation characteristics. The selected acoustical power source is a high-energy magnetostrictive source in a fluid-filled elastomeric sleeve. The receiving transducers are defined to be piezoelectric ceramic stacks. Systems considerations are covered including the probable availability of various classes of hardware, those types which will require additional development, and their impact upon the total integrated system when considered in view of other sensors involved. The appendix concludes by summarizing the preliminary design and defining the preferred components in critical areas.

ACOUSTICAL SENSING SUBSYSTEM TRADE-OFFS

Topics that must be considered in the design of an acoustic subsystem include the following:

- Performance requirements, both from the point of view of sensing and from the point of view of operation of the whole system.
- Candidate approaches to transmitting and receiving transducer.
- The available hardware which can serve as a point of departure for this system.
- Hardware trade-off considerations including the impact upon the system as a whole of the inclusion of specific hardware.
- The interaction, interplay, and information mix between acoustic and other sensors.

These considerations will be discussed in this appendix and a tentative system configuration established. Where additional studies, trade-offs, or information is required, these areas will be identified.

1. PERFORMANCE REQUIREMENTS

The intent of the acoustic subsystem is to aid in locating discontinuities out to a range of 100 ft. (30.5 m) in hard rock. It must be able to record these in a way such that they can be displayed and processed at a later time. Zones of incompetent rock as well as free-water zones are of particular interest. These are areas which present significant hazards in tunnelling. It is also desirable to delineate the joint sets and faults or any other large interfaces by their attitude and spacing. If

possible, the system should provide an estimate of the rock quality designator (RQD). The acoustic subsystem should provide much of this information by itself. Other information can be derived by the system serving to complement the electromagnetic and electrical probes.

From an operational point of view, the performance requirements for the subsystem include operation in a single borehole, wet or dry, of 6-3/4" (17.1 cm) diameter. Insofar as possible, it should incorporate available proven hardware in order to minimize the developmental efforts and costs. This will be especially true in the selection of sensors.

2. ACOUSTIC SUBSYSTEM CANDIDATES

The discussion of candidate approaches for the acoustic subsystem will include consideration of coupling methods, the type and utility of various signals which can be generated, the types of transducers and sensors which can be used, the physical configuration in which they will be deployed, and a review of the existing hardware which can serve as the point of departure for the system.

2.1 COUPLING METHODS

Perhaps one of the most critical elements of the acoustic subsystem is a mechanism by which the acoustic energy is coupled to the borehole wall. The purpose of coupling is to provide an impedance-matched acoustic path between the borehole wall and the transducer. Some of the possible methods of attaining coupling are summarized in Figure 1, as reported by SwRI [1].

The standard method of acoustic coupling for borehole acoustic probes is for the system to operate in a fluid-filled hole. The dry hole operational requirement for this system precludes

Basic Mechanism	Illustration
Elastomeric Boots (Hydraulic or Pneumatic)	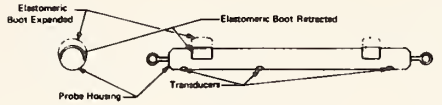
Elastomeric Pistons (Hydraulic or Pneumatic)	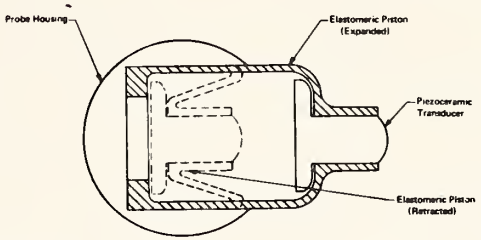
Elastomeric Sleeves (Solid or Fluid-Filled)	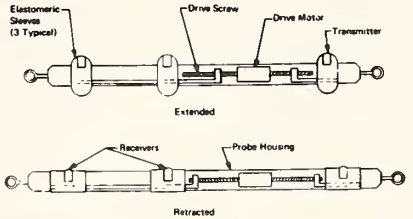

Basic Mechanism	Illustration
Inflatable Elastomeric Mandrels (Hydraulic or Pneumatic)	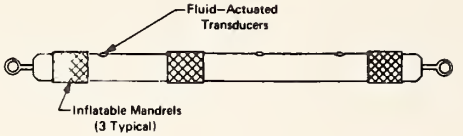
Screw-Driven Mechanical Expanders	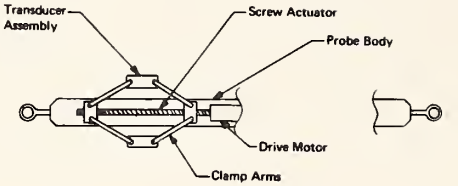
Fluid Cylinder Actuated Cams	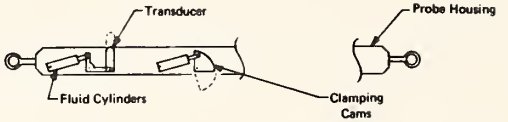
Rigid Pistons (Hydraulic)	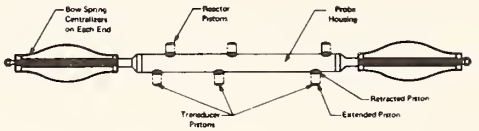

Figure 1. Coupling concepts (After SwRI Ref. 1)

this method. As indicated in Figure 1, another approach to fluid coupling can be achieved by providing the fluid in an elastomeric bag to provide the link between the transducer and the borehole wall. In addition, operation in a dry hole requires the use of force contact. This can be achieved either through the pressurization of the fluid coupling bag or alternatively by physically pushing the transducer against the wall of the borehole in order to provide the coupling needed to get good signals into the rocks and out again. This force can be provided by elastomeric boots, pistons, hydraulic and pneumatic cylinders. Figure 1 also illustrates mechanical expanders and cams as well as the hydraulically operated systems. The contact force required is substantial and will vary from a few pounds to hundreds of pounds.

The coupling and uncoupling times must be fairly short, no more than a few seconds at most, if a reasonable traverse rate is to be maintained down the borehole. If it takes too long to couple and uncouple, it will limit the production rate at which the hole can be scanned. The coupling mechanism will be subject to considerable wear with the possibility of snagging during travestry. It must, therefore, present a minimal silhouette to the borehole. It must be adaptable to minor variations in hole size as one of the fundamental requirements of this system.

Of the options summarized in Figure 1, Southwest Research Institute has developed the system with two rigid hydraulic pistons that expand to force the transducers against the wall of the borehole.

The Southwest Research Institute approach is attractive because of its simplicity and the fact that the acoustic transducer makes direct firm contact with the borehole wall. However, it does not meet all the requirements for this system. The resolution requirements of the system are such that it will either be necessary for the transducer to be scanned around the axis of the borehole or for multiple transducers to be used. (See Appendix C). If the scanning transducer approach is employed, then the coupling mechanism will almost have to be by use of a fluid-filled elastomeric bag. The coupling and decoupling times of the piston-actuated transducer would rapidly become excessive in that the system would have to be decoupled from the borehole wall prior to each incremental azimuthal translation of the transducer. Multiple transducers could be coupled by the use of pistons, but it is impractical to use more than three or four.

2.2 SIGNAL SOURCES

2.2.1 Signal Types

The signal types to be considered as candidates for the acoustic probe fall into two categories: pulsed signals and continuous wave (CW) signals.

The CW signals are used to sense a discontinuity by means of interferometry. They require a rather complicated processing operation to display the images that they generate. They usually are not amenable to quick-look displays and normally require multi-frequency emissions to resolve some of the ambiguities that result from using single frequency CW signals.

The pulsed signals are more amenable to the mapping problem. The pulses can be either true impulses, short bursts of CW signals, or swept frequency signals (chirp signals) that can be processed by correlation processors to obtain a large time

bandwidth product at a low average power. The pulsed signals are intended fundamentally to show the time of flight and transmission loss for shear and compressional waves. From these time of flight and transmission loss measurements, one can derive information about the number, location and attitude of interfaces. This can be ahcieved by much simpler processing than is required for CW signals. Some of the gross in situ properties of rock such as the compressional and shear modulii can also be derived from pulsed signals. However, it is also necessary that the density of the rock be known and the general geometry under which the measurements were made. Indirect measurements of the bulk or rock quality designator can also be derived from measurementsmade of changes in propogation velocity. Excellent correlations have been achieved between these and the fractured density of recovered cores [3].

2.2.2 Signal Parameters

Some of the signal parameters that must be kept in mind in the acoustic system include the relative velocities between compressional and shear waves. In hard rock, compressional waves will propagate at speeds of 10 to 20 feet (3.0 to 6.1 m) per millisecond. Shear waves will propagate somewhat slower than that, five to 15 feet (2 to 4.6 m) per millisecond. These waves will attenuate at roughly a rate of one to two dB per wavelength. This means that the outer limits of the useful frequency band for the acoustic subsystem are going to range between one kilohertz and 100 kilohertz. This will define the resolution and the penetration which the acoustic subsystem may attain. The wavelengths corresponding to these velocities will be in the order of a tenth of a foot (30mm) to about ten feet (3 m). Given an attenuation of one dB per wavelength, the ranges attainable with an attenuation loss of 20 dB are about one foot (0.3 m) for 100 kilohertz and about 100 feet (30.5 m) for one kilohertz. The instantaneous power that will be needed to

sense a reflector at 100 feet (30.5 m) range will vary between milliwatts and kilowatts, depending on the frequency, the kind of sensors in use, and the rock type in which the measurements are being made. Figure 2 summarizes the ranges at which the system will be able to work in different kinds of rocks over the frequency spectrum of interest. However, a word of caution should be interjected. This figure was derived from the cumulative works of a number of authors [4]. Most of these made only a few spot measurements on differing types of rock over at most a very narrow range of frequencies. The curves on Figure 2 were derived by established theoretical formulations. Actually, much more work is required to validate these curves over additional rock types before they can realistically be used as more than general guides to the trends which can be expected in hard rock acoustical probing.

It can be seen in Figure 2 that with limestone, which has good propagation characteristics for acoustic waves, a range of 100 feet (30.5 m) can be attained at frequencies well above ten kilohertz. This means that in a purely limestone environment the system could achieve fairly high resolutions at the maximum ranges of interest [i.e., 100 feet (30.5 m)]. Thus, small targets could be detected at these ranges. At the other end of the hard rock spectrum in a lossy medium like shale, the system will be severely limited to frequencies on the order of a kilohertz in order to get a 100 foot (30.5 m). penetration. This would imply that only gross features could be resolved at these distances. The term "hard rock" as used in this report to define the medium in which the system must operate must be considered to include this complete spectrum. The median rock, in general, would not be anticipated to be as bad as shale as far as attenuation characteristics are concerned. However, there will be certain types of decomposed crystalline rock which might easily approximate shale and its properties. Thus, over the range of properties

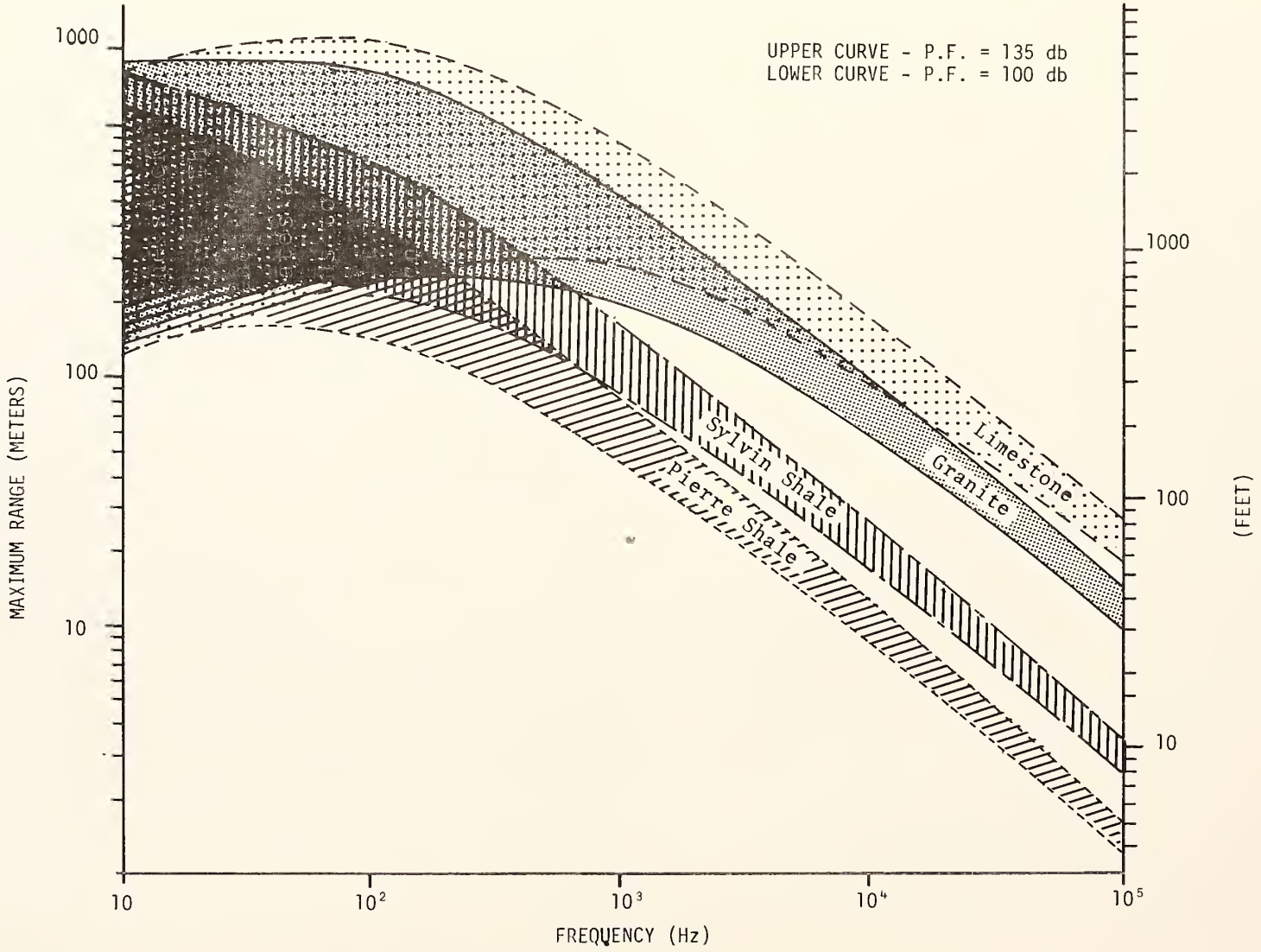

Figure 2. Maximum range for an Acoustic Radar in Typical Rock as a Function of Frequency and Radar Performance Figure (after White (4).

included under the broad generic term of hard rock, a range of 100 feet can be expected to be attainable. However, resolution can be expected to vary from a few inches to the order of tens of feet, depending upon the material in which the measurements are being made.

2.2.3 Transducer Options

One of the prime candidates for both transmitting and receiving transducers is the traditional piezoelectric stack. In general, this consists of a stack of ceramic disc elements of a highly piezoelectric ceramic. The stack consists of a number, perhaps 20 or 30, of discs each of which has a sensitivity of about 20 volts per mil of compressional or transverse displacement. This implies that distortion of the disc by one thousandth of an inch (.025mm) will generate a voltage of approximately 20 volts. Conversely, application of a 20 volt charge to the disc will cause it to physically expand or contract a thousandth of an inch (.025 mm). One mode in which SwRI uses these stacks [1] very successfully as energy sources is in a pulse mode. The stack is charged to approximately a 1,000 volt DC charge level as though it were a multi-element capacitor. It is then rapidly discharged. In the charged state, the stack is physically deformed by the high voltage on the discs. Thus, the rapid discharge of the disc is analogous to the instantaneous release of a spring-loaded mass which generates a pulse of displacement energy as the ceramic stack returns to equilibrium. Experimental configurations have been built where, from a stack of about one cubic inch (16 ml), discharging a 1,000 volt DC potential, will generate a pulse of about 50 millijoules over perhaps a 50 microsecond time interval. This corresponds to a kilowatt of peak power. However, it is generated only over a very short interval of time so that the total average power is small. Its instantaneous intensity is high.

The piezoelectric stack can also be used for the purpose of receiving transducers. The same discussion as used for the transmitting mode now applies in reverse. Acoustical vibrations received from the rock produce microscopic motions of the piezoelectric stack. This in turn generates voltages which can then be amplified.

The piezoelectric stack can also be used in a continuous wave (CW) mode; however, this is not a recommended approach for this particular system application. A possible exception would be to use a short CW burst as an approximation to a pulse signal.

Magnetostrictive stacks for transmit applications behave in a similar manner to the ceramic stacks. However, in place of ceramic, they use discs made of a magnetostrictive metal. They are less fragile than the piezoelectric stacks. The discussion of their operation is similar to that of the ceramic disc except that they deform in the presence of a magnetic field rather than an electro field. At this point in the study, they are considered as preferable to the piezoelectric stacks because of their ruggedness.

Figure 3 is an example of signals generated by the pulse discharge method through ceramic discs. This represents work accomplished by Southwest Research Institute [2] and shows both shear and compressional waves at various distances. This data represents one-way transmission distances varying from 8 feet (2.4 m) to about 20 feet (6.1 m). It can be seen that the stacks generate a sharp pulse and over these ranges the clearly evident P and S signals have ample signal strength for SwRI applications. These measurements were made in volcanic tuff which is a reasonably good propagating medium for acoustic energy. It is estimated that its propagation characteristics approach those of limestone as an environment. It can be seen that these pulses, even extrapolated to greater ranges, pro-

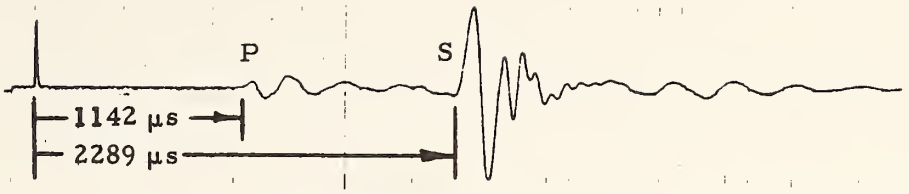

(a) Chart Record #15: P-Wave Receiver Channel
RCVR Station #10: Horizontal Borehole (dry)
XMTR-RCVR Distance 8.067 feet

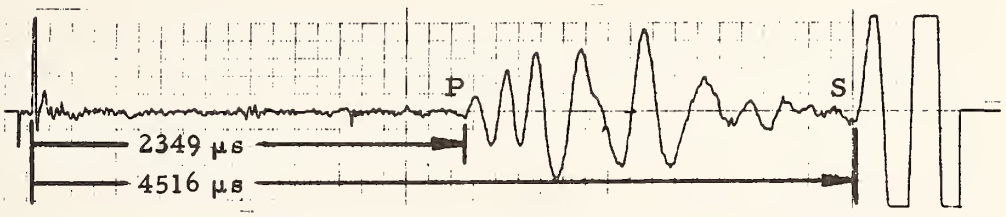

(b) Chart Record #135: S-Wave Receiver Channel
RCVR Station #33: Horizontal Borehole (dry)
XMTR-RCVR Distance 19.567 feet

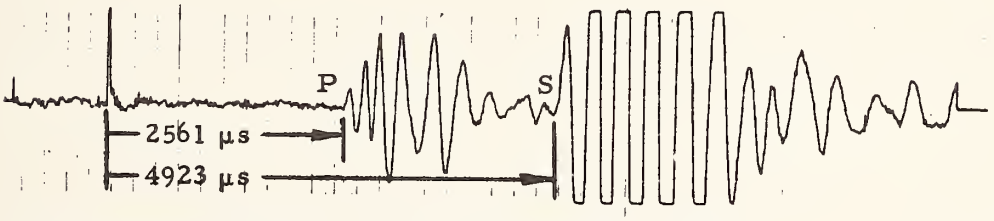

(c) Chart Record #139: S-Wave Receiver Channel
RCVR Station #37: Horizontal Borehole (dry)
XMTR-RCVR Distance 21.567 feet

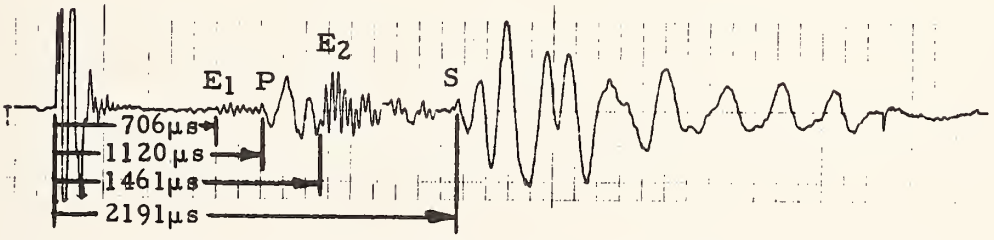

(d) Chart Record #233: P-Wave Receiver Channel
RCVR Station #69: Slanted Borehole (wet)
XMTR-RCVR Distance 10 feet

SAMPLE SEISMIC VELOCITY PROBE WAVEFORMS
NEVADA TEST CENTER (15-17 April 1975)

Figure 3. (After SwRI (2).

vide a signal strength which is adequate to make acoustic pulse measurements useful in hard rock. Southwest Research used

this data to calculate attenuation rates of 0.892 dB/ft. (2.9 dB/m) for compressional waves [2]. With a center frequency of 4000 Hz, this corresponds to attenuation of 2 dB per wavelength. Thus, at least for this case it seems reasonable to estimate that with current equipment it would be possible to map acoustic reflections from 50 to 100 feet (15.4 m to 30.5 m) with energy in the 2 kHz to 6 kHz range.

A transillumination borehole probe developed by Simplec Inc. is currently in operation by the Tennessee Valley Authority. This uses magnetostrictive transmitting transducers and it has been reported that this system is able to resolve joints and gouge zones as little as 1/16" (1.6 mm) thick to distances in excess of 25 feet (7.6 m). The magnetostrictive transducer was specifically chosen for this particular probe in the hard rock environment because of its ruggedness.

Another prime candidate for this system is the sparker. Although the spark discharge approach has been used for years and was the initial form of transducer used in borehole logging, it has only recently been assembled in a form amenable for operation in a dry hole. The sparker basically is a discharge of a high-voltage electrical spark in a fluid. It is currently used extensively in off-shore surveying where extremely high-power, deep-penetrating probes are required. A ten kilovolt spark will generate, over a few microseconds, a peak power in the order of tens of megawatts. In the adaptation for operation in a dry borehole, the spark gap would be mounted in an oil-filled elastomeric bag. The actual physical pulse generated by a sparker comes, not from the high intensity spark directly, but from the

gas bubble generated by the instantaneous vaporization of the fluid in which the spark gap is immersed. Thus, the pulse duration actually transmitted from the system may be considerably longer than the few microseconds it takes to discharge the spark gap.

At the present time, there are no commercially available dry hole sparkers, although several manufacturers including Simplec, Inc. are looking at such a source. For this reason, we do not recommend planning on the use of the sparker for this system. However, if one becomes available, it should be seriously considered.

Similar in operation to the sparker is the exploding wire system. Instead of discharging a spark through an ionized gap, the exploding wire system physically uses a wire which is ionized and literally explodes when a high current is passed through it. This yields extremely high powers in very short times. One unit that is produced by Sonics International is packaged for operation in a five-inch (13 cm) borehole. It can be operated at a pulse repetition rate of about two seconds per pulse. A wire supply goes along with the unit and feeds across the spark gap between pulses. This system puts out a peak power in excess of 25 megawatts. It is not designed as an acoustic source for a system such as this. Its purpose is to physically blast scale and wax accumulations from the walls of pipes in producing oil wells. It is not believed that the exploding wire system would be a desirable candidate for this system. However, it is indicative of the amounts of power which are available using the general concept of the sparker.

A final candidate to be considered is the electrodynamic vibrator. These units are available in a variety of sizes,

shapes, and frequency ranges. They have the advantage that they can be made to be a repeatable, swept frequency source. Physically, a unit that is three inches in diameter and can very easily be packaged to go into a borehole will provide a thrust in the order of ten pounds over a frequency range of from one hertz to ten kilohertz. It is primarily a continuous power rather than a pulsed power device. Thus, the signals must be processed before any display is possible; the pulse system or pulsed CW is considered to be the prime candidate. However, if for any reason the system concept changed so that a CW or a swept CW such as chirp type of system were employed, the electrodynamic vibrator would warrant serious consideration as an highly desirable, rugged, repeatable source of acoustical energy.

A number of factors must be considered in evaluating the best configuration of sensors for this system. Primarily this involves the question of the need for multiple versus single transmitters and receivers. It is possible to obtain a certain degree of azimuthal resolution by using a number of heads, each with directional characteristics and embedded around the circumference of the unit (See Appendix C). Azimuthal resolution can be provided by a single head with some form of either continuous or incrementally stepped rotation.

High longitudinal resolution can be achieved through an array of sensors or through processing where the synthetic aperture type of approach can be used. The total amount of traverse production can be attained by a long array and a long time on station between couplings and uncouplings. The current belief is that the configuration will involve one transmitter and four receivers. Four receivers will be used to provide the azimuthal resolution called for in the specifications. The velocity measurements will be made by the use of a timing pulse added into the received signal.

Although a number of manufacturers build acoustic velocity probes, several of which could be used, the actual hardware availability is extremely limited. Most of these manufacturers are service companies who do not sell equipment which they build. It is available as a leased service only. The best sources found to date for an acoustic probe seem to be Simplec, Inc. and Southwest Research Institute. Southwest Research Institute has developed an experimental dry-hole velocity tool. The pulses from the piezoelectric stack shown in Figure 3 [2] come from this instrument. Figure 4 [1] is a picture of the SwRI instrument. These two organizations seem to be the only viable sources for instruments of this type.

As far as CW imagers are concerned, Holosonics, Inc., is involved in a program for scanning the face of a tunnel in front of the cutting edge of the tool. However, at the present time there are no commercial systems using CW imagers.

2.3 SYSTEM CONSIDERATIONS

At this point in the preliminary development cycle, the dry hole pulse system is the preferred candidate. All indications are that the concept of dry hole pulse transmission is truly feasible. However, it is now necessary to consider a number of factors from the standpoint of total system trade-offs involving available component suppliers and the functions which these components must perform. Most of these have already been mentioned. The signal type and the bandpass at peak power that the unit must provide must be balanced to realistic requirements for the tool. The pulse repetition frequency and the duty cycle which the source can handle dictate the amount of heat which must be transferred into the borehole. This can limit

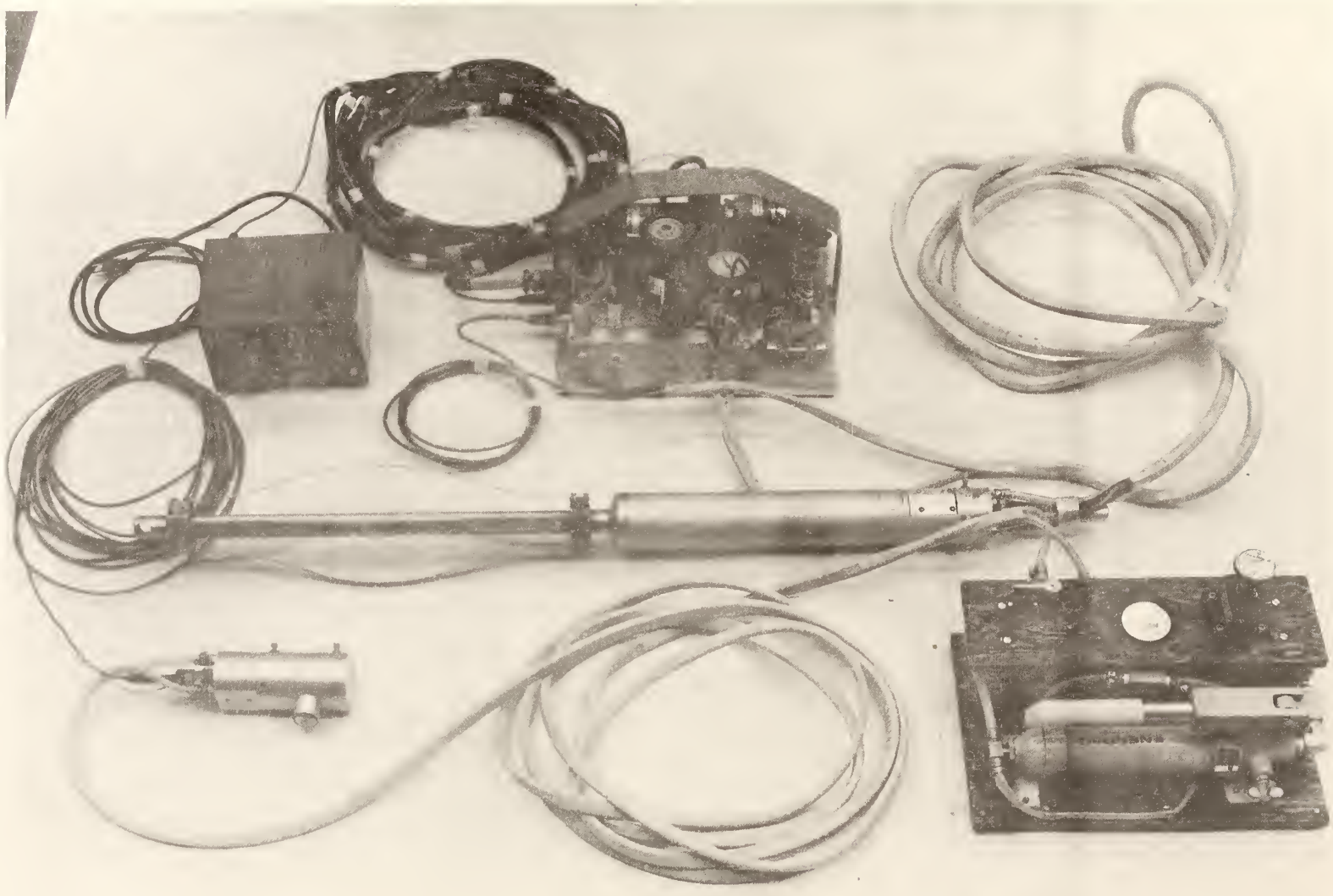

Figure 4. Laboratory model seismic velocity probe system. (Developed by Southwest Research Laboratory (1).

the traverse rate that can be obtained with this system. The physical size of the acoustic probe must be compatible with the borehole size. The lower frequencies required to achieve penetration in certain materials dictate the physical size of the magnetostrictive stack. In order to operate efficiently, their physical dimensions must be an appreciable portion of the lowest wavelength which they are expected to transmit. Thus, the stack must be as large as possible while still keeping the resonant frequency above the highest transmitted frequency. It will be necessary to evaluate the degree of compatibility which the existing acoustic components have when integrated into the whole system with the other types of probes and other system requirements. The physical restraints of the long borehole will reflect into system considerations from the standpoint of certain of the transducers. For example, the high-voltage systems required for an impulsive source cannot tolerate excessively long cables. This would imply that it would be necessary to package, in the limited downhole space, a high-voltage, high-energy discharge system which can be fed from a lower voltage source. All of these are factors which must be considered in the design. It is not sufficient to attempt to design the acoustic probe in a vacuum without considering the complete interplay between it and other probes involved.

There are discrepancies in the availability of the components necessary to fabricate a probe such as this. The majority of components are, however, available off-the-shelf. Some portions, principally the transducer contacting parts, will require additional development to meet the peculiar restraints of this program. Other factors which must be considered include reliability, safety, maintainability, potential traverse rates, and suitability of the signal to advanced signal processing techniques.

One candidate certainly is a magnetostrictive pulse system. It is safe, convenient, and highly reliable. There is ample field experience in collateral areas from which to draw concerning its overall operational suitability. Conversely, it may be limited in range when compared to a sparker. The sparker has many advantages, the chief of which is high power. It has been well proven in high-frequency acoustic surveys under the ocean. However, it does not currently exist in the dry borehole configuration of an oil-filled elastomeric bag. Should such a device become available before the prototype is built, it should definitely be considered for this application.

3. SUMMARY

In summary, the design has progressed to a point where the functional requirements of the components can be defined. We know the types of components which will be needed in the acoustic subsystem and the functional requirements of the system itself. The transmitter will have a signal energy output in the order of one tenth joule to possibly as high as 50 joules. This will depend upon whether the final transmitter is spark or magnetostrictive. These energies, when converted into peak and average power requirements, are sufficient to meet the range requirements for this system in many rock types. The system will have receiving transducers spaced around the periphery to provide azimuthal resolution of the signal.

The source coupling to the medium will be by a fluid-filled elastomeric sleeve. Receivers will be piezoelectric ceramic stacks coupled by hydraulic pistons to the wall. Operating as a standard velocity probe, this configuration will give the fundamental engineering modulii of the surrounding rock. Operating in an acoustic-pulsed echo mode, the system will have a high probability of resolving at least major discontinu-

ities under the majority of rock conditions out to a distance of 100 feet (30.5 m).

4. REFERENCES

1. Owen, Thomas E., Suhler, Sidney A., and King, James H., "Analysis of Borehole Seismic Velocity Tests - Nevada Test Center," Southwest Research Institute Project 14-4095-002, 21 May 1975.

2. Suhler, S. A., Winnie, D. S., and Owen, T. E., "A Laboratory Model Dry-Hole Velocity Probe and Permissible System Design for Operation in Coal Mines," SwRI Project No. 14-3706, 11 February 1974.

3. Bledsoe, J. D., "Development of a Tunnel System Model," Symposium -- The Technology and Potential of Tunneling, Volume I, pp. 183-188, South African Tunneling Conference, Johannesburg, South Africa, 1970.

4. White, J. E., Seismic Waves: Radiation, Transmission and Attenuation, McGraw-Hill, New York, 1965.

APPENDIX F

GROUND-PROBING RADAR

TABLE OF CONTENTS

BACKGROUND STATEMENT

The purpose of this Appendix is to introduce the monocyclic pulse radar, list some typical radar parameters, give some recent measurements of electrical properties of various types of rocks, and obtain estimates of the maximum radar range within the various rock types. While the presentation is somewhat different, this Appendix is essentially a condensation of recent work by Dr. John C. Cook, "Radar Transparencies of Mine and Tunnel Rock," Geophysics, Vol. 40, No. 5 (Oct. 1975), pp. 865-885.

GROUND-PROBING RADAR

ABSTRACT

Ground-probing radar, utilizing short, monocyclic pulses, has been developed for subsurface exploration. The maximum radar range in subsurface media is strongly dependent, among other things, on the attenuation factors of the particular environment and the frequencies in the transmitted pulse. Laboratory measurements on samples of several rock types as a function of frequency have provided estimates of their attenuation factors. These factors are employed in the radar range equation, using realistic radar and target parameters, to estimate the maximum radar range as a function of frequency for a monocyclic pulse radar in various types of rocks. The results indicate that the maximum range decreases with increasing frequency. A maximum range in excess of 100 ft (30.5 m) appears to be achievable in granites and limestones at frequencies on the order of 100 MHz, but will be limited to about 10 ft. (3.1 m) or less in shales and gouge material at 100 MHz. The target is assumed to be a rough surface, oriented normal to the wavefront, and at least as large as the first Fresnel zone. This type target is expected to be representative of various discontinuities of significance in tunneling such as faults, fracture zones, boundaries between rock masses, large water-filled cavities, and voids. System reliability, sources of error, limitations and general performance of a monocyclic pulse radar for detection of rock discontinuities from within horizontal boreholes are discussed.

GROUND-PROBING RADAR

1. INTRODUCTION

The basic monocyclic pulse radar, also referred to as subsurface video pulse radar [2], impulse radar [3], ground-probing radar [4], and electromagnetic sounder [5], was first proposed and demonstrated by Cook in 1956 [1]. Its subsequent development has been largely stimulated by the need to remotely detect buried objects and map features of subsurface structure, as implied by its several names. Notable recent achievements include detection of tunnels through as much as 230 feet (70.2 m) of dry dolomite [5]; the location of interfaces through 28 feet (8.54 m) of coal [4]; detection of faults, joints cavities, and lithologic contrasts (to a depth of 40 feet, or 12.2 m) in soft rock and detection of plastic and metal pipe in the overburden [2]. Other achievements include: penetration to depths of 75 feet (23 m) in a Massachusetts glacial delta and greater than 230 feet (70.2 m) in an Antarctice ice shelf; detection and mapping of various utility lines and pipes; profiling of river and lake bottoms and subbottoms; measurement of fresh and sea water ice thickness; and detection of ice in permafrost [3]. It has very recently been successfully employed from a helicopter to obtain a rapid profile of snow-covered ice [6] and a radar logging capability for drill holes is under development [4]. A major breakthrough is reported [12] in more hostile rock (schistose gneiss) in a project which is covered more fully in Appendix M (Vol. II, Part 2) of this report.

2. RANGE-RESOLUTION

The major attributes of the monocyclic pulse radar are its capability to detect targets at close ranges, and to discriminate between targets closely spaced in range (range resolution)

while operating at low enough frequencies to achieve practicable penetration, or range, in lossy subsurface media. These capabilities are primarily dictated by the transmitted pulse characteristics. The transmitted pulse is approximately a half-cycle of radio frequency (rf) energy (hence called monocyclic) in the time domain, which constitutes a wide spectrum (hence often called video) in the frequency domain.

This is unlike most conventional pulse radars which radiate a pulse-modulated continuous wave containing many cycles of rf energy. The restriction to a narrow half-cycle (or nearly half-cycle) pulse in the monocyclic pulse radar permits a very short transmitter on-time and hence the receiver can be turned on quickly following the transmission. This minimizes receiver dead-time which permits detection of close-in targets. Also, the narrower the pulse, the greater the range resolution. The pulse width τ and high-frequency content in the pulse are related by $\tau = \frac{1}{f}$. Thus, the narrower the pulse, the higher its frequency content. However, subsurface media are generally dispersive at radio frequencies with the attenuation rate being greater at the higher frequencies. Thus, there is a compromise between the maximum range attainable (range increases with decreasing frequency) and the range resolution (resolution increases with increasing frequency).

Because subsurface media are dispersive, the range resolution is also a function of range. As the pulse, which contains a band of frequencies, propagates through the medium, the higher frequency components are attenuated more rapidly than the lower frequency components. This loss of high-frequency content with increasing range results in reduction in the accuracy with which the time of arrival of the received pulse can be measured. Hence, the greater the range, all else being equal, the less the range resolution.

3. PRACTICAL LIMITATIONS

Monocyclic pulse radars developed so far typically have pulse widths of 2 to 70 nanoseconds (corresponding to frequency components as high as 15 to 500 MHz), pulse repetition frequencies of a few hundred Hertz, peak powers of 10's of watts (although they can be much higher) can generally be operated monostatic (transmitter and receiver are co-located) or bistatic (separated antennas) and with linear single or crossed polarization [7]. The monocyclic pulse radar is still in its early stages of development. The more critical design areas are probably the antennas and pulse characteristic. The designs of these are interdependent and also depend upon the environment, intended application, and operational constraints. There is much yet to be learned about the radar capabilities and limitations. Specific applications generally require, at least to some extent, specific design considerations. The maximum range attainable is generally a major consideration in most applications. Attention is now turned to estimates of the maximum range in various rock environments.

3.1 RANGE LIMITATIONS

The maximum range at which a target can be detected by the radar depends upon the radar system parameters, type of signal processing, target characteristics, and the characteristics of the propagation media. The radar equation (Equation 1) will be employed to examine the range dependence in various types of rock. Monocyclic pulse radar parameters that have been obtained in practice will be employed. Characteristics of rock environments will be based on laboratory measurements of their electrical constitutive parameters. The target characteristics are estimated in the form of a radar cross section. The analysis is on the basis of single-pulse detection (i.e., no signal enhancement is assumed by integration or other signal processing techniques).

3.2 RADAR-RANGE EQUATION

The radar transmission equation in free space is given by [8]:

$$P_r = \frac{P_t G_t G_r \sigma_r \lambda^2}{(4\pi)^3 R^4} \qquad (1)$$

where the symbols are defined as:

P_r = received signal power at antenna terminals (watts)

P_t = transmitted peak power at the antenna terminals (watts)

G_t = transmitting antenna power gain

G_r = receiving antenna power gain

σ_r = radar target cross section (meters squared)

λ = wavelength (meters)

R = radar to target distance (range)(meters)

Equation 1 is applicable in the far-field. The far-field of an antenna is at ranges greater than approximately $2D^2/\lambda$ where D is the largest linear dimension of the antenna [8]. The radar equation given above is for free space propagation where attenuation by the propagation medium is negligible. It must be modified for application in a lossy, or attenuating, medium such as subsurface rock environments. The modification is readily obtained by recalling that the phase and attenuation factor for plane, cylindrical or spherical waves is given by $e^{-\gamma R}$ where R is the range and $\gamma = \alpha + i\beta$ is the wavenumber [9]. The symbols α and β denote the attenuation and phase factors, respectively, and are given by [9]

$$\alpha = \omega \sqrt{\frac{\mu\varepsilon}{2}\left(\sqrt{1 + \left(\frac{\sigma}{\omega\varepsilon}\right)^2} - 1\right)} \quad \text{neper/meter} \qquad (2)$$

and

$$\beta = \frac{2\pi}{\lambda} = \omega \sqrt{\frac{\mu\varepsilon}{2}\sqrt{1 + \left(\frac{\sigma}{\omega\varepsilon}\right)^2} + 1} \quad \text{radians/meter} \qquad (3)$$

where ω is the radian frequency, μ is the magnetic permeability of the medium (normally assumed the same as $\mu_o = 4\pi \times 10^{-7}$ henry/meter for free space), $\varepsilon = \varepsilon_r \varepsilon_o$ is the dielectric constant of the medium, ε_r is the relative dielectric constant of the medium, $\varepsilon_o = 8.854 \times 10^{-12}$ farads/meter is the dielectric constant of free space, and σ is the conductivity of the medium in mhos/meter.

The power in an electromagnetic wave is proportional to the square of the absolute magnitude of the field quantities. Hence, the phase and attenuation factors for the power in the wave are $|e^{-\gamma R}|^2 = |e^{-(\alpha+i\beta)R}|^2 = (e^{-R\alpha})^2 = e^{-2\alpha R}$. This represents the attenuation after propagating a range R. The radar equation includes the range to and from the target, hence the modification to the radar equation to account for attenuation will be $e^{-4\alpha R}$. A further modification to the radar transmission equation that places it in a more useful form is to define the received signal-to-noise power ratio P_r/P_n where P_n is the noise power level in the receiving system [8]. The noise power level P_n determines the minimum signal power P_r that can be detected. Including the modification $e^{-4\alpha R}$ and writing the radar Equation 1 in terms of the signal-to-noise power ratio gives

$$\frac{P_r}{P_n} = \frac{P_t G_t G_r \sigma \lambda^2 \, e^{-4\alpha R}}{P_n (4\pi)^3 \, R^4} \qquad (4)$$

It is customary in radar analysis to treat the minimum single pulse signal-to-noise power ratio as $(P_r/P_n)_{min} = 1$. Note from Equation 4 that the statement that the received signal-to-noise power ratio is a minimum implies, with other factors held constant, that the range is a maximum. Setting the single pulse $(P_r/P_n)_{min} = 1$ establishes a convenient basis against which various signal enhancement techniques, most of which are equivalent to the integration of some number of pulses, can be compared. The single pulse P_r/P_n is employed here, but it is noted that improvements in the probability of detection in excess of 15 db are readily achieved by integration [8].

In order to establish a reasonable estimate of the radar cross section σ_r, Cook [1] suggests that practical targets such as fault planes and the surfaces of caverns and abandoned mine workings will be reasonably flat but too rough for coherent, specular reflection. In this case, the first arriving radar echo will be from the nearest point on the reflecting surface, at range R, and will include contributions from all parts of the surrounding circular area that are within the distance $R + \lambda/4$ from the radar. This is the first Fresnel zone and Cook [1] employs its area as the radar cross section

$$\sigma_r = \pi \left(\frac{\lambda R}{2} + \frac{\lambda^2}{16}\right) \simeq \pi \frac{\lambda R}{2}. \tag{5}$$

The radar cross section is, in general, a difficult factor to compute except for targets of simple shape and is usually obtained by measurement in practice. The σ_r of Equation 5 is used here.

3.3 MAXIMUM RANGE

Before proceeding to an examination of the maximum range, it is interesting to examine the transmission loss, called the total propagation loss (T.P.L.) by Cook [1], as a function of range.

Norton [10] defines the transmission loss, denoted here as T.P.L., in decibels as

$$\text{T.P.L.} = 10 \log \left(P_t/P_r \right). \tag{6}$$

Substituting Equations 4 and 5 into 6 and assuming the transmitter and receiver share the same antenna (i.e., $G_t = G_r = G$) yields

$$10 \log \left(\frac{P_t/P_n}{P_r/P_n}\right) = 10 \log \frac{P_t}{\rho_r} = \text{T.P.L.}$$

$$= 10 \log \left(\frac{128\pi^2 R^3}{G^2 \lambda^3}\right) + 10 \log e^{-4\alpha R} \tag{7}$$

or

$$T.P.L. = 10 \log \left(\frac{128\pi^2 R^3}{G^2 \lambda^3}\right) - 2R\,(20\alpha \log e). \qquad (8)$$

But $20\alpha \log e = 8.686\alpha$ nepers/unit distance = A db/unit distance. Thus,

$$T.P.L. = 10 \log \frac{128\pi^2 R^3}{G^2 \lambda^3} - 2RA(db) \qquad (9)$$

Cook [1] further defines a measurable "performance figure" (P.F.) in decibels as

$$P.F. = 10 \log (P_t/\text{minimum detectable signal}). \qquad (10)$$

The minimum detectable signal is $P_{r_{min}} = P_n$ for the single pulse case, and from Equation 7 for $P_r = P_{r_{min}}$

$$T.P.L. = 10 \log \frac{P_t/P_n}{P_r/P_n} = 10 \log (P_t/P_{r_{min}})$$

$$= 10 \log (P_t/P_n) = 10 \log (P_t/P_r) = P.F. \qquad (11)$$

Cook [1] has measured the performance figure for existing radars and found them to be on the order of 100 to 110 db, but suggests that in theory the values of 200 to 230 db should ultimately be feasible.

Equation 9 is now employed, using the values of G = 4 and λ = 3.28 feet (1.00 m) obtained for an existing radar [1], to plot T.P.L. as a function of R for values of A between A = 0 and A = 1 db/ft = 3.28 db/m in Figure 1. These values of A are representative of a wide range of rock types.

The maximum range achieved and identification of the medium using a radar having P.F. = 105 db are shown in Figure 1 along the T.P.L. = 105 db line.

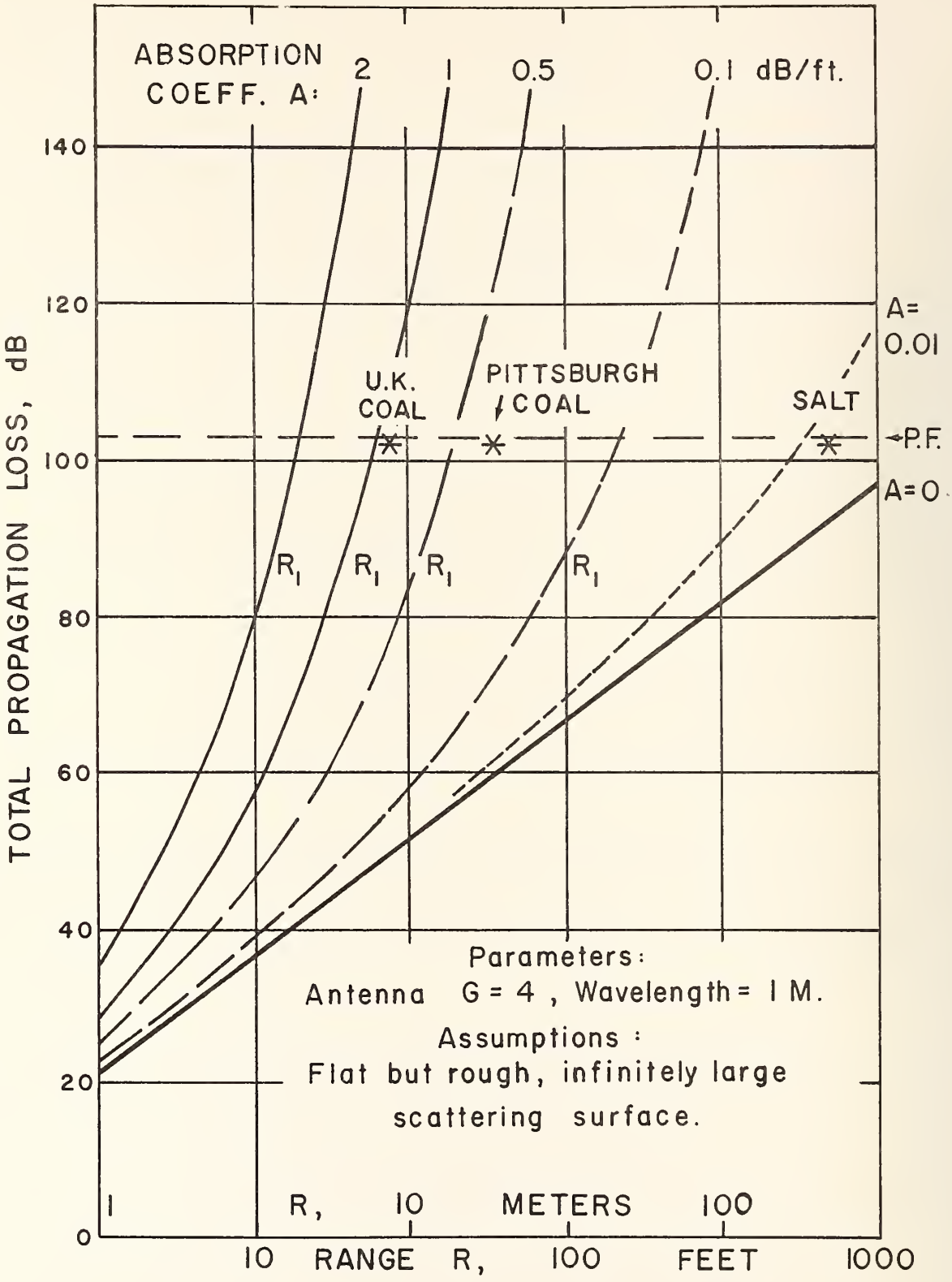

Figure 1. Calculated transmission loss as a function of range and attenuation rate.

Figure 1 shows that the greater the attenuation rate, the greater will be the transmission loss at a particular range. Or, the greater the attenuation rate, the less will be the attainable range for a given transmission loss. The figure also shows that the rate of transmission loss increases with increasing range for fixed attenuation rates. This implies that incremental improvements in system performance will result in smaller increments of range improvement as the range increases.

Figure 1 does not reveal the frequency dependency of the range. This is of major importance and will now be examined. Before proceeding to estimates of attenuation based on measurements of specific rock samples, Equation 9 will be examined with the assumption that the attenuation rate varies directly with frequency. This is generally observed in practice, and Cook [1] employs an rf loss "constant" for rock of $L = A/f$ to specify the frequency dependency. In order to account for all frequency dependent factors, the maximum antenna gain is expressed as $G = 4\pi a^2/\lambda^2$ where a^2 is the aperture area [8]. From Equation 3 with the approximation of $\frac{\sigma}{\omega\varepsilon} << 1$, which is generally true for rock environments at frequencies of interest here, one obtains $\beta = 2\pi/\lambda \simeq \omega\sqrt{\mu\varepsilon}$. This gives

$$\lambda \simeq c/f\sqrt{\varepsilon_r}$$

and $$G \simeq 4\pi a^2 f^2 \varepsilon_r / c^2$$

where $c = 3 \times 10^8$ meter/sec is the velocity of light in vacuum. Substituting these values of L, G and λ into Equation 9 with $(P_r/P_n)_{min} = 1$ (which implies that the range is a maximum, as mentioned) gives

$$P.F. = T.P.L. = 10 \log (8R^3_{max}\, c/a^4\, f\sqrt{\varepsilon_r}) + 2R_{max}\, fL \qquad (12)$$

where R_{max} denotes the maximum range.

Curves of R_{max} as a function of frequency and rock constant are obtained from Equation (12) and plotted in Figure 2 for T.P.L. = P. F. = 100 and 200 dB, for the assumed aperature dimension of a 3.28 ft. (1 m) and assumed value of $\varepsilon_r = 4$. The assumption of $a^2 = 10.8$ ft.^{2} (1 m^2) is based on the fact that the antenna aperture is generally limited in practical applications. The assumption of $\varepsilon_r = 4$ is based on the fact that the ε_r of competent rock generally varies over a small range (approximately 2 to 10) and it does not significantly influence the results of Equation (12) [1].

In Figure 2, the value of L = 0 dB corresponds to free space propagation. The figure clearly illustrates the relatively large effect of attenuation in restricting the maximum range as compared to free space propagation. For example, at 1 GHz and P.F. = 100 dB, the R_{max} = 6.560 feet (2000 m) in air but R_{max} 91.8 feet (28 m) in a relatively low loss rock with L = 1 dB/m=GHz). The curves also indicate that R_{max} tends to increase initially with frequency at the low frequencies and then decrease thereafter with the knee of the curves tending to lower frequencies with increasing L. The decrease in R_{max} with frequency above the knee of the curves is approximately proportional to $f^{-0.9}$.

The chief application of Figure 2 is in the selection of the radar system parameters of frequency and performance figure needed to obtain specified maximum ranges in rock for which the loss constant is known [1].

4. EXPERIMENTAL WORK IN ELECTRICAL PROPERTIES OF ROCK

If the values of the dielectric constant and conductivity for the rock medium of interest are known (or measured) as a function of frequency, the attenuation rate A as a function of frequency can be computed directly from Eq. 2. These values of A can then be used to compute the loss constant L, or A may be employed directly

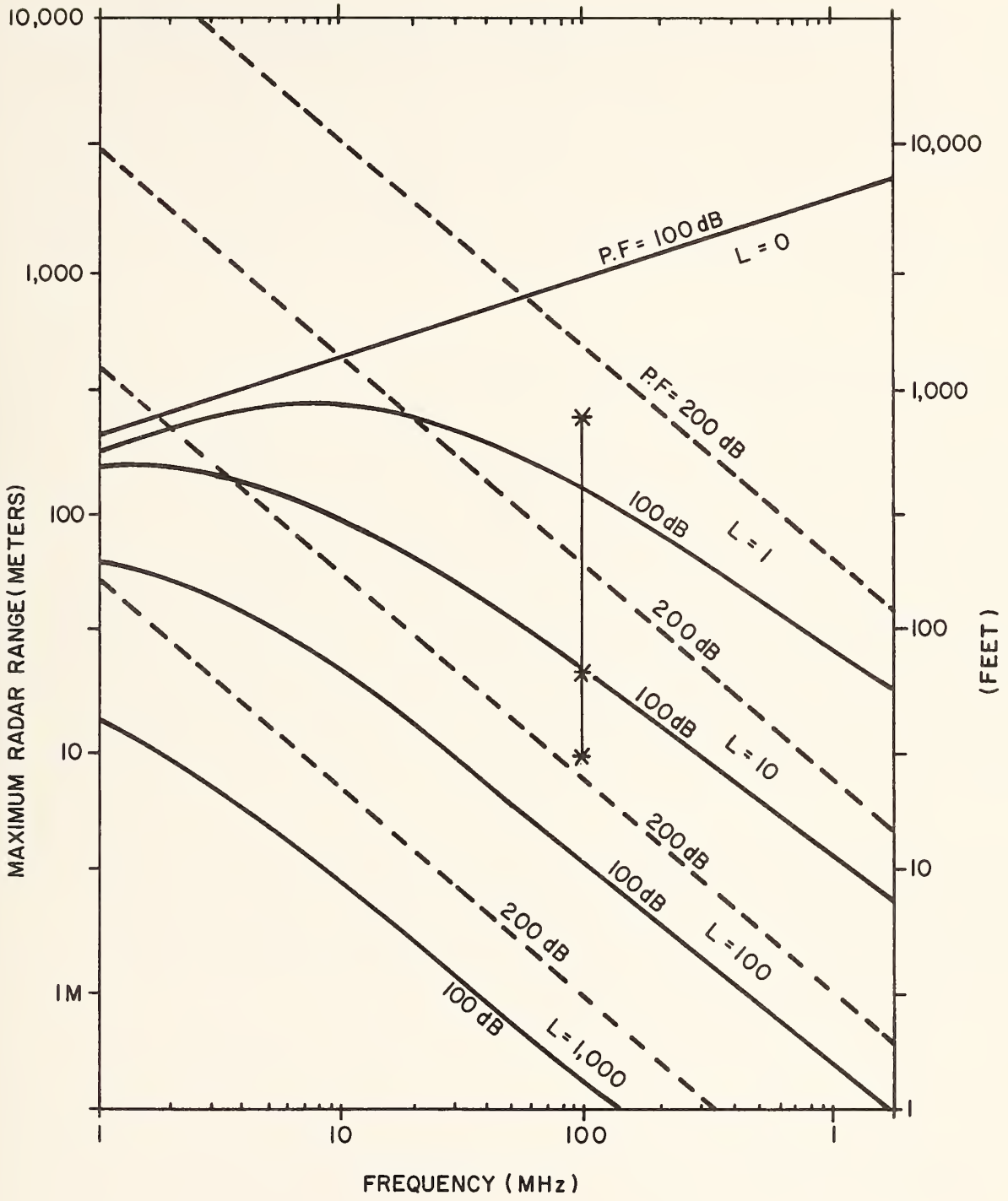

Figure 2. Maximum radar range as a function of frequency, radar performance figure (P.F.) and rock loss constant (L in dB/M-GHz)

in Equation 12 where A = fL. Cook [1] has measured the conductivity and dielectric constant as a function of frequency for several types of rock in laboratory tests of the samples. Resultant values are summarized in Tables 1 through 7 for seven types of materials. These results include measurements of wet and dry samples. For a discussion of the method and details of measurement and the listing of other parameters measured, the reader is referred to [1].

Using A = fL in Equation 12, one obtains:

$$P.F. = T.P.L. = 10 \log (8R^3_{max}\, c/a^4 f\sqrt{\varepsilon_r}) + 2\, R_{max} A$$

The values of A may be determined directly from Tables 1 through 7 for each material, and ε_r is given directly. Using P.F. = 100 and 150 db and again assuming a = 1m, values of R_{max} as a function of frequency are computed for each material of Tables 1 through 7 and plotted in Figure 3. The stars correspond to the maximum ranges achieved by Cook [1] as shown in Figures 1 and 2.

The work of Cook was extended from 100 to 1,000 megahertz for several suites of typical rock and gouge under this contrast. The experimental work and results are covered in Appendix K (Volume II, Part 2) of this report.

Table 1. Conductivity σ and relative dielectric constant ε_r of schist from Washington, D.C. (values of σ are in millimhos/meter).

1 mHz		5 mHz		25 mHz		100 mHz	
σ	ε_r	σ	ε_r	σ	ε_r	σ	ε_r
0.746	7.4	1.222	5.4	2.062	4.8	4.082	4.5
0.621	7.1	1.064	5.4	1.919	4.8	4.082	4.5
0.247	6.0	0.541	4.8	1.029	4.2	1.361	3.9
0.521	6.8	0.901	5.1	1.515	4.4	2.717	3.9
0.238	4.8	0.578	3.9	1.220	3.5	2.857	3.6
0.877	6.4	1.488	4.9	2.770	4.1	4.525	3.8

Table 2. Conductivity σ and relative dielectric constant ε_r of granite from Switzerland (values of σ are in millimhos/meter).

1mHz		5 mHz		25 mHz		100 mHz	
σ	ε_r	σ	ε_r	σ	ε_r	σ	ε_r
0.007	2.5	0.042	2.7	0.070	2.5	0.455	2.4
0.122	3.0	0.286	2.7	0.465	2.6	0.149	2.6
0.016	3.0	0.062	3.08	0.143	2.96	0.391	2.5
0.153	3.78	0.213	3.2	0.311	3.06	0.159	2.6
						0.159	2.5
						0.154	2.3
						0.145	2.4
						0.909	2.7
						0.408	2.96
						0.417	3.10

Table 3. Conductivity σ and relative dielectric constant ε_r of limestone from Italy (values of σ are in millimhos/meter).

1 mHz		5 mHz		25 mHz		100 mhz	
σ	ε_r	σ	ε_r	σ	ε_r	σ	ε_r
0.328	7.1	0.820	5.0	1.724	4.0	1.266	3.7
0.167	5.0	0.388	4.8	1.042	4.5	2.857	3.6
0.022	3.8	0.088	3.5	0.323	3.6	2.545	3.7
0.027	4.1	0.091	3.7	0.222	3.15	0.943	4.1
0.043	5.6	0.160	5.1	0.442	3.6	1.923	4.2
0.120	5.6	0.280	5.1	0.535	4.6	5.556	3.4
0.072	5.4	0.190	5.1	0.588	4.7	0.794	3.4
				0.617	4.2	0.400	3.35
						0.980	3.5
						2.358	4.7
						2.427	4.8
						1.887	5.2

Table 4. Conductivity σ and relative dielectric constant ε_r of shales from Canada and New York (values of σ are in millimhos/meter)

1 mHz		5 mHz		25 mHz		100 mHz	
σ	ε_r	σ	ε_r	σ	ε_r	σ	ε_r
9.709	85.0	14.706	31.0	13.889	8.3	45.455	5.5
11.111	96.0	15.152	30.0	8.850	8.15	40.0	6.6
1.220	27.0	5.128	18.0	30.303	16.0	90.909	12.0
0.248	14.0	1.653	8.3	25.641	13.0	66.667	8.8
2.632	24.0	3.650	8.6	16.949	9.6	43.478	6.1
2.591	23.0	3.546	15.0	6.757	5.1	18.868	3.5
0.120	1.(?)	0.230	1.(?)	6.098	5.0	2.346	4.3
0.119	2.7	0.238	2.3	5.814	4.7	10.417	4.1
0.139	3.0	0.294	2.5	0.513	1.(?)	1.064	1.(?)
				0.465	2.0	1.0	1.9
				0.625	2.1	1.639	2.0

Table 5. Conductivity σ and relative dielectric constant ε_r of coal and clay from Ohio (values of σ are in millimhos/meter).

1 mHz		5 mHz		25 mHz		100 mHz	
σ	ε_r	σ	ε_r	σ	ε_r	σ	ε_r
0.020	3.68	0.117	3.59	0.567	3.48	2.183	3.30
0.024	3.66	0.117	3.59	0.551	3.36	2.326	3.29
0.034	3.97	0.163	3.82	0.759	3.55	2.959	3.39
0.122	5.58	0.426	4.82	1.449	4.31	5.464	3.98
0.095	5.16	0.324	4.59	1.238	4.09	4.739	3.86
0.086	4.61	0.314	4.06	1.145	3.67	4.016	3.46
0.111	5.33	0.415	4.73	1.425	4.95	4.202	3.78
0.116	5.32	0.395	4.43	1.355	3.94	4.785	3.70
0.119	5.68	0.405	4.80	1.488	4.31	5.208	4.02
0.235	7.03	0.746	5.48	2.611	4.45	8.621	3.93
0.282	7.62	0.844	5.63	2.618	4.60	7.937	3.95
0.353	8.19	0.963	6.15	2.717	4.94	9.524	4.42
0.354	7.95	0.887	5.81	2.660	4.78	8.264	4.26
0.474	9.09	1.225	6.46	3.356	5.09	9.901	4.39
1.368	16.60	2.915	9.35	6.024	6.66	15.974	5.74
1.350	15.40	2.710	8.84	5.814	6.38	14.184	5.44
1.330	14.10	2.469	10.60	5.435	6.42	13.680	5.54
2.941	67.80	11.628	39.40	37.594	21.50	131.752	13.60
2.033	46.60	9.709	33.40	29.851	19.10	100.908	13.4

Table 6. Conductivity σ and relative dielectric constant ε_r of gouge material from New Mexico (values of σ are in millimhos/meter).

1 mHz		5 mHz		25 mHz		100 mHz	
σ	ε_r	σ	ε_r	σ	ε_r	σ	ε_r
0.439	9.44	0.926	7.07	2.725	5.88	7.143	5.09
0.840	17.80	2.833	10.20	8.772	6.58	24.390	5.20
0.847	21.90	2.924	13.60	9.009	9.22	23.202	7.02
4.000	17.40	6.289	13.10	14.815	8.42	41.494	6.44
22.936	32.80	23.148	20.00	32.680	14.10	69.930	10.20
16.779	33.60	20.000	19.80	32.895	11.70	75.188	8.33
64.516	34.30	64.935	20.90	70.423	16.10	120.482	12.40
0.758	11.70	1.701	7.87	4.202	8.35	9.259	5.32
0.068	2.93	0.231	5.08	0.565	4.84	2.299	4.78
0.127	6.14	0.273	5.25	0.893	5.03	3.731	5.24

Table 7. Conductivity σ and relative dielectric constant ε_r of coal from Pittsburgh (σ is in millimhos/meter). Data are averaged from Table 2, reference [11].

1 mHz		5 mHz		25 mHz		100 mHz	
σ	ε_r	σ	ε_r	σ	ε_r	σ	ε_r
0.047	3.19	0.217	2.89	0.794	2.64	1.835	2.47
0.008	2.36	0.030	2.34	0.133	2.21	0.647	2.14
0.009	2.63	0.051	2.49	0.165	2.36	0.769	2.21

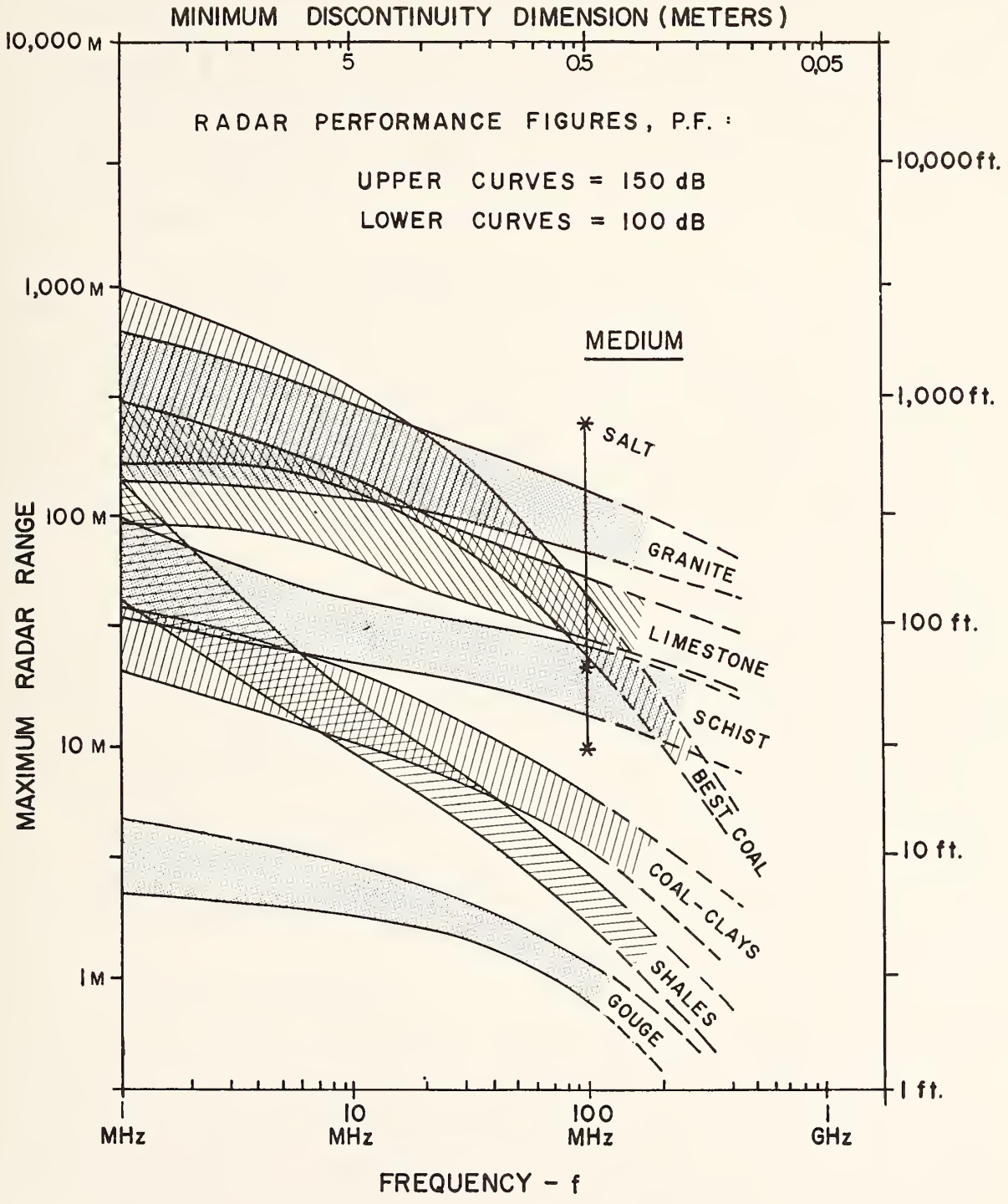

Figure 3. Maximum radar range in typical rock as a function of frequency and radar performance figure.

5. RANGE-RESOLUTION RELATED TO ROCK TYPES

Figure 3 shows that the maximum range achievable depends strongly on the rock type and the frequency. In all cases, the maximum range decreases with increasing frequency. Greater ranges can be achieved in the harder rock, such as granite and limestone. Shale and gouge, however, because of their greater attenuation rate, severely limit the maximum range. Figure 3 shows that maximum ranges of 100 feet (30.5 m) or more are achievable in limestone, granite and some coals at frequencies as high as 100 MHz . For the other coals, schist, shales and gouge materials examined, ranges of 100 feet (30.5 m) do not appear to be achievable even at frequencies as low as 10 MHz. In particular, gouge materials are strongly attenuating and limit the maximum range to a few feet even at frequencies as low as 1 to 10 MHz.

The theoretical performance estimates depicted in Figure 3 provide valuable guidelines in the design of a monocyclic pulse radar for borehole application. The close agreement between the predicted range and measured ranges at 100 MHz tends to confirm the validity, at least qualitatively, of the system parameters and target characteristics employed. Recall also that the P.F. of 100 db is achieved with present monocyclic pulse radar systems and, with system improvements and signal integration techniques presently within the state-of-the-art, the P.F. of 150 db is a realistic estimate.

6. SYSTEM PERFORMANCE EXPECTATIONS

It is premature to specify the optimum system parameters or to accurately predict its performance in operation. Experimentation with such systems in boreholes in rock environment will almost surely be required to firmly specify design and performance parameters and criteria.

However, considerable information is available on the radar system design and performance in other environments and on the types of geologic structures of most interest in tunneling. It seems appropriate to utilize this information and extrapolate from the performance predictions obtained here to examine, albeit qualitatively, the types of targets that might be detectable and point out possible sources of error, reliability and system limitations to be considered in the system design.

6.1 RELIABILITY VERSUS MINIATURIZATION

In terms of system reliability, there appears to be no reason that the system hardware cannot be made sufficiently rugged, waterproof, shock and vibration hardened, temperature and pressure insensitive and otherwise environmentally proofed for field handling and operation inside boreholes. Radar technology is quite advanced. Due to spacecraft, man-portable and similar radar developments, miniaturized radar components and subsystems are available as off-the-shelf items in many cases such that even developmental models and prototypes can be fairly advanced. Further, it has been demonstrated that electromagnetic pulse radar having a peak power of 10 kw into the antenna can be operated in small-diameter boreholes (the sonde was five inches (12.7 cm) in diameter) at in-hole temperatures in excess of 170°F (76.7°C) and at pressures on the order of 10,000 psi (68.948×10^6 Newtons/m^2) [5].

6.2 SYSTEM LIMITATIONS

There are system limitations. The range limitation is perhaps the most serious for general subsurface investigations. The maximum range depends upon the radar system parameters, type of host rock (or bulk medium), and characteristics of the target. For most host rock types, other than gouge materials, a maximum range of some 10 feet (3 m) to 200 feet (61 m) or so appears likely for a monocyclic pulse radar operating at the center frequency of 100 MHz (see Figure 3). It is pointed out that gouge material (or gouge zones) is expected to be a target rather than a host material, in general, and use of the results of Figure

3 in gouge for assessing radar range performance in rock presents an overly pessimistic view.

6.2.1 RANGE

The maximum range, of course, depends on the frequency. The monocyclic pulse radar transmit a narrow pulse in the time domain, which comprises a wide band of frequencies. A bandwidth of 120 MHz centered around 100 MHz is a typical value [3]. From Figure 3, it is clear that the maximum range will not be the same for all frequencies comprising the pulse. The higher frequencies will be attenuated at a greater rate and hence will not achieve the same range as the lower frequencies. The capability to resolve closely spaced targets, to accurately measure range and target extent, and to detect targets very close to the radar also depend on frequency, or equivalently, the pulse width. The narrower the pulse, the better the range resolution, but the higher the frequency content of the pulse with the attendant higher attenuation at those frequencies. Hence, a relatively wide pulse will allow the greater range but with poorer range resolution while a relatively narrow pulse will restrict range but improve range resolution. It is noted that range resolution decreases with increasing range in either case due to the greater attenuation rate of the higher frequency components of the pulse. There are thus limitations on the maximum range resolution as well as range. The main controlling parameter for both is the pulse width and they present opposing requirements on it. Hence, some compromise may be needed. It should perhaps be noted that a compromise between pulse width and bandwidth is a fundamental physical one and not unique to the monocyclic pulse radar. It is a basic consideration in virtually all pulse systems whether they are intended for digital communications, data transmission, radar application or other. However, it is not unusual to employ a variable pulse width to minimize compromises in performance. This is a consideration in the design of the monocyclic pulse radar. A remotely controlled pulse would greatly enhance the flexibility and capability

of the radar. It would permit detailed examination of the target structure at close ranges (narrow pulse) while allowing the detection of gross structures to the maximum range (wide pulse). Further, examination of the targets using different pulse widths would provide additional information on the target (target response is a function of frequency) and hence serve to aid in data interpretation. An adjustable pulse width would also provide flexibility for operating in an optimum manner in different type rock. Thus, while there are limitations to the range resolution achievable, compromises between the two may be minimized and additional capabilities in target data obtained by incorporation of a variable pulse width capability.

6.2.2 RESOLUTION

As a qualitative estimate of resolution, assume minimum pulse width of 2 nanoseconds, which corresponds to frequency components at 500 MHz. Point targets whose dimensions are about $\lambda/4$ and layered structures whose interfaces are separated by about $\lambda/4$ represent reasonable lower bounds as efficient reradiators [8,9]. Assuming a typical relative dielectric constant of 4 for rock, This then gives $\lambda/4 = \simeq$ 3 inches (0.075 m) at 500 MHz. Hence, at the shorter ranges (limited by the attenuation at 500 MHz which could conceivably allow ranges of 100 to 200 feet (30.5 to 61 m) in granite) the maximum resolution is on the order of 3 inches (76 mm). The maximum achievable range (with a wide pulse and poor resolution) is on the order of 1646 feet (500 m) or so, at 10 MHz (see Figure 3 for granite). These would appear to be reasonable bounds on the limitations in the range and resolution. Practical considerations may restrict them further.

6.2.3 DIRECTIVITY

There are other potential limitations. The ability to resolve target positions in planes normal to the borehole is a potential one. Achieving antenna directivity in the transverse plane is not straightforward within the space limitations imposed by the boreholes diameter [perhaps some 6 inches (15 cm), or so]. This

represents a subject for critical laboratory tests in the design phase. However, it is noted that a high degree of directivity is not required to achieve a high degree of target position resolution in the longitudinal or circumferential directions. This is because the targets are stationary in space and the antenna can be rotated and moved longitudinally which, through subsequent data processing, allows the formation of virtual antenna arrays in these directions. This can greatly enhance target circumferential and longitudinal position resolution. The amount of signal processing required to achieve a given resolution will depend on the degree of inherent antenna directivity that can be achieved. The greater the inherent directivity, the less the processing. However, with the use of high-speed digital computers, the data processing does not appear to be an overly restrictive problem provided some degree of inherent directivity is provided. Achieving adequate inherent antenna directivity in the longitudinal direction appears straightforward by simply array techniques. It remains, however, to determine the better approach to achieving inherent circumferential directivity.

6.2.4 ANTENNA LIMITATIONS

The antenna designs, however, pose a potential limitation in general. Their impedance must be matched to the medium for efficient radiation and their dimensions, in particular the length, are critical to realizing the pulse width [2]. Impedance matching to achieve sufficient coupling of energy into the environment is not expected to be a major problem. Adequate radiation (i.e., antenna matching) is achieved in surface systems in the presence of relatively large variations in the intrinsic impedance of the surface medium [3]. However, some empirical efforts will probably be required to arrive at the better matching arrangement. Antenna design to accommodate a range of pulse widths may be far more difficult. Conceivably, a number of antenna lengths and matching networks could be pre-designed and provided such that the proper combination

is automatically selected when a particular pulse width is selected. The practicability of this approach requires careful consideration. The critical laboratory tests performed by Dr. Cook under this contract and reported in Appendix (Volume II, Part 2) provide valuable insights and guidance as to the better approach and the degree of flexibility that can be designed into the antennas.

6.3 SOURCES OF ERROR

In terms of potential errors, the measurement of the range is probably the more obvious. The time elapsed between pulse transmission and reception can be converted directly to range to the target if the velocity of propagation is known. However, the velocity of propagation depends on the electrical properties of the medium and is generally not known in advance. However, if core samples are available, the rock type and hence its electrical properties may be estimated. Also, if prominent localized targets are encountered as the system moves along the borehole, the range as a function of movement will appear as a hyperbola. This defines a curve which is uniquely described by the velocity and travel time, and hence permits velocity to be computed. Also, if a bistatic system is employed having at least two receive antennas at different distances along the borehole from the transmitter, a common data point measurement of targets in general may be made to accurately determine range [3]. Hence, minimization of errors in range measurement appears to be possible in a number of ways.

The more serious errors and uncertainties will probably be in data interpretation, in general. Valuable guidance should be possible through theoretical analysis with various simplified models. However, the complexities of the environment are probably such that direct experimentation in known environments will be required to remove ambiguities, establish definite target signatures, and improve the theoretical models.

7. TENTATIVE PERFORMANCE SPECIFICATIONS

Specification of the overall radar performance and capabilities to detect specific targets of interest in tunneling will also require experimentation. However, some qualitative performance projections can be made on the basis of the theoretical performance depicted in Figure 3 and known rock characteristics of importance in tunneling. First, the most serious problems encountered in tunneling are associated with rock instability which, in many cases, is associated with joints and fractures oriented parallel or subparallel to the tunnel (borehole) axis (see Appendix B). The radar performance in Figure 3 is based on a radar cross section representing a surface of discontinuity so oriented and of dimensions at least comparable to the first Fresnel zone and, hence, represents estimates of the maximum range of detection for such joints and fracture zones. It is also representative of the maximum detection range for large cavities (air or water filled), gouge zones, and discontinuities in general that present extended surfaces oriented approximately parallel to the borehole axis and with dimension at least comparable to the first Fresnel zone. Their thickness should also be on the order of $\lambda/4$ or more and their electrical characteristics different from the bulk media. Further analysis is required, however, to quantatively establish reflection coefficients and radar cross sections for different materials and dimensions likely to be encountered at discontinuities in practice. Orientation of the planes of discontinuity is less critical to detection for a bistatic system, due to the angles of reflection involved. It is interesting to note that such planar types of discontinuities are analogous to the horizontal stratification in general and oblique layering in lake bottoms, for example, that have been successfully detected and mapped with monocyclic pulse radar [3]. A series of planer type discontinuities oriented parallel or subparallel to the borehole can be expected to produce a signature that depicts constructive and destructive interference as a function of range. A series of closely spaced discontinuities would appear to be indicative of a poor rock quality (see Appendix B).

Planes of discontinuity (joints, fracture zones) which intersect or are orthogonal to the borehole should also be detectable upon traversal of the discontinuity if transverse polarization is employed. Further, the thickness of the planes of discontinuity intersecting the borehole is probably not critical to their detection by transverse polarization. An analogy is the detection of buried pipes and thin wires with surface radar [3].

In general, planes of discontinuity (e.g., faults, fractures, boundaries) and regions of discontinuities in general (water or air-filled cavities, gouge zones, etc) will scatter, reflect and/or diffract the incident electromagnetic energy. Major discontinuities can be expected to exhibit large reflection coefficients or radar cross sections. Such discontinuities, and hence the radar returns, are directly related to the major problems of rock instability and water in-flows encountered in tunneling (see Appendix B). Final system capabilities and limitations will depend on other factors as well as the technical ones. In particular, the degree of flexibility and versatility that can be cost effectively incorporated (e.g., variable pulse width, longitudinal and transverse polarization, antenna array size, matching networks, etc.) will be a major consideration. It seems clear that the radar can detect rock discontinuities of significance in tunneling, but design, operational and economic trade-offs beyond the scope of this task are required to provide more quantitative performance estimates. A number of these are covered more fully in Appendix K (Volume II, Part 2).

8. REFERENCES

1. Cook, John C., "Radar Transparencies of Mine and Tunnel Rock," Geophysics, Vol. 40, No. 5 (Oct. 1975), pp. 865-885.

2. Moffatt, David L., "Subsurface Video Pulse Radars," Proc. of Subsurface Exploration for Underground Excavation and Heavy Construction, ASCE, August, 1974.

3. Morey, Rexford M., "Continuous Subsurface Profiling by Impulse Radar," Proc. of Subsurface Exploration for Underground Excavation and Heavy Construction, ASCE, August, 1974.

4. Cook, John C., "Status of Ground-Probing Radar and Some Recent Experience," Proc. of Subsurface Exploration for Underground Excavation and Heavy Construction, ASCE, August, 1974.

5. Dolphin, Lambert T., Bollen, Robert L., and Oetzel, George N., "An Underground Electromagnetic Sounder Experiment," Geophysics, Vol. 39, No. 1, February, 1974.

6. Morey, Rexford M., "Personal Communications".

7. Response to ENSCO, Inc. - conducted "Questionnaire on Subsurface Radar," initiated by L. A. Rubin, March, 1975, (unpublished).

8. Skolnik, Merrill I. (Editor), Radar Handbook, McGraw-Hill, New York, 1970.

9. Ramo, S. and Whinnery, John R., Field and Waves in Modern Radio, John Wiley and Sons, New York, 1953.

10. Norton, K.A., "Transmission Loss in Radio Propagation-II," NBS Technical Note No. 12, 1959.

11. Cook, John C. "RF Electrical Properties of Bituminous Coal Samples," Geophysics, Vol. 35, No. 6, 1970.

12. Rubin, L.A., Griffin, J.N., and Still, W.L., "Final Report, Phase I--Feasibility of Subsurface Site Investigation by Electromagnetic Radar," NSF (RANN) Grant APR75-13414, ENSCO, Inc., March 31, 1976.

APPENDIX G

ELECTRICAL RESISTIVITY PROBES

TABLE OF CONTENTS

BACKGROUND STATEMENT

The choice of sensor types and sensor ensembles was one of the most critical features of the program. This study analyzes the key features of resistivity probes as potential candidates for the sensor system. It was written early in the program and subsequently updated as the overall system configuration evolved.

ELECTRICAL RESISTIVITY PROBES

ABSTRACT

A resistivity probe is a candidate sensor for the horizontal borehole sensory system. The spaced electrode logging method, which measures the average resistivity of the medium around the borehole, is the oldest and most widely accepted routine method used in borehole logging. By judicious choice of the in-hole electrode spacing and array design, the method is capable of measuring the resistivity of resistant zones oriented normal, oblique or concentric to the borehole. The method does not yield circumferential resolution but can, to some extent, control the volume (or range) over which measurements are representative. The measurements encompass the medium to deep ranges comparable to the source/detector electrode spacings. Because of its established reliability, the spaced electrode method is customarily used to provide a back-up in more complex logging operations. This is a specific purpose in this application as well as to provide independent data.

There are standard types of arrays, or electrode spacings, for use in standard logging operations. Some designs are subject to greater error than others. Typical sources of error, performance curves, methods of data interpretation and array designs for various standard type arrays are discussed. Because of the relative simplicity of the theory for data interpretation and array design, quite arbitrary spaced electrode arrays can be designed to accommodate a range of requirements. A flexible lateral array configuration is presented to illustrate the major features required in the spaced multiple electrode array application.

ELECTRICAL RESISTIVITY PROBES

1. HISTORY

Spaced logs were the first type of geophysical well logs used [1]. From the early development of geophysical well logging, which occurred around 1920, until the late 1930s, spaced logs were the only type of geophysical measurements made routinely in boreholes. From about 1940, electric logging has been supplemented by methods based on other measurements, such as radioactivity and acoustic wavespeed, but the measurement of resistivity remains a fundamental measurement. Most well logging measurements now being made use induction logging devices as the primary tool. This has come about because with an induction logging system, the volume of ground from which the response is obtained can be sharply restricted, and induction logs give highly detailed records of the variation of resistivity along a borehole. Resolution is obtained at the cost of increased complexity and reduced reliability of the logging device. Whenever an induction logging device is run in a borehole, a more reliable single-spaced electric resistivity log is also run to provide a backup.

Spaced logs are a direct application of conventional surface-based resistivity techniques. The essential feature is that four or more electrode contacts are used, with at least two serving as current supply electrodes and at least two being used to detect voltage. The use of different electrodes for current supply and for measurements makes it possible to control to some extent the volume of rock over which resistivity is being determined.

Because of the relative simplicity of the theory for direct current flow in conductive media [2] meaningful values of resistivity can be derived from measurements made with quite

arbitrary geometric arrays of electrodes along a borehole. To avoid problems which arise in comparing resistivity measurements made in different boreholes with different arrays, in the early days of commercial development of logging, the companies involved went to considerable lengths to standardize the arrays of electrodes used in electric logging. As a consequence, virtually all logs run commercially are of two array types, which will be discussed in more detail in following paragraphs. However, a point to be made here is that in considering the use of spaced-electrode resistivity surveys for boreholes, it is not immediately obvious that the standard arrays will be the best arrays for a new application. The criteria and techniques for array design are well developed, however, and new array design poses no new problems.

2. NORMAL ARRAYS

The simplest of the commonly used arrays is the "normal" electrode array, as shown in Figure 1. With the normal array, two of the four electrodes, one of which is a current electrode, A, and the other of which is a measuring electrode, M, travel with the sensing head of the logging tool. The other current electrode, B, and the other measuring electrode, N, remain at the surface, or are installed on the logging cable so that they are far enough removed from the sensing head that they have no effect on the measurement. The normal array is characterized by the separation between the electrodes A and M, a distance which is called the "spacing" of the array. In oil well practice, the most commonly used spacings are 16" (40.6 cm) and 64" (1.6 m) (short and long normal logs, in the trade terminology). Analysis shows that the measured voltage is affected to a measurable extent by resistivities in the medium roughly out to a distance comparible with this spacing.

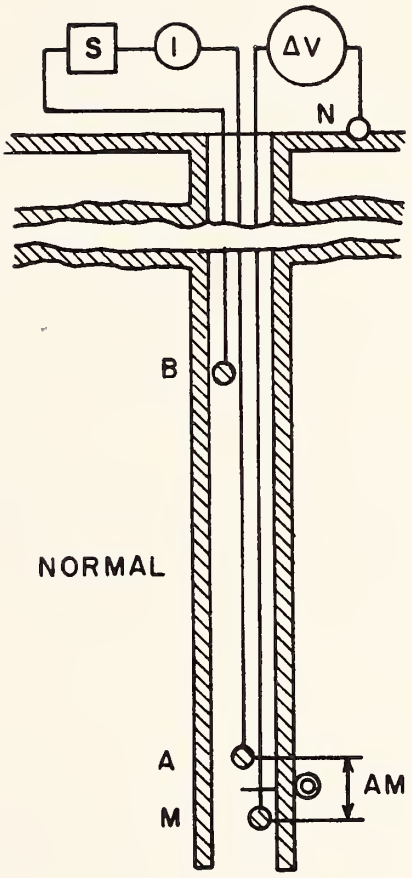

Figure 1. Schematic electrode arrangement for normal resistivity curve. After L. G. Chombart, Factors Involved in Practical Electric Log Analysis (Wichita, Kansas: Schlumberger Well Surveying Corporation, 1949).

Computation of apparent resistivity ρ_a from measurements of voltage and current made with a normal array are based on the assumption of point electrodes situated in a homogeneous medium. Then,

$$\rho_a = 2\pi a \frac{V_m}{I_A} \qquad (1)$$

where a is the $\overline{AM}$ separation and V_m and I_A are the measured values of voltage and current, respectively. Then, more complicated distributions of resistivity are analyzed by observing how values of apparent resistivity change along the borehole, or with spacing. Resistivity changes which occur along planes intersecting the borehole are best studied by observing the pattern of apparant resistivity along the borehole, while resistivity changes that occur at interfaces concentric with the borehole, or not intersecting the borehole, are best studied with resistivity measurements made using a sequence of spacings.

The theory for determining resistivity patterns for any geometry of real resistivity values is straight-forward and well advanced. All such analyses are based on the solution of Laplace's equation

$$\nabla^2 U = 0 \qquad (2)$$

where U is the electric potential throughout the medium. The method of solution depends on the nature of the interfaces separating regions with different resistivities. If these interfaces are a sequence of parallel planes either normal to or inclined to the axis of the borehole, the simplest approach is the use of a series of Kelvin images. If the interfaces are in part concentric cylinders about the borehole, a solution of Laplace's equation by the Hankel transform method provides tractable results. If the shape of the interface is more arbi-

trary, a solution to eq. (2) can be obtained by integrating a Green's function over the interface by numerical methods or by using a finite-difference method. All of these are described in the basic treatises on electric logging [2,3,4] and extensive catalogs of responses for various earth models have been compiled.

Many of the features of the behavior of the normal array are summarized in the computed profiles in Figure 2. Here are shown the apparent resistivity curves that would be recorded on passage of a normal array through a high-resistivity zone of limited extent. If the zone is relatively thick compared to the AM spacing, (Fig. 2a), the response of the logging system records the actual resistivity faithfully except for short transition zones at the boundaries. (On these computed curves, the dashed ones refer to measurements made in a drained borehole, while the solid curves refer to measurements that would be made with the hole filled with slightly conductive water). If the thickness of a high-resistivity zone is comparable to the $\overline{AM}$ spacing (Fig. 2b), the response of a normal logging array is less reliable, with the peak value being significantly less than the actual resistivity. This erroneous response becomes most pronounced when the thickness of the resistant zone is less than the $\overline{AM}$ spacing (Fig. 2c), in which case, the apparent resistivity passes through a minimum as the electrode array passes the resistant zone.

The essential characteristics of the response of a normal logging array are that the recorded resistivity profile has a simple symmetric form, and records the actual resistivity faithfully if the dimensions of various zones are considerably larger than the $\overline{AM}$ dimension of the array. This behavior poses a quandary for the designer; large spacings are required for deep sensing of resistivities, but short spacings are necessary in order to obtain resolution required to detect thin zones. Usually, this problem is solved by using several spacings with widely different dimensions.

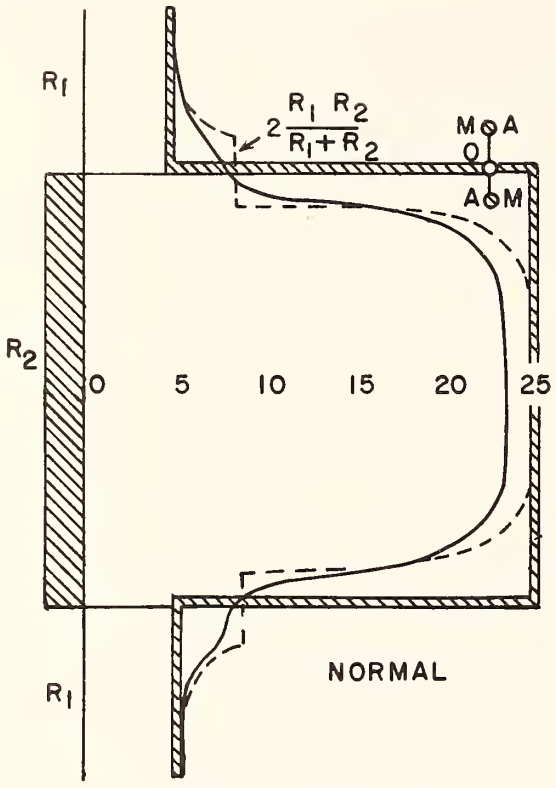

a. Normal curve shape--
thick resistive bed.

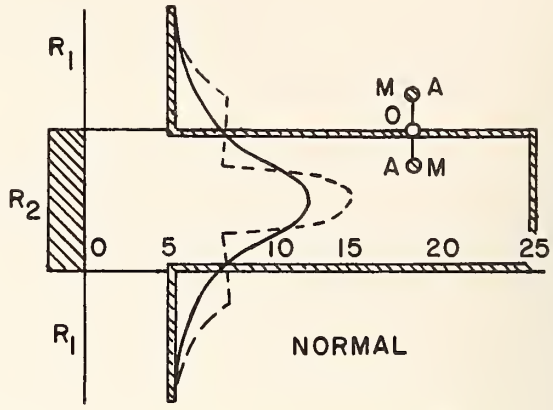

b. Normal curve shape (e=2AM).

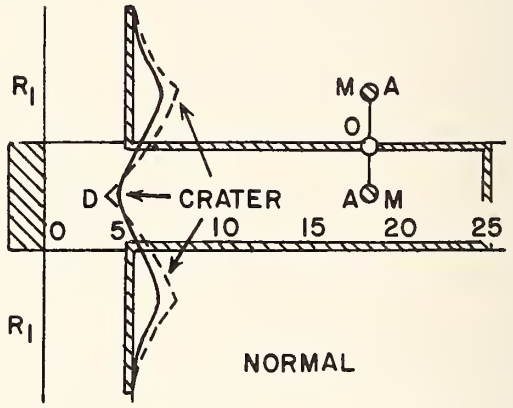

c. Normal curve shape (e=AM).

Figure 2. Normal curve shapes. Figures after L. G. Chombart, Factors Involved in Practical Electric Log Analysis (Wichita, Kansas: Schlumberger Well Surveying Corporation, 1949).

The use of several normal spacings to obtain information about the variation of resistivity as a function of distance from the borehole, rather than as a function of distance along a borehole, is illustrated in Figure 3. This illustration shows a method for cross-plotting two resistivity values, one recorded with a 16 inch (40.6 cm) normal array and the other recorded with a 64 inch (1.6 m) normal array. It is assumed in compiling this chart that the resistivity bed thickness is relatively large, so that the apparent resistivity recorded at the center of a zone is a reliable value. The physical dimensions for which the chart is valid are indicated; the borehole diameter is 7-7/8' (20 cm), and is surrounded by an annular region of resistivity, R_i, that is different than the resistivity at larger distance, R_t. The quantity R_m is the resistivity of the material filling the borehole, and D_i/d is the ratio of the diameter of the annular region to the diameter of the borehole. The various curve parameters indicate the resistivity contrasts between the various zones. In practice, values of apparent resistivity recorded with the two normal arrays are used to define the abscissa and ordinate of a single point on the plot; then the dimensions of the areas with different resistivites are determined from the parameters of the pair of curves passing through that point. With more than two resistivity measurements, a similar type of interpretation can be made using each pair of values, when the appropriate families of curves are available.

In the example shown in Figure 3, it is assumed that the diameter of the annular zone is known to be 120 inches (3.05 m), measured possibly by acoustic or radar means. The measured resistivity on the 64-inch (1.6 m) and 16-inch (41 cm) normal arrays are 325 and 230 ohmmeters respectively. The borehole fluid is measured to be 10 ohmmeters. Thus, the respective resistivities of the inner shell and the outer country rock are 150 and 400 ohmmeters.

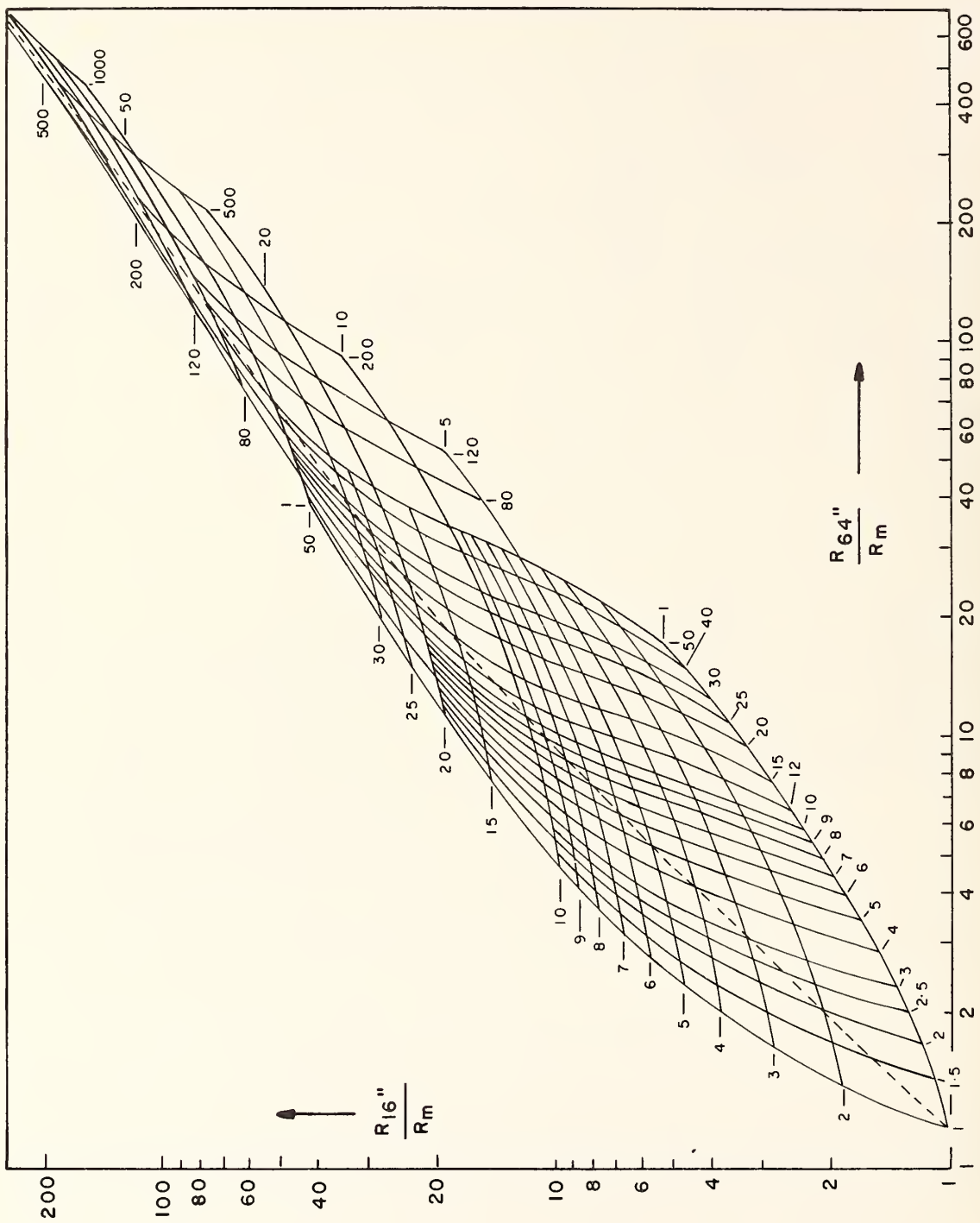

Figure 3. Cross-plotting of two resistivity values.

3. LATERAL ARRAY

The problem of studying resistivity in thin zones can be attacked by using a somewhat different electrode array, the lateral array, shown in Figure 4. Here, three moving electrodes are used in the borehole, and only one is fixed remotely on the logging cable or at the surface. One of the moving electrodes, A, is used to provide current, and this is returned to a remote electrode, B. Voltage is then detected with a closely-spaced pair of electrodes, M and N, on the moving tool. If the $\overline{NM}$ separation is much smaller than the AM orAN spacing, then the $\overline{MN}$ pair can be considered to be a dipole pair. The ratio of voltage to dipole length is approximately equal to the electric field component in the $\overline{MN}$ direction. With the lateral array, apparent resistivity in a uniform medium is computed using the formula:

$$\rho_a = \pi \frac{\overline{AO}^2}{\overline{MN}} \cdot \frac{V_{MN}}{I_{AB}} \qquad (3)$$

where $\overline{AO}$ and $\overline{MN}$ are the distances indicated on Figure 4. The spacing of the lateral array is defined as the distance $\overline{AO}$, and this represents the distance into the medium at which there is a significant sensitivity to the presence of resistivity boundaries.

The response of the lateral array as it traverses a resistant zone is quite different than that of a normal array (see Figure 5. Here, it may be seen that apparent resistivity values portray the presence of a thick zone rather faithfully (Figure 5a), and that as the zone becomes thin relative to the electrode spacing, a peak in apparent resistivity is seen even when the layer is quite thin compared to the spacing. The lateral array does not fail to respond to a single thin layer, as does the normal array. However, there is a "fluid" zone in the

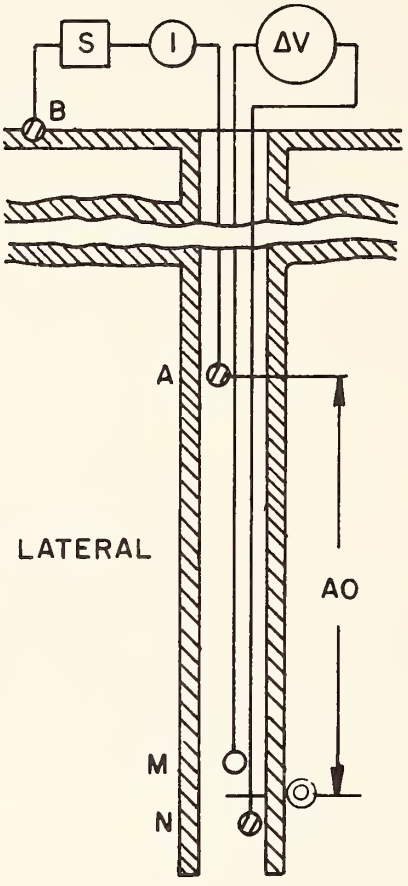

Figure 4. Schematic electrode arrangement for lateral resistivity curve. After L. G. Chombart, Factors Involved in Practical Electric Log Analysis (Wichita, Kansas: Schlumberger Well Surveying Corporation, 1949).

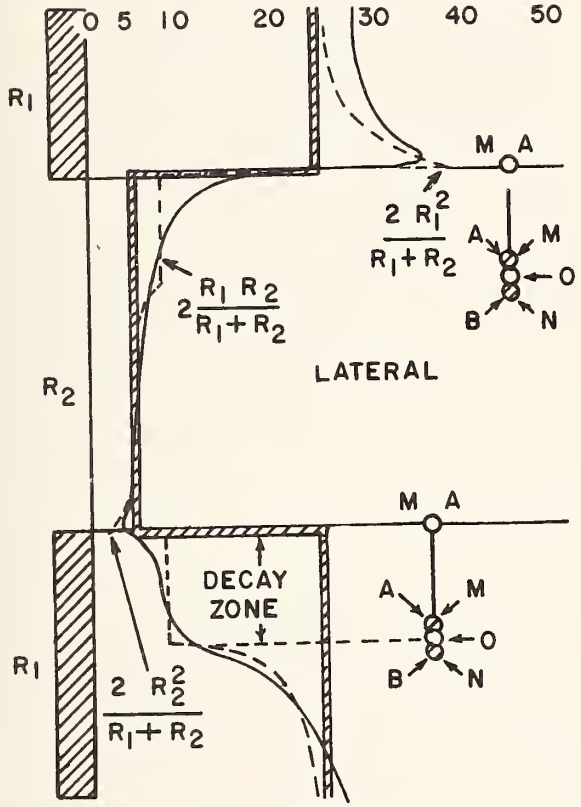

a. Lateral curve shape--thick conductive bed.

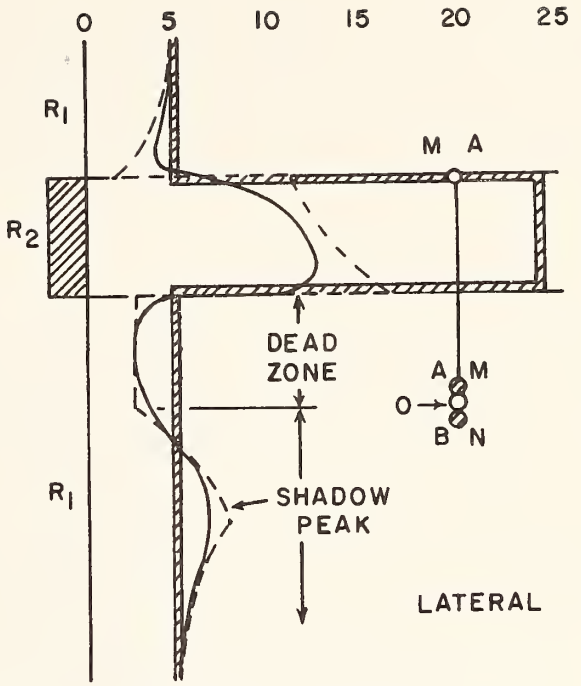

b. Lateral curve shape--resistive thin bed (e=1/2 AO).

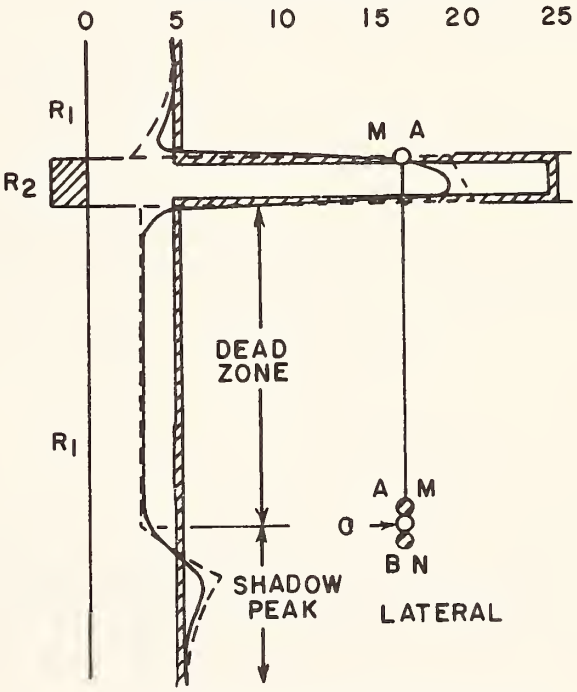

c. Lateral curve shape--resistive thin bed (e=AO).

Figure 5. Lateral curve shapes. Figures after L. G. Chombart, Factors Involved in Practical Electric Log Analysis (Wichita, Kansas: Schlumberger Well Surveying Corporation, 1949).

response of a lateral array as it passes through a resistant layer. If a second resistant layer were present in the fluid zone, which lies between the electrode pair $\overline{MN}$ and the current electrode A, it will be poorly represented on the log.

4. LIMESTONE ARRAY

In contrast to the normal array, the lateral array does not generate a symmetric curve on passing through a boundary in resistivity. For example, if the electrode array is reversed in a borehole, the position of the blind zone can be shifted from one side to the other of resistant zones. As a consequence, there is often an advantage in recording lateral logs with both orientations of the array along the borehole. Such an array of two lateral arrays is sometimes called a "limestone" array (5) (see Figure 6). Such an array has been used in the past for detection of thin, water-bearing zones in resistant rock such as limestone.

5. DESIGN REQUIREMENT

In view of the wealth of interpretive material that has been built up for the standard logging arrays, there would be an advantage in using these standard arrays in new applications. Let us now consider the design requirements for such systems.

5.1 FREQUENCY

First of all, we should consider the AC frequency which can be used and yet have the flow of current characterized by Laplace's equation. The condition for this to be true with no more than 2% error in computed responses is as follows:

$$\omega < \frac{0.02}{\mu\sigma L^2} \qquad (4)$$

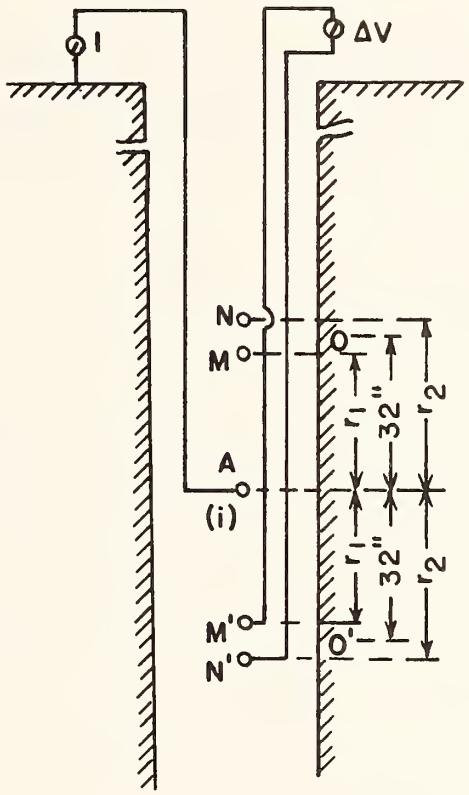

Figure 6. Schematic measuring arrangement for the 32-inch limestone sonde. After Wright and Pirson, "Porosity-Profile Determination from Electric Logs," Bull. Am. Assoc. Petroleum Geol., Vol. 35, No. 2 (1952), p. 299.

where ω is frequency in radians per second, μ is magnetic permeability ($4\pi \times 10^{-7}$ Henrys per meter), σ is the maximum value of conductivity in mhos per meter to be routinely recorded, and L is the maximum spacing to be used. Setting L = 30 meters and σ = 0.1 mho/m, we find that the maximum permissible frequency is about 177 radians per second (about 28 Hertz).

5.2 POWER

Next, we need to know what the power requirements are. This also is done quite simply by inverting either equation (3) or (1). Considering the lateral array [equation (3)], the amount of current needed is:

$$I = \pi \frac{\overline{AO}}{\overline{MN}}^2 \cdot \frac{V_{MIN}}{\rho_{MIN}} \qquad (5)$$

where V_{MIN} is the lowest voltage which can be recorded faithfully and ρ_{MIN} is the lowest value of resistivity which is to be recorded routinely. Taking $\overline{AO}$ = 30 meters, $\overline{MN}$ = 1 meter, $V_{MIN} = 10^{-4}$ volts and ρ_{MIN} = 10 ohm-meters, we have

$$I = 3.1416 \times \frac{30^2}{1} \cdot \frac{10^{-4}}{10}$$

$$= 28.3 \text{ milliamperes.}$$

5.3 CONTACT RESISTANCE

The voltage needed to drive this amount of current into the rock depends on the quality of contact that can be made with the electrode A in the borehole (with electrode B located at the ground surface, its resistance can be reduced to arbitrarily low values). The contact resistance in the borehole can be evaluated approximately using curves developed by Tagg [6].

Curves for elongate cylindrical electrodes are shown in Figure 7 for a rock resistivity of 50 ohmmeters. For a two-foot (0.6 m) electrode wedged in a 3-inch (7.6 cm) hole, the grounding resistance would be roughly 100 ohms. The contact resistance is a linear function of the resistivity of the medium, so that in a rock with a high resistivity (1000 ohmmeters), the contact resistance would be about 2000 ohms. At the other end of the range of resistivities, say 10 ohmmeters, the grounding resistance would be roughly 20 ohms. To provide 28.3 milliamperes of current to a 20 ohms grounding circuit would represent a power requirement of approximately 16 milliwatts.

As the resistivity and the grounding resistance increase, less current is needed to provide a measurable voltage of 10^{-4} volts at the receiver electrodes. Consequently, no greater power is required in high resistivity rock. However, if a simple constant-current logging system is used, provision of 28.3 milliamperes of current to a grounding resistance of 2000 ohms would require about 1.6 watts.

6. ILLUSTRATIVE CONFIGURATION

The 30-meter lateral array considered here requires higher operating power than any shorter lateral or normal array, and so consideration of this one array specifies the maximum power required by a system with several electrode arrays. Because fabrication of expandable, contacting electrodes is required, the system to be used in the present application should attempt to use a small number of electrodes in various combinations to provide a large number of spacings. One such array is shown in Figure 8.

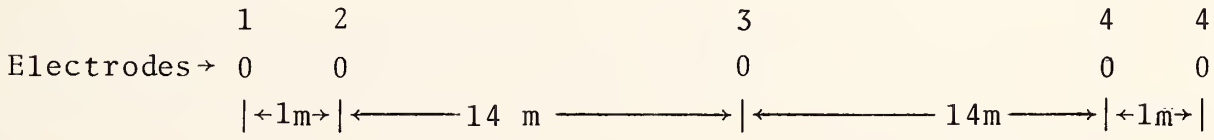

Figure 8. Composite electrode array.

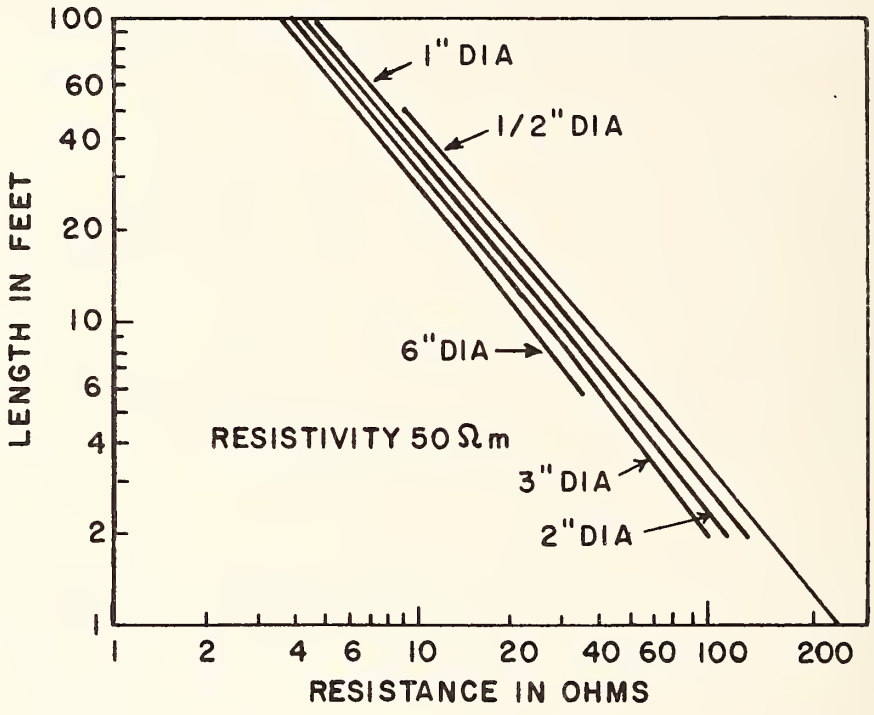

Figure 7. Resistance of driven rod calculated from ellipsoid formula.

Here, the following arrays can be formed by interchanging the roles of the five electrodes by using a simple stepping switch.

1. 1→A; 2→M; 1 meter spacing normal array
2. 1→A; 3→M; 15-meter spacing normal array
3. 1→A; 5→M; 30-meter spacing normal array
4. 3→A; 1, 2→M,N; 14.5 meter spacing lateral array
5. 3→A; 4,5 →M,N; reversed 14.5 meter spacing lateral array
6. 5→A, 1, 2→M,N; 29.5 meter spacing lateral array
7. 1→A, 4, 5→M,N; reversed 29.5 meter spacing lateral array
8. 1,5→A, A'; 2, 4,→B, B' and 3=M, 14.5 meter limestone array

Other arrays can also be made. The better design for the subject borehole application will depend on overall system considerations as well as resistivity measurement requirements.

7. DISCUSSION

The resistivity probe array of paragraph 6 should be considered as illustrative of the use of multiple electrodes to achieve different array configurations. There are several system trades which must be made before a final configuration can be specified.

The probe must have a length equal to, or greater than, the probing depth. Thus, it will be long and slender. Its configuration may have to depend upon such factors as the location of the in-hole thrust device. Does it pull or push the probe? The resistivity probe differs from the other sensors being considered in that it measures bulk characteristics rather than locations of interfaces. Thus, it could be of greatest value when used in conjunction with these instruments. It could act as a bell ringer to alert the operator to significant changes in the surrounding medium, which could then be more precisely located by the acoustic or radar probes.

Resistivity probes in their own right can obtain range resolution by use of multiple spacing of electrodes. The degree to which

this should be exploited will depend upon the sensitivity and interpretability of the data from the other probes.

Fortunately, the resistivity device is a very simple tool. Its development can lag that of the other two sensors if necessary to define the best configuration to support the system.

8. CONCLUSION

The concept which should be employed would be to consider the probe not as a single unit but rather as an unspecified number of single electrodes. These can then be assembled in any configuration of numbers and spacings, the selection being made on the basis of the operational problem to be solved. The electrodes would be stepped through a sequence of configurations, possibly by a patch board programmable stepping relay. This would provide the most flexible configuration for the problem at hand.

9. REFERENCES

1. Schlumberger, C. and M., and E.G. Leonardon, "Electrical Coring: A Method of Determining Bottom Hole Data by Electrical Measurements," AIME Geophysical Prospecting, 1934.

2. Keller, G. V., and F.C. Frischknecht, Electrical Methods in Geophysical Prospecting, Pergamon Press, Oxford, 1966, 517 pp.

3. Dakhnov, V.M., "Geophysical Well Logging," Colorado School of Mines Quarterly, Vol. 57, no. 2, 1962, pp 1-445.

4. Pirson, S.J., Handbook of Well Log Analysis, Prentice-Hall, Englewood Cliffs, N.J., 1963, 326 pp.

5. Wright, T. R., and S.J. Pirson, "Porosity Profile Determination from Electric Logs," Bull Am. Associ. Petr. Geol., Vol. 36, No. 2, 1952, pp. 299.

6. Tagg, G. F., Earth Resistances, Pitman, N.Y., 1964, 258 pp.

APPENDIX H

SIGNAL PROCESSING TECHNIQUES APPLICABLE TO SUBSURFACE INVESTIGATION OF ROCK MASSES THROUGH BOREHOLES

TABLE OF CONTENTS

BACKGROUND STATEMENT

A study was performed to determine how computerized processing of sensor data can enhance the interpretability of the data.

This appendix covers that topic from a theoretical viewpoint, leading to suggestions of certain processes which seem relevant.

Another appendix (M) makes reference to experimental results carried out on radar sensing data in metamorphic rock.

SIGNAL PROCESSING TECHNIQUES APPLICABLE TO SUBSURFACE INVESTIGATION OF ROCK MASSES THROUGH BOREHOLES

ABSTRACT

Signal processing techniques and computer programs have been in use, particularly in the seismic industry, for some time and are widely used today. These programs take the raw signals recorded in the field and process them to enhance the detectability of geologic structures that are small, distant, or of low contrast and to improve the geometric representation of the structures in terms of distance, direction, attitude, size and configuration. Some of these techniques were modified and used for a similar application; i.e. for processing signals received from subsurface radar used for investigation of rock masses through pilot tunnels and eventually through boreholes. A description of these signal processing techniques is given in this section.

The techniques described are Digitizing, Background Removal, Whitening, Filtering, Velocity Analysis, and Migration. The functional description, and in some cases the mathematical background, of these techniques is given. Appropriate illustrations are used to aid the description. Relevant references are cited at the end of the appendix.

SIGNAL PROCESSING TECHNIQUES APPLICABLE TO INVESTIGATION OF ROCK MASSES THROUGH BOREHOLES

1. INTRODUCTION

There are a number of standard signal processing techniques and resulting software packages that are commonly used today, particularly in the seismic industry, that are extensively described in the literature.

Basically, these processing techniques serve two purposes:

- to enhance the detectability of geologic structures that are small, distant, or of low contrast, and
- to enhance the geometric representation of structures in terms of distance, direction, attitude, size, and configuration.

A description is given in this section of those signal processing techniques that can be applied directly or with minor modifications for processing signals received and recorded from subsurface acoustic and electromagnetic radar used for investigation of rock masses through tunnels or boreholes.

The following techniques will be described:

- Digitizing - to convert the analog field data into the requisite format for computer processing.
- Background Removal - to remove the background noise from the raw field data.
- Whitening - to enhance weak signal returns from features of interest.

- Filtering - to remove interference and noise from the data.
- Velocity Analysis - to obtain the velocity function to be used in the Hyperbolic Stacking process.

2. SIGNAL PROCESSING TECHNIQUES

2.1 DIGITIZING

The raw data will be recorded in the field on an analog FM tape recorder. For processing by digital computers, this data needs to be digitized. During digitizing, it is necessary to choose the correct number of bits per value and data values per record in order to get good resolution and to store identifying information, such as record number, profile number, etc., in each digitized record. The digitizing process must be fast enough so as not to require excessive conversion time. This requirement necessitates a judicious choice of the analog tape speed, and the frequency of interrupts from the A/D interface. The digitizing rate and the number of words per record are determined by the highest frequency in the received signal and the length of time reflections can be expected to be received. The minimum number of bits per value for such a system should be 10.

2.2 BACKGROUND REMOVAL

The raw field data can have extensive background noise distributed over the entire traverse. A principal cause of this noise is periodic reverberations between the antenna and the walls of the borehole. The intensity of these reverberations depends on the geometry of source-receiver antennas, the material content of the walls, and size of the borehole. Therefore, the field data recorded with a reflection system in a borehole in many cases is masked by uniform-intensity background noise over sections of the traverse. The background removal algorithm computes the average of the contaminated signal along constant time-of-flight lines over specified sections of the traverse and subtracts

this average from instantaneous signal values, again along the same constant time-of-flight lines. This process reduces the effects of reverberations from the signals and leaves data that represents aperiodic returns from the subsurface zones.

One form of the background removal algorithm can be expressed mathematically as

$$fb_i(n) = f_i(n) - a_j(n), \text{ for } i = j \text{ to } j+N_a-1$$

where

$$a_j(n) = \frac{1}{N_a} \sum_{k=j}^{j+N_a-1} f_k(n)$$

$fb_i(n)$ = Background removed value of $f_i(n)$

$f_i(n)$ = Instantaneous value of $f_i(t)$ at instant $n\Delta t$

$f_i(t)$ = Analog signal return corresponding to the i^{th} transmitted pulse

Δt = Sampling interval

$a_j(n)$ = Average value of noise at instant $n \cdot \Delta t$

N_a = Number of records over which the average is being taken

N = Total number of records being processed

j = Record number at which the computation of average is started.

The above form of the algorithm is quite flexible in that by choosing a different set of values for j and N_a different averaging effects can be achieved. Thus, by making

- $j = 1$ and $N_a = N$, only one average is computed for one instant in time over the entire set of N records, which results in a constant background noise being substracted from the value of the signal at that instant. This form of average will be referred to as "global" average.

- $1<j<N$ and $1<N_a<N-j$, the average is computed over the N_a number of records starting at the j^{th} record. This form of average will be referred to as "block" average.

- $j = i$, $1<N_a<N-i$, for $1 \leq i \leq N-N_a$, the average to be subtracted from the i^{th} record is computed over the next N_a records. This form of average will be referred to as "forward moving" average.

- $j=i-N_a+1$, $1<N_a<N-i$, for $N_a \leq i \leq N$, the average to be subtracted from the i^{th} record is computed over the previous N_a records. This form of average will be referred to as "backward moving" average.

The choice of how to use this algorithm is made by examination of the data. In order to keep from removing reflection data it is desirable to use as large a averaging block as possible. The size of the block should be limited only by the changes in the reverberation pattern.

2.3 WHITENING

Whitening is a form of filtering that can be used to advantage in signal pulses that are attenuated in one frequency band more than in another. The pulse is intended to provide a wide band transient for use in time-of-flight measurements. However, the attenuation can obscure the onset time of the pulse. Such problems can be improved by whitening the signal. Whitening is done by transforming the time-domain signals to their spectral form, compressing or truncating the large spectral lines in the spectrum in a way that does not alter their phase relations, and then transforming the modified spectrum back to the time domain. The resulting signal, called the whitened signal, emphasizes the pulse return characteristics and de-emphasizes repetitive, or oscillatory, returns.

Signal oscillations that are prominent in the transmitted signal and the main reflections from the tunnel walls tend also to predominate in the received signal so that returns from small targets or thin interfaces can go undetected. Therefore, a type of signal enhancement rhat is of value involves displaying profiles of signals whose spectra have been altered in a way intended to increase the resolution of small features. The whitening process described above can be used for this type of enhancement, since the whitened spectrum tends to more closely approximate a spike.

One form of whitening algorithm can be expressed mathematically as

$$fw_i(n) = \text{I.F.T. } FW_i(m),\ i = 1 \text{ to } N$$

where $FW_i(m) = F_i(m) \cdot A_i(m)$

$$A_i(m) = \left(\frac{a + \varepsilon}{F_i(m) + \varepsilon} \right)^c$$

$fw_i(n)$ = whitened signal $f_i(n)$

I.F.T. = Inverse Fourier Transform

$F_i(m)$ = Fourier spectrum of $f_i(n)$

$A_i(m)$ = Whitening factor

$|F_i(m)|$ = absolute value of $F_i(m)$

a = maximum value of $|F_i(m)|$ or of the average of $|F_i(m)|$ over all the N records

ε = empirical constant to eliminate indeterminate solutions

c = empirical exponent, usually less than one.

Flexibility in the choice of a, ε and c makes this algorithm versatile.

2.4 BANDPASS FILTERING

The effective recording of pulse data requires the recording of a large band of frequencies. In general, the transmitted pulse seldom contains energy at all of the frequencies. Therefore, it becomes advantageous to filter out the frequencies in which the noise power is significantly greater than the signal power. This is done by weighting the appropriate frequencies by a given filter function. The process must be versatile so that any predetermined filter function can be applied to the data. This will allow the passing of wide-band data or the notching out of narrow-band noise.

2.5 VELOCITY ANALYSIS

Variations in signal propagation speed with depth can be estimated by analysis of the variations in travel time observed in groups of records having a common datum point (CDP). These records are obtained by bistatic profile runs where the transmitter and the receiver are moved longitudinally away from each other and in equal steps starting from a common point, as shown in Figure 1. A sequence of summation traces is then displayed, each trace representing a CDP stack employing normal move out (NMO) corrections that are based on a different constant propagation velocity. A wide enough range of velocity values is used to insure that the true propagation velocities are covered. The sum traces are laid out in order of increasing velocity values. This forms a display of sum signal amplitude

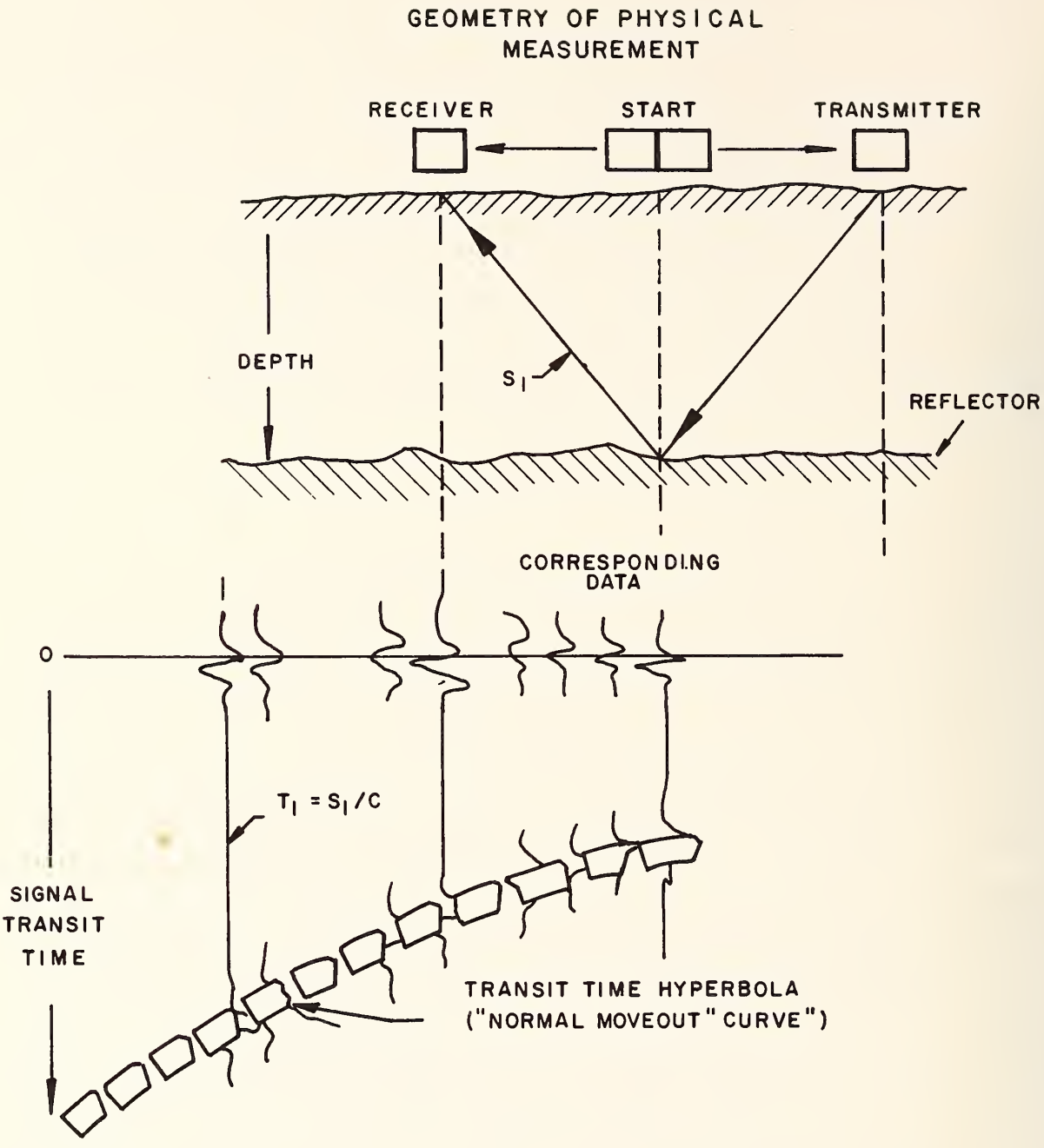

Figure 1. The bistatic profile and "normal moveout".

as a function of reflection time and of normal move out correction velocity as illustrated in Figure 2. The peaks in this function will usually trace out a line that represents a good estimate of average velocity versus reflection time from which a velocity can be defined as function of depth.

Velocity analysis is important for two reasons. It provides the velocity functions needed to maximize the effectiveness of CDP stacking when detecting weak interfaces and its multiple reflections. It is also useful as an interpretation tool in its own right. It identifies changes in interval velocities that are directly related to changes in dielectric constant and hence to changes in the lithology. However, since the prototype as it is currently designed collects data with a fixed separation between source and receiver, this type of processing is not feasible. If future developments allow multiple offsets, then velocity analysis will be important.

2.6 MIGRATION

When reflection records are displayed in the form of profiles showing time-of-flight versus distance along the line of traverse, these profiles bear a superficial and misleading resemblance to geologic cross sections. However, the fact that the vertical scale is time-of-flight rather than depth means that many of the most striking features in the profiles are not geologic structures at all. For example, the dislocation of a strong reflecting horizon by faulting will cause the occurrence of strong diffraction and scattering of the signal at the points where the reflector is broken. These diffraction patterns will show up as hyperbolic tracks across large sections of profiles and can sometimes be mistaken for other reflections from beneath the reflectors, which they are not.

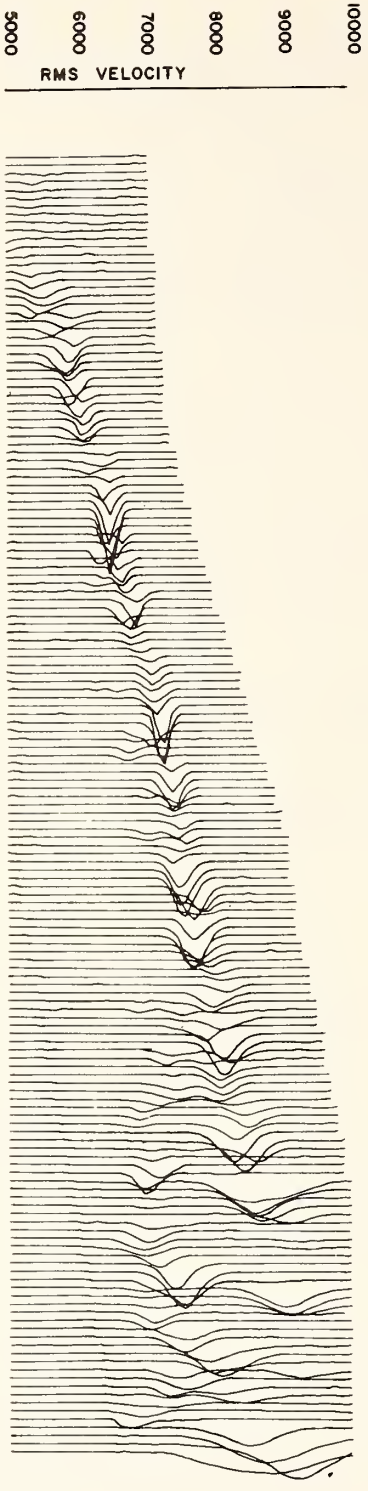

Figure 2. Example of "velocity spectrum". (From: Geophysics, Vol. 34, No. 6, Dec. 1969 P. 9.867.)

These distortions can be corrected by a process called "migration" which in essence is reconstruction of a depth profile from the time-of-flight profile, based on the known propagation speeds in recording locations.

Consider the volume of rock probed by the transducer beam to be composed of many small individual unit scattering volumes. The returning signal can be thought of as the sum of all the returns from all of these scattering volumes. Thus, if the recorded signal at station (i) is identified by $[f_i(t)]$, the signal can be approximately defined by

$$f_i(t) = \sum_k a_{ik}\, g(t-T_{ik})$$

where

$g(t)$ is the transmitted signal

a_{ik} is a complex coefficient representing transmission loss and scattering strength for the k^{th} unit scattering volume sensed at the i^{th} station

T_{ik} is the round-trip signal transit time from the i^{th} station to the k^{th} unit scattering volume.

Suppose there is a small cavity located opposite the i^{th} station of the line of traverse (at a distance of x_i along the line of traverse and a radial distance r_k away from it) and the cavity begins to enter the field of view of the antenna when the antenna has approached to within m stations distance. Then, from Figure 3,

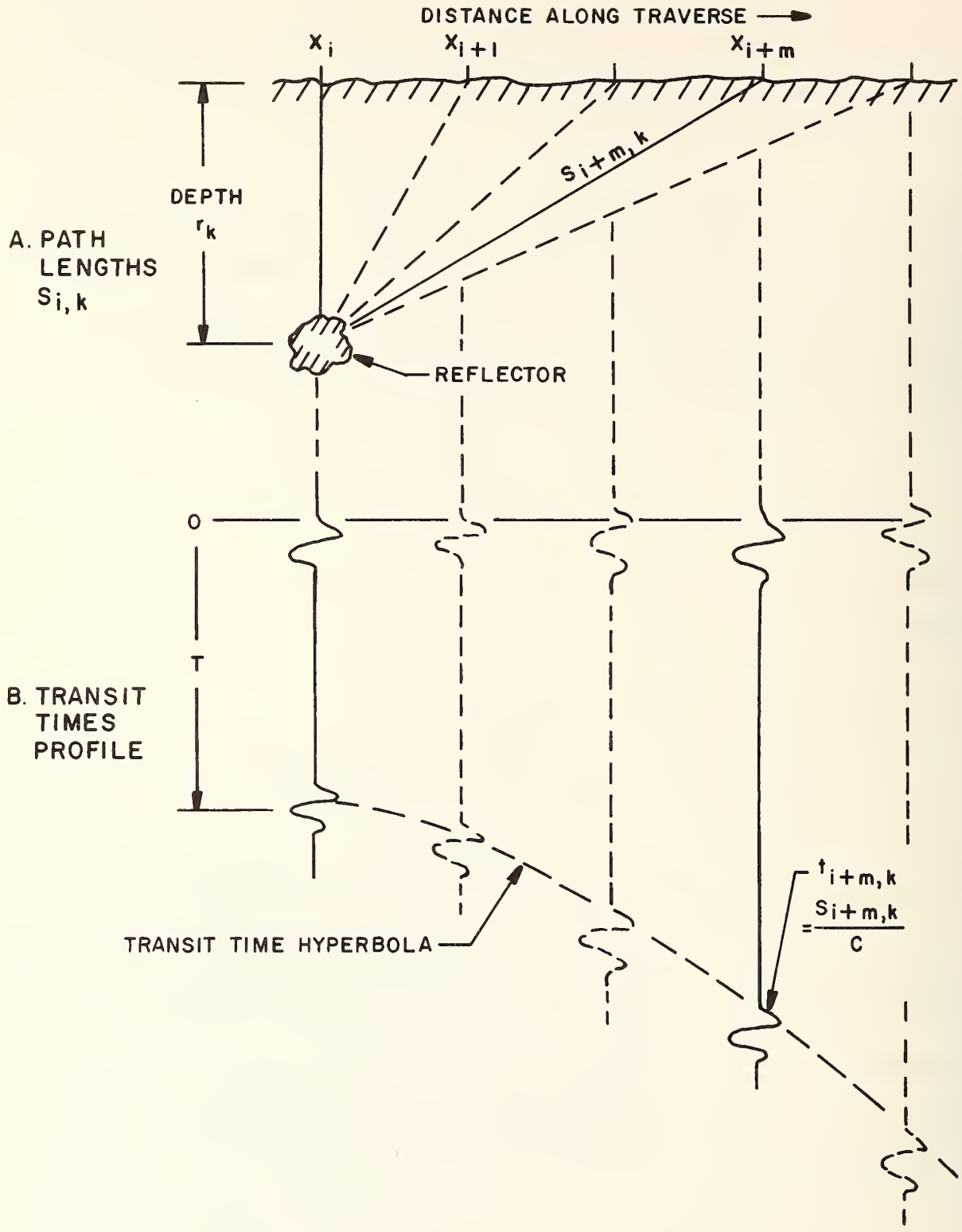

Figure 3. Origin of hyperbolic features in profile.

$$\left(\frac{1}{2} \; c_{jk} \; T_{jk}\right)^2 = \left(X_j - X_k\right)^2 + r_k^2$$

where $j = i-m$

$m = 0,1,.....M$

c_{jk} = average speed of signal propagation

r_k = depth of reflector directly below the k^{th} station.

This becomes an equation for a hyperbola of the form

$$\frac{x^2}{a^2} - \frac{y^2}{b^2} = 1$$

where $x = T_{jk}$

$y = X_j - X_k$

$a = 2 \; r_k/c_{jk}$

$b = r_k.$

Therefore, as the antenna moves along the traverse, a hyperbolic trace that begins where the scatterer enters the beam and ends where it leaves the beam will appear on the reflection profile, the hyperbolic "tails" being caused by the signal transit time changes as a beam passes over the target.

Thus, one form of signal enhancement that can be provided for any profile traverse signal will be to display the profiles that result from averaging of the signals along hyperbolic paths. This process, in effect, probes each elemental volume within the array beam to see if that volume contains a source of scattering or reflection. The probe of a single unit volume is conducted by summing all of the received

signals from a series of different recording positions, after having time-shifted them to remove the expected travel time for that particular unit volume based on the estimated velocity function. If a significant amount of signal energy did indeed scatter from within that volume, the signal sum will show a local maximum at the time and distance coordinates of that particular unit volume.

The effect of this averaging will be to concentrate all the signal energy in each hyperbolic "tail" into a zone near the vertex of the hyperbola. This will result in an intensification of the traces in the profile that correspond to bedding planes, as well as a less distorted representation of the configuration of the bedding planes. This enhancement will reduce the likelihood that faults or gouge zones will be missed.

The "migration" for monostatic data consists of generation of a function $h_i(t)$ that may be displayed in the same format as the raw signal profiles $f_i(t)$. The function will be of the form:

$$h_i(t) = \sum_{m=-M}^{M} f_{i+m}\,(t + T_m) \Bigg/ \sum_{m=-M}^{M} f_{i+m}\,(t)$$

where

$$T_m = \frac{1}{c}\left[(x_i - x_{i+m})^2 + (ct)^2\right]^{1/2}$$

This function represents the normalized sum of a set of 2M+1 instantaneous signal values from the M adjacent stations on either side of the transverse position x_i, after all the values

of the set have been time-aligned as though they had come with speed c from an imaginary source located at the same position x_i along the traverse and a perpendicular distance r = ct away from the line of traverse. Thus, any signal components for which this is true will interfere constructively in the sum, causing a local maximum in the display at coordinate x_i, t. The process is illustrated in Figure 4.

The expected effect of this processing is illustrated in Figure 5 which is from an advertisement of a petroleum exploration company showing the effect of this type of signal processing on a seismic exploration profile. The raw distorted profile analogous to f(t) is shown at the top; the corrected profile analogous to h(t) is at the bottom. The main feature in both profiles is a strong reflection from a discontinuous bedding plane. Note how much clearer the discontinuities appear after processing than before.

At the present time, these programs require large amounts of computer time to implement, and the signal to noise problems are such that migration does not help the data. Therefore, the implementation of this type of processing should wait until there is a need established by the users.

3. EXAMPLES OF PROCESSED DATA

The purpose of this section is to show how the processing techniques described in the previous sections can be applied to field data. In this case, the field data is from electromagnetic radar work ENSCO has performed under other contracts.

The first example is shown in Figure 6. This is a series of returns from a traverse in a Washington Metro tunnel with a low frequency (approximately 100 MHz) radar. This is part of the NSF work described in Appendix M. Figure 6 shows the

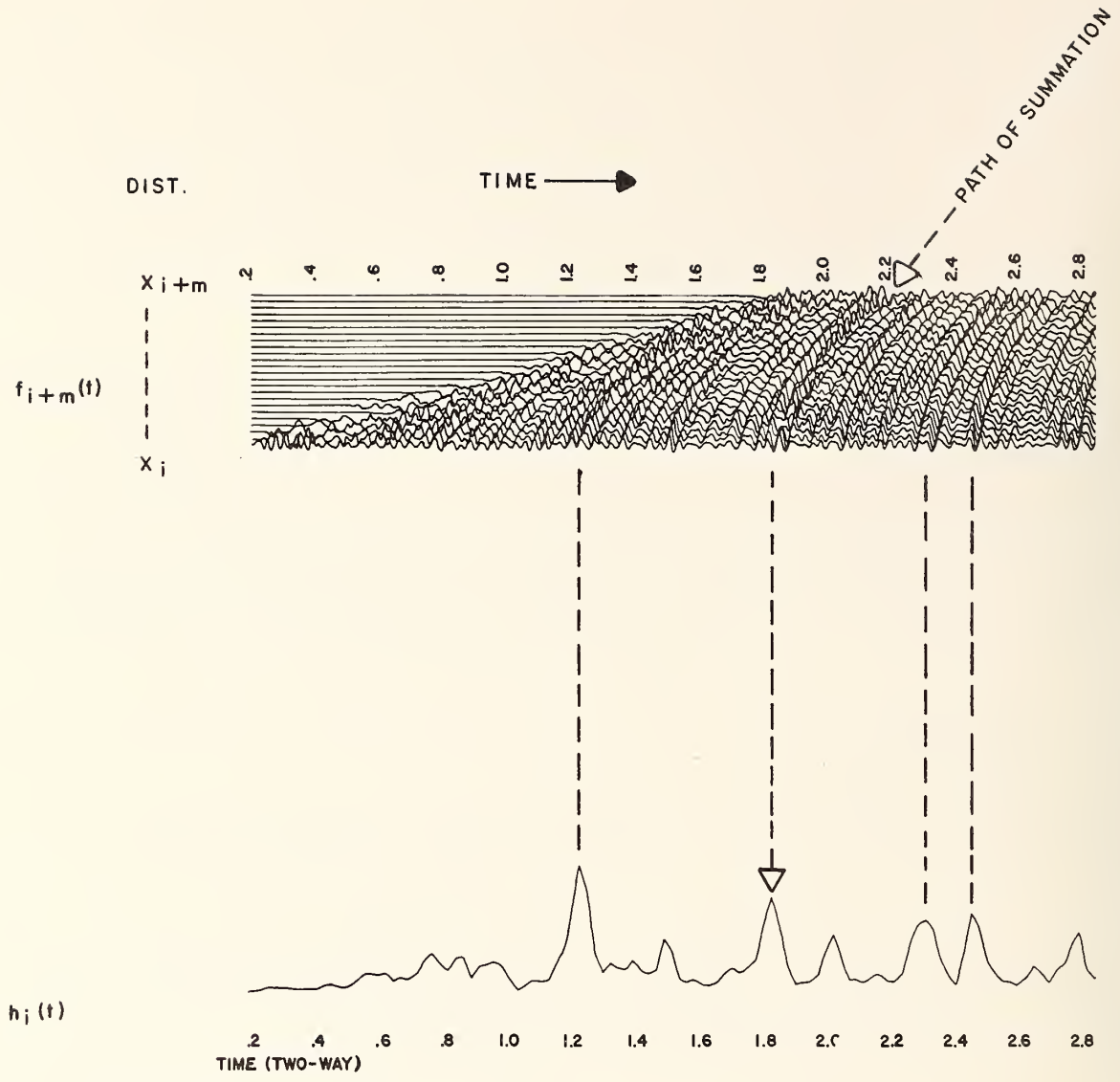

Figure 4. "Hyperbolic Stacking". In the processed profile, the summed function $h_i(t)$ replaces the raw scan function $f_i(t)$ (2).
(From: Geophysics, Vol. 34, No. 6, December 1969, P. 867.

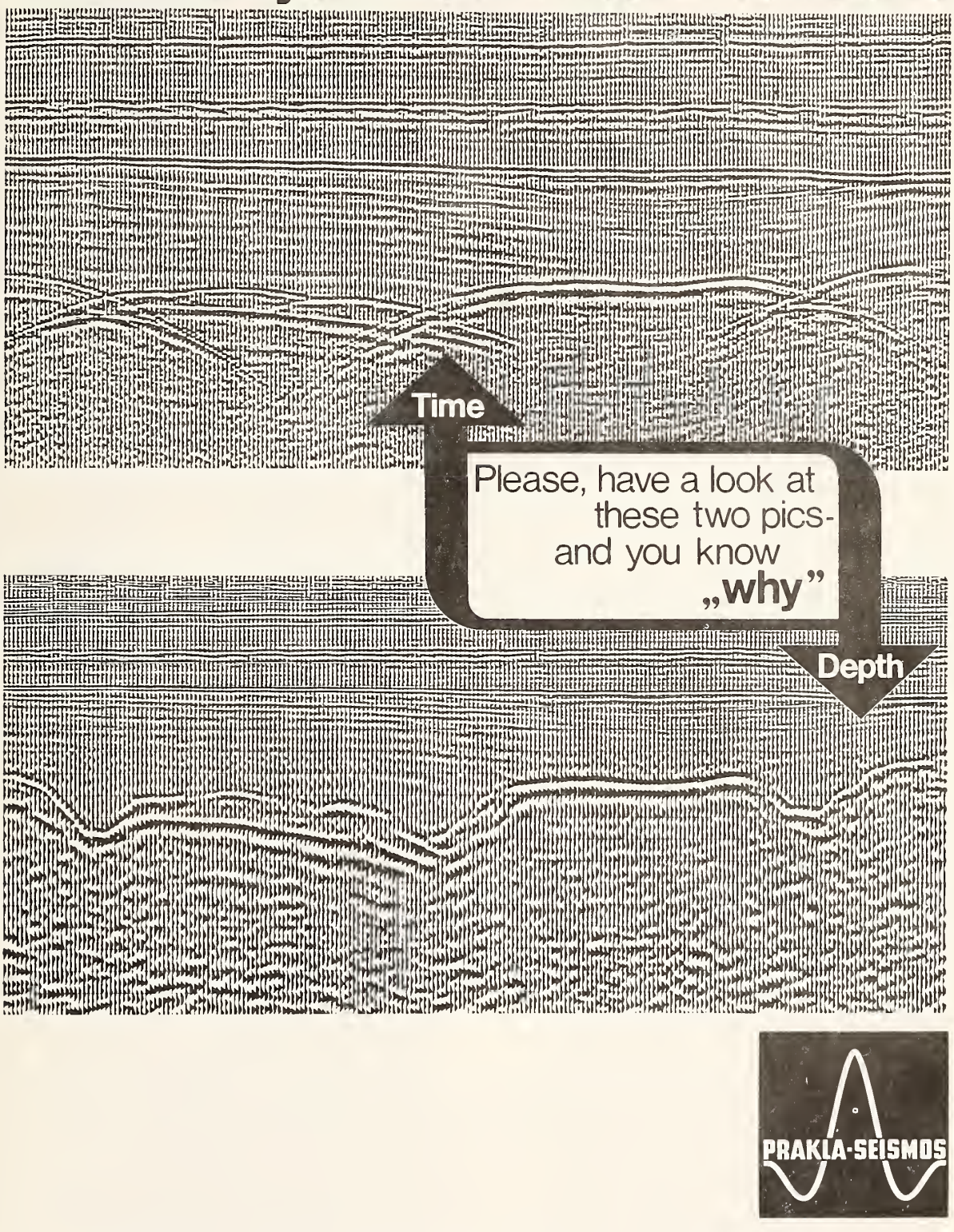

Figure 5. Example of the use of one form of "migration" to improve resolution of discontinuities on a bedding plane (10).
(From: Geophysics, Vol. No. 3, June 1972, P. A-39.

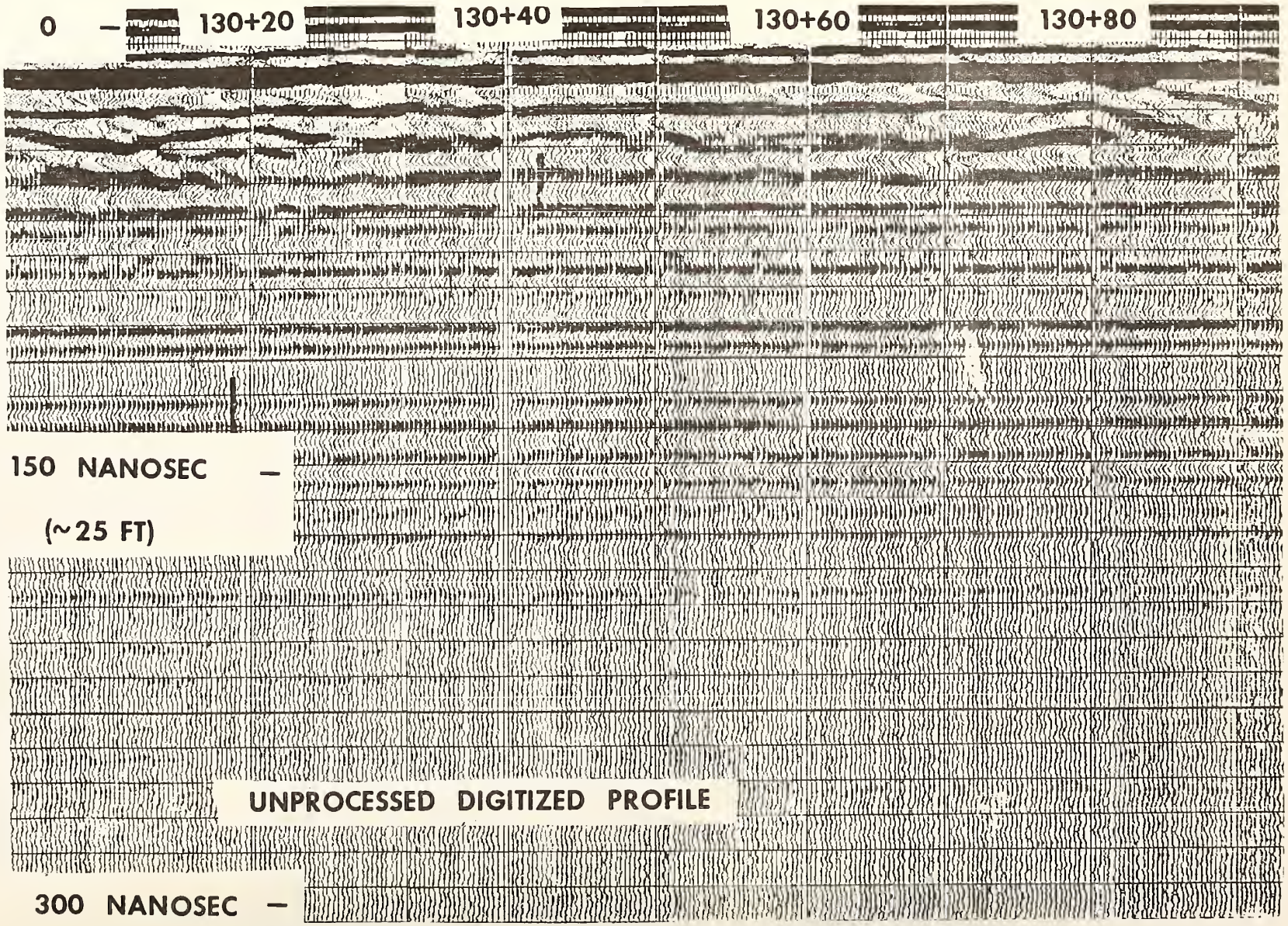

Figure 6. Unprocessed digitized profile.

data after it was digitized. The next step in processing was to apply a gain correction to the data to increase the level of the reflections from longer distances. Figure 7 shows the data after scaling. The raw field data has excessive background noise distributed over the entire traverse. The main cause of this noise is periodic reverberations from the walls within the tunnel. The intensity of the recorded reverberation depends on the distance of the antenna from the walls and on the material content of the walls. This noise can be seen as the dark horizontal streaks in the plots of Figures 6 and 7. A weak slanted feature (marked in pen) can also be seen in the lower right-hand corner of Figure 7 going from left to right at an angle of about 30° to the horizontal. Background removal was applied to the data to try to remove the effects of the reverberation. Figure 8 shows the section after the background was removed using a "global" average. The reverberations are reduced and the slanted feature at the right is now much more prominent. Also, a number of hyperbolic features are visible over the central section of the figure.

The next stage of the process was to try to enhance the wide band returns by applying a whitening operator. This operator should have the effect of enhancing the wideband reflections while discriminating against the narrow band reflections. Figure 9 shows the data after whitening. It can easily be seen that the whitening enhanced the reverberations. This implies two things:

- The first background removal was not 100% complete.
- The reverberations are probably more wideband in nature than they appear.

A second pass at background removal was tried and the results are shown in Figure 10. The reverberation has been removed but at the penalty of a tremendous decrease in overall contrast. However, the net result is an overall increase in the

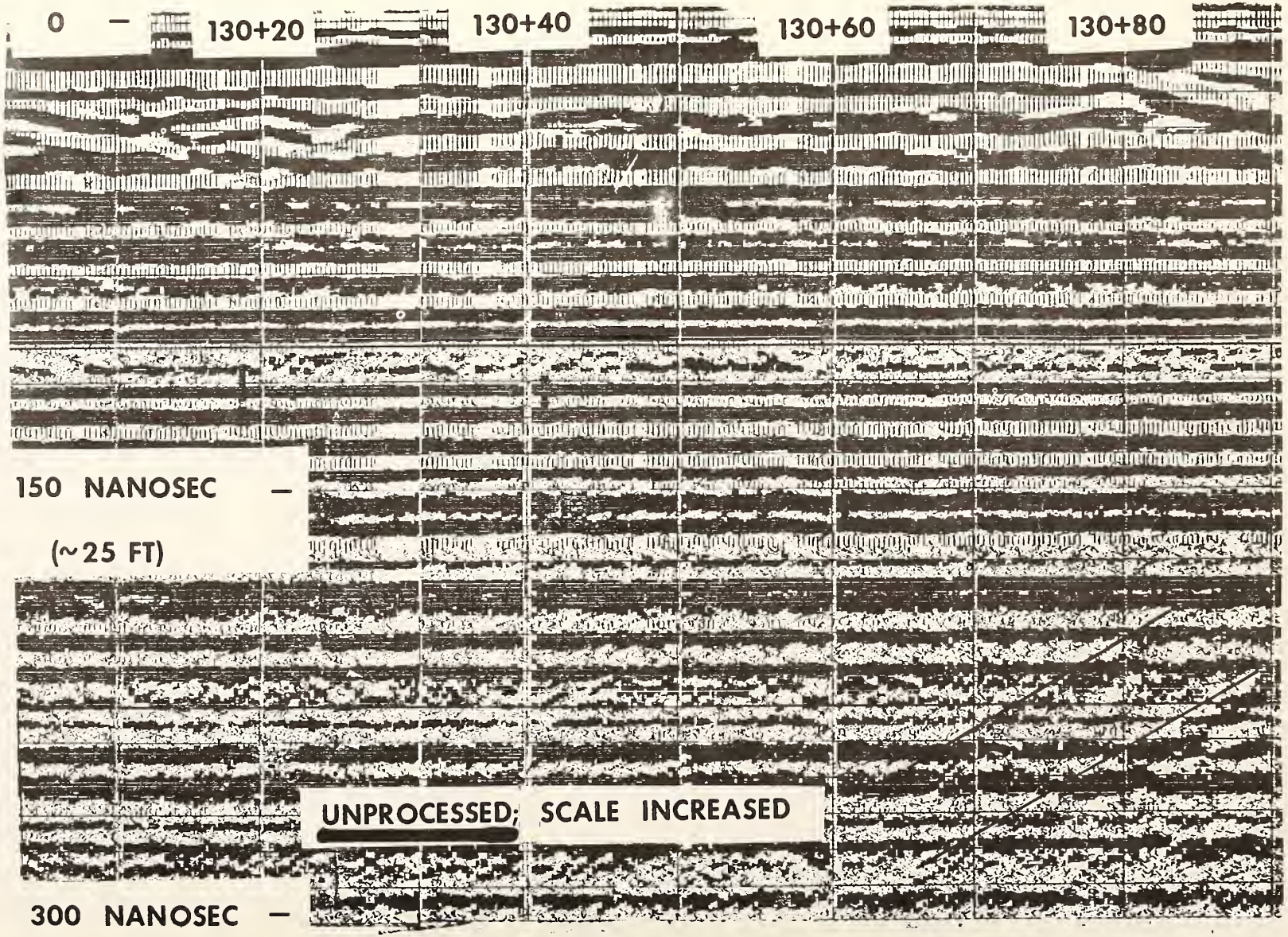

Figure 7. Unprocessed; scale increased.

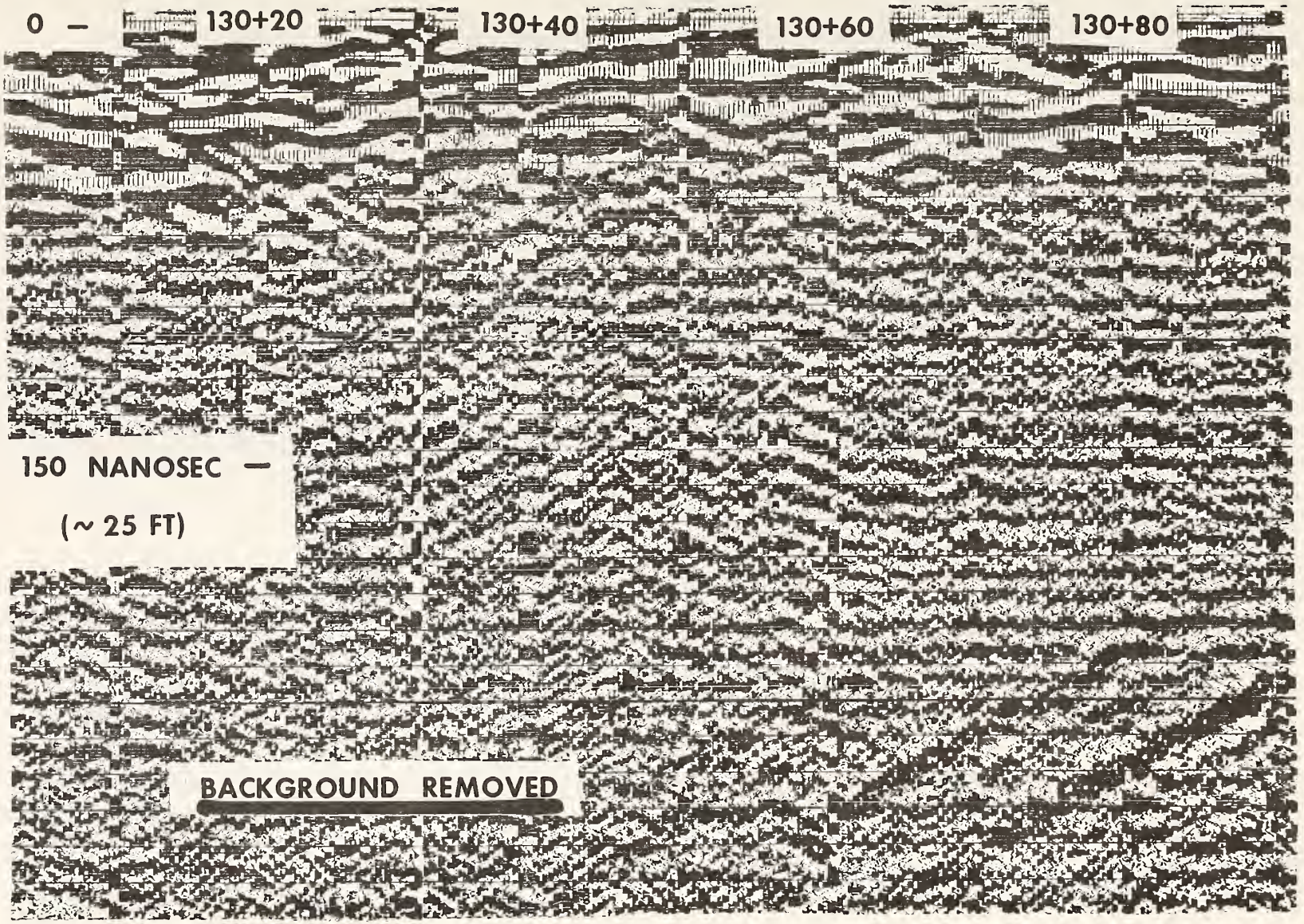

Figure 8. Background removed.

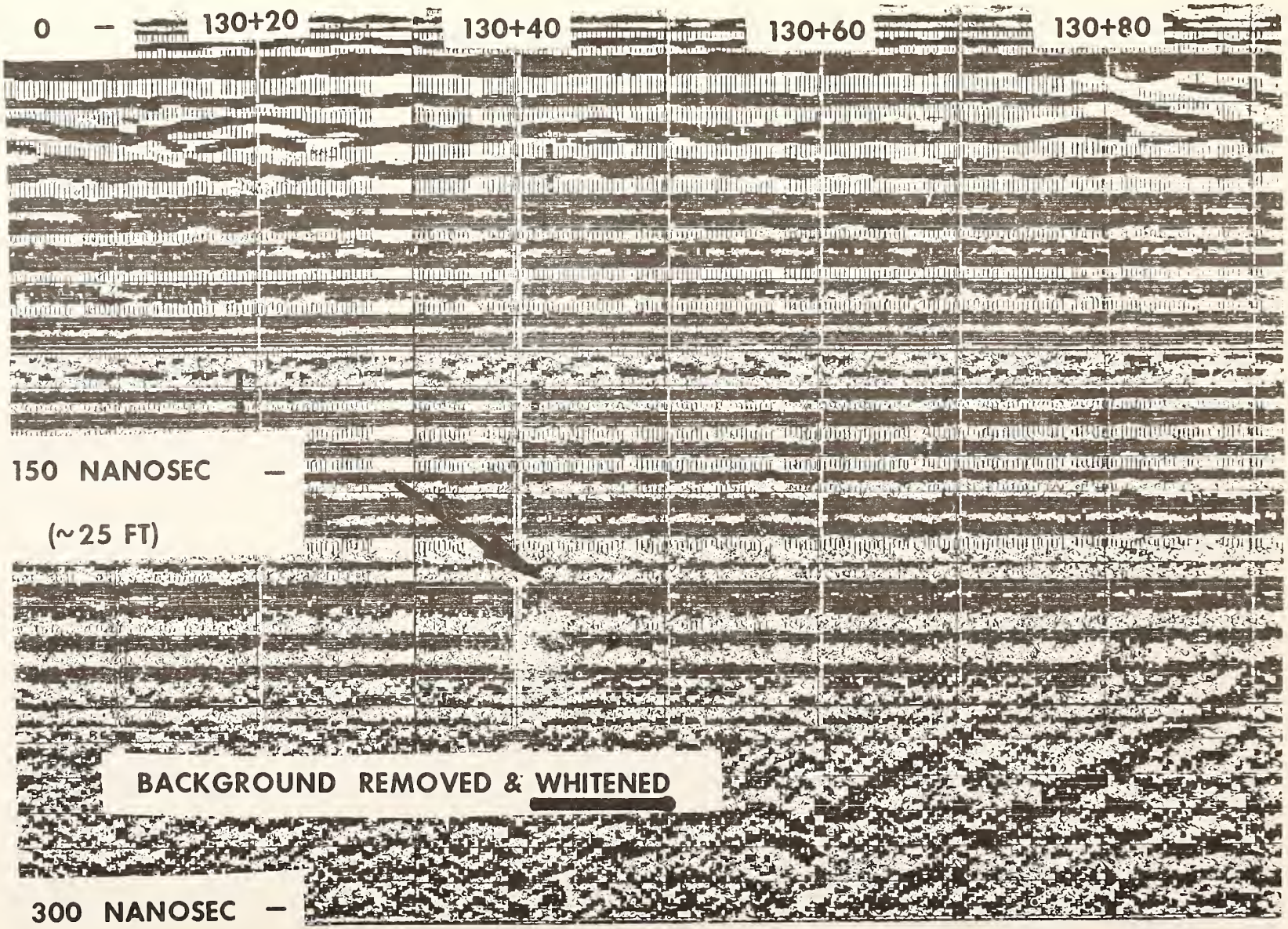

Figure 9. Background removed & whitened.

Figure 10. Background removed - second pass.

amount of interpretable data. Many fine-grained details of features are now visible. Figure 11 is a repeat of Figure 10 but with the features marked on the section.

A second set of data is now shown to demonstrate the value of frequency filter. This data was obtained from a U. S. Bureau of Mines project in which a high-frequency (100 MHz to 1 GHz) EM radar was used to measure coal thickness along a mine tunnel. Figure 12 shows some of this data. The bottom trace on this figure is a typical trace from a single radar transmission. The feed-through pulse arrives between o and 3 nanoseconds, then there is a large low-frequency peak before the return from the roof (at 7.5 nanoseconds) arrives. This low-frequency return (artifact) masks the arrival of the roof return. In order to study the data more carefully, a series of filters was applied to the trace. Figure 13 shows the bandpass characteristics of the filters. The first five traces of Figure 12 show the results of passing the raw data trace through each of the filters.

The low-frequency return can be seen of the first trace very easily, while the roof reflection is more visible on the third trace. From examination of the data, it can be seen that the fifth trace which is a 400 MHz to 800 MHz version of the data seems to pass the reflection while filtering out the artifact.

4. CONCLUSIONS

Several processing techniques have been described in this section. With the exception of digitizing, the application of the rest of the techniques must be determined by examination of the data. This is done by careful examination of both the reflection traces and their spectra. From this noise and signal parameters can be estimated and the proper processing can be applied. Each step of the processing must be monitored separately and care taken that the results are indicative of the true earth returns and are not generated by the processing

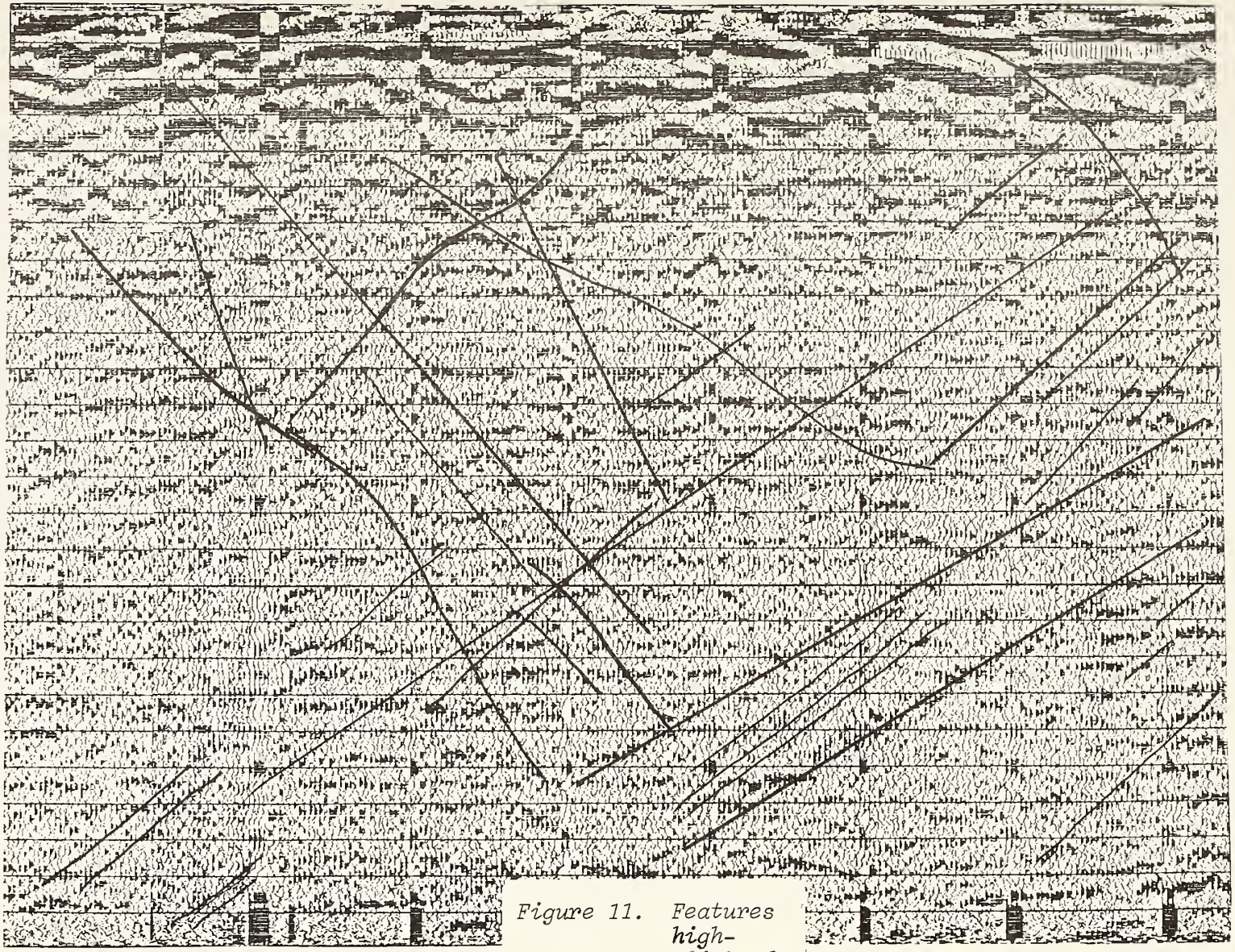

Figure 11. Features highlighted.

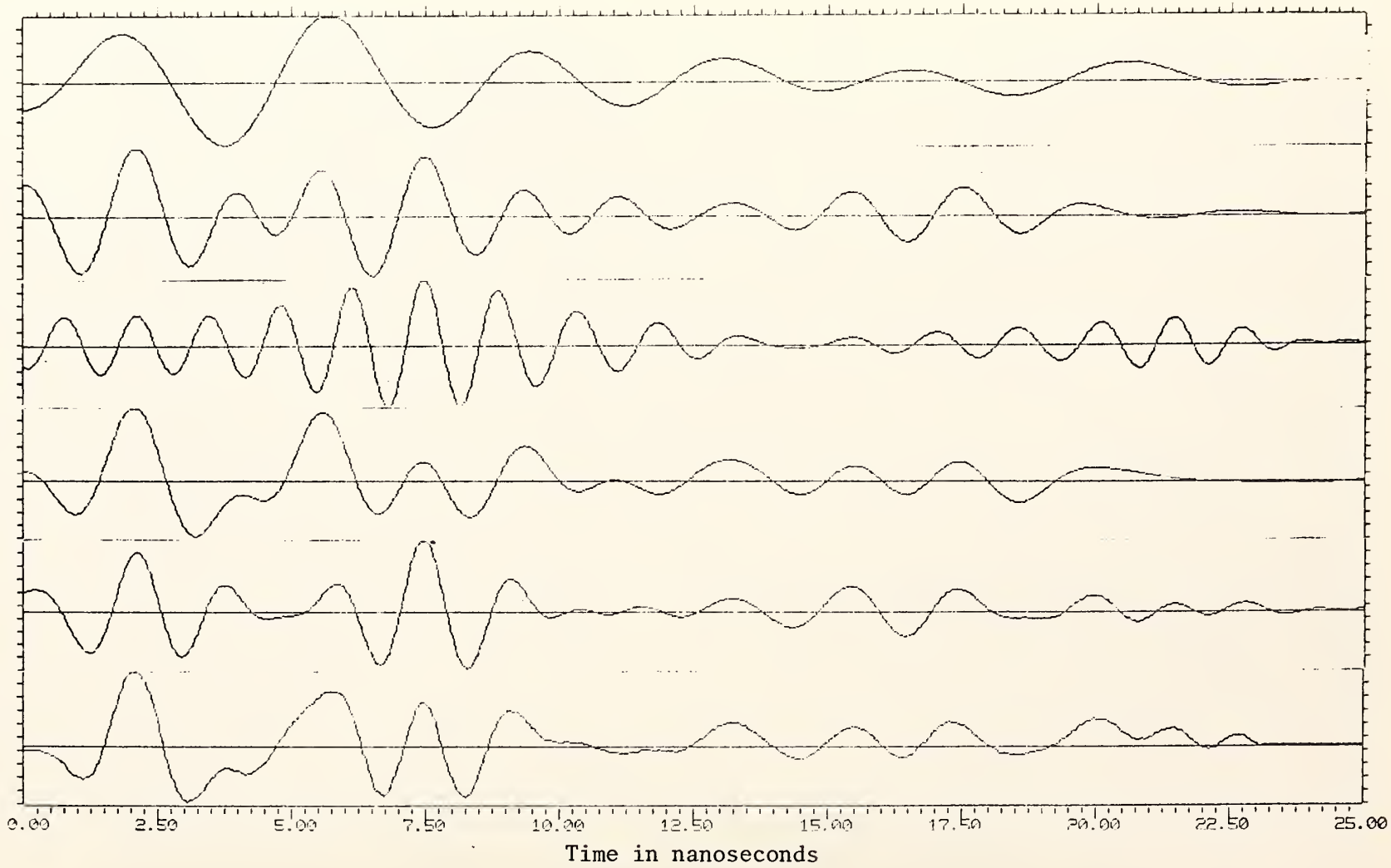

Figure 12. Frequency band playouts of EM radar data.

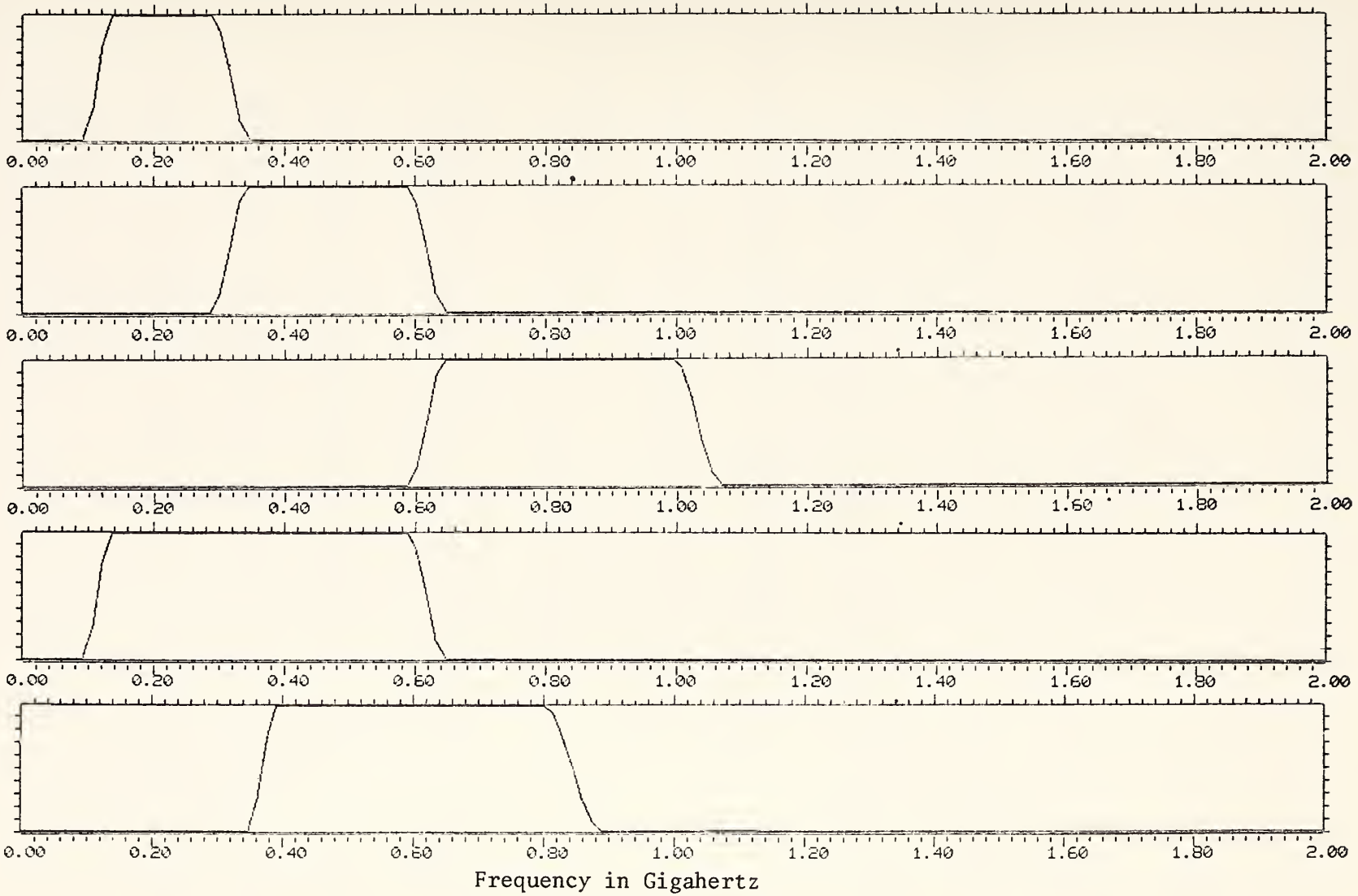

Figure 13. Frequency bands used.

system. Once this is done, the processing system can become a powerful tool for the interpreter to use in producing a geologic interpretation.

5. REFERENCES

1. Oppenheim, A. V., "Generalized Linear Filtering," Digital Processing of Signals, McGraw-Hill Publishing Company, 1969, pp. 233-264.

2. Taner, M. T., and Koehler, F., "Velocity Spectra-Digital Computer Derivations and Applications of Velocity Functions," Geophysics, Vol. 34, No. 6, (December 1969), pp. 859-861.

3. Bogert, Bruce P.; Healy, J. J. R.; and Tukey, John W., "The Frequency Analysis of Time Series for Echoes," Proceedings of the Symposium on Time Series Analysis at Brown University, June 11-14, 1962, pp. 209-243.

4. Kunetz, G., and Fourmann, J. M., "Efficient Deconvolution of Marine Seismic Records," Geophysics, Vol. 33, No. 3, June 1968, pp. 412-423.

5. Mueller, R. K., "Acoustic Holography," Proc. IEEE, Vol. 59, No. 9, September 1971, pp. 1319-1334.

6. Claerbout, J. F., and Doherty, S. M., "Downward Continuation of Moveout-Connected Seismograms," Geophysics, Vol. 37, No. 5, October 1972, pp. 714-768.

7. Plutchok, R., and Broome, P., "Hydroacoustic and Seismic Signal Analysis for the Identification and Classification of Underwater Events," ARL Report 68-1, Earth Sciences, A Teledyne Company, 17 April 1968.

8. Sherwood, J. W. C., "The Seismoline, An Analog Computer of Theoretical Seismograms," Geophysics, Vol. 27, No. 1, February 1962, pp. 19-34.

9. Rice, R. B., "Inverse Convolution Filters," Geophysics, Vol. 27, No. 1, February 1962, pp. 4-18.

10. Prakla-Seismos GMBH. Advertisement in Geophysical Prospecting, Vol. 20, No. 2, June 1972, p. xxii.

APPENDIX I

CONCEPTUAL DESIGN STUDY OF HARD ROCK SENSOR CONVEYANCE DEVICE

TABLE OF CONTENTS

BACKGROUND STATEMENT

A major effort of the program was to design a self-propelled conveyance device. This study is one of the documents produced in this effort. The fact that the final system as specified does not include a conveyance such as this does not nullify the value of the work.

The decision not to incorporate a self-propelled thruster was made on the basis of other factors.

- The state-of-the-art of horizontal drilling is such that it is doubtful that, in the same time frame as the first hardware of this program, there will be holes long enough to need a self-propelled device.
- The sensor concept must first be field proven before a device such as this is needed. Thus, it is possible to separate the development of the thruster from that of the sensor.

CONCEPTUAL DESIGN STUDY OF HARD ROCK SENSOR CONVEYANCE DEVICE

ABSTRACT

A design study to determine the best conceptual design for a conveyance system to transport a hard-rock sensor package through a two-mile (3.2 km) horizontal borehole is described. Various design concepts for the conveyance system and associated power sources are formulated and examined in an effort to determine the most efficient, cost-effective, and reliable system.

The study resulted in a recommendation for either electric or pneumatic power supplied through the umbilical. Two conveyance concepts were found to be of equal potential to perform satisfactorily. These concepts are both variations of the "worm." It was also recommended that a modular approach consisting of multiple forward power modules be adopted.

1. INTRODUCTION

1.1 BACKGROUND AND OBJECTIVE

This report describes the work conducted by ENSCO, Inc. to determine the best conceptual design for a conveyance system to transport a hard-rock sensor package through a two-mile (3.2 km) horizontal borehole. The work corresponds to Task B-5 of Contract DOT-FH-11-8602 entitled "A New Sensing System for Pre-Excavation Subsurface Investigation for Tunnels in Rock Masses."

The device conceived in this task is to be part of an overall sensor system consisting of surface support equipment, data processing equipment, an umbilical cable, sensor modules, a borehole penetrator and the conveyance system itself. The various subsystems must all interact in such a way that the most efficient and reliable total system is achieved.

In this report, various design concepts for a conveyance system and associated power sources are analyzed in an effort to determine the most cost-effective and reliable method for the conveyance systems design.

1.2 PERFORMANCE CRITERIA

Before considering the individual concepts which have potential for transporting the sensor package, a statement of the performance criteria which all devices must meet is necessary.

- The conveyance device must be capable of pulling itself, the sensor package, and the umbilical cable for a distance of up to two miles (3.2 km) in an existing horizontal borehole. In conjunction with the umbilical, it must be capable of retracting the downhole package.

- The device must be capable of being built for a borehole diameter, in the range of 4-3/4" (12.1 cm) to 9" (23 cm). The borehole is essentially horizontal but may have an up or down grade to it. [The horizontal curvature is greater than 500 ft. (152 m) radius and not considered a limiting factor.]

- The conveyance device must be able to operate in the presence of a down-hole hydraulic head as high as 500 psi (3.45 MPa).

- The device must be capable of a repeated stop-and-go motion with movement of approximately 6" (15 cm) to 12" (30 cm) per cycle. These pauses are necessary for the acoustic sensor operation.

- The device should be capable of operating in a borehole which is drilled out of material varying in consistency from soft ground to hard rock.

- The conveyance device should have the ability to traverse a borehole in which there are adjacent voids which effectively increase the diameter of the borehole by at least two or three times. The length of the voids to be considered are no greater than 2 feet (0.6 m) in length.

- The speed of the device should be 50 fpm (0.254 m/s), however, in order to cut down power demands, the speed may be allowed to taper off by 10% at distances approaching the 2-mile (3.2 km) limit.

- The device should have the ability to transform its motive power into crushing power should the device be stalled by rubble or other fragments that are in its path. It must also provide space for the passage of crushed debris.

- The device must allow cables and hoses to pass through it as required by equipment ahead of it.

- The device must be adaptable for modular system design.

2. CONVEYANCE SYSTEM DESIGN STUDY

2.1 SOURCES OF DOWN-HOLE POWER

One of the prime considerations for the self-powered conveyance device of the down-hole sensor system is the type of power and its source. The weight of the power source, appearing either as increased umbilical weight or down-hole energy storage device weight, affects the power requirements of the conveyance device and hence its size, weight, and complexity. It is important, therefore, to explore this area before a study of the actual conveyance device design is attempted. The power source is a system which can be studied irrespective of the final device configuration. The types of power which are feasible are:

- Electric (umbilically supplied)
- Electric (self-contained battery)
- Pneumatic (umbilically supplied)
- Hydraulic (umbilically supplied)

General features of these power sources and their applicability to the present problem are discussed in this section.

2.1.1 Electric (Umbilically Supplied)

Since the sensor package requires electric power, use of electric power for the conveyance device is very convenient. Also, it is easily transmitted over the required distances with lightweight cables. Due to the stop-and-go movements of the sensor package required for acoustical sensor coupling, it would be most efficient for an electric-powered system to be used in conjunction with a down-hole hydraulic system (electro-hydraulic) so that the required electric motor could be run at

constant speed. The hydraulic power could be stored in an accumulator for providing the cyclic capability. The electric power can be AC or DC; however, the weight of the umbilical cables for DC power can be lower due to lower peak voltage requirements.

Motor Size

The motor size should first be gauged to see if it is possible to find a motor with the required power that will fit in the borehole.

The power requirements depend basically on how much power is required to drag the umbilical and down-hole package along the borehole for a distance of two miles (3.2 km). The net power required to drag the umbilical and down-hole package depends on the product of the frictional force (F) exerted on the umbilical and the package, and the speed of transit (v). The frictional force, F, is given by

$$F = \mu_1 W_1 + \mu_2 W_2(\ell) \qquad (2\text{-}1)$$

where

μ_1 = coefficient of friction between the package and borehole

W_1 = the weight of the downhole sensor package

μ_2 = coefficient of friction between umbilical and borehole

$W_2(\ell)$ = weight of umbilical unwound at a distance ℓ from entry point of sensor package.

It can be seen that the frictional force (F) to be overcome by the driving mechanism increases with penetration (ℓ) into the borehole.

For the speed of transit, it is desirable (from the performance requirements) that 50 ft/min (.254 m/s) be attainable at the start of the sensing activity although this should be relaxed somewhat at the end of travel to avoid excessive power consumption. Assuming the velocity at the start is v_i and drops off linearly at the end (L) to v_f, the velocity at any penetration (ℓ) is

$$v(\ell) = v_i \left(1 - \frac{\ell}{L} + \frac{v_f}{v_i}\frac{\ell}{L}\right) \qquad (2\text{-}2)$$

The power required at any penetration (ℓ) is

$$P = kFv(\ell) \qquad (2\text{-}3)$$

where k is a constant; F is the force to overcome friction (2-1) and $v(\ell)$ is the velocity at penetration ℓ.

It can be shown that the maximum power required will be at a penetration $\ell_{P_{max}}$ given by

$$\ell_{P_{max}} = L \left\{ \frac{1}{2\left(1 - \frac{v_f}{v_i}\right)} - \frac{\mu_1}{2\mu_2}\frac{W_1}{W_2} \right\} \qquad (2\text{-}4)$$

provided $\ell_{P_{max}} < L$. If not $\ell_{P_{max}} = L$

For the systems envisioned here this max power will occur at penetrations approaching the maximum penetration, L. For example for a typical system

W_1 = 500 lb (227 kg) (down-hole package)

$W_2(L)$ = 2776 lb (1.259 Mg) [(umbilical weight for 10,560 ft (3.2187 km)] (See Annex A).

μ_1 = 0.5 (friction for sensor package against borehole)

μ_2 = 0.5 (friction for dragging cable against borehole)

v_i = 50 ft/min (.254 m/s)

v_f = 45 ft/min (.229 m/s)

we find $\ell_{P_{max}} = L$

Consequently, the net maximum power required at L from (2-3) is

$$P_{max} = 2.23 \text{ hp } (1.66 \text{ kw})$$

Assuming the efficiency of the hydraulic motor which the electric motor drives is 80%, then the motor power required is of the order of 2.79 (2.08 kw) or about 3 horsepower (2.23 kw).

Electric motors of the 3 horsepower (2.23 kw) range do not normally come off the shelf in diameters small enough to fit into holes ranging from 4-3/4" (12 cm) to 9" (3 cm) diameter unless they are of the submersible type or are specially built. Most motors built in small frames for special applications (such as electric drills) require open frames with fan cooling. Such a design would not provide adequate down-hole cooling when placed inside a casing necessary for environmental protection. An enclosed water cooling system would be necessary for sufficient heat dissipation. Since submersible pump motors require water submersion for cooling, this would be the most likely candidate and a water jacket which distributes the heat would have to be built. The size of this jacket is governed by the cooling required on the motor as discussed in the next section.

Cooling Requirements

For an electric motor encased in a cooling jacket, the heat generated from the motor is absorbed by the cooling water. This heat is in turn transferred out of the water to the air by radiation and convective heat transfer from the surface of the cooling jacket. (Conduction heat transfer is considered minor.) The critical parameter to be decided here is the required amount of surface area of the cooling jacket to ensure heat is transferred out at a fast enough rate to keep the motor from overheating. It is understood from the motor manufacturers that if the cooling jacket surface temperature is kept to 150°F (65.6°C) the motor will not overheat. As far as the amount of heat to be dissipated, this

averages around 20% of the power rating of the motor. With this information, the dimensions of the jacket can be determined by considering the heat transfer from the jacket.

As the motor package moves through the borehole, the flow of air over the cooling jacket will cause heat to be dissipated through forced convection. Some heat will also be dissipated in radiation so that the heat to be dissipated (q) is therefore given by

$$q = \bar{h}A\ (T_w - T_\infty) + \sigma A(T_w^4 - T_\infty^4) \qquad (2\text{-}4)$$

where the first term relates to the convective mode and the second to the radiative heat transfer mode. Here $\bar{h}$ is the average value of the convective heat transfer coefficient, A is the surface area of the cooling jacket, T_w is the temperature of the jacket outside wall, T_∞ is the ambient temperature of the borehole, σ is the Stefan-Boltzmann radiation constant.

For the convective heat transfer the average heat transfer coefficient depends on the speed of flow of air over the cylinder, and the hydrodynamic and thermodynamic properties of the air. Specifically it can be shown*

$$\bar{h} = \frac{2Nu_L k}{L} \qquad (2\text{-}5)$$

where Nu_L is the Nusselt number evaluated at the end of the cooling jacket of length L and k is the thermal conductivity of the air. For a cylindrical surface* the Nusselt number is given by

$$Nu_L = 0.332\ Re_L^{1/2}\ Pr^{1/3} \qquad (2\text{-}6)$$

where Re and Pr are the Reynolds and Prandtl numbers for the flow respectively. Assuming the cooling jacket is 6" (15 cm) diameter and moves through the 9" (23 cm) diameter hole at 50 ft/min (0.254 m/s), the average air speed, u over the cylinder is 1.5 ft/sec

* Holman, J.P., "Heat Transfer," McGraw-Hill, 1963, Chapter 5.

(0.46 m/s). The Reynolds number, Re, at the location L is given by

$$Re_L = \frac{uL}{\nu} \qquad (2\text{-}7)$$

where ν is the kinematic viscosity. For air at 50°F and atmospheric pressure, $\nu = .5488\ ft^2/hr$. The Prandtl number for air under these conditions is Pr = 0.712 and the thermal conductivity k = .0143 btu/hr ft-°F. Consequently

$$Re_L = \frac{1.5\ (3600)\ x\ L}{.5488}$$

$$= 9839.7\ L$$

and

$$Nu_L = 0.332\ Re_L^{1/2}\ Pr^{1/3}$$

$$= 0.332 \times 99.19 \times L^{1/2} \times (0.712)^{1/3}$$

$$= 29.41\ L^{1/2}$$

This gives the average heat transfer coefficient as

$$\bar{h} = \frac{2Nu_L k}{L}$$

$$= \frac{.841}{L^{1/2}}\ \text{btu/hr - ft}^2\text{-°F.}$$

The surface area of the cooling jacket is

$$A = \pi dL$$

$$= 1.57L\ ft^2 \text{ for a 6" diameter jacket}$$

Next, for the radiative heat transfer we assume the cooling jacket is an ideal black body with $\sigma = 0.1714 \times 10^{-8}$ btu/hr-ft^2-°F. The ambient temperature is assumed to be 50°F which implies $T_\infty = 510°R$. The jacket temperature is to be held to $T_w = 610°R$.

Substituting the above information into equation (2-4) yields an expressive for the length of cooling jacket (L) that is required. For the case of a 2.5 hp (1.9 kw) motor, the length required for a 6" (15 cm) outer diameter cooling jacket is approximately 5 ft. (1.5 m). Consequently, for the sizes of motors that are required in the conveyance device, the cooling jackets will be of the acceptable size.

2.1.2 Electric (Battery Supplied)

In this configuration, electric power would be supplied to the conveyance device by use of batteries rather than using cables running down from the surface. Here we don't have to worry about the power for dragging along the supply cables (however we still need an umbilical cable). On the other hand, the batteries have to have enough capacity to power the device over the two miles of travel which means they may be bulky and possibly too large to fit in the borehole. This question of battery size is discussed in the next section.

Battery Size

First of all, the power required to propel the system must be computed. Again it can be split into two parts - the power required to drag the umbilical and the power required to drag the sensor package and the power pack.

Sensor & control cable weight	= 2100 lb
Friction force	= 2100 x 0.5
	= 1150 lb_f
Power required at speed of 50 ft/min to drag umbilical	= 1.735 hp
Weight of sensor package, power pack and battery	= (500 + battery weight) lb
Friction force	= (500 + battery weight) x 0.5 lb_f

Power required at speed of 50 ft/min to drag sensor and power pack

$$= (500 + \text{batt. wt.}) \times 0.5 \times 0.83/550 \text{ hp}$$

$$= \underline{(0.075 + \text{batt.wt.} \times .00075)\ \text{hp}}$$

The energy required to move the device over the two mile range and back at 50 ft/min is given by the instantaneous power x the time. For the umbilical the power requirements increase linearly (since only part of the cable is being dragged) from zero to a maximum of 1.735 hp at the maximum distance. Thus the energy E required is given by

$$E = (\frac{1.735}{2} + 0.075 + \text{Batt.Wt.} \times 0.00075) \times 746 \times 7.11 \text{ W-h}$$

$$= (4601 + 397.8 + \text{Batt.Wt.} \times 4.0) \text{ W-h}$$

Based on an efficiency of 95% for the electric motor and an 80% for the hydraulic system to propel the conveyance device the energy required E at the battery is given by

$$E = 1.315\ (4999 + \text{Batt.Wt.} \times 4.0) \text{ W-h.}$$

In order to find the battery weight the energy density of the battery must be known. Several types may be considered. A very efficient silver oxide cadmium battery developed by the Yardney Electric Corporation has the following specifications:

Type Y_S 60

1.4 volts

60 amph

2.76 lb

30.43 w-h/lb

29 in^3/cell

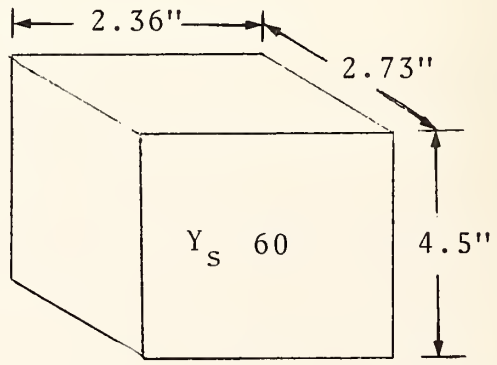

Using this specification in the above equation gives

$$30.43 \times \text{Batt.Wt.} = 1.315\ (4999 + \text{Batt.Wt.} \times 4.0)$$

$$\text{Batt.Wt.} = \frac{6573.8}{25.17}$$

$$= \underline{261\ \text{lb}}.\ (118\ \text{kg})$$

Thus approximately 95 cells would be required. If the cells were arranged in pairs, this would mean a total battery package length of 11 ft. (3.4 m) which is feasible although cumbersome. However, this power estimate includes only that power required to operate the conveyance and does not include sensor package power requirements. These requirements would further increase the battery package size and weight. Also it is doubtful that the batteries could be packaged so tight without cooling problems.

2.1.3 Pneumatic

Pneumatic (compressed air) power offers many advantages over other forms of power. The actual power supply, which consists of the air compressor system, can be located on the surface; the pneumatic transfer normally requires only one light weight hose from the compressor to the down-hole package; the light weight of the umbilical (lighter than electric cable) allows for a light weight device with low footprint pressure; pneumatic devices give off a negligible amount of heat (which eliminates the down-hole cooling problem); the presence of water or other contaminents poses no problem from a sealing point of view.

The major problem for the pneumatic power is the potential presence of a high hydraulic head down-hole. Thus if the water in the borehole amounts to a head of 500 psi (3.45 MPa), at the end of the 2-mile (3.2 km) travel, the pneumatic cylinder either has to exhaust against this or a return hose has to be provided. In the first case, a special high-pressure system

would have to be installed so that on exhaust the cylinder pressure is greater than 500 psi (3.45 MPa). Since the high pressure pneumatics are potentially dangerous, this is not really desirable. If a hose were to burst, the rapid expansion of the air (44 times volume increase) would be explosive. The other alternative, a return air line, is more attractive. It can be shown that these hoses are not excessively large or cumbersome and could be easily integrated into the umbilical.

Hose Sizes

These hose sizes, both for supply and return, depend upon the flow rate and the desired pressure drop. Since the flow rate is tied to the power requirement of the conveyance, which itself is dependent on the hose weight, the calculation of the hose size has to be done iteratively.

It was found that a flow rate of approximately 8 cfm (0.004 m^3/s) is required to provide sufficient power to propel the sensor system at 50 ft/min (0.254 m/s) and overcome the drag of the umbilical and sensor package. To provide this flow rate with an acceptable pressure drop of approximately 75 psi (517 kPa), a supply hose of 1/2" (1.3 cm) ID is required. To return 150 psi (1.03 MPa) air which is expanded down to atmospheric pressure of 14.7 psi (101 kPa), a return hose of 1.15" (2.92 cm) ID or two return hoses of 0.75" (1.9 cm) ID are required. The details of these calculations are given in Annex B.

2.1.4 Hydraulic

Hydraulic power is similar to pneumatic in that a fluid is pumped under pressure from the surface through the umbilical line to the conveyance device. The hydraulic system tends to have some disadvantages with respect to the pneumatic system. The major one being the weight of the hose and the weight of the associated fluid. This increases the load on the device

requiring more power and consequently larger hose size. Also hydraulic fluids have much higher viscous resistance in the hoses, requiring larger diameter hose or higher pressure hose, either of which increases weight. Hydraulics normally tend to run at higher pressures than pneumatics which increases the possibility of a hose bursting. Hydraulic hoses tend to be less flexible than pneumatic as a result of their greater wall thickness. On the other hand, one advantage of hydraulics is that the pumps and motors are smaller becuase of the higher system pressures compared to pneumatics.

Hose Sizes

Calculation shown in Annex C indicates that a 1-1/4" (3.2 cm) diameter supply hose is required with a 2500 psi (17.24 MPa) capability. This amounts to a weight of 1.73 lb/ft (2.57 kg/m) or approximately 18,250 lb (8.2781 Mg) for the whole umbilical length. In the case of the return, a 1.5" (3.8 cm) diameter hose is required with a weight of 1.02 lb/ft (1.52 kg/m) or approximately 11,800 lb (5.3524 Mg) for the total length. In addition, the fluid weight comes to 13,700 lb (6.2142 Mg) so that the total hydraulic supply system weighs approximately 43,800 lb (19,867 Mg).

While a lower fluid supply pressure might be used to reduce this umbilical weight, the weight of the hydraulic fluid alone makes use of a hydraulic system extremely unattractive.

2.2 GENERAL CONVEYANCE SYSTEM DESIGN FEATURES

In a previous section, the performance criteria pertaining to all conveyance concepts were established. In this section, general design features pertaining to all conveyance system concepts will be discussed. It is felt that certain system features are common regardless of the specific design of the conveyance device.

Since the basic layout of the down-hole package will be one of individual modules linked together to form a train-like consist, one of the basic system considerations is the placement of thrust modules in the consist. Within the consist there will be one or more thrust modules. Since the umbilical, which connects all components of the consist, cannot act in a compressive mode, the power modules must work in a "puller" mode. This establishes that at the lead of the consist there will be at least one thrust module.

The lead thrust module can be designed to provide all of the motive power or only a portion of it. If it provides a portion of the power, then the remainder can be made up by additional thrust modules either behind it or spaced out throughout the length of the consist. Thus, we have three possible configurations for thrust module placement:

- Single forward thrust module
- Multiple adjacent forward thrust modules
- Distributed thrust modules

The single forward thrust module has the advantage of lowest cost and system simplicity. By building only one thrust module, the number of parts is reduced which reduces cost and simplifies the system. The single module must, however, be built to power the system for a 2-mi. (3.2 km) range when in many applications this range of 2 mi. (3.2 km) may not be required.

The multiple forward thrust modules provide the same capability as the single, but allow the removal of modules for shorter runs. This configuration also provides duplicity in case of component failure. If one module fails, the others can take over with only the sacrifice of traversal speed. The multiple forward modules also allow the normal force to be spread out to

lower footprint pressure. Traversal of void spaces is also simplified since traversing modules can be pulled by the others which are not over voids.

In the distributed system, the thrust modules are spaced at intervals along the length of the umbilical. For instance, within the 10,560 ft (3.2187 km), four thrust modules could be distributed at 2,640-foot (804.7 m) intervals. Then, if a shorter run were to be made, the length of umbilical and appropriate number of thrust modules could be left off.

A design problem which is common to all system concepts is that of traversing a void space in the borehole. First of all, it can be seen that an upper design limit must be specified for void space length that is to be traversed. If a void space greater than this length is found, then it will be necessary to retract the device and grout the hole before continuing. Thus, it will be necessary to have a sensor up front which can indicate void space length before the device has proceeded to the point of no return. One way to do this is to have an extension to the thrust module ahead of any of the contacting feet or tracks. The length of the extension is the maximum traversable void space length. At the tip of this extension are three or four mechanical feelers evenly spaced around the perimeter which indicate borehole radius. This data, along with current traversed distance data, could be sent back to the surface and displayed on a console and run through a computer to determine when limits have been exceeded.

Traversal of void spaces can be done in one of two ways--the first way would be to design the conveyance device tracks or feet of sufficient length to span the void space. Since this would either result in very long feet (or tracks) or a capability of traversing only short void spaces, the second alternative, that of redundant feet (or tracks), is advantageous. This

redundancy can best be handled with multiple forward power modules. If one power module is spanning the void space, other modules could provide power. Front and rear extensions of the power modules would allow traversal of the consist even when the feet (or tracks) were completely suspended across the borehole. Figure 2-1 illustrates this concept. For this reason, when going to the modular approach, use of the multiple forward thrust modules is recommended.

Removing potential blockage from the borehole is another design consideration common to all conveyance concepts. One way to considerably reduce this problem is to reduce the cross-sectional area of the device so as to allow the device to pass over much of the rubble. Since it can be safely assumed that the rubble will be lying on the bottom of the borehole, allowing clearance below the device is best. Since prevention of arbitrary rotation of the device is impossible, the device should be designed radially symmetric, allowing three-to-four clearance channels around the periphery. This clearance must, of course, be carried through the entire consist or else blockage will occur at a later point. In cases where rubble exceeds traversable size, a rock crusher device located on the leading end of the consist would have to be called into play. This crusher will divert power normally used for thrust into crushing power. Thus, the device will slow up and move at a pace equivalent to that dictated by the crusher capacity. To conserve power, the rock crusher will only operate when needed and not run constantly with consist movement through the hole.

The concept proposed for a rock-crushing device is that of a rotating cone fitted with tungsten carbide teeth. The diameter of the large end would be such as to allow a given radial clearance. The bit can be spring-loaded longitudinally such that upon reaching a blockage, the forward thrust of the device

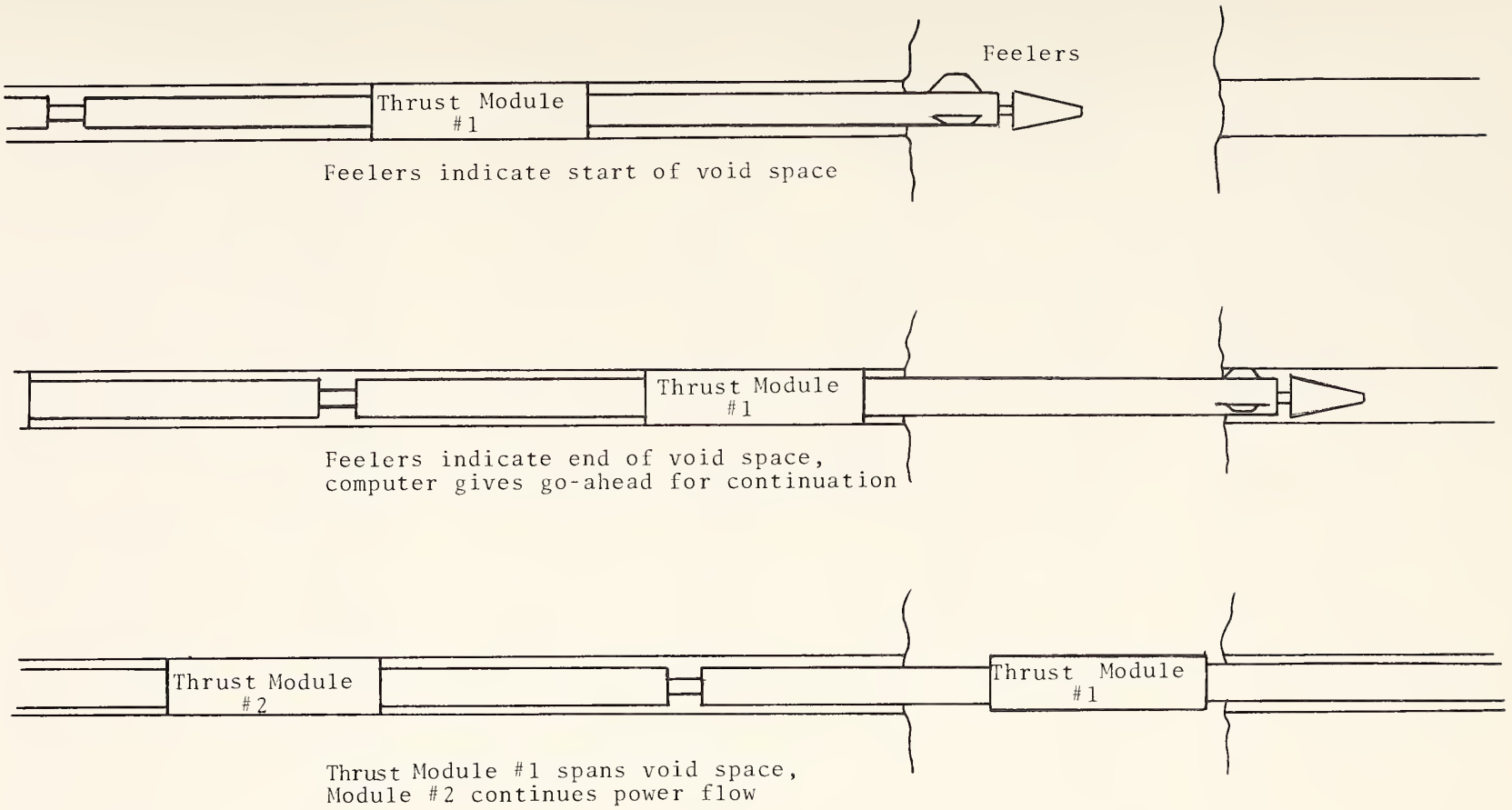

Figure 2-1. Void space traversal by borehole sensor system.

will push the device toward the bit compressing the spring. The bit will engage a switch thereby starting bit rotation and grinding up the blockage. When the blockage has been cleared, the bit will no longer depress the switch and rotation will cease. Figure 2-2 demonstrates this concept.

2.3 POTENTIAL CONVEYANCE DEVICE CONCEPTS

2.3.1 Worms

The worm is a concept which is especially suited to the small diameter borehole environment. Because of the small diameter of the hole, tractive normal forces must be gained through outward expansion of the conveyance device. Since it is not feasible to build enough weight into the device to gain the needed tractive force, the worm gains a footing in the hole by expanding outward to the borehole wall.

Because of the small diameter of the hole and the resultant volume restrictions, it is important to supply motive force in the most efficient manner. Use of wheels, tracks, screws, etc., require rotational torque from a motor to be transferred into longitudinal thrust. A much more efficient method is to use the expansion of a high-pressure fluid to provide thrust directly. Hydraulic or pneumatic cylinders could provide this power in the worm design.

The basic concept of the worm operation is shown in Figure 2-3. First, the secondary (rear) anchoring devices clamp firmly to the borehole wall. Next, the cylinder expands and pushes the primary (forward) anchor forward. Next, the primary anchoring device clamps to the borehole wall and the secondary releases. Finally, the cylinder retracts pulling the consist forward. There are several adaptations of the basic worm concept concerned with the method of gaining tractive force. These adaptations are discussed in the following sections.

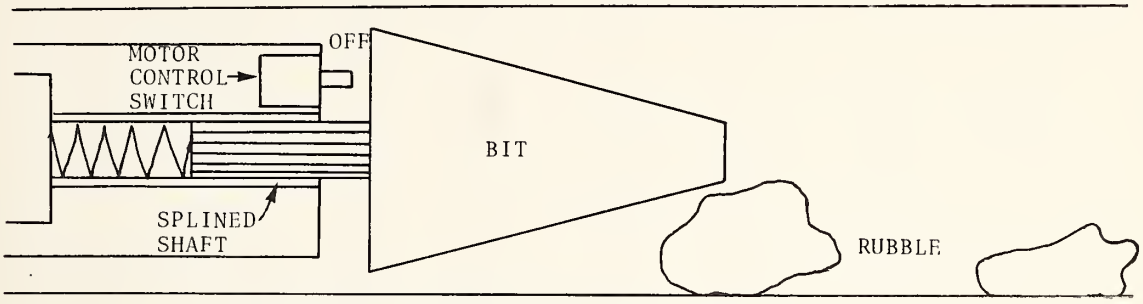

NO RUBBLE ENCOUNTERED , NORMAL MOVEMENT

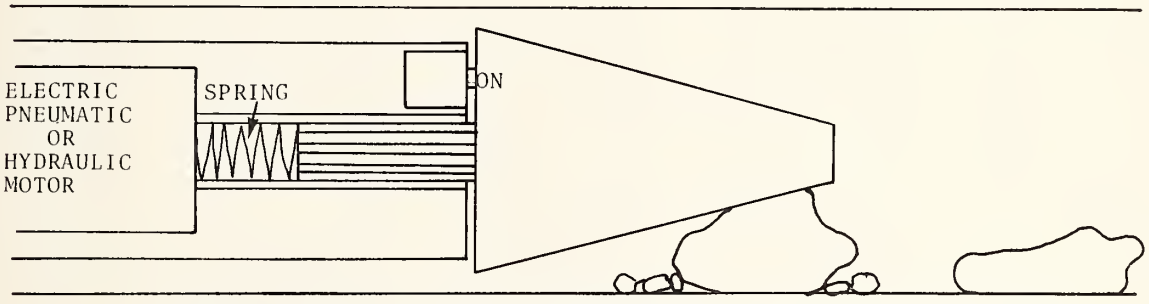

RUBBLE BLOCKS PATH, SPRING COMPRESSES, BIT TURNS GRINDING RUBBLE

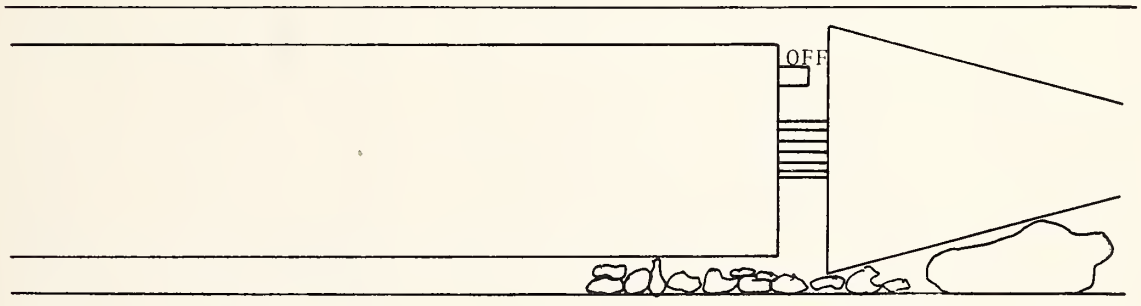

RUBBLE CLEARED, NORMAL MOVEMENT PROCEEDS UNTIL NEXT BLOCKAGE

Figure 2-2. Borehole clearing operation by conveyance device.

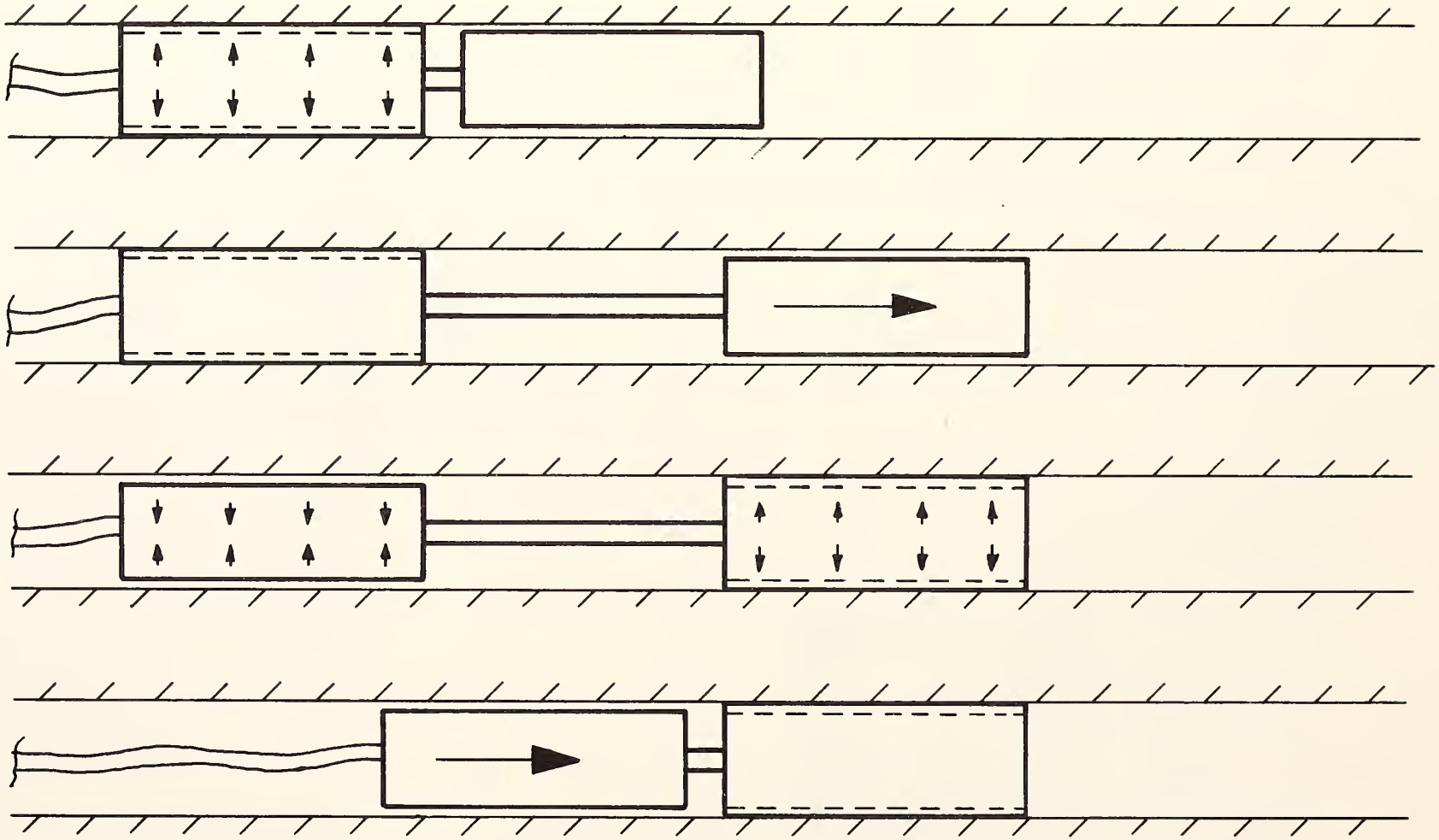

Figure 2-3. Sequential movements of the worm conveyance device.

Wedge-Worm

This device, as shown in Figure 2-4, incorporates the concept utilizing the consist load for wedging a temporary anchor radially in the borehole. The anchors are composed of arms extending radially from the center of the hole which pivot at a point on each arm. The arms are angled backward from the center wall and have feet connected to their ends. By applying a force in the direction opposite to the travel direction the arms will wedge the feet into the borehole and anchor the device. Applying a force in the direction of travel retracts the feet. This concept is shown schematically in Figure 2-5.

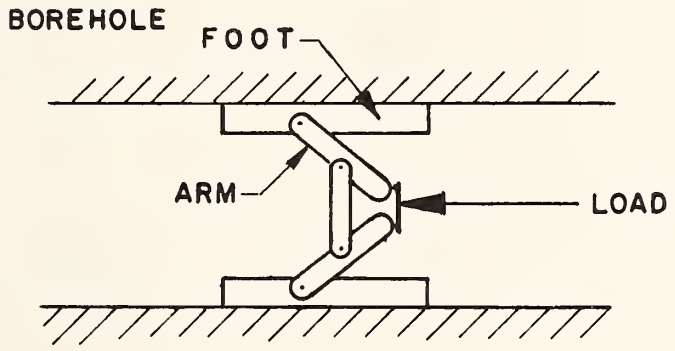

Figure 2-5. Anchoring mode of wedge worm

Two of these anchors are used by placing one on either end of a double-acting hydraulic or pneumatic cylinder. When the cylinder expands, the rear (secondary) anchor wedges in and the forward (primary) anchor collapses and is pushed ahead. Retracting the cylinder causes the primary anchor to take hold and the secondary anchor together with the consist are pulled forward. This action is repeated and the device traverses through the borehole.

The device requires a light outward spring loading on the arms to keep the feet in contact with the wall at all times. This is necessary to allow the wedging of the arms to take place. Without this and friction, the anchors would not jam into position.

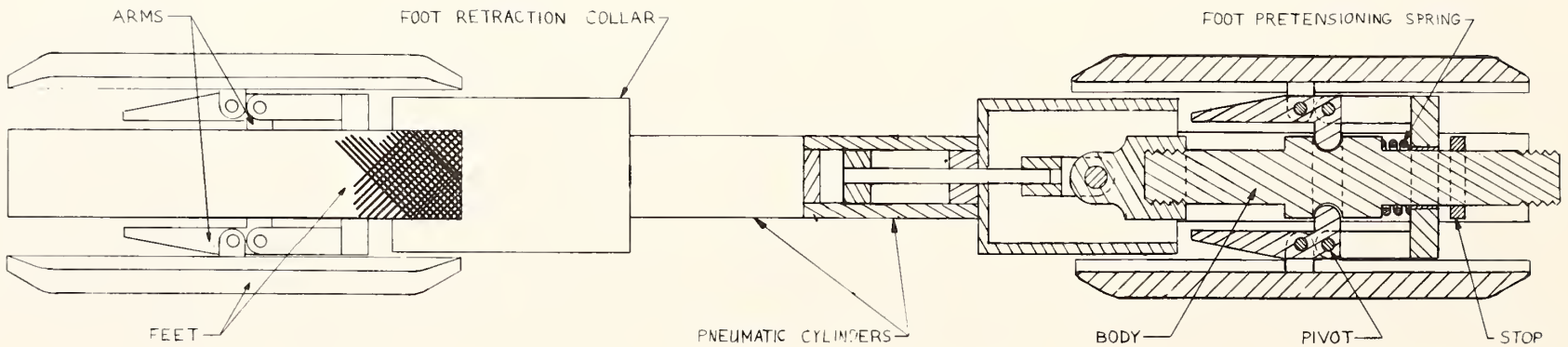

Figure 2-4. Wedge worm concept.

The major drawback of this concept is its irreversibility. The automatic anchoring prevents the device from traversing in the opposite direction. To overcome this problem, the device has been conceptually designed so that at full retraction of the power cylinder the feet retract and no longer anchor the device. To remove, a reversed conveyance device at the rear of the consist provides rearward motive power.

Another major drawback is with the footprint pressure equalization. Because all of the arms and feet move together, if a stone becomes lodged beneath one foot, the other feet would not contact the borehole properly. Use of rubber pads on the feet can partially overcome this problem by allowing some local shoe deformation.

Traversal of void spaces is also a problem because when in an open space the shoes will expand outward and possibly pivot, and can get caught on the opposite side of the void space. The feet can therefore only span a void space distance which is less than half their length.

Inflatable Elastomeric Shoe Worm

This concept utilizes inflatable elastomeric rubber shoes (or rings) located on the outside of the device to expand out to the borehole wall and provide normal tractive force. The rubber shoe is cast as a single casting with an inflation tube and metal core as an integral part as shown in Figure 2-6. Applying pneumatic or hydraulic pressure to the shoe causes the shoe walls to expand.

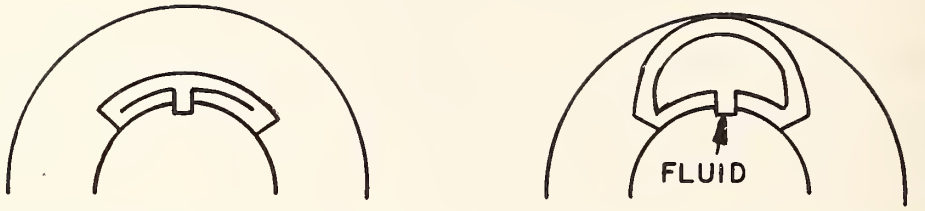

Figure 2-6.

Typical elastomers will expand up to 700%, but 20% is considered a safe limit for repeated elastic expansions. As an example, such an expansion would allow an 8.0" (20 cm) diameter ring to expand to a diameter of 9.6" (24 cm).

The inflatable shoe (or ring) concept has one major drawback in this application. When operating in a high-pressure water environment, the internal inflation pressure of the shoe will be directly opposed by the downhole water pressure (P). Therefore, to overcome a 500 psi (3.45 MPa) head, an internal pressure of ΔP above 500 psi (3.45 MPa) must be provided. This will necessitate either a regulated high-pressure fluid source (or self-compensating amplifier) to maintain internal pressure at the correct level but avoid high pressures from being introduced into the shoe when the down-hole pressure is low. The latter problem could produce damaging over-inflation of the shoes and possible rupture. While the shoe could be designed to be strong enough to resist possible over-inflation, this would make it too stiff to operate at high down-hole pressures because the pressure differential would be too small for sufficient expansion.

To accomplish the needed pressure regulation, a pressure equalizer can be employed as shown in Figure 2-7. The idea here is to use hydraulic fluid whose pressure is determined by the existing down-hole pressure to pressurize the inflatable shoes. Pressurized air is pumped from the surface through the umbilical cable. A portion of this air is used to operate the pneumatic cylinders while the remainder is used to power a hydraulic pump. A double-solenoid, two position valve controls air flow to the double-acting pneumatic cylinders. Sequencing of this valve is controlled by micro-switches located at either end of the primary shoe system stroke.

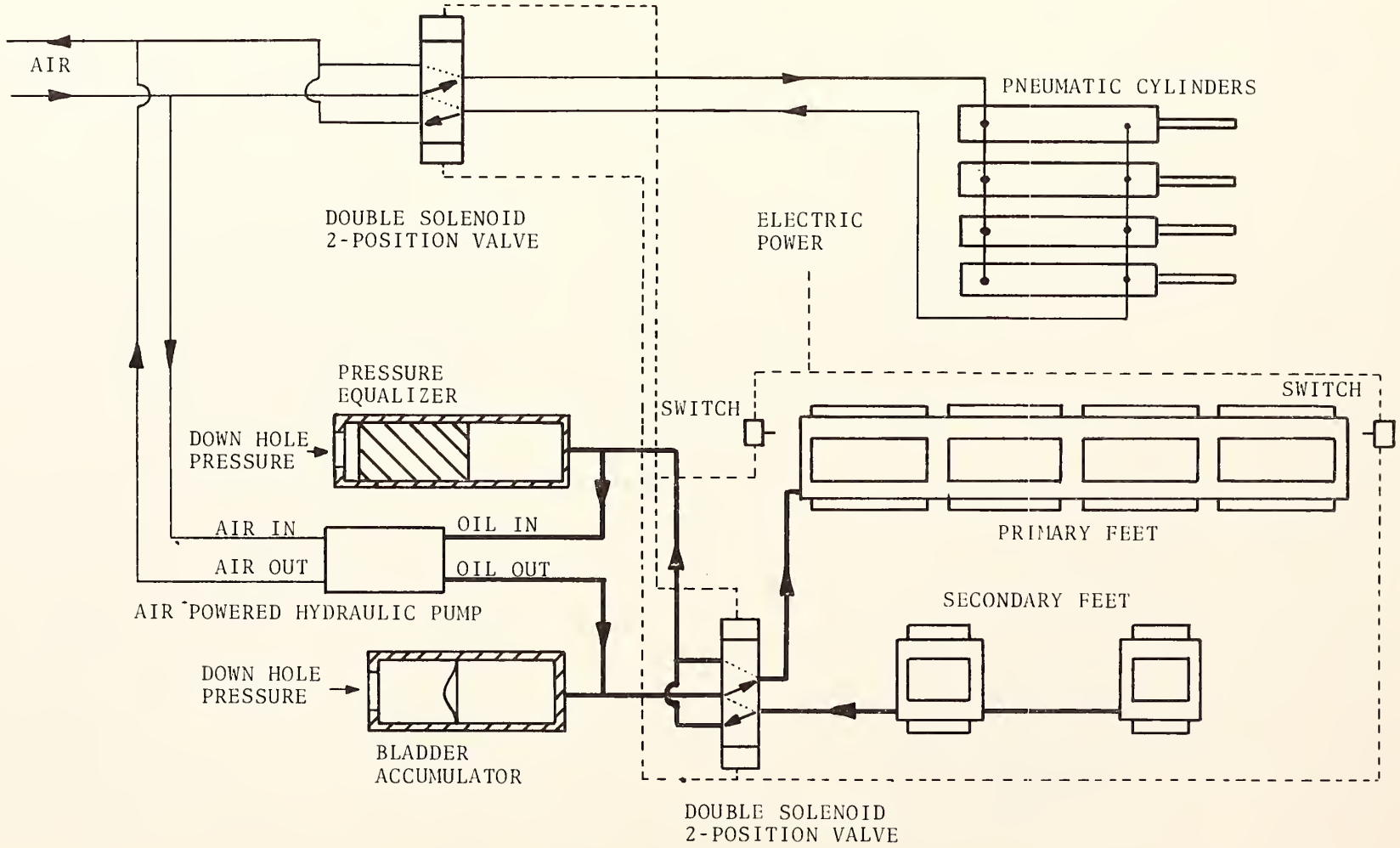

Figure 2-7. Inflatable shoe worm fluid power system schematic.

The hydraulic system operates at down-hole pressure (P) on the pump suction side and at P+ΔP on the pump pressure side. A bladder accumulator evens out pump demand. Because this accumulator must operate at various internal fluid pressures, it uses down-hole pressure on the external side of the bladder. A double-solenoid two-way valve controls the hydraulic fluid flow to the shoes. It too is sequenced by the same micro-switches which control the pneumatic cylinders.

The concept proposed for the inflatable shoe worm device itself, Figure 2-8, is designed around a cylindrical pipe core. This core allows easy routing of the umbilical through the device. The primary anchoring shoes are mounted on an outer cylinder (reciprocating primary shoe pod) in four longitudinal rows radially spaced at 90° intervals. This arrangement provides natural "troughs" for passage of debris. Because of the size limitations imposed by the design, four small pneumatic cylinders rather than one large cylinder are used to move the outer cylinder. A hose coiled around the central pipe supplies hydraulic fluid to the outer cylinder. Secondary shoes are located at either end for holding the device in place when the primary shoe pod is moving backwards.

Mechanical Piston Worm

To overcome the complications in the inflatable shoe worm, resulting from high down-hole pressures a mechanical analogy to the elastomeric shoe worm has been developed. This design uses three longitudinal banks of pistons located circumferentially at 120° intervals. The pistons extend out to contact the walls of the borehole and provide tractive normal force. The pistons overcome the down-hole pressure problem by being designed as pneumatic pressure amplifiers. The 0.5" (1.3 cm) diameter end of the piston exposed to the water has only 1/9 the surface area of the internal pressurized end [1.5" (3.8 cm) diameter]. Thus with an internal pressure of 150 psi (1.03 MPa) and an external down-hole pressure of 500 psi (3.45 MPa), there is a net outward force on the piston of approximately 170 lb (77.1 kg).

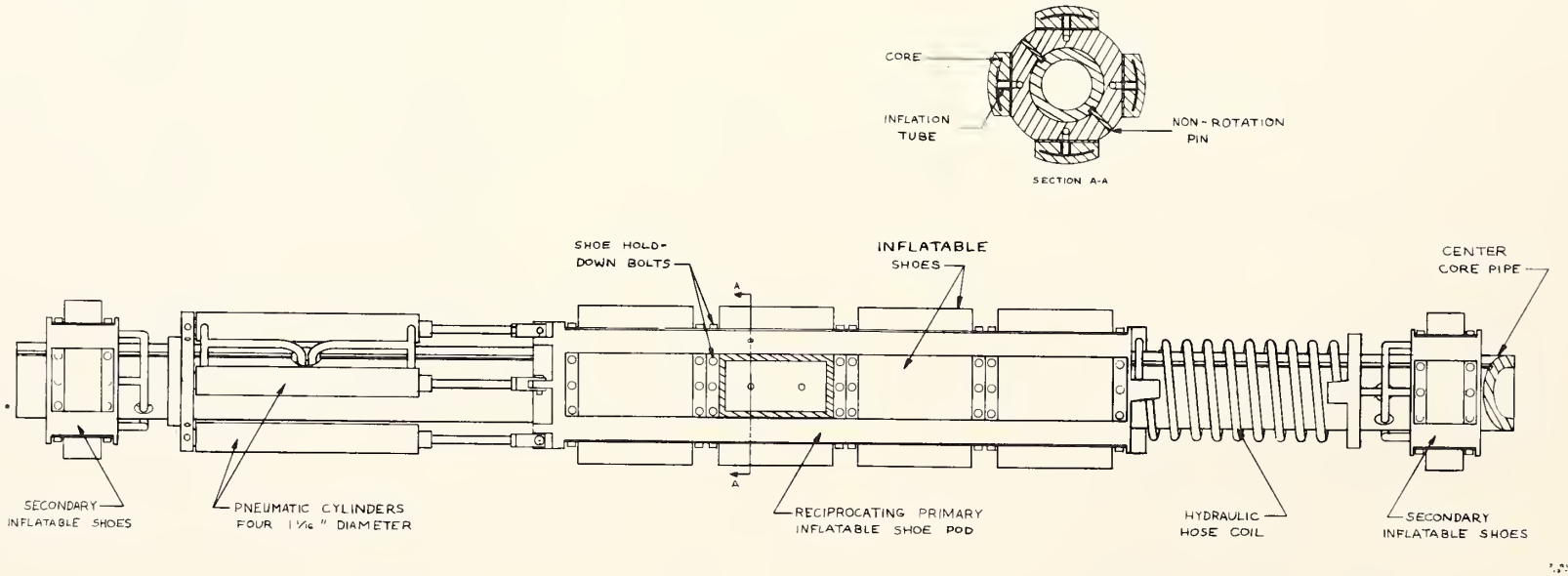

Figure 2-8. Inflatable shoe worm concept.

Thus the device will operate with a large hydraulic head, the only penalty being a slower speed of piston extension. When the piston contacts the wall, the outward force will return to 265 lb. (120 kg) since the water pressure no longer acts counter to movement. The device in the example can operate at down-hole pressures up to 1350 psi (9.31 MPa) providing that the rest of the device is designed to withstand those pressures.

The conceptual design for this device is shown in Figure 2-9. The device employs three radial banks of pistons bolted to a central air supply core. The entire cylinder bank system reciprocates within the confines of three end plates which also provide troughs for hoses and cables. A single pneumatic cylinder provides motive power for the device. The pistons are provided with return springs and feet, the latter feature being used for better footprint pressure distribution.

A fluid power system which is much simpler than that of the inflatable shoe piston can be utilized. The system would consist of an air storage tank, a double-solenoid/two-piston pneumatic valve, two valve sequencing switches, and related hoses and fittings.

The major concern with this design is sealing of the pistons against the harsh environment of high-pressure water, which contains abrasive compounds. However, this problem has been solved in similar mining applications.

2.3.2 Continuous Motion Devices

Tracked (Caterpillar) Conveyance

The tracked conveyance is a continuous motion device as compared to the discrete action of the worm device. This poses a problem due to the stop-and-go motion required by the acoustic sensor. Consequently a logic system for stopping and starting the device at predetermined intervals must be provided with the this design.

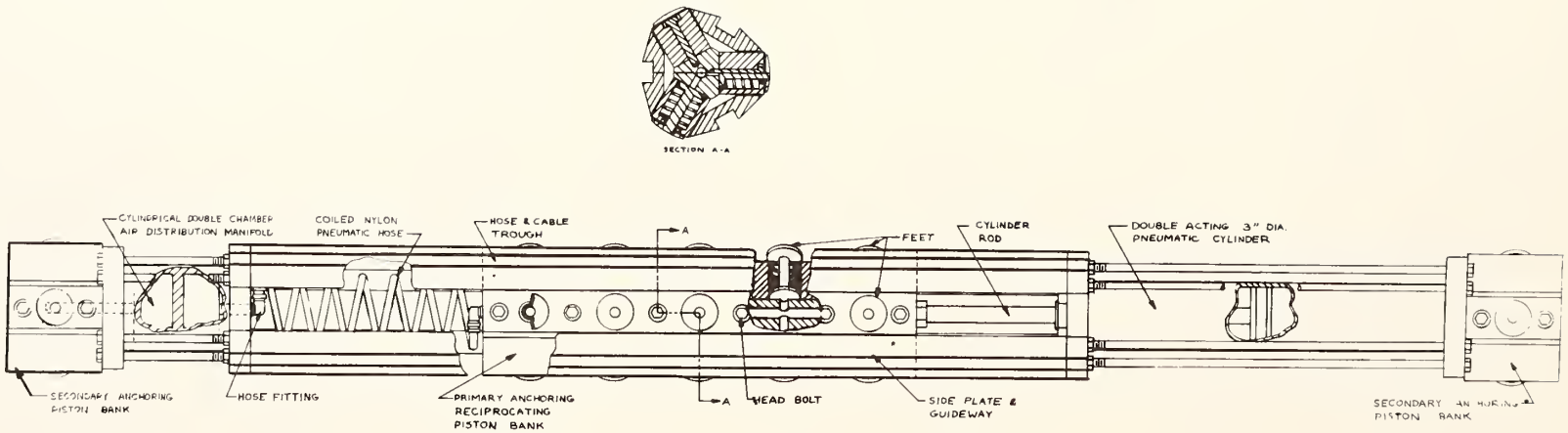

Figure 2-9. Mechanical piston worm concept.

The tracked conveyance (Figure 2-10) has three track belts located 120° apart around the periphery of a power screw. As the power screw turns, it engages with teeth on the belts. Each track belt runs around a series of bogies (rollers) which supply the normal force to the tracks. This normal force is obtained from action of a hydraulic or pneumatic cylinder which compresses the series of bogies and bunches them up creating an outward normal force component. The drive torque is supplied to the power screw directly from an electric, pneumatic, or hydraulic motor. The device could employ, as an example, a 3" (7.6 cm) diameter quadruple ACME thread power screw with a 1" (2.5 cm) pitch. This screw has an efficiency of approximately 60%.

The track belt could be a chain of special links or a reinforced rubber belt, with an ACME thread on the outside and a raised notch on the inside. The notch keeps the belt from coming off of the bogies which are designed with a groove to mate with the notch. The belts are contoured on the outside surfaces with a radius to match the borehole wall.

One major problem with this system is one of complication and associated reliability. The large number of small interacting parts invites failure. Many wear surfaces are exposed to the harsh environment. Failure of one track system would require a complete test abort. The design is also extremely susceptible to jamming from stones, especially at the belt-power screw interface.

Auger Screw Conveyance Device

The auger screw device (Figure 2-11) uses four auger type screws located 90° apart circumferentially to convert rotational torque into thrust. Each pair of diagonally opposite screws has the reverse thread of the other pair. Opposite rotation of these pairs prevents the gross rotation of the device

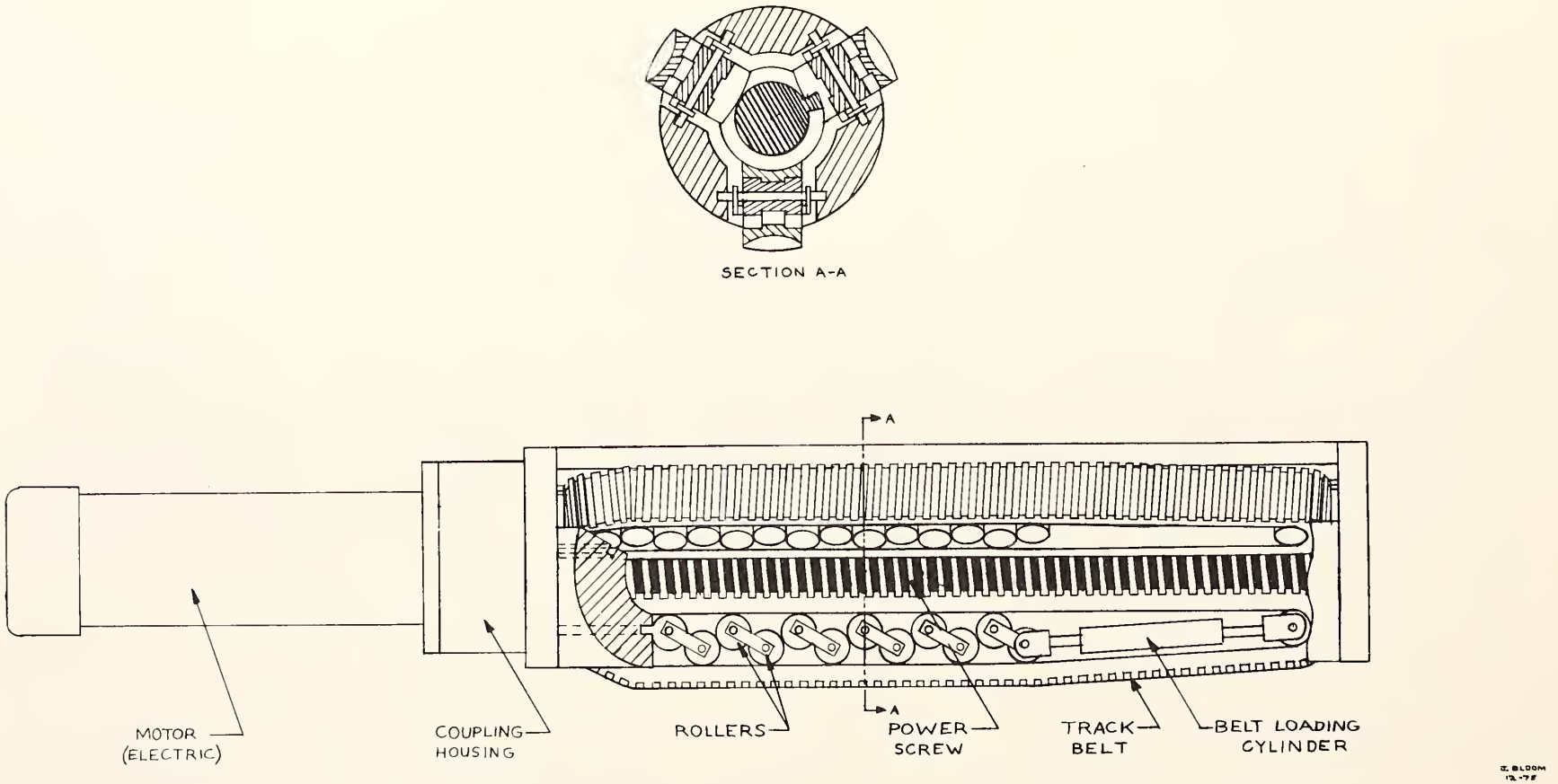

Figure 2-10. Tracked conveyance concept.

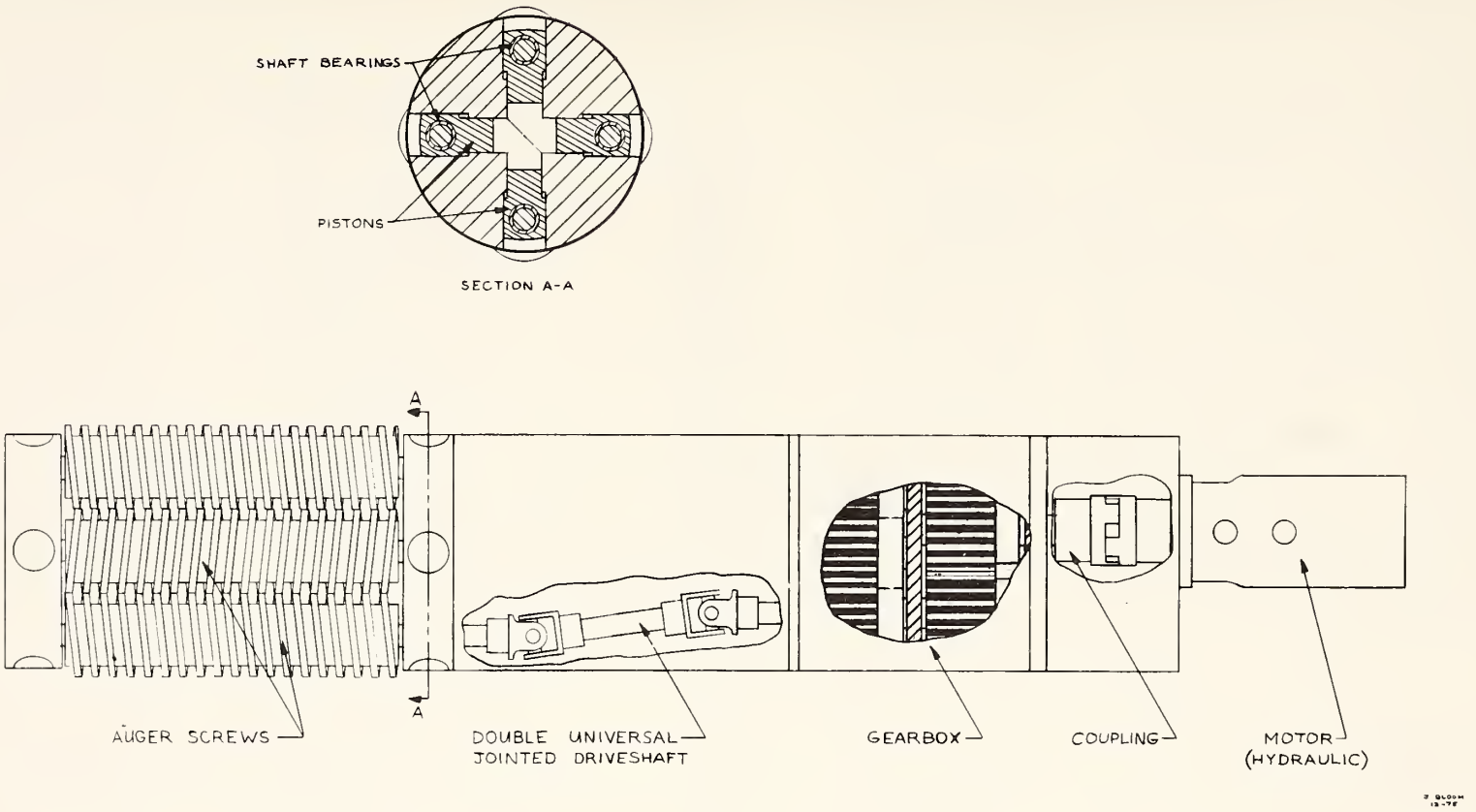

Figure 2-11. Auger screw concept.

which would occur if all screws turned the same direction. The screws are held to the frame of the device at a bearing point at both screw bosses. These bearings are fixed to radial pistons which through hydraulic or pneumatic pressure force the screw against the borehole wall. Each screw is connected by a double universal jointed drive shaft to a gear box with four output shafts. Inside the gear box are four equal size gears which mesh in a square pattern giving opposite rotation to each diagonally opposite pair. Power comes from either an electric, hydraulic or pneumatic motor.

The screws are of a composition contruction consisting of a steel center core rod with cast rubber body and threads. The rubber allows the screws some local deformation to fit around small rocks and nonuniform surfaces. It also has better traction properties than a solid metal screw would.

As with the tracked conveyance, the auger screw conveyance is a continuous motion device with the same associated logic system requirements.

2.4 ANCILLARY EQUIPMENT

2.4.1 Surface Support Vehicle

The surface support vehicle shown conceptually in Figure 2-12 is a truck to convey the borehole sensor system to the test site and provide support during the testing operation. The vehicle contains all support equipment except for data collection and monitoring equipment.

The basic vehicle is a flatbed truck 325" (8.26 m) long with a 204" (5.18 m) wheelbase and 240" (6.10 m) loadbed. The vehicle has a crew cab with seating for five persons. In addition to the standard vehicle fuel tank, there are two 125 gallon (473 l) fuel tanks to provide approximately a week's supply of fuel for borehole sensor system power. The vehicle carries

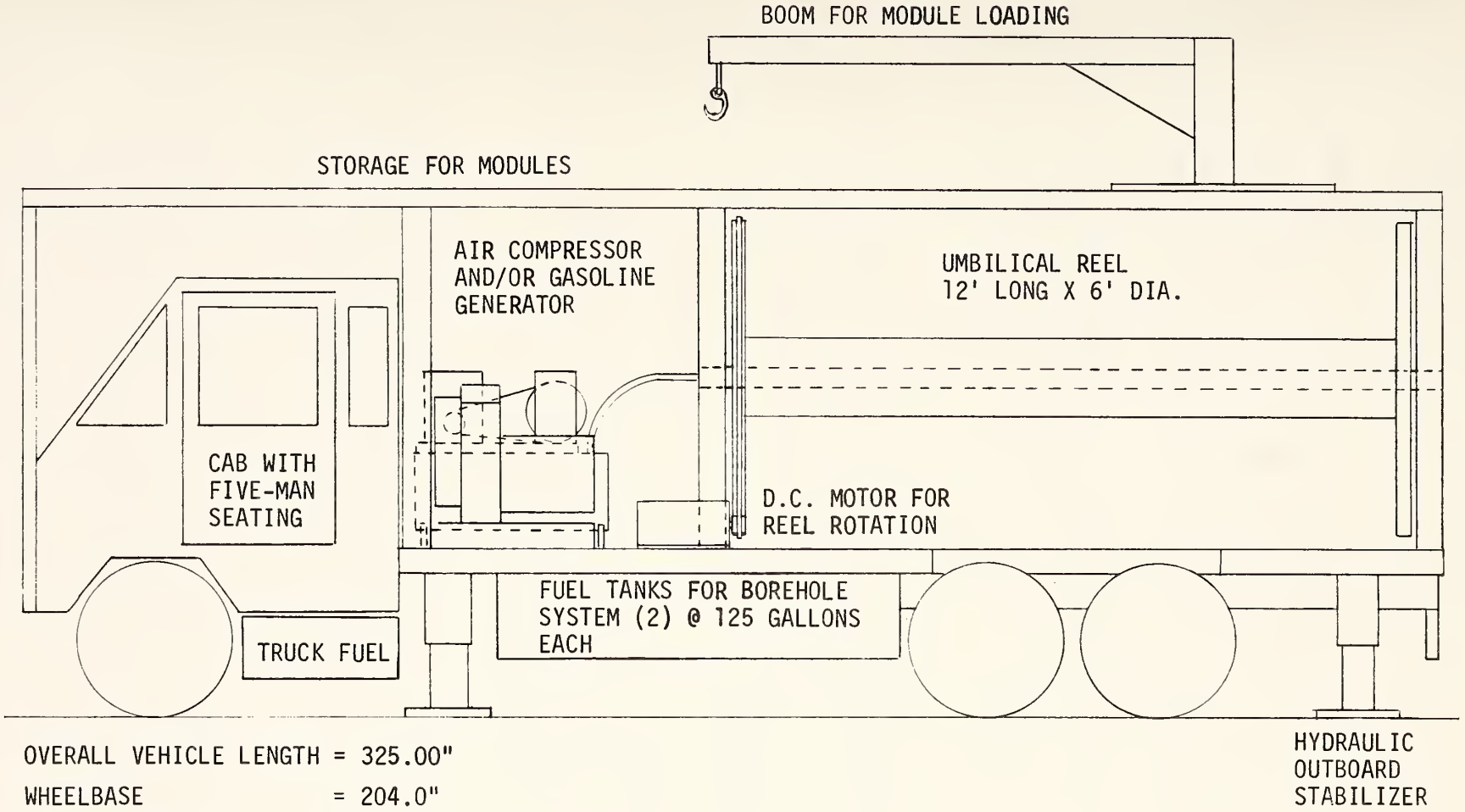

Figure 2-12. Borehole sensor surface support vehicle.

a 12' (3.7 m) long by 6' (1.82 m) O.D. (1.5' [0.46 m] I.D.) umbilical cable reel. This size reel is capable of carrying two miles (3.2 km) of 2.0" (5 cm) diameter umbilical cable. The reel rotates about a horizontally-mounted axle. A variable speed D.C. motor drives the reel through a belt or chain drive arrangement. Rotational speed is controlled by a feedback system (not shown) which monitors umbilical tension at the reel and speeds up or slows down in order to maintain a constant tension.

The vehicle contains all the required power transmitting devices such as electric generator, air compressor and/or hydraulic pump. The power is transferred to the reel through rotating couplings or slip rings.

The vehicle structure includes an overhead storage area where modules are carried during transporting. The modules are picked up at their c.g. by a boom which rotates and lowers them to the ground. While in overhead storage, the modules are strapped into place to prevent movement.

2.4.2 Umbilical Cable

The umbilical cable must be designed to serve three functions: supplying power and control to the down-hole package, transmitting sensor signals, and retrieving the sensor package.

The first function means that the umbilical must contain power cables and/or pneumatic lines and control cables. If the conveyance is pneumatic powered, small power cables must be provided for sensor package power in addition to the supply and return pneumatic lines. An electric powered conveyance will require heavy-duty electric power cables. Since AC cables are designed for the peak voltage as opposed to the usable RMS voltage, DC power allows lighter weight cables and should be used. For control, four pairs of #22 control cable are anticipated.

The third function of the umbilical, that of returning sensor signals, will be handled by a single coaxial cable.

For retrieval of the package, the umbilical must be capable of a tensile force sufficient to pull its own weight and that of the down-hole package. A safety factor must be provided in case of snagging and resultant force peaks. Since electric cables and pneumatic lines were not designed for this purpose, it is proposed that the umbilical be jacketed with phillystran fiber. This fiber has a tensile-strength-to-weight ratio about ten times as great as steel cable. It is used for applications such as helicopter hoists, balloon tethers, and mooring cables where light weight is important.

Shown in Figure 2-13 are four examples of pneumatic umbilical cable designs which demonstrate some of the considerations that must be made in designing an umbilical.

The first design has all small diameter hoses because they have better kink resistance with thinner walls and lighter weight than larger hoses. They also are more readily available and can use standard fittings on the ends. The configuration, however, is less flexible and more difficult to wind on a reel because the various cables bend at different radii.

The second design is more flexible along one axis than the first and is easier to wind on a reel provided it does not twist. The hoses are larger diameter and more susceptible to kinking than in the first design. Also, special fittings are required on the ends.

The third and fourth designs are very similar, both being symmetrical, flexible and easy to wind up. However, the outer hoses are extremely susceptible to kinking and must be of a very thick wall to resist it. Consequently, they would be heavy. Also, special fittings would be required to connect the pneumatic lines to the compressor and the down-hole device.

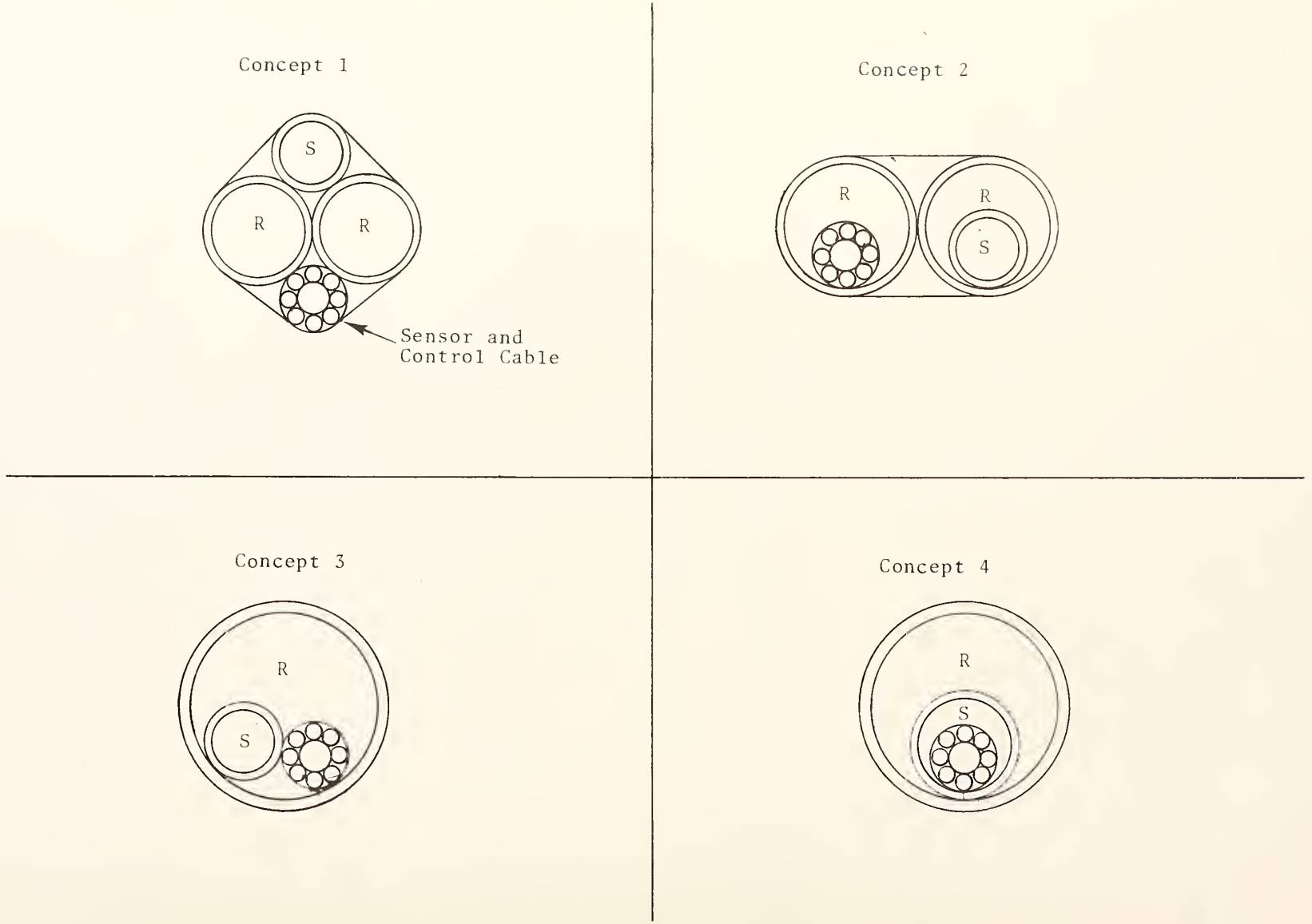

Figure 2-13. Pneumatic power umbilical cable concepts S = supply; R = return.

3. TRADEOFF STUDY FOR BOREHOLE CONVEYANCE DEVICE

A tradeoff study has been conducted with the emphasis on a fair and impartial evaluation of each of the potential concepts. In the study, each concept appears to be of equal potential in each of the following areas:

- Umbilical features
- Sensor package constraints
- Length
- Modular construction feasibility
- Surface support equipment

The concepts were evaluated in all areas which were considered to have any bearing on the success or failure of the project. Each concept was evaluated for each of 22 tradeoff criteria. A ranking was given from 1 (worst) to 5 (best) for each case. A justification for the ranking is included in each case also. Because some criteria have greater importance than others, a weighting was also given for each of the 22 criteria. The weightings, made on the basis of importance to success of the project, were: 3 for vital; 2 for important; and 1 for minor importance. Weightings were multiplied times the ranking and a total score arrived at.

Because it is recognized that the ranking is subjective, anything below a 10% difference in score cannot be interpreted as being significant for discrimination between two or more devices. Therefore, a second basis of comparison has been instituted. If a device receives a ranking of 1 (worst) on a vital criteria, that will serve as an additional basis for nonacceptance. Such a ranking means that in a vital area, this concept is sorely lacking.

TRADEOFF CRITERIA FOR CONVEYANCE DEVICE CONCEPTS

1. Power requirements and efficiency
2. Relative complexity of design
3. Adaptability for stop-and-go movement
4. Traversal of void spaces without over-expansion of feet
5. Ability to apply normal force evenly over rough surfaces (e.g., over protruding pebbles)
6. Ability to operate under hydraulic head
7. Requirement for new technology and special manufacturing techniques for implementation of design
8. Estimated reliability of conveyance system
9. Need for close tolerance in device
10. Potential damage from dirty or wet environment
11. Likelihood of pebbles or dirt jamming the device and preventing movement
12. Probability that failure could prevent removal by umbilical retraction
13. Footprint pressure on borehole
14. Relative cost
15. Difficulty of routing wires and hose past conveyance
16. Difficulties of power transfer mechanism
17. Adaptability to various borehole sizes
18. Smallest borehole diameter that is feasible
19. Ease of converting motive power for use in rock crushing mode
20. Speed capability
21. Fail-safe characteristics of device
22. Probable maintenance required

BOREHOLE CONVEYANCE TRADEOFF STUDY

TRADEOFF CRITERION: 1. Power requirements and efficiency

IMPORTANCE TO SUCCESS: Not critical but reflects on cost and weight

CONVEYANCE CONCEPT	DISCUSSION OF TRADEOFFS	RANKING 5=best 1=worst
WEDGE WORM	Horsepower ≈ 2.5 (1,9 kw) High efficiency due to utilization of load force in anchoring device	5
INFLATABLE SHOE WORM	Horsepower ≈ 3.0 (2.2 kw) Good efficiency resulting from direct utilization of pneumatic power in cylinder, little power required for anchoring device	4
EXTENDABLE PISTON WORM	Horsepower ≈ 3.0 (2.2 kw) Same as above	4
TRACKED DEVICE	Horsepower ≈ 5.0 (3,7 kw) Losses due to power transfer in power screw result in decreased efficiency	3
AUGER DEVICE	Horsepower ≈ 6.0 (4,5 kw) Power transfer losses in gear box, universal joints and slippage of augers on borehole wall result in poor efficiency	2

BOREHOLE CONVEYANCE TRADEOFF STUDY

TRADEOFF CRITERION: 2. Relative complexity of design

IMPORTANCE TO SUCCESS: Greater complexity leaves more room for error in design

CONVEYANCE CONCEPT	DISCUSSION OF TRADEOFFS	RANKING 5=best 1=worst
WEDGE WORM	Very simple design with few parts; can be analyzed thoroughly by conventional kinematic methods	5
INFLATABLE SHOE WORM	Design relatively simple, very few moving parts; however, design of inflatable shoes may need development	3
EXTENDABLE PISTON WORM	Design relatively simple, large number of parts, however.	3
TRACKED DEVICE	Most complex design, large number of interacting parts	1
AUGER DEVICE	Fairly simple design, number of parts is not too large	4

BOREHOLE CONVEYANCE TRADEOFF STUDY

TRADEOFF CRITERION: 3. Adaptability to stop-and-go movement

IMPORTANCE TO SUCCESS: Fairly important

CONVEYANCE CONCEPT	DISCUSSION OF TRADEOFFS	RANKING 5=best 1=worst
WEDGE WORM	Automatic stop and go movement as part of operation. Length of stop period can be adjusted by changing length of stroke	5
INFLATABLE SHOE WORM	Same as above	5
EXTENDABLE PISTON WORM	Same as above	5
TRACKED DEVICE	Downhole logic system required to tell device when to stop-and-go	3
AUGER DEVICE	Same as above	3

BOREHOLE CONVEYANCE TRADEOFF STUDY

TRADEOFF CRITERION: 4. Traversal of void spaces without over expansion of feet.

IMPORTANCE TO SUCCESS: Vital

CONVEYANCE CONCEPT	DISCUSSION OF TRADEOFFS	RANKING 5=best 1=worst
WEDGE WORM	Traversal capability is poor due to possible over expansion of foot	1
INFLATABLE SHOE WORM	Possible over inflation of shoes may result.	3
EXTENDABLE PISTON WORM	Pistons expand out and stop. Spring loading of pistons prevents snagging on opposite void wall.	5
TRACKED DEVICE	Tracks expand outward until they stop; may have trouble on opposite void wall with snagging.	4
AUGER DEVICE	Same as above for screws.	4

BOREHOLE CONVEYANCE TRADEOFF STUDY

TRADEOFF CRITERION: 5. Ability to apply normal forces evenly over rough surfaces

IMPORTANCE TO SUCCESS: Fairly important

CONVEYANCE CONCEPT	DISCUSSION OF TRADEOFFS	RANKING 5=best 1=worst
WEDGE WORM	Uneven surface can prevent all feet from touching surface and overload some arms.	1
INFLATABLE SHOE WORM	Good adaptability to variations in surface conditions. Rubber shoes can inflate to mold to uneven contours.	5
EXTENDABLE PISTON WORM	Excellent ability to adapt to large variances in surface conditions. Each piston can move radially a different amount.	5
TRACKED DEVICE	Fair ability of track to mold to contour changes	3
AUGER DEVICE	Screw pitch can be designed so that largest pebble sizes can fit between threads.	4

BOREHOLE CONVEYANCE TRADEOFF STUDY

TRADEOFF CRITERION: 6. Ability to operate under hydraulic head

IMPORTANCE TO SUCCESS: Very important

CONVEYANCE CONCEPT	DISCUSSION OF TRADEOFFS	RANKING 5=best 1=worst
WEDGE WORM	No problem.	5
INFLATABLE SHOE WORM	Shoe cannot inflate unless inflation pressure exceeds hydraulic head pressure. Downhole pressure amplifier and regulation system required.	2
EXTENDABLE PISTON WORM	Hydraulic head pressure creates only minor retarding action on piston travel.	4
TRACKED DEVICE	No problem.	5
AUGER DEVICE	No problem.	5

BOREHOLE CONVEYANCE TRADEOFF STUDY

TRADEOFF CRITERION: 7. Requirements for new technology and special manufacturing for implementation of design

IMPORTANCE TO SUCCESS: Minor

CONVEYANCE CONCEPT	DISCUSSION OF TRADEOFFS	RANKING 5=best 1=worst
WEDGE WORM	None.	5
INFLATABLE SHOE WORM	Development of inflatable elastomer shoes required.	2
EXTENDABLE PISTON WORM	Piston seals may pose a problem in regard to grit contamination.	2
TRACKED DEVICE	Track belt must be specially manufactured for this device.	2
AUGER DEVICE	Auger screws must be specially manufactured for this device.	2

BOREHOLE CONVEYANCE TRADEOFF STUDY

TRADEOFF CRITERION: 8. Estimated reliability of conveyance system

IMPORTANCE TO SUCCESS: Very important

CONVEYANCE CONCEPT	DISCUSSION OF TRADEOFFS	RANKING 5=best 1=worst
WEDGE WORM	Reliability estimated to be extremely high because of the simplicity of device.	5
INFLATABLE SHOE WORM	Good reliability foreseen, however, much testing required.	4
EXTENDABLE PISTON WORM	Good reliability foreseen; seal wear may be a problem.	4
TRACKED DEVICE	Reliability is estimated to be fairly low because of the large number of moving and interacting parts and possible track failure.	1
AUGER DEVICE	Good reliability foreseen.	4

BOREHOLE CONVEYANCE TRADEOFF STUDY

TRADEOFF CRITERION: 9. Need for close tolerances in device

IMPORTANCE TO SUCCESS: Dirty environment makes close tolerances undesirable

CONVEYANCE CONCEPT	DISCUSSION OF TRADEOFFS	RANKING 5=best 1=worst
WEDGE WORM	Sloppy tolerance can be allowed.	5
INFLATABLE SHOE WORM	Tolerances need not be very close.	4
EXTENDABLE PISTON WORM	Only pistons require close tolerances in bore.	3
TRACKED DEVICE	Fairly close tolerances required between exposed interacting parts.	1
AUGER DEVICE	Fairly close tolerances required inside gear box and piston bores.	2

BOREHOLE CONVEYANCE TRADEOFF STUDY

TRADEOFF CRITERION: 10. Potential damage from dirty, wet environment

IMPORTANCE TO SUCCESS: Can result in premature failure or heavy wear

CONVEYANCE CONCEPT	DISCUSSION OF TRADEOFFS	RANKING 5=best 1=worst
WEDGE WORM	Very little damage foreseen.	5
INFLATABLE SHOE WORM	Very little damage foreseen, some sealing against water required; dirt can wear mating surfaces of telescoping cylinders.	4
EXTENDABLE PISTON WORM	Very little damage foreseen, pistons must be sealed against water, sliding surfaces can wear from dirt.	3
TRACKED DEVICE	Many surfaces to wear from grit, however, water poses no problems.	2
AUGER DEVICE	Pistons used to push augers outward must be sealed, as must gear box; several potential wear problems from grit.	2

BOREHOLE CONVEYANCE TRADEOFF STUDY

TRADEOFF CRITERION: 11. Likelihood of pebbles or dirt jamming device and preventing movement

IMPORTANCE TO SUCCESS: Vital

CONVEYANCE CONCEPT	DISCUSSION OF TRADEOFFS	RANKING 5=best 1=worst
WEDGE WORM	Very little.	4
INFLATABLE SHOE WORM	None.	5
EXTENDABLE PISTON WORM	Very little.	4
TRACKED DEVICE	Small pebbles becoming lodged in tracks can jam device when screw threads mate with belt.	1
AUGER DEVICE	Large pebbles could lodge between auger screws.	3

BOREHOLE CONVEYANCE TRADEOFF STUDY

TRADEOFF CRITERION: 12. Probability that component failure could prevent removal by umbilical retraction.

IMPORTANCE TO SUCCESS: Vital

CONVEYANCE CONCEPT	DISCUSSION OF TRADEOFFS	RANKING 5=best 1=worst
WEDGE WORM	Failure of cylinder return springs could prevent retraction of feet and thereby prevent retraction from borehole.	3
INFLATABLE SHOE WORM	None.	5
EXTENDABLE PISTON WORM	None.	5
TRACKED DEVICE	Very little.	4
AUGER DEVICE	Auger screw shaft failure could cause screw to become lodged in borehole and prevent retraction.	3

BOREHOLE CONVEYANCE TRADEOFF STUDY

TRADEOFF CRITERION: 13. Footprint pressure on borehole.

IMPORTANCE TO SUCCESS: High force concentration can cause problems in soft borehole.

CONVEYANCE CONCEPT	DISCUSSION OF TRADEOFFS	RANKING 5=best 1=worst
WEDGE WORM	Footprint pressure can be low with long feet; however, uneven loading can occur.	3
INFLATABLE SHOE WORM	Footprint pressure low and even.	5
EXTENDABLE PISTON WORM	Forces are concentrated at points; however, large number of pistons lower required individuals loadings as do feet on ends of pistons.	4
TRACKED DEVICE	Low footprint pressure, good force distribution.	4
AUGER DEVICE	Low footprint pressure.	4

BOREHOLE CONVEYANCE TRADEOFF STUDY

TRADEOFF CRITERION: 14. Relative cost.

IMPORTANCE TO SUCCESS: Important because of limited available funds

CONVEYANCE CONCEPT	DISCUSSION OF TRADEOFFS	RANKING 5=best 1=worst
WEDGE WORM	Lowest cost.	5
INFLATABLE SHOE WORM	Medium cost.	3
EXTENDABLE PISTON WORM	Medium cost.	3
TRACKED DEVICE	Highest cost.	1
AUGER DEVICE	Medium cost.	3

BOREHOLE CONVEYANCE TRADEOFF STUDY

TRADEOFF CRITERION: 15. Difficulty of routing wires and cables past conveyance

IMPORTANCE TO SUCCESS: Important for modular usage

CONVEYANCE CONCEPT	DISCUSSION OF TRADEOFFS	RANKING 5=best 1=worst
WEDGE WORM	Difficult; requires hollow center shaft or necessity of running wires and cables between arms.	1
INFLATABLE SHOE WORM	Rather easy.	5
EXTENDABLE PISTON WORM	Side plates can be designed as troughs.	4
TRACKED DEVICE	Side plates can be designed as troughs.	4
AUGER DEVICE	Rather difficult, must run between auger screws.	1

BOREHOLE CONVEYANCE TRADEOFF STUDY

TRADEOFF CRITERION: 16. Power transfer mechanism difficulties.

IMPORTANCE TO SUCCESS: Design problems only.

CONVEYANCE CONCEPT	DISCUSSION OF TRADEOFFS	RANKING 5=best 1=worst
WEDGE WORM	Very little problems.	5
INFLATABLE SHOE WORM	Minor problems only.	4
EXTENDABLE PISTON WORM	Minor problems only.	4
TRACKED DEVICE	Many problems associated with mating of belt and power screw; take-up-roller problems.	1
AUGER DEVICE	Minor problems in gearing; designing proper auger for this application may be difficult.	2

BOREHOLE CONVEYANCE TRADEOFF STUDY

TRADEOFF CRITERION: 17. Adaptability to various borehole sizes.

IMPORTANCE TO SUCCESS: Minor importance but allows more versatility

CONVEYANCE CONCEPT	DISCUSSION OF TRADEOFFS	RANKING 5=best 1=worst
WEDGE WORM	Arms can be designed for large radial show travel, however, mechanical advantage changes. Thickness of feet can be changed also.	4
INFLATABLE SHOE WORM	Limited to range of elastomeric expansion, different shoes could be substituted.	4
EXTENDABLE PISTON WORM	Pistons can expand within large range with no mechanical advantage loss. Longer pistons can also be substituted.	5
TRACKED DEVICE	Limited travel, substitution of parts difficult.	2
AUGER DEVICE	Limited travel, substitution of parts difficult.	2

BOREHOLE CONVEYANCE TRADEOFF STUDY

TRADEOFF CRITERION: 18. Smallest borehole diameter that is feasible.

IMPORTANCE TO SUCCESS: Minor importance; but allows more versatility.

CONVEYANCE CONCEPT	DISCUSSION OF TRADEOFFS	RANKING 5=best 1=worst
WEDGE WORM	Probably 6" (15 cm) minimum.	2
INFLATABLE SHOE WORM	Probably 3" (7.6 cm) minimum with sacrifice in power.	5
EXTENDABLE PISTON WORM	Probably 4" (10 cm) minimum with sacrifice in power and piston throw range.	4
TRACKED DEVICE	Probably 8" (20 cm) minimum.	1
AUGER DEVICE	Probably 6" (15 cm) minimum because of motor.	2

BOREHOLE CONVEYANCE TRADEOFF STUDY

TRADEOFF CRITERION: 19. Ease of converting thrust power for use in rock crushing mode.

IMPORTANCE TO SUCCESS: Simplicity of device.

CONVEYANCE CONCEPT	DISCUSSION OF TRADEOFFS	RANKING 5=best 1=worst
WEDGE WORM	Power can be diverted forward to rock crusher.	5
INFLATABLE SHOE WORM	Same as above.	5
EXTENDABLE PISTON WORM	Same as above.	5
TRACKED DEVICE	Same as above.	5
AUGER DEVICE	Same as above.	5

BOREHOLE CONVEYANCE TRADEOFF STUDY

TRADEOFF CRITERION: 20. Speed capability.

IMPORTANCE TO SUCCESS: Minor but can allow more efficient usage.

CONVEYANCE CONCEPT	DISCUSSION OF TRADEOFFS	RANKING 5=best 1=worst
WEDGE WORM	Sufficient capability but not high speed.	3
INFLATABLE SHOE WORM	Same as above.	3
EXTENDABLE PISTON WORM	Same as above.	3
TRACKED DEVICE	Good speed potential.	5
AUGER DEVICE	Same as above.	5

BOREHOLE CONVEYANCE TRADEOFF STUDY

TRADEOFF CRITERION: 21. Fail-safe characteristics.

IMPORTANCE TO SUCCESS: Important

CONVEYANCE CONCEPT	DISCUSSION OF TRADEOFFS	RANKING 5=best 1=worst
WEDGE WORM	Failure of one arm or foot would not prevent continuation of traversal.	5
INFLATABLE SHOE WORM	Rupture of shoe would cause loss of system pressure.	2
EXTENDABLE PISTON WORM	Leakage of piston would reduce power, pistons provide redundancy of loading devices.	4
TRACKED DEVICE	Failure of one track could prevent movement.	1
AUGER DEVICE	Failure of one universal joint would not prevent traversal, leakage of piston would reduce power.	4

BOREHOLE CONVEYANCE TRADEOFF STUDY

TRADEOFF CRITERION: 22. Probable maintenance required.

IMPORTANCE TO SUCCESS: Minor.

CONVEYANCE CONCEPT	DISCUSSION OF TRADEOFFS	RANKING 5=best 1=worst
WEDGE WORM	Very little.	5
INFLATABLE SHOE WORM	Periodic shoe replacement.	3
EXTENDABLE PISTON WORM	Periodic seal replacement.	4
TRACKED DEVICE	Frequent track, roller, and power screw replacement.	1
AUGER DEVICE	Periodic auger screw replacement.	2

FINAL RANKING

Tradeoff Criterion	Weighting	Score									
		Wedge Worm		Inflat. Shoe		Extend. Piston		Tracked		Auger	
		Unwtd.	Wtd.	Unwtd.	Wtd.	Unwtd.	Wtd	Unwtd.	Wtd.	Unwtd.	Wtd.
1	1	5	5	4	4	4	4	3	3	2	2
2	1	5	5	3	3	3	3	1	1	4	4
3	2	5	10	5	10	5	10	3	6	3	6
4	3	1	3	3	9	5	15	4	12	4	12
5	2	1	2	5	10	5	10	3	6	4	8
6	3	5	15	2	6	4	12	5	15	5	15
7	1	5	5	2	2	2	2	2	2	2	2
8	3	5	15	4	12	4	12	1	3	4	12
9	1	5	5	4	4	3	3	1	1	2	2
10	1	5	5	4	4	3	3	2	2	2	2
11	3	4	12	5	15	4	12	1	3	3	9
12	3	3	9	5	15	5	15	4	12	3	9
13	2	3	6	5	10	4	8	4	8	4	8
14	2	5	10	3	6	3	6	1	2	3	6
15	2	1	2	5	10	4	8	4	8	1	2
16	1	5	5	4	4	4	4	1	1	2	2
17	1	4	4	4	4	5	5	2	2	2	2
18	1	2	2	5	5	4	4	1	1	2	2
19	1	5	5	5	5	5	5	5	5	5	5
20	1	3	3	3	3	3	3	5	5	5	5
21	2	5	10	2	4	4	8	1	2	4	8
22	1	5	5	3	3	4	4	1	1	2	2
	TOTAL		143		148		156		101		125
No. of critical areas with low score.		1		0		0		2		0	

4. RECOMMENDATIONS

The following recommendations are made in regard to the design of a conveyance system as a result of the findings made in this study.

- At this time, it is felt that either electric or pneumatic power are viable prime power sources for the conveyance system. Further research is needed to determine which of these power sources will be selected for use in the final design.

- As a result of the tradeoff study, it is felt that the inflatable shoe worm and the mechanical piston worm have equal potential as satisfactory conveyance concepts. Further study will be conducted to refine the two concepts and determine the best overall design.

- It is recommended that the multiple forward module approach be utilized in the conveyance system. This configuration is best from the aspects of borehole range adaptation, void space traversal, rock-crushing power capability, and speed of traversal.

ANNEX A

ESTIMATES OF CABLE WEIGHT FOR ELECTRICAL UMBILICAL POWER

Driving the electric motor down-hole from the surface requires power cables:

2 #12 wires @ .032 lb/ft (47.6 g/m) for 10,560 ft (3.2187 km) (2 miles)	=	675 lb. (306 kg)

Certain control functions down-hole on the conveyance device require control cables:

4 pairs #18 wires @ .012 lb/ft. (17.9 g/m) for 10,560 ft. (3.2187 km)	=	1014 lb. (459.9 kg)

Transmitting the sensor signals requires:

Coaxial cable @ 0.08 lb/ft. (119 g/m) for 10,560 ft. (3.2187 km)	=	845 lb. (383 kg)

Bundling up all the wires (coaxial and control) and providing tensile strength requires:

Phyllistran jacket 3/8" (9.5 mm) diameter @ 0.023 lb/ft. (34.2 g/m) for 10,560 ft. (3.2187 km)	=	242 lb. (110 kg)
Total Weight	=	2776 lb. (1.259 mg)

ANNEX B

ESTIMATES OF HOSE WEIGHT AND POWER REQUIREMENTS FOR PNEUMATIC UMBILICAL POWER

PARAMETER ASSUMPTIONS:

- Down-hole air pressure = 150 psi (1.03 MPa)
- Speed of conveyance = 50 fpm (0.254 m/s)
- Flow rate of air = 8 cfm (0.23 m^3/min.)
- Length of hose = 10,560 ft (3.2187 km)

SUPPLY HOSE SIZE AND WEIGHT:

From hose pressure drop table in Aeroquip catalog 236, a total pressure drop of 74 psi (510 k Pa) will be seen with the assumed flow rate and hose length in .50" (12.7 mm) I.D. hose. This hole in Aeroquip FC 121 Nylon weighs .08 lb/ft. (119 g/m).

Weight of supply hose = .08 lb/ft (119 g/m) x 10,560 ft. (3.2187 km) = 845 lb. (383 kg)

RETURN HOSE SIZE AND WEIGHT:

It is assumed that the compressed air is expanded adiabatically from 150 psi (1.03 MPa) to 14.7 psi (101 kPa) when being used. The governing equation for adiabatic expansion is:

$$P_S V_S^{1.4} = P_R V_R^{1.4} \qquad \text{(B-1)}$$

where:

P_S = supply pressure
P_R = return pressure
V_S = supply volume
V_R = return volume

Assuming the expanded air is returned at the same speed as the supply air, equation B-1 can be changed to the following equation:

$$D_R = 2\left[\frac{P_S}{P_R}\left(\frac{D_S}{2}\right)^{2.8}\right]^{.357142857} \qquad \text{(B-2)}$$

where D_R = return hose I.D,

D_S = supply hose I.D.

D_R = 1.15" (29.2 mm) (this is equivalent in cross sectional area to two .75" (19 mm) I.D. hoses.)

The .75" (19 mm) I.D. hoses in Aeroquip FC 121 Nylon weigh .12 lb/ft (179 g/m) each.

Weight of return hose = (2).12 lb/ft x 10,560 ft. = 2534 lb.
[(2)179 g/m x 3.2187 km = 1.149 Mg

Total hose weight = 3379 lb. (1.533 Mg)

WEIGHT OF OTHER UMBILICAL CONSTITUENTS:

Air in pressure hose	= 11 lb.	(5.0 kg)
Coaxial cable	= 845 lb.	(383 kg)
4 pairs #18 control wire	= 1014 lb.	(459.9 kg)
Phyllistran jacket	= 242 lb.	(110 kg)
	2112 lb.	(958.0 kg)
Total Umbilical Weight	= 5491 lb.	(2.491 Mg)

THRUST REQUIREMENT OF DEVICE:

$$F = W_u{}^{\mu} = W_D{}^{\mu} \qquad \text{(B-3)}$$

Where:

F = thrust

W_u = total umbilical weight

μ = friction coefficient $\simeq .5$

W_D = weight of downhole package ≈500 lb. (227 kg)

F = 2995 lbf (13.32 kN)

CHECK ON ASSUMED FLOW RATE:

$$Q = F \times S/P_s \qquad \text{(B-4)}$$

Where

W = flow rate
S = speed of downhole package

$Q = 6.93\ ft^3/min\ (0.196\ m^3/min)$

The remaining flow rate is required to expand the clamping device.

HORSEPOWER REQUIREMENT:

$$HP = Q \times P_s/550 \qquad \text{(B-5)}$$

= 5.24 horsepower (3.91 kW)

ANNEX C

ESTIMATES OF HOSE WEIGHTS FOR HYDRAULIC UMBILICAL POWER

ASSUMED PARAMETER VALUES:

- Umbilical length = 10,560 ft. (3.2187 km)
- Speed of conveyance = 50 ft/min (.254 m/s)
- Downhole Hydraulic Pressure = 1000 psi (6.895 MPa)
- Flow rate of fluid = 30 gal/min (1.9 l/s)
- Weight of hydraulic fluid = 62.4 lb/ft^3 (1000 kg/m^3)

SUPPLY HOSE SIZE AND WEIGHT:

From a table in Aeroquip catalog 236, it can be determined that for a flow rate of 30 gal/min (1.9 l/s) a 1.25" (31.8 mm) I.D. hose has a pressure drop of 950 psi (6.55 MPa) for the entire length. This pressure drop is within reason, the hose is the smallest hose size that can be used. The weight of Aeroquip 2781 double wire braid hose, working pressure 2500 lb. (17.24 MPa), is 1.73 lb/ft (2.57 kg/m).

Supply hose weight = 1.73 lb/ft x 10,560 ft. = 18,269 lb.
(2.57 kg/m x 3.2187 km = 8.2866 Mg)

RETURN HOSE SIZE AND WEIGHT:

Since we cannot tolerate a 950 psi (6.55 MPa) drop in the return line, we must go to a larger size. However, we can use a lower working pressure hose. A 1.5" (38 mm) I.D. hose would have a pressure drop of 400 psi (2.76 MPa) over the entire return trip. The weight of this hose, Aeroquip 2681 - working pressure 700 psi (4.83 MPa), is 1.12 lb/ft (1.67 kg/m).

Weight of return hose = 1.12 lb/ft x 10,560 ft. = 11,827 lb.
(1.67 kg/m x 3.2187 km = 5.3647 Mg.

WEIGHT OF HYDRAULIC FLUID:

To find the weight of the fluid, we assume that the hoses are full of fluid.

$$\text{Hose Volume} = 10{,}560 \text{ ft.} \left(\left(\frac{1.25}{2}\right)^2 + \left(\frac{1.50}{2}\right)^2\right) \frac{}{144}$$

$$= 2.19.6 \text{ ft}^3$$

$$\text{Fluid Weight} = 219.6 \text{ ft}^3 \times 62.4 \text{ lb/ft}^3 = 13{,}703 \text{ lb.}$$

$$(6.218 \text{ m}^3 \times 1000 \text{ kg.m}^3 = 6.216 \text{ Mg})$$

Total hose and fluid weight = 43,799 lb. (19.867 Mg)

Total umbilical weight = 45,900 lb. (20.820 Mg)

THRUST REQUIREMENTS OF DEVICE:

$$F = W_u \mu + W_D$$

where:

F = Thrust

W_u = Umbilical weight

W_D = Downhole device weight = 500 lb. (227 kg)

μ = Friction coefficient = .5

F = 23,200 lbf. (103.20 kN) (C-1)

CHECK ON FLOW RATE:

$$Q = F \times S/P_s \qquad \text{(C-2)}$$

where:

Q = Flow rate

P_s = Supply pressure

S = Speed of device

$$Q = 8 \text{ ft}^3/\text{min } (.0038 \text{ m}^3/\text{s})(3.8 \text{ dm}^3/\text{s})$$

$$= 60 \text{ gal/min. } (3.8 \text{ l/s})$$

The initial assumption of 30 gal/min (1.9 l/s) was low, which means that this system would only be capable of 25 ft./min (0.127 m/s) unless the umbilical size is further increased.

APPENDIX J

APPLICABILITY OF DRILL RIGS AS PROPULSION DEVICES

TABLE OF CONTENTS

BACKGROUND STATEMENT

This study is based on similar work which was done in examining the problems of horizontal drilling. It was performed late in the program to investigate the probable limits to which a drill rig could be used as a substitute to the in-the-hole thrust generation device which was originally part of the system.

It concludes that the drill rig will be of sufficient utility as a thrust device to make it a desirable replacement for the thruster, but only to relatively shallow depths.

APPLICABILITY OF DRILL RIGS AS PROPULSION DEVICES

ABSTRACT

A drill rig has only limited utility as a propulsion device to push a survey package into the hole. The hole will be drilled by a well-lubricated rotating drill string. It will therefore be operating with a dynamic coefficient of friction. The package must be pushed into the drill hole with only the residual lubrication. Because of the twisting of the umbilical, it cannot be rotated. Thus, it will see the much higher static coefficient of friction. The drill string will buckle and join with the package attached at much shorter hole lengths, than if it were being rotated.

The critical lengths are such that the drill rig can probably be used to hole lengths of a few thousand feet. As hole lengths increase, it will be necessary to employ an in-the-hole thrust device to propel the package.

APPLICABILITY OF DRILL RIGS AS PROPULSION DEVICES

1. INTRODUCTION AND SUMMARY

This study investigates the applicability of drill rigs as propulsion devices for the sensor package. The investigation concerns itself primarily with the compressive forces, causing a drill string to buckle, lock up, and suddenly release at extended depths. It concludes that, because of differing hole and operating conditions, there is no sure way of guaranteeing the drill hole will be completely usable with any form of propulsion from the surface. However, the maximum probability of successfully using a drill rig would be to employ the same one w-ich drilled the hole, provided strict operational procedures and enforced to prevent overstressing the package.

As a cost-effective intermediate approach, the drill rig should be used for propulsion in shallow holes and the development of the downhole thruster deferred until more is known about the problems of system operation. Although the study recommends the deferral of the development of the downhole thruster, it may be the only satisfactory method of propelling the package to greater hole depths. Thus, its development should be deferred but not abandoned.

2. COMPRESSIVE FORCES ON THE DRILL STRING

The linear forces acting on the drill string are the forces due to:

- The frictional drag due to the package weight
  $$F_p = W_p f$$
- The reserve force allocated to pushing through minor blockages, F_r

- The frictional drag due to the weight of the drill string, $F_d = WLf$

- Buckling forces of the drill string against the borehole wall. $F_b = F_w f$

where:

W_p = the weight of the package, lbs.

F_r = the allocated reserve force, lbs.

W = the drill string weight, lbs/ft.

L = the length of the drill string, ft.

f = the coefficient of friction of the drill string against the borehole wall.

F_w = the perpendicular component of the total force (F_t) to the borehole wall, applied by the buckling of the drill string:

$$F_w = N F_t \sin\theta \quad (1)$$

θ = the angle between the buckled drill string and the borehole wall

N = the number of buckling contacts with the borehole wall.

Eulers long column buckling formula with fixed ends is:

$$L_b = (K/6)\left(\frac{EA}{F_t}\right)^{\frac{1}{2}} \text{ ft.} \quad (2)$$

where

L_b = the length at which the column will buckle, ft.

K = least radius of gyration, in.

E = modulus of elasticity, 3×10^7 psi

A = structural area, sq. in.

$$K = \left(\frac{D_o^2 + D_i^2}{8}\right)^{\frac{1}{2}} \quad (3)$$

$$A = \frac{\pi(D_o^2 - D_i^2)}{4} \quad (4)$$

D_o = outside diameter of the drill string, in.

D_i = inside diameter of the drill string, in.

F_t = the total applied force before buckling

$$F_t = F_r + (W_p + F_b + WL) f \tag{5}$$

The number of times the drill string buckles will be

$$N = \frac{L}{L_b} \tag{6}$$

Although N should assume only integer values, little error is introduced if equation (6) is taken to be a continuous function.

$$N = \frac{6\,L}{K} \left(\frac{F_t}{EA}\right)^{\frac{1}{2}} \tag{7}$$

$$\sin \theta = \frac{D_h - D_o}{12\,L_b} = \frac{(D_h - D_o)}{24K} \left(\frac{F_t}{EA}\right)^{\frac{1}{2}} \tag{8}$$

D_h = the hole diameter, in.

It is now possible to better define the buckling force, F_b, by combining equations (1), (3), (7), (8). F_b becomes

$$F_b = \frac{6\,L(D_h - D_o)}{K^2 EA} \left[F_b f + (WL + W_p) f + F_r\right]^2 \tag{9}$$

equation (9) can be manipulated to solve the quadratic in F_b

$$F_b = \frac{K^2 EA}{24\,L(D_h - D_o) f} \left[1 - \left(1 - \frac{6\,L(D_h - D_o)}{K^2 EA} \left[\left(WL + W_p\right) f + F_r\right]\right)^{\frac{1}{2}}\right]^2 \tag{10}$$

It will be noted that F_b becomes complex when the quantity under the radical goes negative. This occurs when the buckling of the drill string produces a lock-up condition. Further input force will merely produce more buckling and will not advance the package.

Examination of (10) will show that if $W_p = F_r = 0$, then there is a critical length $L_{(crit)}$ beyond which an unincumbered drill string will not go. This will be examined first.

$$L_{(crit)} = \left(\frac{K^2 EA}{6\Delta DWf} \right)^{\frac{1}{2}} \tag{11}$$

3. USE OF LIGHTWEIGHT DRILL ROD FOR PUSHING PACKAGE

One propulsion concept which has been considered is the use of a light drill rig and small drill rod to push the package into the hole. This study will consider first the critical hole length behond which a drill rod will not work in a 6-3/4 inch (17 cm) hole. Table 1 is taken from Ref. 1, p. 133, Appendix A.

Table 1. Values for friction coefficients*.

Drilling Fluid	Friction Coefficient	
	Static, f_s	Dynamic, f_D
Water	0.47	0.38
Bentonite-Water Mud	0.38	0.28
Bentonite-Water Mud with Lubrication Additive	0.1	∿0.06-0.1

*Measured by Baroid Oil Field Products Laboratory

To prevent entanglement of the umbilical, the drill string will not be rotating while the package is being inserted. Thus, the static coefficient is assumed. f is taken to be 0.38 from Table 1. Table 2 presents the calculated parameters for AQ and BQ drill rod as well as for API standard 4.5" (11.43 cm) drill pipe, which would probably be used to drill the hole.

Table 2. Critical lengths for f=.38 with various drill rods.

Drill Rod Type	AQ	BQ	4.5"
D_o in.	1.75	2.18	4.5"
D_i in.	1.437	1.875	3.985
W lbs	2.68	3.45	13.75
K in.	.8	1.02	2.125
A in^2	.783	1.00	3.43
$L_{(crit)}$ ft.	707	902	2567

The assumptions made in deriving equation (11) are such that the results of the calculation will be conservative. Thus, the actual critical lengths will probably be in excess of those shown in Table 2.

However, the relative values between the various drill rods should be realistic. It should also be remembered that the hole will probably be drilled by rotary drilling, where the dynamic coefficient of friction would apply. It would seem that, if the hole has any appreciable depth, it could only be penetrated by a downhole thruster, or by a rotating drill string of a size equivalent to that with which it was drilled. Thus, the probability of being able to use a light drill rig to maneuver the package much beyond a thousand feet (304.8 m) would seem to be slim. However, the flexibility and low cost of the light rig make it very attractive during the early testing of the system.

This study has not considered the possibility of using stabilizers to stiffen the drill rods. However, this introduces added complications which tend to make either drill rig unattractive.

4. FRICTION FORCES

Coefficients of friction are statistical in nature. Any measurement will show a wide group of variations around the published means. In addition, as the package on the drill rod is moved into the hole, it must be stopped each time the ram on the drill rig is retracted. Thus, the thrust will consist of that caused by a force build up and minor buckling of the drill rod until the static coefficient of friction is overcome. The package will then jump forward on the basis of the lower dynamic coefficient of friction, as can be seen by reference to Table 1. The package will continue to move as the drill rod releases the potential energy absorbed in buckling.

Because of the added weight, needed wall thickness and sensitivity of the instruments will be infeasible to design the downhole package to absorb the same impact loading as a drill bit. These same statistical indeterminants and non-linear effects are anticipated to limit the applicability of providing thrust from the

surface in drilling long boreholes. If the borehole is at the practical limit of drilling depth, then it is highly unlikely that the much more delicate package could be successfully inserted by the drill rig.

The frictional force on the drill rig has been shown to be expressible by (12) on the basis of empirical relationships [1]

$$F_f = 1.8\ D_o^{1.44} Lf \qquad (12)$$

where

F_f = the frictional forces acting on a drill rig, pounds.

D_o = the outside diameter of an API drill string, inches.

L = the depth into the hole, feet.

f = the coefficient of friction as a random variable.

Equation 12 does not consider the locking forces due to buckling. Table 1 shows that in a wet, lubricated hole f can vary as

$$0.06 < f < 0.47$$

The system is specified to be able to operate in dry as well as wet holes. Thus, the upper limit of f could be even higher. By way of illustration, even at a hole depth of 2,500 feet, (762.0 m) the transition from static to dynamic coefficients of friction could generate forces high enough to damage the package.

Let

L = 2,000 feet

D_o = 4.5 inches

$$f = \begin{matrix} 0.38 \text{ static} \\ 0.28 \text{ dynamic} \end{matrix}$$

The differential force released the instant the package starts to move would be

$$\Delta F_f = 1.8x(4.5)^{1.44}x2000(.38-.28) = 3,140 \text{ lbs.}$$

The package itself would be subject to the retarding force

$$F_p = \Delta F_f - W_p f_d$$

where

W_p = weight of the package, assume 500 pounds

f_d = dynamic coefficient of friction, assume .28

F_p = 3,000 lbs.

This would represent an inertial acceleration of:

$$a = \frac{F_p g}{W_p}$$

a = inertial acceleration in g units

g = acceleration of gravity, 1

thus

a = 6 g's

This would be a normal loading to be expected and the package could easily be stressed to absorb it.

However, consider the case for the same distance of 2,000 feet but with a higher value of f. Here the drill string is near its critical length for f=0.6, which is a reasonable 3 σ bound for f-0.4. The drill string buckles and releases added energy when it breaks loose now:

$$\Delta F = (1.8\ D_o^{1.44}L+F_b)f_s-1.8\ D_o^{1.44}Lf_d \qquad (13)$$

where

F_b = the buckling force calculated from equation (10)

L = 2,000 feet

f_s = static coefficient of friction, assumed to be 0.6 for the upper 3σ bound

f_d = dynamic coefficient of friction, assumed to be 0.28 for the upper 3σ bound.

The values necessary to calculate F_b are given in Table 2. When applied to (13) give:

$$\Delta F = 11,510 \text{ pounds}$$

and

$$a = 23 \text{ g's}$$

It is not reasonable to stress the package to withstand forces and accelerations such as this. However, these numbers are near the upper limit of feasibility. Compressive loading of 10,000 pounds and longitudinal accelerations of 20 g's are as high as could be expected considering the functions and length of the package.

It must be remembered that f is a random variable, the tabular values are for the median (50% value). Thus, there will be an

appreciable portion of the time that these values and stresses will be exceeded. In the example given, the design stresses are just exceeded. For a standard deviation, $\sigma = 0.1$, these stresses would be exceeded only 0.5% of the time. However, there is no safety factor. Thus, the design is marginal.

5. DISCUSSION

The problems of designing, building and testing a sensing system such as this are separable from those of penetration. However, this is obviously only true for shallow depths. At present, and probably for the near future, there are no boreholes of the size and length which will tax the use of the drill rig for propulsion. The concept that, if the drill rig can bore the hole, it can insert the package, does not seem realistic except for shallow depths.

It makes good sense to defer the development of a down hole thrust device for a self-propelled version of the system. However, it must be stressed that, pending field experience which will verify or refute the results of this study, the self-propelled system cannot be eliminated if full penetration depths are to be achieved. The down hole thruster has the advantages of maneuverability, controllability, and flexibility. Countering this is the fact that it is a development which will be sterile unless the sensor system first proves its utility. Thus, the total system development can be divided into two steps: one to prove the value of the sensor system and the second to extend its range capability with a downhole thruster.

It seems highly probable that various forms of down hole thrust devices will be developed on co-lateral programs in other areas. These could lead the procurement of this system. Thus, the final decision whether to use the drill rig or a down hole thrust device should be reexamined on the basis of current data, prior to any final commitment to the propulsion concept.

6. CONCLUSION

- The drilled hole will probably be lubricated and drilled with rotary drilling. If the hole is near its maximum length, it may not be possible to reinsert the package to full hole length even with the same drill rig. This would be due to the differences between the coefficients of static and dynamic friction.

- Even with the package strength specified to the limit of reasonable design, the design is marginal for insertion by a full-size drill rig. Thus, where the full size drill rig is used, it will be necessary to rely upon operational procedures to insure that the package is not destroyed by the insertion process.

- The probability of being able to use a light drill rig with corresponding lightweight drill rod, except for comparatively shallow depths, seems low. However, the flexibility of, and lower stresses generated by, the lightweight system is sufficient to justify its use for the majority of data gathering required during the early stages of prototype testing.

- The only sure way of guaranteeing that the hole can be completely utilized is with a downhole thrust device.

- This study has been based upon severe oversimplification of a complex problem. The results should be conservative; however, the numbers fall so close to critical design limits that they should be verified experimentally.

- Before any final firm commitments are made, a reexamination of the status of borehole thrust devices, developed on co-lateral programs, should be made.

7. REFERENCES

1. "Drilling and Preparation of Reusable, Long Range Horizontal Bore Holes in Rock and Gouge," J. C. Harding (et al) of Foster-Miller Associates, Inc., Volume III. (Soon to be published).

APPENDIX K

INVESTIGATIONS OF THE PHYSICAL PROPERTIES OF LOW-POROSITY ROCK A CRITICAL LABORATORY EXPERIMENT

TABLE OF CONTENTS

BACKGROUND STATEMENT

From the very beginning of this project, the need for more information about the physical properties of low-porosity rock was quite evident.

After the Task A effort was complete, and the decision to use acoustics, electromagnetics, and electrical sensors was made, it was apparent that a need to have relevant correlations among the electrical, acoustic, electromagnetic, and strength parameters had to be satisfied.

A contract was negotiated with Colorado School of Mines to conduct this study. The results are included in the appendix. A most significant result for this program is that for these rocks, once the frequency is well above the conductive/dielectric crossover, the attenuation is simply due to the range-dependent spreading loss, and no longer dependent on frequency. The consequence of this is that for borehole-sized antennas (optimum frequencies between 500 MHz and 2 GHz), the radar is actually more efficient with increasing frequency.

As an administrative exception to the rule, this Appendix is presented with tables and figures grouped at the end.

Department of Geophysics
Colorado School of Mines
Golden, Colorado 80401

May 24, 1976

Final Report:

Investigations of the physical properties of low-porosity rocks

by

George V. Keller
Jeff Given
James Crompton

Abstract

Acoustic, mechanical and electrical properties have been measured on suites of low-porosity rocks. Three rock types were represented in these suites; gneiss and schist, granite, and metarhyolite. All are similar in chemical makeup, but differ materially in texture. The three rock types exhibited a wide range in unconfined compressive strengths, ranging from 5000 to 75000 pounds per square inch. Many of the measured properties, such as density, acoustic wavespeeds, and dielectric constant, show a pronounced correlation with strength. However, in each case, a significant number of data contradict these correlations, so that the correlations would have to be used cautiously in inferring rock conditions from geophysical measurements.

Measurements of electrical properties indicate that conductivity and dielectric constant in water-bearing samples are nearly independent of frequency out to frequencies of approximately 1 gigahertz. Attenuation rates for electromagnetic waves at frequencies ranging from 100 megahertz to 1 gigahertz should be 0.6 to 6 db per meter, for rock resistivities ranging from 100 to 1000 ohm-meters. These estimates bode well for the use of radar imaging in the more resistant parts or rock masses consisting of gneiss, granite, or rhyolite.

Introduction

In the field of geo-engineering, many problems arise in which indirect determinations of rock properties can be of great value in planning or carrying out subsurface excavations. Direct evaluation of rock strength and structure requires drilling test holes or pilot bores, and performing laboratory strength tests circetly on the recovered cores. Even direct investigations are insufficient at times because features such as faults or joints may not be intersected by drill holes or bores. Therefore, there is a requirement for an indirect means of studying rock properties and structures, if such methods can be demonstrated to be predictably reliable and economical.

Two approaches to investigating the properties of the rock immediately around subsurface openings have been proposed in recent years. In one approach, some property of the rock around a small opening is measured by geophysical means, and this property is correlated with rock strength to provide an indication of the character of the rock. Both measurements of volume electrical resistivity (Keller, 1962, 1974; Donaldson, 1974) and the speed of transit of seismic waves (Wantland, 1963) have been used experimentally on various occasions over the years. In the other approach, energy reflected back from discontinuities in properties in the rock mass is detected, and travel times are used to determine the locations of such discontinuities. Again, both electromagnetic fields (Morey, 1974; Moffatt, 1974; Cook, 1974) and acoustic fields (Price, 1974; Hipkins and Whitney, 1974) have been used in recent years. However, with imaging methods, much higher frequencies must be used that in the case of volume determinations of properties. The imaging methods operate at frequencies normally associated with radar transmissions and ultrasonic acoustic ranging.

With either volumetric determinations of physical properties or imaging of structures using high frequencies, success in surveys must be based on knowledge of the interrelations between properties established by laboratory studies. With volumetric studies, these correlations are essential in order to convert measured values of resistivity or acoustic wavespeed to useful values of rock strength. With imaging methods, the same information is needed to determine attenuation and propagation speeds for use in converting reflections to images.

Many diverse studies of the physical properties of rocks have been carried out in recent years, but relatively few pertain directly to the problem of excavating shallow subsurface crystalline rocks. Extensive studies have been made of the properties of porous rocks that serve as petroleum reservoir rocks, and the results of such studies are summarized in many places (Keller, 1971, for example). More recently, great interest has developed in the properties of rocks in the deep crust, and many studies are under way on the electrical and acoustic properties of crystalline rock at high temperatures and pressures. In these studies, it appears that properties relate primarily to the development of porosity in the form of microfractures, rather than to the presence of primary porosity in the form of intergranular voids (Wang and others, 1975; Spencer and Nur, 1976; Nur and Simmons, 1969: O'Connell and Budiansky, 1974; Brace and others, 1965). Results indicate that correlations between physical properties in crystalline rocks with porosity as microfractures differ in significant respects from similar correlations previously developed for clastic rocks with intergranular porosity.

Many determinations of physical properties will be required before the statistically reliability of correlations between various physical properties can be established. A majority of studies presently under way involved detailed studies carried out on a relatively few samples of a given rock type; only a very few include measurements on a large enough suite of samples to provide information about the variability of properties (Wang and others, 1975; Johnson and Wenk, 1974). The objective of the study described in this report is to fill this gap to some extent, by providing data on the various physical properties of three suites of crystalline rock.

All three suites of rocks were obtained from the shallow suboutcrop of the rock units being sampled. It was desired to obtain samples characterized by the type of weathering one would expect to encounter in shallow subsurface excavations. Two suites of samples were obtained in areas where extensive excavations are either underway or contemplated; one suite from Washington, D.C., where excavations for the Washington Metro have been underway for some years, and another suite from the vicinity of Atlanta, Georgia, where planning for a metro system is well under way. The third suite of samples was obtained on outcrop from the Calico Mountains in northwestern Nevada. This suite has no significance

in terms of planned excavations, but provides variety to the rock types covered by the sample suites. Physical properties tests were of three general types; electrical, acoustic, and mechanical. In the electrical measurements, properties were studied both for a range of low frequencies, such as are used for volumetric determinations of properties in place, and for several frequencies in the low gigahertz part of the spectrum, comparable to frequencies being used for radar imaging. For the acoustic measurements, the transit times for acoustic pulses containing frequencies in the ultrasonic part of the spectrum were used. In the mechanical tests, deformation of samples under uniaxial stress was observed up to the breaking point. Details of the measurement techniques and of the results obtained are included in the following sections.

Experimental Procedure

A. Source of samples and mode of preparation:

Three suites of samples were taken as material for physical properties tests. Suite 1 was obtained from excavations being carried out for the Metro System in Washington, D.C. Approximately 50 source samples were taken from rock being hauled from the excavations in Washington. These source samples were selected from the more competent parts of the rock debris, and consisted of fragments with weights generally of 10 to 20 kilograms. Examination of the samples reveals that about half are gneiss, and half schist. These rock types are typical of most of the Precambrian rock units underlying the District of Columbia.

Suite 2 was obtained by sampling in roadcuts and at exposures of particularly resistant bedrock in the vicinity of Atlanta, Georgia. Here, extensive excavations are planned for construction of a Metro system, but none had yet been started when sampling was carried out. Samples consisted almost entirely of non-foliated granite or granitic gneiss. A very few samples were schist or metasiltstone. Again, these samples are characteristic of the Precambrian bedrock in north central Georgia.

Suite 3 was taken from samples previously collected on outcrops in the Calico Mountain Range, located approximately 110 miles north of Reno, along the northwest edge of the Black Rock Desert. The Calico Mountains represent a Quaternary volcanic complex of rhyolitic-dacitic composition. The samples consisted of ash-flow tuffs and intrusive rhyolites. Extensive deposition of secondary hydrothermal silica has virtually destroyed original porosity, and these samples are best described as metarhyolite, despite their geologic youthfulness.

In preparation of subsamples for physical properties tests, at least two shaped samples were cut and machined from each source sample. One of these two subsamples was prepared in the form of a thin disc (7 mm. thickness by 45 mm. diameter) for use in some of the electrical properties determinations. The other subsample was prepared in the form of a cylinder (40 mm. length by 20 mm. diameter), and was used for measurements of density, acoustic wavespeeds and strength. The density of each sample was determined from its weight, and its volume calculated from the dimensions of the shaped samples.

B. Acoustic wavespeed measurements:

Both compressional and shear wavespeeds were measured by observing the transit time for acoustic pulses along the cylindrical subsamples. Pulses were generated by driving an electrical signal into a set of piezoelectric transducers at one end of a sample, and observing the electrical output from a second set of piezoelectric transducers at the other end. The transducers used in generating compressional waves were oriented with their active axes inline with the sample. Shear waves were generated and detected using sets of transducers forming rings in the plane perpendicular to the axis of the cylindrical sample.

The transducers and sample form a stack which is inserted in a piston arrangement to provide uniaxial confining pressure, which can be controlled over a wide range. The stack is then immersed in a pressure vessel, in which a hydrostatic pressure can be applied to the stack using oil as a pressuring medium. In this way, the uniaxial pressure loading the mineral framework of a sample can be controlled separately from the pressure on the pore fluids.

Because we wish to simulate the environment encountered in shallow subsurface excavations, ideally the uniaxial frame pressure, which represents gravity loading, should be a few tens of metric tons per square meter (we expect lithostatic pressure to increase with depth at a rate equal to the density 2.2 to 3.1, in tons per square meter, per meter of depth). Similarly, because many excavations are done above the water table, or only a short distance below it, the pressure on the pore fluids should be roughly atmospheric.

In attempting to make measurements at very low confining pressures, however, it was found that acoustic coupling through the stack was too poor to permit accurate observation of the arrival times. The transmitted pulses were either 1 microsecond in duration (for compressional waves) or 3 microseconds in duration (for shear waves). The received signal, displayed on an oscillograph screen to read arrival times, contains a wide spectrum of frequencies, but shows dominant frequencies of some tens of kilohertz. It was necessary to apply uniaxial confining pressures in order to obtain adequate coupling through the stack to make accurate determinations of arrival times.

It has been observed by many investigators (Walsh, 1965; Birch, 1960, 1961; Simmons, 1964; Christensen, 1965, 1966) that significant changes in acoustic wavespeed take place as the pressure on a rock is increased from nothing to a few tens of tons per square meter (one ton per square meter = 0.1 bars), with the effect being largest in undersaturated rocks. It is generally considered that this initial increase in wavespeed at low confining pressures is real and is caused by closing of microfractures under pressure. Therefore, for our purposes, we indeed do need the wavespeeds at confining pressures of a few tens of tons per square meter.

The procedure finally adopted was to measure wavespeeds over a range of uniaxial loading pressures, selected to be 700, 2000, 3500, 5000, 7000, and 14000 tons per square meter. For some samples, paticularly the schistose samples from the Washington area, the increase in wavespeeds over this range amounted to as much as 5 percent. For the remainder of the samples, wavespeed changes amounted to only a few percent. Because of the small scale of these changes, only a single value for each wavespeed is reported here (see Tables 2 and 6).

The acoustic wavespeed data, along with the density determinations, were used to compute values for the dynamic elastic moduli. Poisson's ratio was computed directly from the ratio of compressional and shear wavespeeds:

$$\sigma_p = \frac{1}{2}\,\frac{R^2 - 2}{R^2 - 1} \qquad \ldots 1$$

where σ_p is poisson's ratio and R is the ratio of compressional to shear wavespeeds. Young's modulus (computed dynamic value) was determined from the ratio of wavespeeds and the density:

$$E_c = \frac{\delta V_s^2\ (3R^2 - 4)}{R^2 - 1} \qquad \ldots 2$$

where V_s is the shear wavespeed, δ is the specific gravity, and E_c is the computed value for Young's modulus. Other forms of the elastic moduli may be computed using the relationships given by Birch (1966, p. 100).

C. Electrical measurements:

Electrical properties determinations were made using three experimental approaches. These consisted of determination of dielectric constant and conductivity in the dry state over a range of low frequencies from 1 to 100 kilohertz, determination of conductivity in the wet state over the same low frequency range, and determination of conductivity at two discrete high frequencies, 0.915 and 2.450 gigahertz.

For the low-frequency measurements on dry samples, the disc-shaped subsamples were dried for a prolonged period (several days) at a temperature of 150°C, to remove all free or loosely associated water. The flat faces of the discs were coated with conductive paint, so that each sample could be inserted as a lossy capacitor in one arm of a Schering capacitance bridge. The bridge was then balanced to yield values for the real and imaginary components for the impedance representing the sample in one arm of the bridge. Measurements were made with the sample at a temperature between 100 and 120°C, so that no moisture could condense from the atmosphere to the sample. The bridge was rebalanced with the rock sample removed from the unknown arm, so that the effect of stray capacitances in the setup could be removed from the measured impedance. Measurements were made at frequencies of 1, 2, 5, 10, 20, 50 and 100 kilohertz.

In converting the measured impedance to values for the electrical properties of the sample, the real part of the impedance was identified with ohmic resistance and the imaginary part with faradaic capacitance:

$$Z = R + \frac{i}{\omega C} \qquad \ldots 3$$

where R is resistance, C is capacitance, Z is impedance, and ω is frequency, in radians per second. For the purposes of this report, we have elected to define resistivity as

$$\rho = R \cdot \frac{A}{\ell} \qquad \ldots 4$$

where ρ is resistivity, A is the base area of the disc-shaped samples, and ℓ is the sample thickness. Although this definition of resistivity has been widely used in the past, it has recently been suggested that a somewhat different approach be used (Olhoeft, 1976). It is commonly observed that both the real and imaginary

components of the observed impedance are frequency dependent:

$$Z = \frac{1}{S_{DC} + S(\omega)} + \frac{1}{\omega(C_\infty + C(\omega))} \qquad \ldots 5$$

where S_{DC} is the ohmic conductance at zero frequency, $S(\omega)$ is the added frequency-dependent conductance at higher frequencies, C_∞ is the limiting capacitance at high frequencies, and $C(\omega)$ is the added frequency-dependent capacitance at lower frequencies. As may be inferred from this formula, one expects the frequency dependent conductance to increase with frequency, and the frequency-dependent capacitance to decrease. According to Olhoeft (1976), the conductivity is computed using only the constant part of the impedance in (5):

$$\frac{1}{\rho} = S_{DC} \cdot \frac{\ell}{A} \qquad \ldots 6$$

and the remainder of the real part of the impedance is considered to represent an imaginary dielectric constant. In this report, however, we will use the more conventional definition of resistivity (or its inverse, conductivity) given in eq. 4.

The observed values for resistivity and dielectric constant are tabulated in Table 7. The general behavior of these measurements is that reported previously by investigators who have measured the electrical properties of fully dry rocks (Keller, 1971; Olhoeft and others, 1973). The resistivity decreases almost linearly with frequency, and the dielectric constant decreases slightly with frequency. This behavior is summarized in Figures 1 and 2, where average values for each of the major groups of samples are plotted as a function of frequency. In Figure 1, the nearly linear increase in conductivity with frequency is apparent over the entire spectrum of frequencies used in measurement, except that the data for samples from Atlanta and from Nevada show a tendency to flatten out at low frequencies. It is apparent from these data that the frequency-independent limit of conductivity has not been determined. It can be said only that the value is less than 10^{-8} mhos/meter, and may be orders of magnitude less.

In Figure 2, the limiting dielectric constant at high frequencies has been estimated from the observations:

Washington I samples (gneiss), $\epsilon_\infty = 5.0$

Washington II samples (schist), $\epsilon_\infty = 6.5$

Atlanta III samples (granite), $\epsilon_\infty = 6.0$

Nevada samples (metarhyolite), $\epsilon_\infty = 5.5$

The frequency-dependent part of the dielectric constant has been plotted separately as the ratio $(\epsilon - \epsilon_\infty)/\epsilon_\infty$, on Figure 2. These relationships are highly linear, at least over the range of frequencies used for the measurements. The slope of the dielectric constant vs frequency curves is small, lying between 0.1 and 0.2. The gross disparity between the slopes of the conductivity and the dielectric constant curves indicates that these two phenomena are unrelated; each has a separate explanation.

Measurements made on completely dry samples are not directly applicable to field applications, because natural rocks always contain some water. However, the presence of water in a rock sample leads to electrochemical reactions when one attempts to measure the impedance of a sample that make the dielectric constant appear to be far larger than it really is (Parkhomenko, 1967). No method has yet been devised to measure accurately the dielectric constant of wet rocks. The best approach appears to be determination of the dielectric constant of the solid frame of the rock, and then the use of a mixing rule, such as Lichtenecker's rule (von Hippel, 1954, p. 231):

$$\log \epsilon = (1 - \theta_1) \log \epsilon_\infty + \theta_1 \log \epsilon_w \qquad ...7$$

where ϵ is the dielectric constant for a wet rock at high frequency, ϵ_w is the dielectric constant for water (78.3), and θ_1 is the volume fraction of water in the rock. Computed high-frequency dielectric constants for the four groups of samples are given in Figure 3.

Low-frequency conductivity was measured on these same disc-shaped samples, after they had been resaturated with a 1.0-normal solution of sodium chloride in water ($\rho_w = 0.12$ ohm meters at 20°C). This is roughly twice the salinity of sea water, and is not intended to simulate normal ground water, which would have a much lower salinity above the water table in most places. However, resaturating the samples with a high-salinity solution assures that we know the

salinity of the fluid in the pore spaces, because any salt remaining in the rock from the original ground water will be relatively insignificant in amount.

Resistance between opposing faces of the disc-shaped samples was determined by measuring the ratio of voltage to current as an AC current was driven through the samples. Measurements were made at frequencies of 1, 10 and 100 kilohertz. The results are tabulated in Table 8.

Finally, conductivities were determined at two discrete frequencies, 0.915 and 2.450 gigahertz. Normal impedance bridge measurements become progressively more difficult to make and less reliable as the frequency is raised above 1 megahertz because of the effects of stray capacitances in the measurement system and the finite lengths of connections. An alternate method of determining conductivity was devised for use at micro-wave frequencies. Microwave heaters were used to induce loss currents in the samples; the intensity of the loss current induced by an electromagnetic field of fixed strength is proportional to the conductivity of the sample at that frequency. Loss currents are totally absorbed and converted to heat in the rock. The effect will be a rise in temperature of the sample, with the amount of rise being determined by the heat capacity of the sample.

In making measurements, a sample was illuminated with a microwave field of fixed intensity, either at a frequency of 0.915 gigahertz or at a frequency of 2.450 gigahertz for a fixed length of time (ten seconds). The temperature rise in the sample was then measured using a thermistor probe having a low heat capacity. Most temperature rises were in the range 5° to 15°C, though a few were considerably higher or lower. The heat capacities of the samples were determined by standard calorimetry; that is, each sample was heated to a specified temperature, and the amount of heat required was determined by letting the samples cool in water-filled calorimeters.

Because the intensity of the fixed microwave fields was not known, computation of conductivity had to be done by comparison of the heating that occurred in the unknown rock samples with heating observed in similar standard reference materials with known properties. The reference materials used were:

	Resistivity 0.915 GHz	Resistivity 2.450 GHz	Density	Heat Capacity
Carbon tetrachloride	3722 ohm-m	1087 ohm-m	1.604	0.207 cal/gm
Bromo benzene	39.7	7.75	1.495	0.231
Ethylene glycol	1.48	0.553	1.109	0.571
Chloroform	175.5	24.71	1.453	0.276
Acetone	58.85	7.55	0.792	0.52
Pyridine	42.57	5.917	0.982	0.43

Conductivities for these materials were taken from von Hippel (1954b).

In converting the observed temperature rises for the various rock samples to conductivities, the change in enthalpy, ΔH_{VOL} per cc of sample was computed as follows:

$$\Delta H_{VOL} = \Delta T \cdot H_{SP} \cdot \delta \qquad \ldots 8$$

where ΔT is the temperature rise, H_{SP} is the specific heat of a sample per unit weight, and δ is the density of a sample. The conductivity was then determined by comparing this change in enthalpy with a calibration curve prepared from similar measurements made on the standard reference materials (the calibration curve at 0.915 gigahertz is shown in Figure 4, as an example).

Average values for conductivity in each of the major subgroups of samples are listed in Table 2. All of the conductivity measurements, both wet and dry, high and low frequency, are summarized graphically on Figure 5. It is most interesting to find that the frequency-dependent dry conductivity values become comparable to the frequency-independent wet conductivity values at frequencies near 1 gigahertz. This indicates that for lower frequencies, the non-dispersive low-frequency conductivity values, which are determined by the water content of a rock, are valid, while at higher frequencies, the dispersive conduction mechanisms in the solid part of the rock become dominant.

D. Mechanical measurements:

Static determination of Young's modulus and unconfined compressive strength were made by the Excavation Engineering and Earth Mechanics Institute at the Colorado School of Mines. The samples used were cylinders, with end faces machined flat with a thousandth of an inch to avoid differential loading of the sample.

Each sample was then progressively loaded in a load frame with a one-million pound load capacity. The rate of loading and the strain of the sample were monitored and computer controlled. Deformation curves, such as the one shown in Figure 6, were recorded for each sample. Compression of each sample was continued until compressive failure occurred.

Young's modulus was taken from each sample as the stress vs strain relation over the portion of the stress-strain curve where nearly linear deformation was taking place (this linear segment of the stress-strain curve is indicated in Figure 6). Values for strength and Young's modulus are listed in Tables 6 and 9. A cross plot of dynamic and static values for Young's modulus is shown in Figure 7. As is usually the case, the static values for Young's modulus are generally lower than the dynamic values from wavespeeds and density.

Discussion of Results

We must now examine data provided by these measurements of physical properties to determine what they indicate in terms of the use of geophysical measurements in evaluating geo-engineering parameters. All three rock-types studied are similar, in that they are low-porosity rocks with roughly the same chemical makeup, that of a granitic rock. Yet, a cross plot of density with rock strength indicates that fabric, which does distinguish one rock type from another, is an important factor differentiating the rock types (see Figure 8). For each of the three major classes of rock (schist and gneiss, granite, and rhyolite), there is a pronounced tendency for strength to increase in proportion to bulk density. The three groups of samples each cover about the same range in density, but the ranges in strength for each are significantly different. The rhyolite samples (open circles) show the highest strength for a given density, while the schist and gneiss samples from Washington (crosses) show the lowest strength.

A crossplot of compressive strength and compressional wave-speed is shown in Figure 9. A reasonable direct correlation is seen between these two parameters for a majority of the data, but about half the samples of schist and gneiss from the Washington area show anomalously high wavespeeds. A crossplot of the ratio of compressional to shear wavespeeds with compressive strength (Figure 10) indicates that there is a strong tendency for this ratio to lie along the value corresponding to a Poisson's ratio of 0.25; only at strengths lower than 30,000 psi do the measured values increase significantly above 0.25.

Figure 11 is a crossplot between observed dielectric constant (dispersed value observed at 1 kilohertz) and strength. As with other parameters, there is a tendency for a majority of the points to lie along a correlation, but again, there are a significant number of points that lie far from the correlation at low rock strengths.

The average values for dielectric constant and electrical conductivity may be used to estimate expected attenuations for transmission of radar fields. A typical range of frequencies used in high resolution ground-penetrating pulse radiar is 0.1 to 1 gigahertz. At these frequencies, the loss tangent is:

$$\tan \delta = \frac{1}{\omega \epsilon \rho} \qquad \ldots 9$$

At these frequencies, the resistivities measured on samples saturated with salt water generally ranged from 10 to 100 ohm-meters; the resistivity of the same samples saturated with less-saline water would be 100 to 1000 ohm-meters, or higher. The water content in competent rock is 2% or less, so that a reasonable value for dielectric constant is 6. At a frequency of 100 megahertz, the range of loss tangents corresponding to resistivities of 100 to 1000 ohm-meters is

0.03 to 0.3

At a frequency of 1 gigahertz, the corresponding range of loss tangent value is

0.003 to 0.03

At these frequencies, these rocks behave as lossy dielectrics with low to moderate loss. Loss, measured in decibels per meter, can be computed as follows (von Hippel, 1954):

$$\alpha = 8.686 \cdot \frac{2\pi}{\lambda_o} \left[\frac{1}{2} \epsilon \left\{ (1 + \tan^2 \delta)^{1\ 2} - 1 \right\} \right]^{1/2} \qquad \ldots 10$$

at 100 megahertz, the corresponding attenuation factors are:

0.67 to 6.6 db/meter

At 1.0 gigahertz, the attenuation rates are the same for the same range in resistivity. These values for attenuation bode well for the application of radar imaging in the more resistant portions of rock masses made up of schist and gneiss, granite or metarhyolite.

Conclusions

Acoustic, mechanical, and electrical properties have been measured on suites of low-porosity rock, consisting of schist and gneiss, granite, and rhyolite as rock types. Properties which depend on the chemical makeup of a rock, such as density and dielectric constant, cover similar ranges of values for each of the rock types. Strength and acoustic properties show a strong dependence on the rock type, despite the similarity in chemical composition.

The three rock types exhibit a wide range in strength, with the metarhyolite rocks having strengths as great as 75,000 pounds per square inch and the gneisses and schists having strengths as low as 5000 pounds per square inch. Many of the measured properties, such as density, acoustic velocity and dielectric constant, show a pronounced tendency to correlate with strength. Unfortunately, with each of these correlations, there are a significant number of data which lie anomalously far from the correlation lines, so that in applying such correlations in the field to evaluate rock character involves a finite element of risk.

The most significant result of these studies is the comparison of electrical conductivity measurements made at low frequencies with those made at high frequencies. For completely dried samples, it was observed that at low frequencies, conductivity in the solid minerals is very low but increases nearly linearly with increasing frequency. This behavior has been observed by many previous investigators, but never adequately explained. It is generally believed that the dispersion of conductivity values in dry rock is somehow related to conduction by impurity ions and interfacial effects in rock crystal species. In the present measurements, this same dispersion was observed at frequencies up to 2.45 gigahertz, using an induction heating technique for measuring conductivity. It was also observed that when wet samples are used in the measurements, the conductivity is essentially frequency-independent up to frequencies of approximately 1 gigahertz. For rock resistivities of 100 to 1000 ohm-meters, electromagnetic attenuation rates of 0.6 to 6 db per meter are to be expected, with attenuation being essentially the same from a frequency of 100 megahertz to 1 gigahertz. This bodes well foe the application of radar imaging in moderately resistant rocks such as gneiss, granite and rhyolite.

References

Birch, F., 1960, The velocity of compressional waves in rocks to 10 kilobars, 1: Jour. Geophys. Res., vol. 65, pp 1083-1102

Birch, F., 1961, The velocity of compressional waves in rocks to 10 kilobars, 2: Jour. Geophys. Res., vol. 66, pp 2199-2224

Birch, F., 1966, Compressibility; elastic constants: in Handbook of Physical Constants, Geol. Soc. Am. Memoir 97, New York, pp 97-174

Brace, W. F., Orange, A. S., and Madden, T. M., 1965, The effect of pressure on the electrical resistivity of water-saturated crystalline rocks: Jour. Geophys. Res., vol. 70, no. 22, pp 5669-5678

Christensen, N., 1965, Compressional wave velocities in metamorphic rocks at pressures to 10 kbar: Jour. Geophys. Res., vol. 70, p. 6147

Christensen, N., 1966, Shear-wave velocities in metamorphic rocks at pressures to 10 kbar: Jour. Geophys. Res., vol. 71, p. 3549

Cook, J. C., 1974, Status of ground-probing radar and some recent experience: in Subsurface exploration for underground excavation and heavy construction: Am. Soc. of Civil Eng., New York, pp 175-194

Cook, J. C., 1975, Radar transparencies of mine and tunnel rocks: Geophysics, vol. 40, no. 5, pp 865-885

Donaldson, P. R., 1974, Rock resistivity and geo-engineering parameters: Ph.D. Thesis T-1689, Colorado School of Mines, Golden, CO., 95 pp

Hipkins, D. L., and Whitney, L. A., 1974, Acoustic techniques suitable for use in soil: in Subsurface exploration for underground excavation and heavy construction; Am. Soc. of Civil Eng., New York, pp 159-177

Johnson, L. R., and Wenk, H. R., 1974, Anisotropy of physical properties in metamorphic rocks: Tectonophysics, vol. 23, p. 79

Keller, G. V., 1962, Electrical resistivity of rocks in the area 12 tunnels, Nevada Test Site, Nye County, Nevada: Geophysics, vol. 27, no. 2, pp 242-252

Keller, G. V., 1971, Electrical characteristics of the earth's crust: in Electromagnetic probing in geophysics, Boulder, Co., Golem Press, pp 13-75

Keller, G. V., 1974, Engineering applications of electrical geophysical methods: in Subsurface exploration for underground excavation and heavy construction, Am. Soc. of Civil Eng., New York, pp 128-143

Moffatt, D. L., 1974, Subsurface video pulse radars: in Subsurface exploration for underground excavation and heavy construction, Am. Soc. of Civil Eng., New York, pp 195-203

Morey, R. W., 1974, Continuous subsurface profiling by impulse radar: in Subsurface exploration for underground excavation and heavy construction, Am. Soc. of Civil Eng., New York, pp 213-232

Nur, A., and Simmons, G., 1969, The effect of saturation in velocity in low porosity rocks: Earth & Planetary Sci. Lett., pp 183-193

O'Connell, R. J., and Budiansky, B., 1974, Seismic velocities in dry and saturated cracked solids: Jour. Geophys. Res., vol. 79, no. 35, pp 5412-5426

Olhoeft, G. R., 1976, Electrical properties of rocks: in The Physics and Chemistry of Rock and Minerals, Wiley, London, pp. 261-270

Olhoeft, G. R., Strangway, D. W., and Frisillo, A. L., 1973, Lunar sample electrical properties: in Proceedings of the Fourth Lunar Science Conference; Supplement 4, Geochemica et Cosmochimica Acta, vol. 3, pp 3133-3149

Parkhomenko, E. I., 1967, Electrical properties of rocks: Plenum Press, New York

Price, T. O., 1974, Acoustical holography as a tool for geologic prediction: in Subsurface exploration for underground excavation and heavy construction, Am. Soc. of Civil Eng., New York, pp 172-174

Simmons, G., and Nur, A., 1968, Granites: relation of properties in situ to laboratory measurements: Science, vol. 162, pp 789-791

Spencer, James W., Jr., and Nur, Amos M., 1976, The effects of pressure, temperature, and pore water on velocities in Westerly Granite: Jour. Geophys. Res., vol. 81, no. 5, pp 899-904

von Hippel, A. R., 1954, Dielectrics and waves: Wiley, New York

von Hippel, A. R., 1954, b, Dielectric materials and applications: Wiley, New York

Walsh, J. B., 1965, The effect of cracks on the compressibility of rocks: Jour. Geophys. Res., vol. 70, pp 381-389

Wang, Chi-yuen, Lin, Wunan, and Wenk, Hans-Rudolf, 1975, The effects of water and pressure on velocities of elastic waves in a foliated rock: Jour. Geophys. Res., vol. 80, pp 1065-1069

Wantland, D., 1963, Geophysical measurements of rock properties in situ: in State of stress in the earth's crust, New York, American Elsevier Pub. Co., pp 408-443

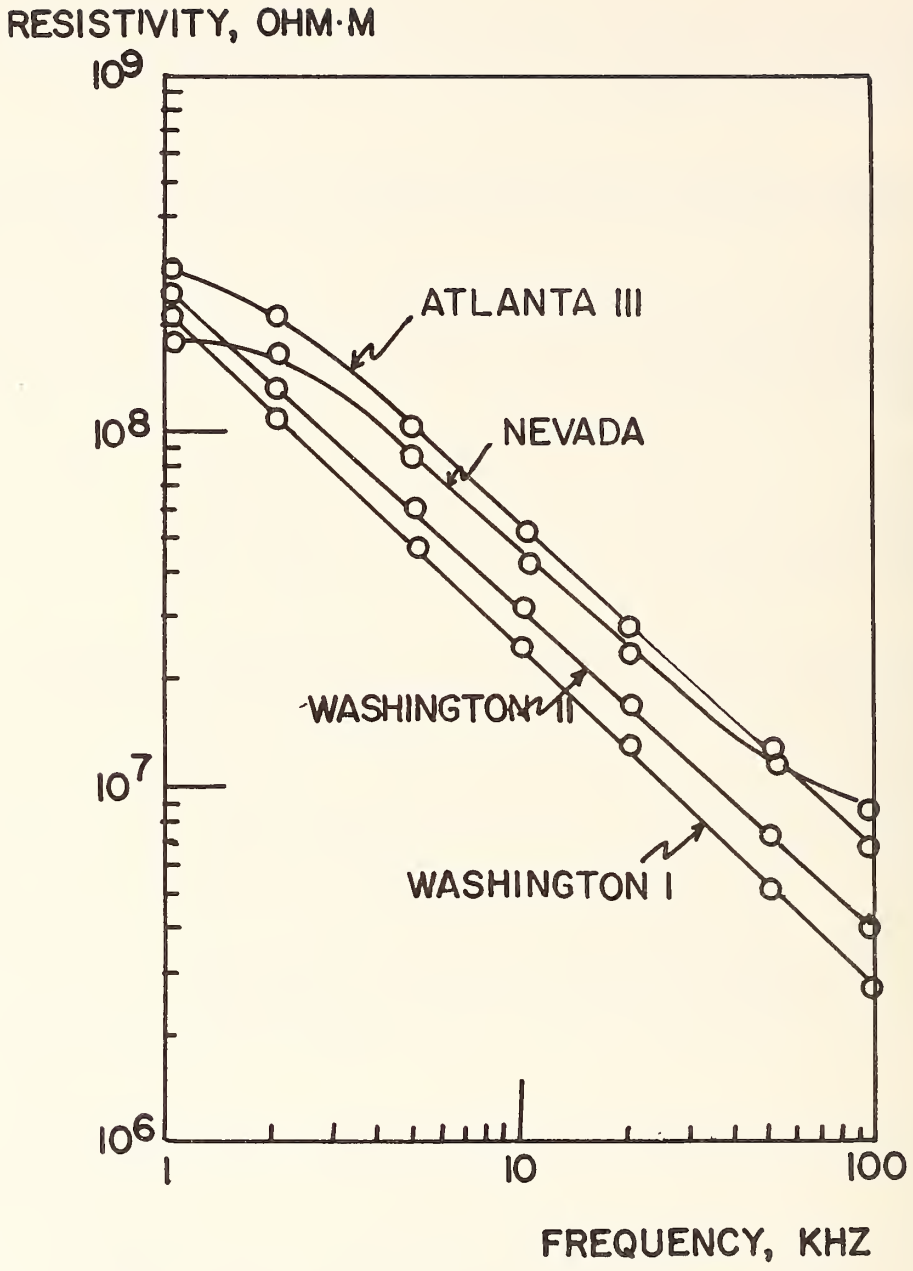

Figure 1. Average values of resistivity determined on dry samples.

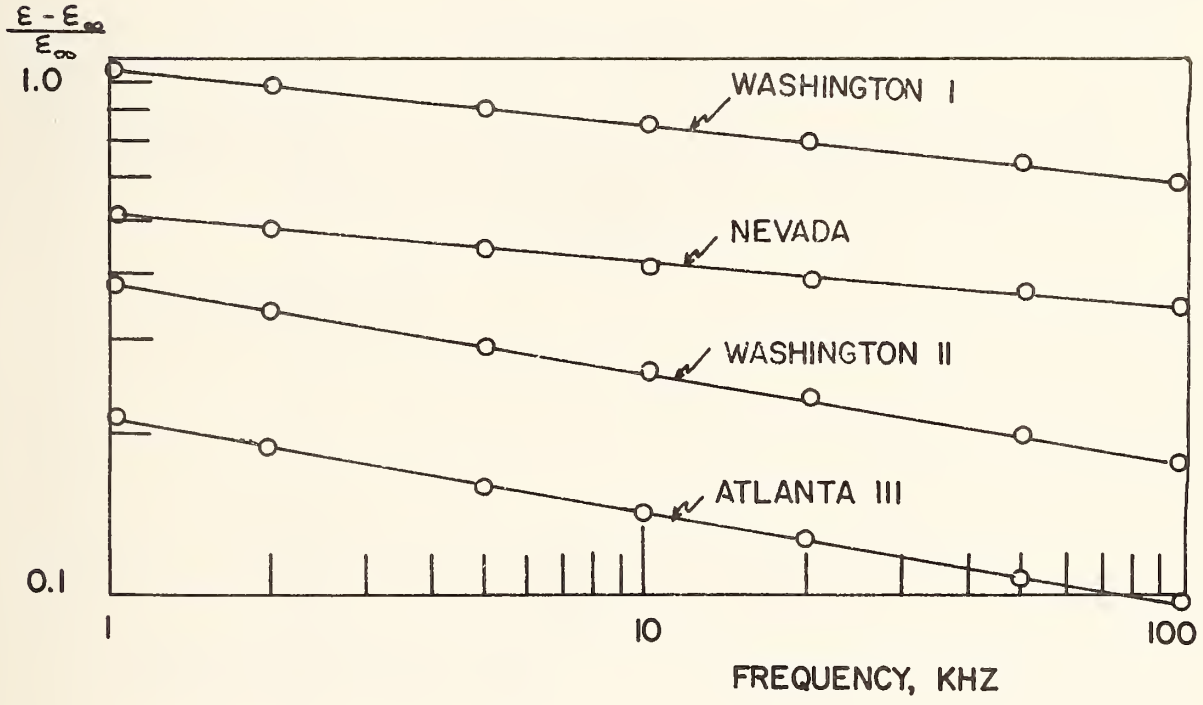

Figure 2. Average values of reduced dielectric constant determined on dry samples. The dielectric constant at high frequencies, ε_∞, has been subtracted from each plotted average.

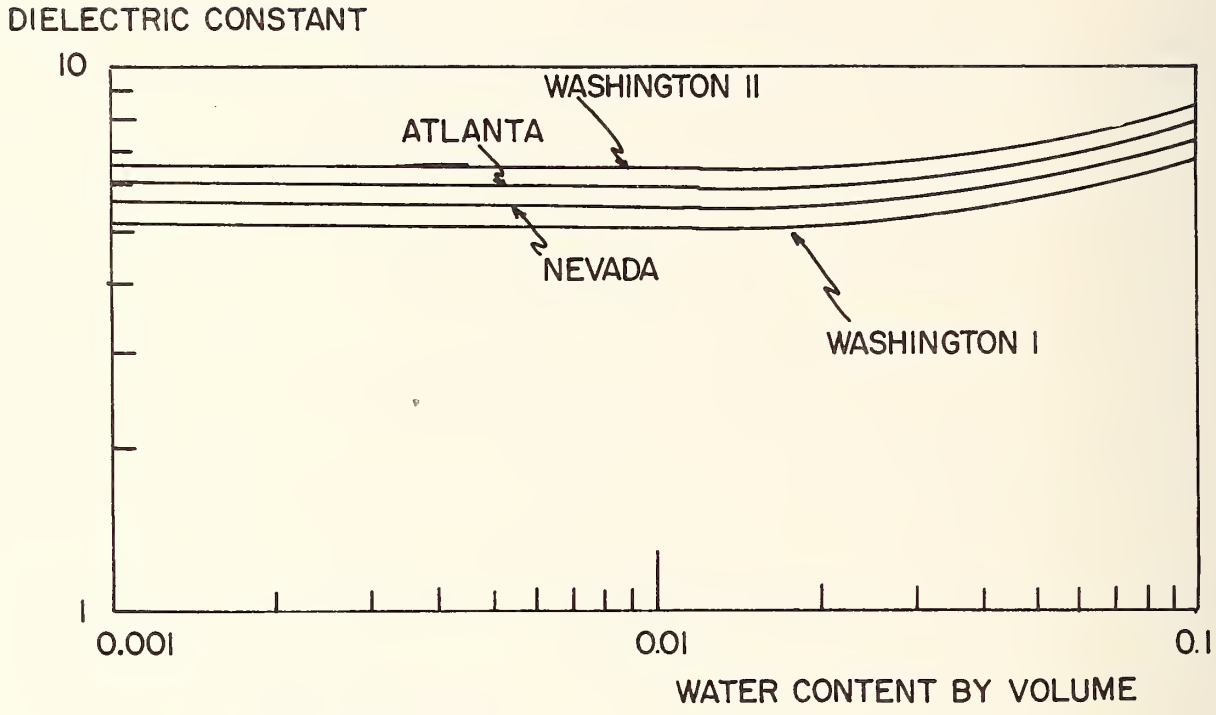

Figure 3. Dielectric constant for water-bearing samples based on the application of Lichtenecher's mixing rule.

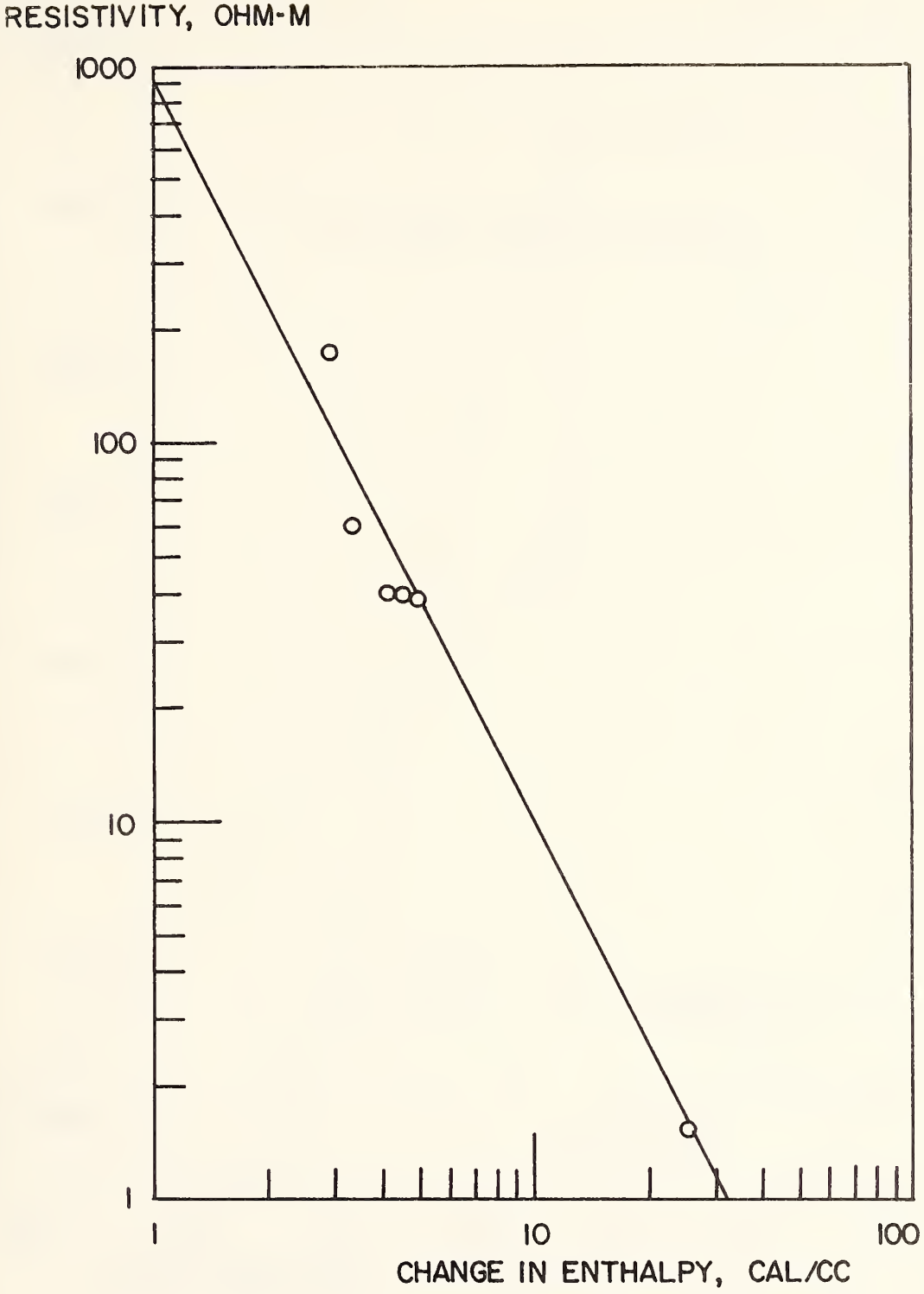

Figure 4. Calibration used in converting heat rise to resistivity for microwave heating at 0.915 gigahertz. The circles are standards.

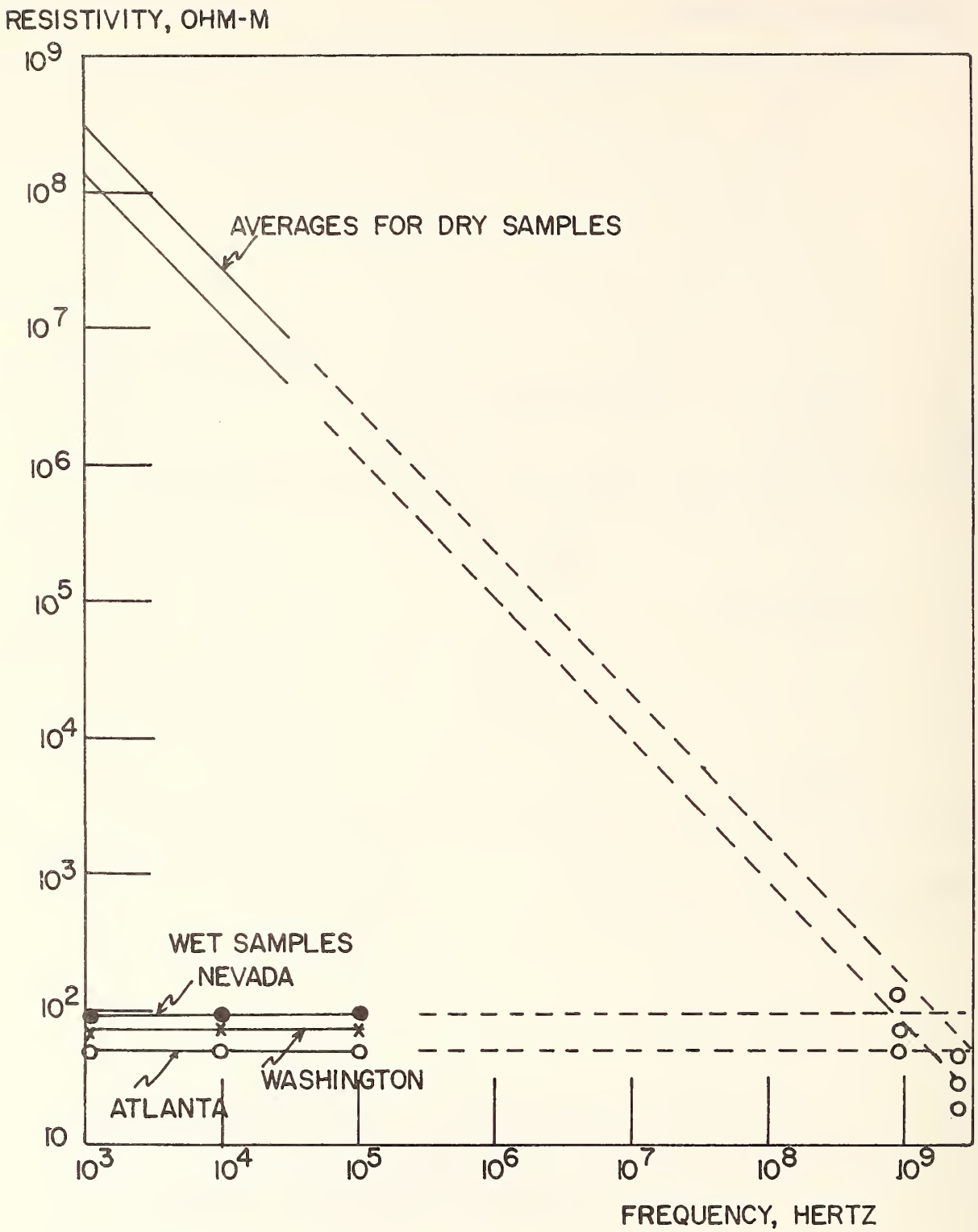

Figure 5. Comparison of all average resistivity determinations at high and low frequencies, and wet and dry samples.

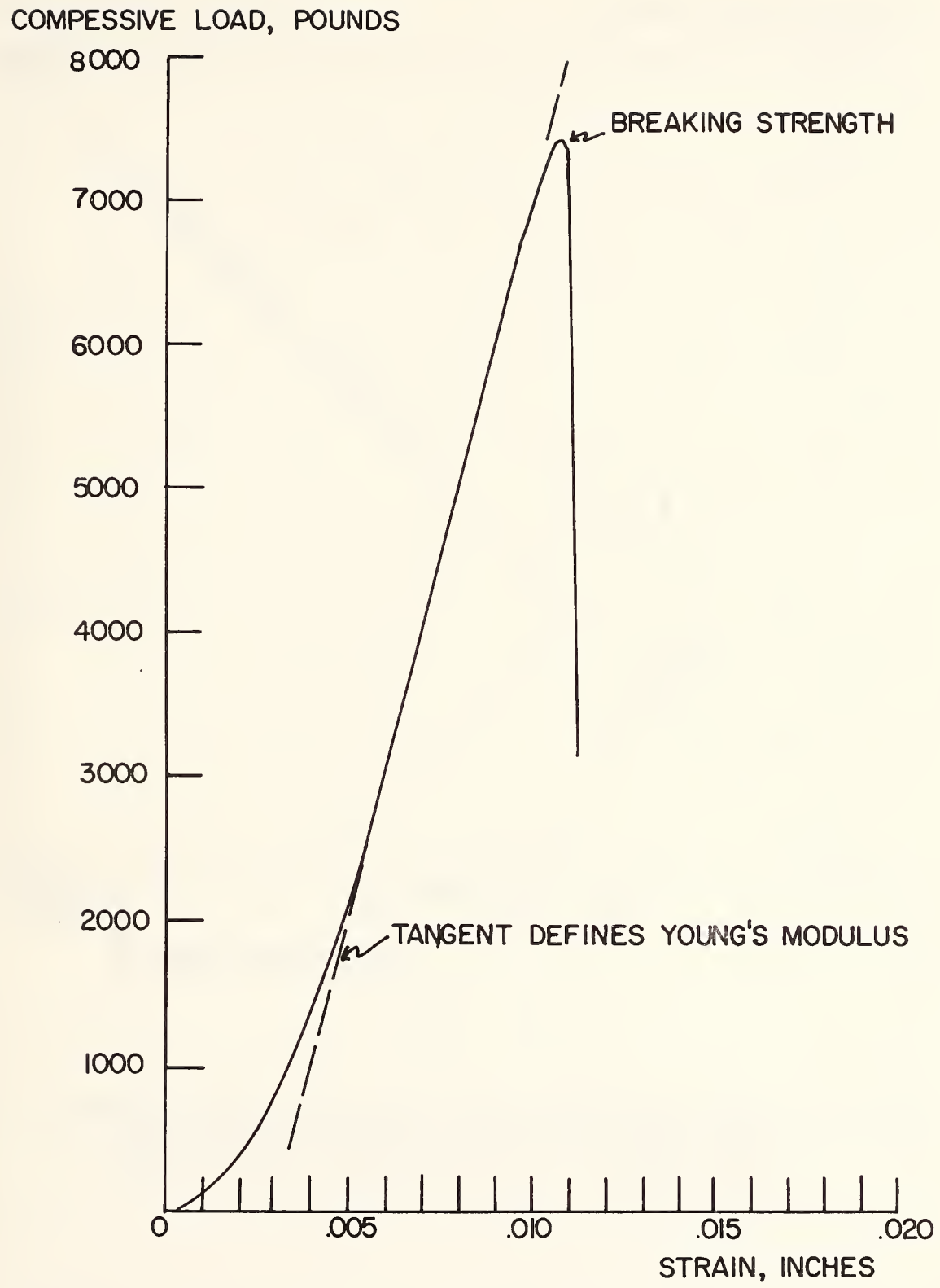

Figure 6. Typical stress-strain curve (sample III).

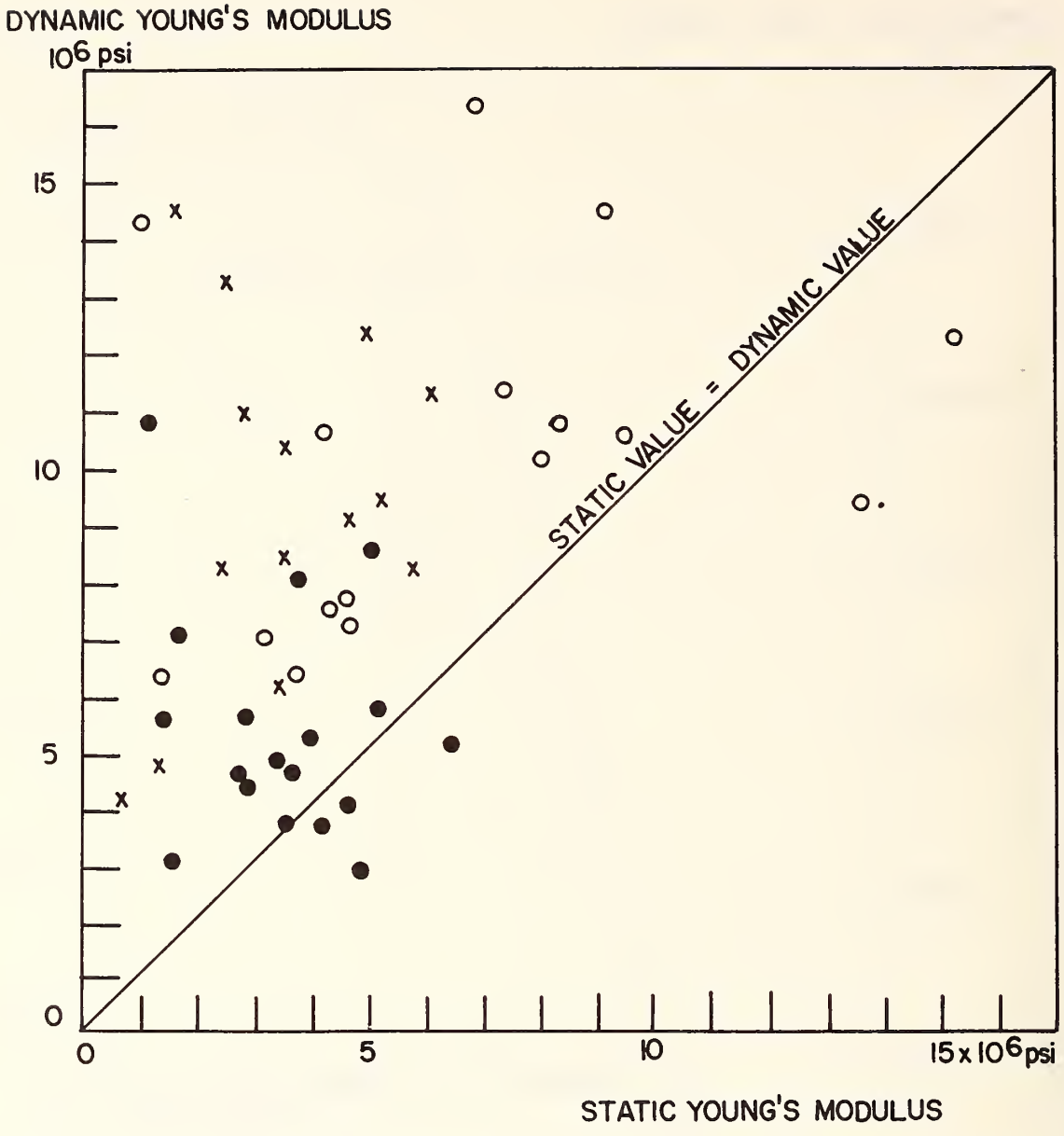

Figure 7. Correlation plot of values of Young's modulus determined from acoustic wave speeds (dynamic value) and from compression of a cylindrical sample (static value).

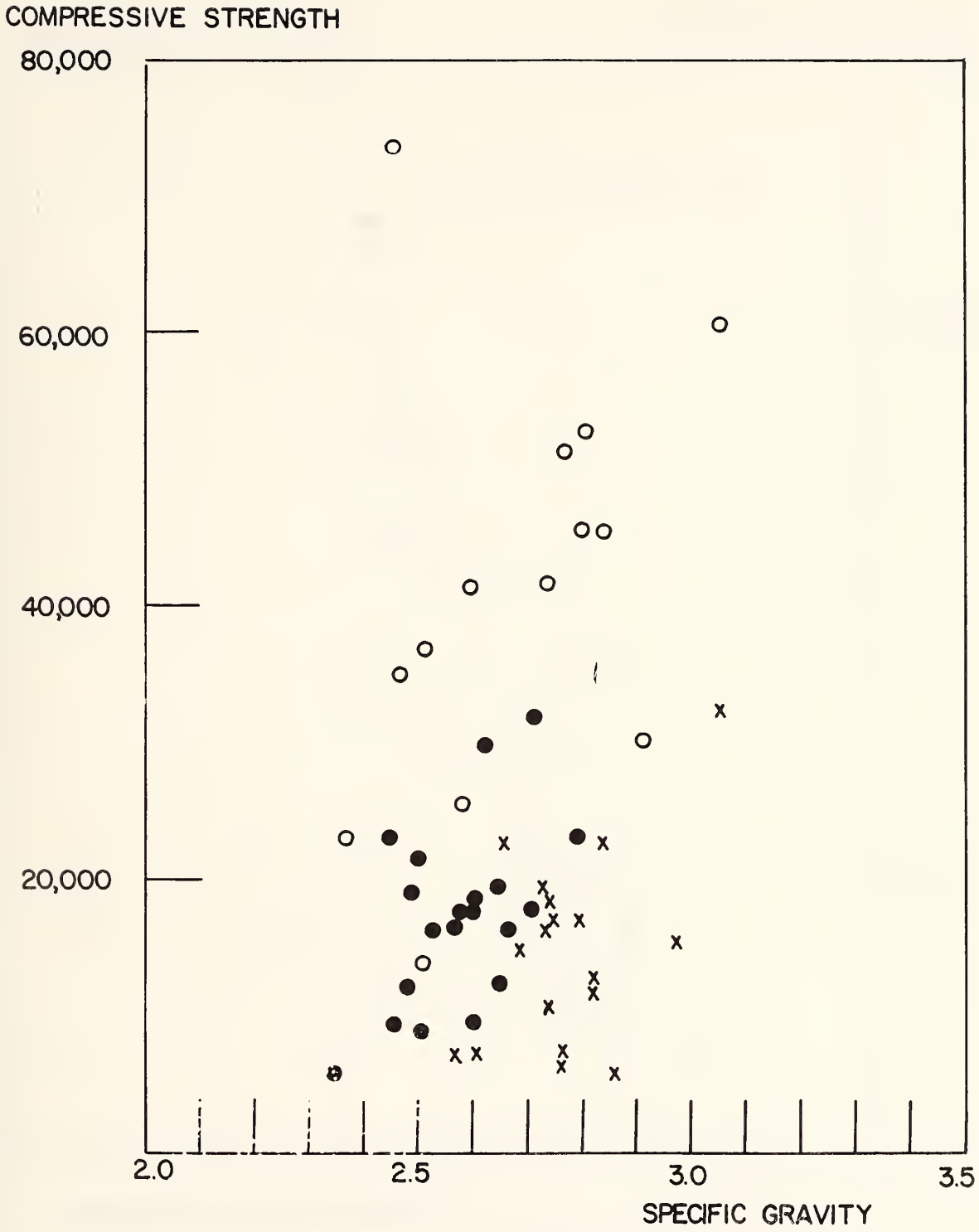

Figure 8. Correlation plot for density values and strengths. Open circles are Nevada samples, filled circles are Atlanta samples and crosses are Washington samples.

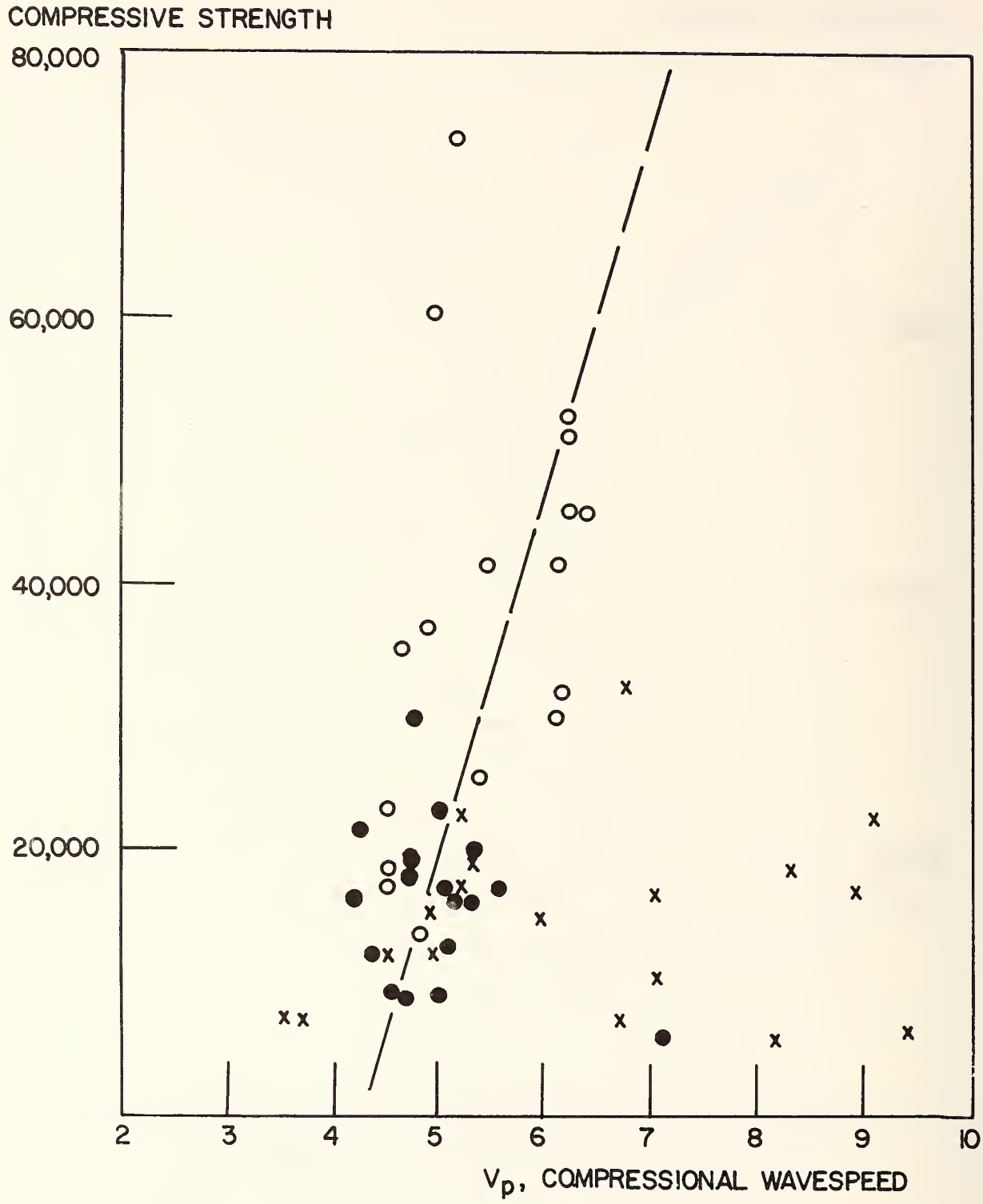

Figure 9. Correlation plot for compressional wavespeeds and strengths. Open circles are Nevada samples, filled circles are Atlanta samples, and crosses are Washington samples.

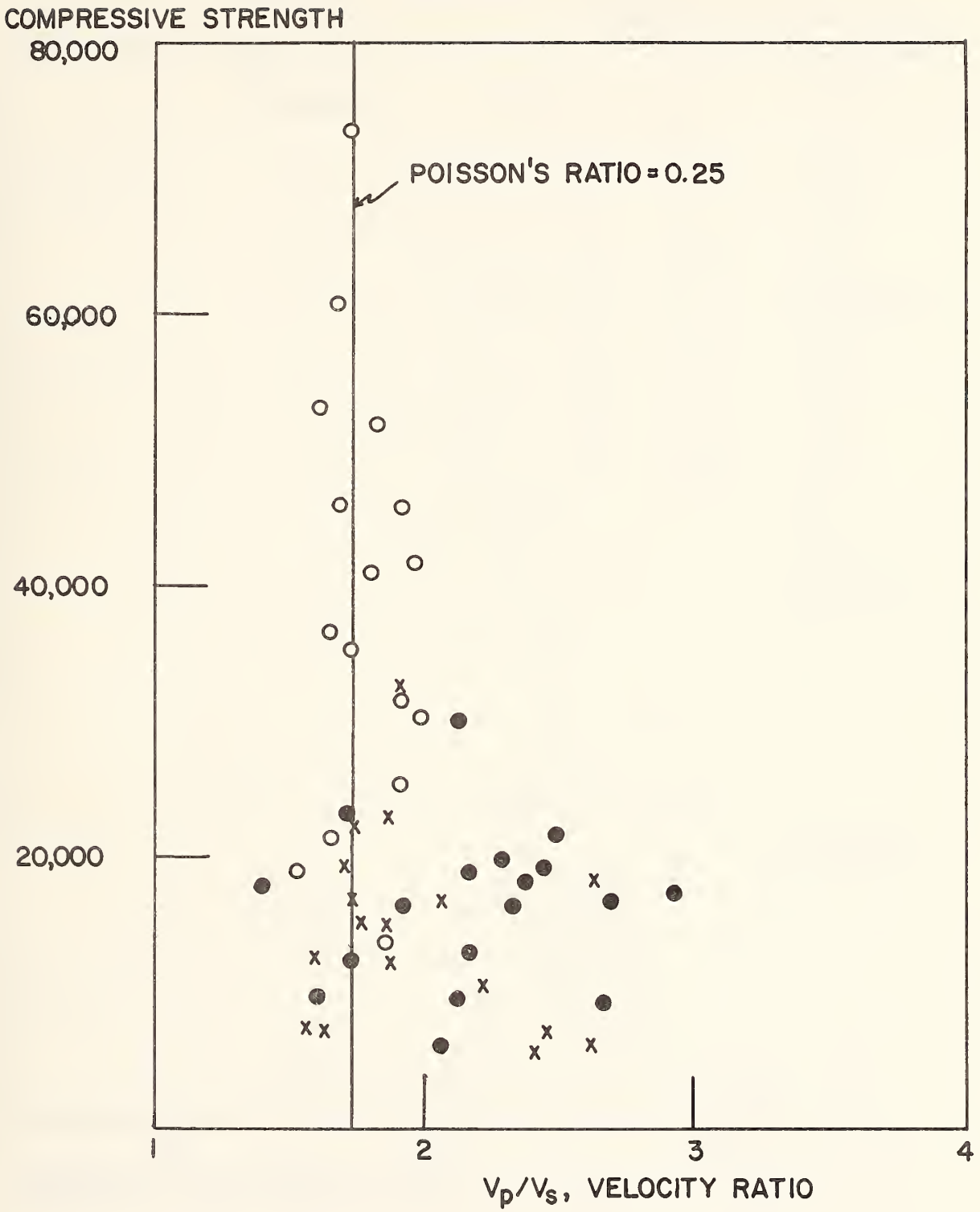

Figure 10. Correlation plot of V_p/V_s velocity ratio and strength. Open circles are Nevada samples, filled circles are Atlanta samples, and crosses are Washington samples.

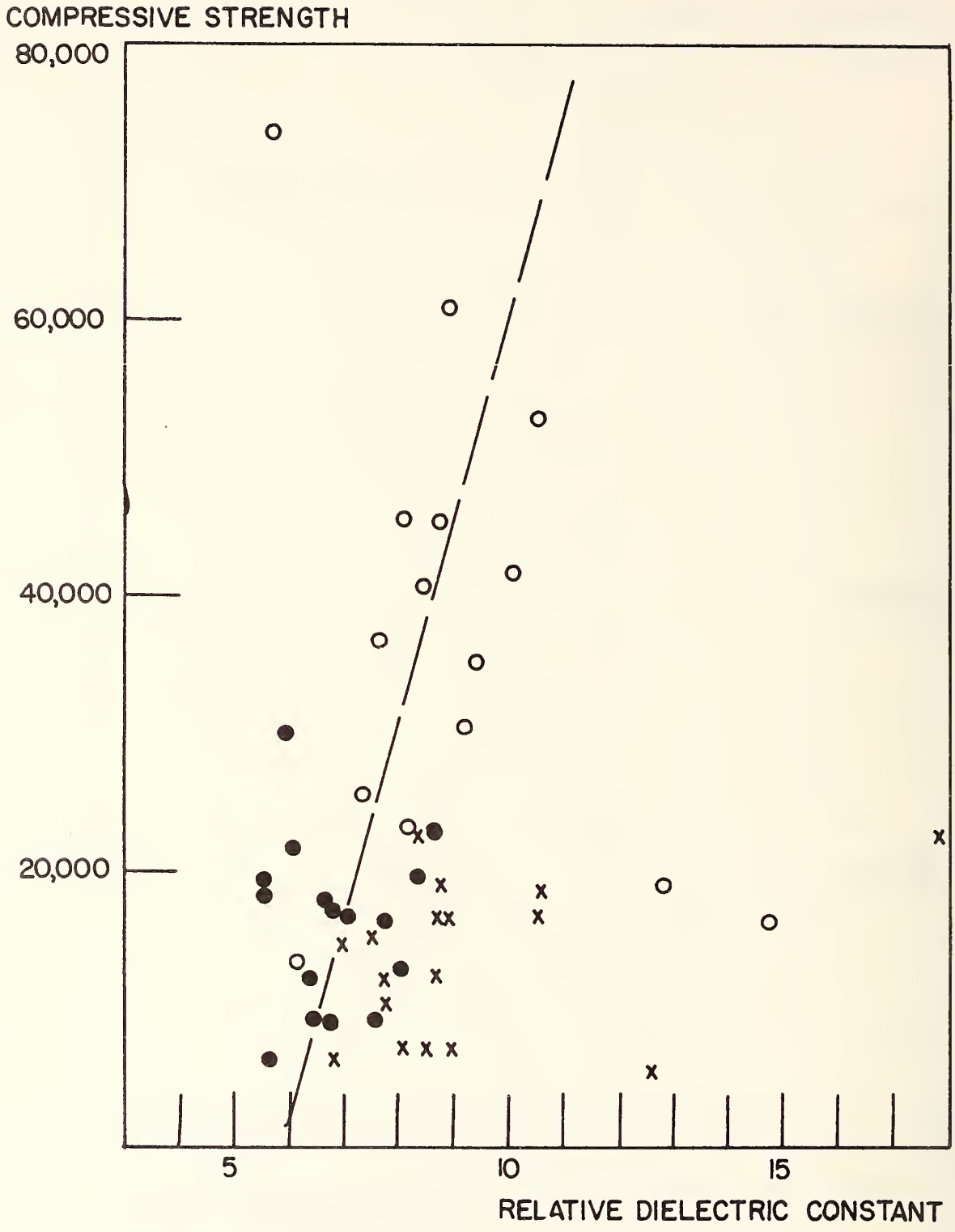

Figure 11. Correlation plot of dielectric constant at 1 kilohertz and strength. Open circles are Nevada samples, filled circles are Atlanta samples, and crosses are Washington samples.

Table 1. Density, in g/cm^3

		No. of samples	Range	$\bar{X}$	St. Dev.
Black Rock		50	3.05 - 2.20	2.62	.21
Atlanta	1	6	2.77 - 2.60	2.69	.07
	2	15	2.79 - 2.34	2.53	.09
	3	28	2.94 - 2.49	2.66	.11
	4	3	2.60 - 2.51	2.54	.05
Total		52	2.94 - 2.34	2.51	.12
Washington	1	22	2.86 - 2.59	2.76	.06
	2	19	2.92 - 2.61	2.76	.07
	3	3	3.14 - 3.05	3.10	.05
	4	3	2.97 - 2.57	2.81	.21
Total		47	3.14 - 2.57	2.79	.11

Table 3. Acoustic velocity, in km/sec

		No. of samples	V_p		$R = V_p/V_s$	
			$\bar{X}$	St. Dev.	$\bar{X}$	St. Dev.
Black Rock		50	5.37	.63	1.84	.34
Atlanta	1	6	4.79	.31	1.47	.14
	2	15	4.94	.69	2.13	.36
	3	28	4.94	.31	2.05	.39
	4	3	4.58	.41	2.02	.24
Total		52	4.90	.46	2.01	.40
Washington	1	22	5.62	1.41	1.94	.33
	2	19	5.63	1.79	2.58	.43
	3	3	7.10	.84	2.03	.16
	4	3	4.15	.68	1.75	.12
Total		47	5.63	1.58	1.96	.37

Table 2. Summary of microwave measurements.

Washington	ρ_{915}	st. dev.	ρ_{2450}	st. dev.	heat capacity
I	39	21	14	6	
II	40	24	13	4	
I-II T	26	16	14	5	
III	17	11	8	5	
IV	37	29	18	15	
All Washington Samples	35	21	14	7	0.19
Atlanta					
I	85	--	32	--	
II	293	159	110	18	
III	296	163	94	32	
IV	39		15		
All Atlanta Samples	272	167	93	36	0.17
Black Rock	56	65	28	26	0.19
Fault Gouge	5	0.5	3	0.6	

Table 4. Young's Modulus x 10^6psi

	No. of samples	Range	$\bar{X}$	St. Dev.
Black Rock	16	2.51 - 10.55	6.53	4.02
Atlanta	21	2.07 - 4.95	3.51	1.44
Washington	19	1.56 - 5.81	4.25	2.69
Atlanta I	1	-- --	3.68	--
II	7	1.03 - 4.23	2.63	1.60
III	12	2.84 - 5.28	4.06	1.22
IV	1	-- --	2.82	--
Total	21	2.07 - 4.95	3.51	1.44
Washington I	9	2.55 - 5.51	4.03	1.48
II	3	3.44 - 8.38	5.91	2.47
III	1	-- --	12.25	--
I-II T	4	2.24 - 3.00	2.62	0.38
IV	2	0.00 - 4.10	2.03	2.07
Total	19	1.56 - 5.81	4.25	2.69

Table 5. Unconfined compressive strength x 10^3

	No. of samples	Range	$\bar{X}$	St. Dev.
Black Rock	16	23.6 - 55.2	39.4	15.8
Atlanta	21	10.9 - 22.3	16.6	5.7
Washington	19	7.8 - 21.4	14.6	6.8
Atlanta I	1	---	17.5	--
II	7	7.7 - 18.7	13.2	5.5
III	12	14.3 - 23.9	19.1	4.8
IV	1	---	9.3	--
Total	21	10.9 - 22.3	16.6	5.7
Washington I	9	8.6 - 18.4	13.45	4.85
II	3	15.5 - 24.7	20.14	4.55
I-II T	4	6.1 - 14.9	10.52	4.42
III	1	---	32.14	--
IV	2	5.5 - 16.9	11.15	5.70
Total	19	7.8 - 21.4	14,63	6.76

Table 6. Individual acoustic and mechanical properties

Black Rock Desert Samples

Sample id	δ	V_p/V_s	σ	V_p	V_s	E_m	S_u	E_c
300	3.05	1.68	0.23	4.95	2.95	13.61	60,600	65.10
302	2.93	2.05	0.34	5.34	2.60			
304	2.76	1.63	0.20	6.01	3.69			
305	2.73	1.41	--	5.75	4.08			
306	2.75	1.62	0.19	5.94	3.67			
307	2.37	1.65	0.21	4.49	2.72	4.18	23,100	73.12
308	2.40	1.68	0.23	4.57	2.72			
310	2.58	1.90	0.31	5.34	2.81	4.46	25,540	53.31
312	2.57	1.97	0.33	5.41	2.75			
315	2.73	1.95	0.32	6.09	3.12	8.04	41,800	70.27
316	2.46	1.73	0.25	4.64	2.68	3.60	35,660	44.17
317	2.48	1.79	0.27	4.48	2.50			
318	2.45	1.51	0.11	4.52	2.99	3.22	19,040	48.59
319	2.41	2.00	0.33	4.94	2.47			
321	2.52	2.16	0.36	4.79	2.22			
322	2.82	1.90	0.31	5.93	3.12			
323	2.84	1.68	0.23	6.34	3.77	1.03	45,530	99.01
325	2.45	1.73	0.25	5.16	2.98	6.85	73,760	113.21
326	2.46	1.13	--	5.20	4.60			
327	2.44	1.82	0.28	5.21	2.86			
328	2.55	1.64	0.20	5.10	3.11			
329	2.51	1.84	0.29	4.82	2.62	1.21	13,970	44.49
332	2.81	1.91	0.31	6.23	3.26	7.34	45,720	78.26
333	2.76	1.63	0.20	5.74	3.52			
334	2.67	1.93	0.32	6.04	3.13			
336	2.73	2.05	0.34	6.34	3.09			
337	2.71	1.91	0.31	6.14	3.21	9.38	31,970	73.18
338	2.80	3.63	0.46	6.12	1.69			
340	2.80	1.60	0.18	6.22	3.89	9.06	52,780	99.95
341	2.25	2.20	0.37	4.46	2.03			
342	2.24	1.73	0.25	4.25	2.46			
343	2.20	1.78	0.27	5.09	2.86			
344	2.24	1.77	0.27	4.96	2.80			
345	2.28	1.92	0.31	4.95	2.58			
347	2.31	2.36	0.39	4.90	2.08			
353	2.60	2.23	0.37	4.86	2.18			
355	2.58	1.68	0.23	5.04	3.00			
356	2.59	1.79	0.27	4.95	2.77	4.64	41,320	50.58

Sample id	δ	V_p/V_s	σ	V_p	V_s	E_m	S_u	E_c
358	2.53	1.79	0.27	4.95	2.77			
359	2.51	1.66	0.22	4.87	2.93	4.34	36,850	52.41
362	2.53	1.67	0.22	5.26	3.15			
364	2.87	1.76	0.26	5.50	3.13			
365	2.84	1.82	0.28	5.97	3.28			
366	2.77	1.81	0.28	6.24	3.45	15.25	51,760	84.45
367	2.82	1.86	0.30	5.89	3.17			
368	2.81	1.90	0.31	6.34	3.34			
370	2.89	1.97	0.33	6.10	3.10			
371	2.91	1.97	0.33	6.10	3.10	8.22	30,350	74.16
373	2.71	1.43	0.02	4.36	3.05			
374	2.77	1.57	0.16	5.70	3.63			
	g/cm^3			km/sec	km/sec	psi		
				Atlanta Samples				
226	2.77	1.44	0.03	4.50	3.13			
243	2.71	1.40	--	4.50	3.21	3.68	17,510	55.71
245	2.60	1.42	0.01	5.05	3.56			
247	2.72	1.76	0.26	5.11	2.90			
255	2.71	1.40	--	4.54	3.24			
260	2.60	1.42	0.01	.505	3.56			
201	2.79	1.71	0.24	5.00	2.92			
202	2.50	2.48	0.40	4.25	1.71	4.78	21,660	20.51
208	2.52	1.86	0.30	4.90	2.63			
210	2.55	1.86	0.30	4.20	2.26			
211	2.48	1.73	0.25	4.35	2.51	1.40	12,370	39.06
212	2.58	2.14	0.36	4.62	2.16			
214	2.54	2.14	0.36	4.71	2.20			
218	2.50	2.66	0.42	4.66	1.75	1.48	9,080	21.71
223	2.53	2.28	0.38	5.05	2.21			
225	2.46	1.60	0.18	4.62	2.89	1.60	9,330	48.47
227	2.34	2.05	0.34	7.06	3.44	1.07	6,050	74.45
236	2.57	2.68	0.42	5.27	1.97	4.51	16,630	28.31
252	2.58	2.37	0.39	5.05	2.13	3.60	17,300	32.58
258	2.51	2.52	0.41	5.52	2.19			
259	2.52	1.86	0.30	4.90	2.63			
200	2.79	1.71	0.24	5.00	2.92	5.04	23,070	58.97
203	2.49	2.43	0.40	4.72	1.94	3.48	19,170	26.19
204	2.53	1.45	0.05	4.92	3.39			

Sample id	δ	V_p/V_s	δ	V_p	V_s	E_m	S_u	E_c
206	2.53	1.92	0.31	4.22	2.19	2.70	16,270	31.89
209	2.74	1.98	0.33	5.62	2.84			
213	2.73	1.61	0.19	5.21	3.24			
215	2.49	1.79	0.27	5.05	2.82			
216	2.67	2.30	0.38	4.64	2.02			
217	2.79	1.96	0.32	4.68	2.39			
220	2.85	1.38	--	4.86	3.52			
221	2.58	1.85	0.29	4.77	2.58			
222	2.60	2.17	0.37	4.73	2.18	3.36	18,470	33.75
228	2.62	2.12	0.36	4.75	2.24	6.41	29,990	35.66
231	2.56	2.60	0.41	4.74	1.82			
232	2.80	2.54	0.41	4.57	1.80			
237	2.66	2.32	0.39	5.15	2.22	3.92	16,460	36.35
238	2.73	1.45	0.05	5.36	3.70			
240	2.65	2.27	0.38	5.32	2.34	5.08	19,710	40.04
242	2.65	2.16	0.36	5.06	2.34	2.86	17,720	39.59
244	2.73	1.33	--	5.14	3.86			
246	2.60	2.93	0.43	5.52	1.88	4.09	17,110	26.35
248	2.71	2.40	0.39	5.05	2.10			
249	2.94	1.76	0.26	4.64	2.64			
250	2.63	2.29	0.38	5.21	2.28			
251	2.58	2.37	0.29	4.71	1.99			
256	2.62	2.12	0.36	4.75	2.24			
257	2.65	2.16	0.36	5.06	2.34			
261	2.62	2.12	0.36	4.75	2.24			
233	2.52	2.18	0.37	4.56	2.09			
235	2.60	2.13	0.36	4.99	2.34	2.82	9,290	30.57
241	2.51	1.75	0.26	4.18	2.39			
				Washington Samples				
100	2.76	2.10	0.35	5.36	2.55			
103	2.76	2.62	0.41	9.40	3.59	1.64	6,320	100.63
104	2.74	1.73	0.25	5.16	2.98	5.02	16,730	60.83
105	2.59	2.53	0.41	6.01	2.38			
106	2.74	2.62	0.41	8.31	3.17	6.06	18,210	77.89
109	2.75	1.64	0.20	4.79	2.92			
111	2.74	2.05	0.34	6.98	3.40	4.97	16,690	85.16
114	2.80	2.02	0.34	6.15	3.04			
127	2.86	2.41	0.40	8.16	3.39	2.52	5,770	91.74
129	2.79	1.68	0.23	5.09	3.03			

Sample id	δ	V_p/V_s	σ	V_p	V_s	E_m	S_u	E_c
131	2.73	1.76	0.26	5.80	3.30			
133	2.82	1.70	0.24	4.05	2.38			
134	2.82	1.87	0.31	4.51	2.41	3.44	12,270	42.57
135	2.68	1.63	0.20	4.68	2.87			
138	2.72	1.83	0.29	4.89	2.67			
145	2.84	2.11	0.36	5.60	2.65			
146	2.79	1.80	0.28	4.72	2.62			
148	2.80	1.63	0.20	4.93	3.02			
149	2.71	1.74	0.25	4.02	2.31			
150	2.73	1.70	0.24	5.28	3.11	5.23	19,140	65.24
153	2.74	1.92	0.31	4.86	2.53			
155	2.82	1.60	0.18	4.92	3.08	4.61	12,540	63.11
102	2.78	3.28	0.45	8.39	2.55			
107	2.80	1.77	0.27	6.98	3.94			
110	2.76	2.46	0.40	6.70	2.72	2.46	7,260	57.20
112	2.79	1.73	0.25	8.91	5.15	3.82	16,750	184.99
113	2.66	1.73	0.25	9.07	5.24	8.47	22,660	182.59
116	2.82	2.16	0.36	5.37	2.49			
117	2.66	2.28	0.38	3.98	1.75			
118	2.75	1.64	0.20	4.89	2.98			
122	2.74	2.22	0.37	7.02	3.16	2.84	10,580	75.15
126	2.83	2.83	0.43	5.79	2.05			
130	2.84	1.86	0.30	5.18	2.78	5.72	22,880	56.93
132	2.69	1.85	0.29	5.94	3.21	3.55	14,890	71.74
136	2.92	1.79	0.27	2.92	1.63			
137	2.70	1.57	0.16	4.55	2.90			
141	2.61	1.56	0.15	3.69	2.37	1.34	7,500	33.75
142	2.80	1.73	0.25	4.77	2.76			
151	2.76	1.98	0.33	3.74	1.89			
152	2.77	1.73	0.25	4.31	2.49			
154	2.81	1.74	0.25	4.78	2.75			
108	3.05	1.89	0.31	6.73	3.56	12.25	32,140	15.03
119	3.12	2.21	0.37	8.06	3.65			
120	3.14	1.99	0.32	6.50	3.27			
101	2.57	1.63	0.20	3.56	2.18	0.56	7,120	29.26
123	2.89	1.87	0.30	3.99	2.13			
144	2.97	1.76	0.26	4.89	2.78	3.49	15,180	57.89

Table 7. Dielectric constant and resistivity, dry state

Sample	Frequency kHz 1	2	5	10	20	50	100
Washington Group I							
100	10.67*	10.13	9.55	9.22	9.01	8.71	8.50
	160**	86	46	27	12.0	5.30	3.00
103	6.86	6.73	6.61	6.43	6.33	6.28	6.18
	2800	280	130	70	28	12	6.0
104	10.52	10.03	9.45	9.22	8.81	8.50	8.25
	130	210	38	240	11	4.50	2.10
105	10.83	10.04	8.97	8.38	7.86	7.61	7.14
	97	80	23	13	14	41	1.70
106	10.57	9.52	8.73	8.25	7.79	7.48	7.15
	100	59	29	15	16	3.50	1.90
109	11.58	11.04	10.55	10.21	9.85	9.44	9.07
	180	87	41	18	8.70	3.50	1.80
111	8.80	8.57	8.19	7.96	7.76	7.50	7.24
	520	2100	57	27	12	5.90	3.20
114	11.79	11.45	10.89	10.4	9.98	9.35	8.93
	270	91	37	14	6.4	2.6	1.4
127	12.60	12.29	11.88	11.57	11.42	10.96	10.70
	130	68	27	13	6.2	2.3	1.1
129	8.86	8.34	7.76	7.54	7.28	6.96	6.96
	140	85	48	32	16	7.3	5.0
131	13.95	13.60	13.45	13.29	13.09	12.59	12.33
	130	1300	61	20	7.0	2.3	1.1
133	13.15	12.60	11.91	11.31	10.62	9.77	9.08
	97	53	20	8.7	4.3	1.8	0.93
134	7.72	7.57	7.42	7.16	7.21	7.21	7.11
	430	220	85	260	26	9.0	3.9
135	9.30	8.69	7.96	7.52	7.24	6.85	6.63
	110	62	29	16	9.9	4.9	2.8
138	8.53	8.23	7.93	7.78	7.63	7.43	7.38
	270	160	70	53	23	9.4	4.7
145	13.37	12.95	12.38	11.91	11.60	10.92	10.45
	110	56	21	11	5.2	2.0	0.93
146	6.76	6.45	6.40	6.29	6.19	5.98	5.93
	310	190	96	81	30	15	6.8

Sample	1	2	5	10	20	50	100
148	10.19	9.66	9.19	8.87	8.56	8.14	7.88
	110	73	36	20	9.6	4.3	2.2
149	7.95	7.80	7.60	7.36	7.36	7.21	7.11
	370	220	110	74	34	13	7.1
150	8.82	8.52	8.26	7.91	7.91	7.66	7.46
	240	140	58	55	15	6.2	3.0
153	9.12	8.97	9.02	9.12	9.08	8.97	8.86
	350	100	83	170	58	13	5.2
155	8.74	8.55	8.26	8.07	7.97	7.68	7.53
	250	130	62	33	18	7.0	3.6
Washington Group II							
102	8.88	8.60	8.27	8.09	7.89	7.79	7.63
	590	350	83	42	20	7.9	5.5
107	9.80	9.15	8.50	8.16	7.80	7.64	7.44
	140	340	43	24	44	5.5	3.7
110	8.96	8.68	8.21	7.99	7.69	7.54	7.35
	300	--	57	33	--	6.1	3.1
112	8.71	8.24	7.77	7.54	7.35	7.15	7.05
	190	100	59	34	17	8.2	4.3
113	17.84	17.58	17.43	17.38	17.13	16.62	16.21
	120	130	47	16	5.1	1.5	0.70
116	9.45	8.91	8.48	8.20	7.84	7.74	7.43
	150	--	54	28	8.0	4.9	2.4
117	9.87	9.60	9.33	9.13	9.00	8.41	8.86
	230	--	87	53	24	12	6.1
118	12.32	11.11	10.39	10.03	9.60	9.42	9.34
	110	310	37	19	23	20	5.0
122	7.78	7.07	6.77	6.57	6.51	6.31	6.21
	250	100	43	24	14	6.0	4.2
126	10.65	10.29	9.93	9.72	9.57	9.21	8.95
	140	100	53	27	12	4.0	1.8
130	8.45	8.15	7.90	7.80	7.60	7.40	7.15
	240	150	70	38	19	7.0	3.8
132	6.95	6.90	6.80	6.69	6.69	6.59	6.54
	450	230	110	54	28	12	7.9

Sample	1	2	5	10	20	50	100
136	12.17	11.42	10.72	10.27	9.73	9.03	8.63
	130	70	28	14	6.5	2.3	1.0
137	7.31	7.17	6.98	6.88	6.79	6.64	6.60
	350	220	92	63	37	15	7.3
141	8.02	7.96	8.07	7.85	7.80	7.69	7.69
	610	330	91	57	27	10	4.1
142	7.83	7.56	7.23	7.12	7.01	6.69	6.74
	240	130	57	43	22	15	6.4
143	10.21	10.00	9.74	9.54	9.38	9.12	8.76
	260	160	66	31	13	3.9	1.6
151	7.50	7.35	7.45	7.45	7.40	7.29	7.24
	440	--	--	--	--	28	8.3
152	6.81	6.71	6.65	6.55	6.60	6.50	6.50
	610	330	160	79	42	17	11
154	12.93	12.60	12.16	11.83	11.61	11.00	10.67
	110	59	23	11	5.4	1.9	0.86
Washington Group III							
108	19.95	18.80	18.28	17.86	17.51	16.93	16.42
	66	220	58	21	7.5	2.5	1.2
119	7.68	7.51	7.28	7.15	7.05	6.95	6.90
	4200	280	150	53	28	11	4.7
120	19.37	18.00	17.44	16.89	16.63	16.18	15.82
	39	110	58	42	11	3.5	1.8
Washington Group IV							
101	8.52	8.30	7.93	7.79	7.42	7.27	7.12
	510	--	58	29	83	6.7	3.1
123	6.72	6.52	6.37	6.22	6.27	6.17	6.08
	320	240	160	89	47	25	12
144	7.50	7.41	7.26	7.17	7.22	7.07	7.03
	410	220	110	55	30	11	6.3

Sample	1	2	5	10	20	50	100
Atlanta Group I							
226	7.99 420	7.89 260	7.73 130	7.63 82	7.73 44	7.58 18	7.52 9.0
229	7.93 350	7.82 190	7.60 90	7.49 46	7.38 24	7.22 11	7.22 5.5
243	6.83 430	6.78 210	6.62 88	6.56 30	6.51 22	6.35 7.5	6.24 3.6
245	5.62 740	5.51 540	5.46 770	5.40 300	5.46 140	5.35 52	5.35 19
247	5.07 2000	5.07 1200	4.99 570	4.96 400	4.99 180	4.96 76	4.96 57
255	8.36 260	8.14 150	7.83 61	7.46 46	7.51 14	7.14 5.3	6.93 2.6
260	10.60 240	10.40 120	10.34 --	10.24 --	10.08 27	9.77 7.0	-- --
Atlanta Group II							
201	5.61 540	5.44 270	5.28 150	5.22 110	5.22 74	5.17 77	5.17 38
202	6.05 520	6.00 310	5.89 160	5.94 91	5.83 44	5.78 22	5.51 9.8
208	6.39 430	6.21 220	5.97 110	5.85 64	5.79 35	5.67 18	5.79 18
210	6.73 300	6.44 170	6.16 80	6.05 52	5.94 30	5.83 17	5.88 13
211	6.37 330	6.24 190	6.06 120	6.06 58	6.00 35	5.93 20	6.06 8.6
212	5.67 400	5.52 220	5.31 140	5.21 88	5.21 74	5.16 41	5.16 41
214	5.41 670	5.36 370	5.47 110	5.24 120	5.30 68	5.19 38	5.19 38
218	6.69 230	6.35 120	6.02 73	5.80 45	5.74 28	5.63 17	5.74 13
223	6.57 390	6.24 220	6.08 120	6.02 45	5.91 38	5.86 17	5.91 8.7
225	6.46 340	6.24 170	6.08 77	6.02 45	5.91 26	5.80 12	5.80 6.4

Sample	1	2	5	10	20	50	100
227	5.64 300	5.53 170	5.37 110	5.31 60	5.31 36	5.20 18	5.20 11
236	6.97 350	6.70 180	6.44 85	6.33 48	6.22 28	-- --	6.12 7.2
252	6.73 390	6.56 210	6.33 110	6.27 65	2.62 43	6.10 25	6.16 12
258	13.98 190	13.81 180	13.76 300	13.70 35	13.43 9.1	13.32 2.6	13.10 1.1
259	8.22 340	8.00 160	7.72 70	7.50 38	7.39 21	7.23 44	7.28 4.8
Atlanta Group III							
200	8.60 78	8.02 68	7.60 50	7.23 150	7.39 28	7.23 12	7.18 8.0
203	5.57 820	5.51 570	5.39 490	5.34 330	5.45 230	5.39 150	5.39 37
204	6.61 250	6.33 210	6.17 140	6.06 120	6.11 45	6.00 22	5.94 11
206	7.74 220	7.50 190	7.26 120	7.14 58	7.08 28	6.90 10	6.90 4.5
209	10.69 97	10.29 46	9.84 24	9.34 15	9.24 7.3	8.84 3.3	8.58 1.7
216	7.49 91	6.97 89	6.56 73	6.27 --	6.39 26	6.22 16	6.16 9.2
217	5.27 670	5.06 660	5.17 200	4.95 140	5.17 170	5.06 27	5.11 13
220	6.30 480	6.24 270	6.36 86	6.13 73	6.13 37	6.02 11	6.02 12
221	7.22 470	7.17 230	7.00 110	6.94 46	6.88 22	6.71 9.4	6.71 4.7
222	5.59 890	5.54 460	5.49 320	5.54 130	5.54 59	5.43 18	5.43 8.0
224	7.10 110	6.60 98	6.27 69	6.05 44	6.05 28	5.88 12	5.83 6.4
228	5.90 780	5.90 460	5.90 240	5.79 140	5.90 74	5.85 39	5.79 19

Sample	1	2	5	10	20	50	100
231	6.36	6.25	6.14	6.08	6.03	5.98	6.03
	410	230	129	57	29	16	7.1
232	9.04	8.56	8.13	7.71	7.76	7.39	7.23
	140	89	45	39	13	5.1	2.9
237	14.68	14.10	13.98	13.68	13.37	12.80	12.27
	110	--	180	31	8.8	2.4	1.0
238	7.68	7.08	6.69	6.31	6.42	6.15	6.04
	110	81	55	76	17	8.2	5.5
240	8.26	7.98	7.71	7.49	7.32	7.16	7.05
	490	130	62	32	17	8.1	4.3
242	7.97	7.75	7.58	7.41	7.41	7.30	7.19
	160	100	47	28	14	4.7	2.4
244	8.18	7.74	7.31	6.87	6.93	6.60	6.49
	130	87	49	55	15	6.8	3.5
246	6.75	6.64	6.53	6.47	6.47	6.30	6.30
	320	190	100	45	24	10	5.1
248	6.16	6.10	6.04	5.93	6.04	5.99	5.93
	370	230	130	84	39	21	12
249	8.61	8.43	8.26	8.14	8.02	7.91	8.02
	120	85	42	27	15	7.6	4.0
250	7.70	7.60	7.65	7.39	7.33	7.33	7.39
	450	250	83	51	26	10	4.5
251	6.57	6.46	6.41	6.41	6.02	6.35	6.30
	610	320	160	50	8.6	--	8.6
256	6.17	6.17	6.06	6.06	6.11	6.06	6.06
	800	510	260	200	88	39	26
257	7.47	7.36	7.25	7.13	7.08	6.91	6.79
	280	150	71	38	19	7.1	3.1
261	6.73	6.78	6.67	6.61	6.67	6.56	6.56
	920	430	220	140	63	25	38
Atlanta Group IV							
205	7.77	7.65	7.47	7.41	7.29	7.18	7.24
	460	240	100	46	23	9.6	6.0
233	7.28	6.80	6.37	6.00	6.11	5.95	5.90
	140	96	50	97	23	11	6.6

Sample	1	2	5	10	20	50	100
234	8.21	8.11	8.11	7.84	7.79	7.63	7.68
	530	260	84	51	25	11	5.0
235	7.49	6.98	6.59	6.13	6.19	6.02	5.97
	150	98	48	67	20	11	7.5
241	6.60	6.48	6.29	6.23	6.17	6.04	6.11
	480	290	150	88	44	21	8.6
Nevada							
301	8.91	8.96	8.87	8.87	8.91	8.87	8.87
	330	650	440	260	120	59	--
303	10.25	--	10.19	10.43	10.31	10.01	9.77
	570	--	--	31	12	4.0	2.0
304	12.07	12.01	11.77	11.71	11.58	11.28	11.03
	200	200	72	33	14	4.6	2.4
305	8.73	8.62	8.45	8.28	8.05	7.77	7.60
	41	340	150	61	24	9.3	4.7
307	8.24	7.79	7.22	6.94	6.66	6.43	6.32
	58	41	24	16	9.9	5.6	4.2
308	6.93	6.68	6.24	5.93	5.99	5.74	5.56
	87	73	39	37	14	8.1	6.9
309	8.01	7.24	6.42	6.01	5.71	5.36	5.18
	33	25	15	11	7.0	3.9	2.8
310	7.29	7.29	7.35	7.17	7.11	7.05	6.99
	260	390	--	87	41	18	18
314	10.01	9.72	9.27	9.10	8.92	8.64	8.52
	97	74	38	22	12	5.9	3.7
316	9.27	8.99	8.44	8.00	7.89	7.56	7.34
	92	63	30	21	9.2	--	2.8
317	10.14	9.46	8.66	8.20	7.80	7.34	7.06
	59	35	17	11	6.2	3.0	2.0
318	12.83	11.55	10.17	9.22	8.67	7.94	7.50
	30	19	10	6.6	3.8	1.8	1.2
319	7.29	7.24	7.04	6.94	6.89	6.78	6.78
	220	210	94	53	29	13	14
320	6.54	6.54	6.60	6.43	6.43	6.37	6.32
	250	350	--	88	43	22	38

Sample	1	2	5	10	20	50	100
321	6.13	6.07	5.96	5.96	5.91	5.85	5.85
	270	380	200	95	52	26	--
322	9.50	9.44	9.27	9.16	9.16	9.04	8.98
	190	200	110	53	27	12	9.2
323	8.73	8.99	8.78	8.73	8.67	8.57	8.46
	200	210	100	55	28	13	10
324	8.42	8.31	8.15	8.09	7.98	7.93	7.81
	190	200	96	60	29	17	9.6
325	5.74	5.68	5.50	5.50	5.44	5.38	5.32
	190	230	120	75	41	21	7.2
326	6.73	6.61	6.39	6.28	6.11	5.94	5.88
	150	130	58	35	19	10	6.3
328	7.11	7.16	7.00	6.95	6.95	6.84	6.79
	260	340	150	79	40	20	20
329	6.13	6.13	6.02	--	6.02	5.96	5.91
	280	430	200	--	61	31	39
331	8.13	8.02	7.85	7.85	7.80	7.69	7.63
	180	190	100	67	36	19	19
334	12.05	11.90	11.54	11.44	11.24	11.03	10.93
	140	80	36	20	9.0	4.0	2.2
335	12.23	11.90	11.36	10.93	10.76	10.49	10.33
	100	62	29	21	9.1	3.9	2.3
338	11.55	10.13	9.61	9.40	9.14	8.77	8.61
	69	93	46	26	13	4.9	2.4
339	10.41	10.35	10.14	9.97	9.86	9.48	9.32
	320	160	62	31	13	4.8	2.6
340	10.54	10.43	10.16	9.83	9.89	9.56	9.40
	280	140	59	47	13	5.0	3.2
341	6.63	6.57	6.40	6.35	6.35	6.24	6.18
	230	270	140	74	40	19	19
343	4.54	4.64	4.93	4.71	4.66	4.61	4.61
	270	390	120	120	53	23	40
344	6.24	6.24	6.07	6.02	6.02	5.96	5.90
	640	400	170	100	57	22	39

Sample	1	2	5	10	20	50	100
345	4.98	4.92	4.81	4.81	4.81	4.75	4.70
	290	470	250	130	67	30	75
347	8.62	7.86	7.04	6.45	6.28	5.86	5.69
	52	34	19	13	7.3	3.7	2.6
348	9.75	9.12	8.37	7.80	7.68	7.28	7.10
	65	38	21	15	7.8	4.2	2.6
350	4.96	4.91	4.80	4.75	4.75	4.64	4.64
	210	250	140	83	46	27	20
353	8.04	8.04	8.04	7.83	7.78	7.72	7.67
	260	320	--	86	45	20	20
357	8.42	8.31	8.14	8.09	7.98	7.93	7.82
	160	160	91	59	30	16	13
358	7.12	7.12	7.18	6.96	6.96	6.90	6.85
	280	460	--	120	61	39	78
359	7.62	7.57	7.51	7.45	7.51	7.39	7.39
	280	460	210	140	58	30	37
361	7.58	7.58	7.64	7.41	7.41	7.29	7.24
	250	340	--	92	42	21	37
362	8.02	8.02	7.86	7.92	7.86	7.81	7.76
	280	550	200	120	59	23	40
363	9.69	9.63	9.46	9.34	9.28	9.11	8.99
	210	220	91	49	22	7.3	4.5
364	9.56	9.51	9.30	9.25	9.19	9.04	8.88
	220	230	95	46	22	8.5	4.5
365	10.50	10.40	10.19	9.82	9.82	9.40	9.14
	290	150	56	--	11	3.7	1.9
367	8.30	8.24	8.14	8.14	8.09	8.03	7.98
	270	360	160	94	46	18	13
370	10.11	10.05	9.87	9.87	9.81	9.75	9.63
	210	250	120	70	36	16	35
371	9.14	9.09	8.91	8.91	8.85	8.74	8.74
	220	280	130	73	40	21	18
373	9.88	9.77	9.55	9.45	9.34	9.12	8.91
	210	200	75	36	15	5.6	3.0

Sample	1	2	5	10	20	50	100
3.74	9.33	9.28	9.06	8.95	8.84	8.63	8.46
	200	200	74	39	17	6.5	3.6
375	8.67	8.61	8.43	8.31	8.19	8.01	7.83
	200	210	79	38	18	6.8	3.5
376	8.12	8.12	7.91	7.85	7.80	7.58	7.42
	230	240	98	45	20	6.8	36

*Dielectric constant, ϵ/ϵ_o, as dimensionless ratio

** Resistivity, ρ, x 10^6 ohm-meters

Table 8. Resistivities measured wet

1. Black Rock Desert samples

Sample	$\rho_{1\ kHz}$	$\rho_{10\ kHz}$	$\rho_{100\ kHz}$
300	21	21	20
307	16	16	16
317	110	105	101
324	121	123	128
328	187	176	168
335	87	83	79
341	30	28	27
350	22	21	20
358	128	127	125
361	50	46	44
367	67	65	64
374	89	90	92

(Samples with resistivities too high to measure: 303, 320, 326, 339, 364, 370).

2. Atlanta samples

208	65	56	51
210	23	23	22
211	24	23	24
212	4	4	4
214	24	23	22
215	17	17	16
218	5	5	5
221	19	19	19
233	10	9	8
234	183	152	128
244	-	-	202

(Samples with resistivities too high to measure: 219, 226, 229, 235, 244).

3. Washington samples

101	21	21	21
105	12	11	11
108	230	221	210
111	203	198	193
119	234	232	223
135	69	66	64
142	201	199	212
143	5	5	5
144	133	131	131
150	124	122	117
152	53	51	49
154	124	116	108

(Samples with resistivities too high to measure: 112 and 127).

Table 9. Results of mechanical tests

Specimen Identification	Diameter (inches)	Length (inches)	Unconfined Compressive Strength	Young's Modulus 10^6 psi
W101	.75	1.484	7,120	.564
W103	.75	1.468	6,320	1.64
W110	.75	1.531	7,260	2.46
W111	.75	1.453	16,690	4.97
W112	.75	1.5	16,750	3.82
W113	.75	1.515	22,660	8.47
W115	.75	1.531	16,790	3.45
W122	.75	1.562	10,580	2.84
W124	.75	1.453	12,290	2.20
W125	.75	1.531	7,600	1.43
W130	.75	1.578	22,880	5.72
W134	.734	1.578	12,270	3.44
W144	.75	1.609	15,180	3.49
W150	.734	1.546	19,140	5.23
A240	.64	1.39	19,710	5.08
A237	.625	1.359	16,460	3.92
A222	.625	1.281	18,470	3.36
A207	.625	1.359	22,380	4.78
A206	.625	1.343	16,270	2.70
A243	.625	1.359	17,510	3.68
A228	.625	1.375	29,990	6.41
A224	.625	1.375	21,260	4.83
337	.625	1.375	31,970	9.38

Specimen Identification	Diameter (inches)	Length (inches)	Unconfined Compressive Strength	Young's Modulus 10^6 psi
323	.625	1.39	45,530	1.03
A225	.625	1.375	9,330	1.6
A218	.625	1.359	9,080	1.48
A203	.625	1.328	19,170	3.48
A201	.625	1.375	13,100	2.55
A246	.625	1.354	17,110	4.09
A242	.64	1.375	12,720	2.86
A252	.625	1.375	17,300	3.60
A251	.625	1.359	12,540	2.13
A236	.625	1.39	16,630	4.51
A235	.625	1.328	9,290	2.82
A227	.625	1.281	6,050	1.07
356	.625	1.375	41,320	4.64
325	.625	1.312	73,760	6.85
B310	.625	1.375	25,540	4.46
B307	.625	1.39	23,100	4.18
A211	.625	1.39	12,370	1.40
332	.625	1.406	45,720	7.34
371	.625	1.39	30,350	8.22
340	.625	1.328	52,780	9.06
B315	.625	1.359	41,800	8.04
B318	.625	1.39	19,040	3.22
359	.625	1.39	36,850	4.34
A219	.625	1.375	22,540	5.79
A202	.625	1.359	21,660	4.78
A200	.625	1.375	23,070	5.04

Specimen Identification	Diameter (inches)	Length (inches)	Unconfined Compressive Strength	Young's Modulus 10^6 psi
W127	.75	1.593	5,770	2.52
B300	.625	1.39	60,600	13.61
366	.75	1.609	51,760	15.25
329	.75	1.656	13,970	1.21
W155	.75	1.5	12,540	4.61
W141	.765	1.468	7,500	1.34
W132	.734	1.468	14,890	3.55
W121	.75	1.468	3,160	.85
W108	.75	1.5	32,140	12.25
W106B	.75	1.5	13,350	2.79
W106A	.734	1.546	18,210	6.06
W104	.734	1.468	16,730	5.02
B316	.625	1.375	35,660	3.60

APPENDIX L

TRANSVERSE-DIPOLE BOREHOLE ANTENNAS
A
CRITICAL LABORATORY EXPERIMENT

TABLE OF CONTENTS

BACKGROUND STATEMENT

After the Task A report was published, it became important to investigate the capability of radar antennas to resolve the location of anomalies in planes normal to the borehole.

To this end, Dr. John C. Cook, ENSCO consultant, and ground-probing radar pioneer, performed a study on various antenna configurations. The results of this work are included in this appendix.

TRANSVERSE-DIPOLE BOREHOLE ANTENNAS

ABSTRACT

Short-pulse, meter-wavelength radar has frequently been proposed for electromagnetic exploration of the rock mass surrounding a borehole. In reasonably radar-transparent rock, such radar should be capable of detecting caverns, faults and other anomalous ground conditions, and of giving their positions along the borehole and their distances from it. It would be highly desirable for the radar to show also in what direction from the borehole the anomaly is located.

Dr. John C. Cook has explored this possibility by employing a transverse-dipole type of antenna, which may have a radiation pattern containing nulls (directions of zero sensitivity) in the plane transverse to the borehole. If such an antenna were rotated so that a null zone embraced the anomaly, its reflected signal should vanish. This would provide the needed localization. The work was performed to test the general feasibility of such a technique.

For speed, convenience and least cost, these experiments have all been performed in air rather than in rock; it is likely that the results obtained in air are applicable to any other isotropic medium of propagation, providing the rules of electromagnetic modeling are kept in mind. In general, the antenna dimensions, or operating frequency, must be reduced by the factor $\sqrt{n}$ when an antenna operating in a medium having magnetic and dielectric constants ($\mu\varepsilon$) is immersed instead in a medium of constants $\mu'\varepsilon'=n(\mu\varepsilon)$.

All of the tests have been made with magnetic dipoles (loops) as receiving antennas, because these are readily made with the plane of polarization in line with the borehole. This in turn is compatible with the electric-dipole type of borehole antenna already developed for transmitting.

The transverse magnetic-dipole antenna must simultaneously fulfill three requirements:

1. Directivity in the plane transverse to the borehole, with at least one null.

2. Reasonable efficiency. This in turn means as large an area as is permitted by the wavelength, and a fair impedance match to the 50-ohm transmission line and receiving equipment.

3. Broad-bandedness of one or more octaves, to receive short rf ("monocycle") pulses without excessive distortion.

The objectives have all been achieved, as detailed in the following:

1. A magnetic dipole antenna has been found which is capable of being used in a four-inch diameter borehole, which receives 100 to 200 MHz "monocycle" radar pulses without serious distortion at acceptable sensitivity, and has broadside "null" zones of at least 20 dB lower sensitivity than the edgewise maximum zones. Other borehole loop designs also shown promising directivity and higher sensitivity.

2. The width of the null zones of this same antenna is of the order of 10 degrees. The direction of a "point" source or specular reflector could be determined to within 5 degrees, or better.

3. The 180° ambiguity expected seldom occurs in practice. One radiation lobe is generally stronger than the other. Some antennas have only one maximum and one minimum.

This work has been confined to the exploration of feasibilities. Directional borehole antennas are almost certainly possible. Practical engineering designs for such antennas will require additional development work.

TRANSVERSE-DIPOLE BOREHOLE ANTENNAS

by

Dr. John C. Cook

Background:

Short-pulse, meter-wavelength radar has frequently been proposed for electromagnetic exploration of the rock mass surrounding a borehole. In reasonably radar-transparent rock[1], such radar should be capable of detecting caverns, faults and other anomalous ground conditions, and of giving their positions along the borehole and their distances from it. It would be highly desirable for the radar to show also in what direction from the borehole the anomaly is located.

The writer recently proposed to Ensco, Inc. that this might be done by employing a transverse-dipole type of antenna, which may have a radiation pattern containing nulls (directions of zero sensitivity) in the plane transverse to the borehole. If such an antenna were rotated so that a null zone embraced the anomaly, its reflected signal should vanish. This would provide the needed localization. The work reported here was performed to test the general feasibility of such a technique.

For speed, convenience and least cost, these experiments have all been performed in air rather than in rock; it is likely that the results obtained in air are applicable to any other isotropic medium of propagation, providing the rules of electromagnetic modeling[2] are kept in mind. In general the antenna dimensions, or operating frequency must be reduced by the factor $\sqrt{n}$ when an antenna operating in a medium having magnetic and dielectric constants $(\mu\epsilon)$ is immersed instead in a medium of constants $\mu'\epsilon' = n(\mu\epsilon)$.

All of the tests have been made with magnetic dipoles (loops) as receiving antennas, because these are readily made with the plane of polarization in line with the borehole. This in turn is compatible with the electric-dipole type of borehole antenna already developed for transmitting.

The transverse magnetic-dipole antenna must simultaneously fulfill three requirements:

1. Directivity in the plane transverse to the borehole, with at least one null.
2. Reasonable efficiency. This in turn means as large an area as is permitted by the wavelength, and a fair impedance match to the 50-ohm transmission line and receiving equipment.
3. Broad-bandedness of one or more octaves, to receive short rf ("monocycle") pulses without excessive distortion.

---

1. References are listed at the end of this report.

Experimental Arrangements:

The basic tests employed the arrangement shown in Figure 1. To avoid the complications of reflected signals, a one-way transmission path was used. To avoid multipath effects and reflections from the ground and surrounding objects, only the first-arriving cycle of the received pulse train was used. See Figure 2. The remainder, or "coda", was ignored; a portion of the coda arose from multipath effects, but most of it was generated in the Terradar type A-T transmitting antenna, which was designed to radiate into rock and was subject to mismatch reverberation when operated in air. Representative tests were performed in an outdoor area well-separated from reflecting obstructions. However, it was found that indoor tests employing only the first-arrival were usually valid. Unfavorable weather and the greater convenience of indoor tests have led to most of them being done indoors.

Since the transmitted waveform contained mainly frequencies in the range from 70 to 300 MHz, tests were confined to this range.

Theory and Results:

A. The "small"magnetic dipole:

Magnetic loop antennas that are "small" compared to the wavelength (the radius under $\lambda/6$, for example) have been used for direction-finding in the broadcast and long-wave frequencies for many years. The signal voltage V from such a loop is given by standard texts[3] as follows:

$$V = \frac{2\pi}{\lambda} NAE \cos\theta$$

Here N is the number of turns and A the area of the loop, E the impinging electric field parallel to the plane of the loop, and θ the angle between the plane of the loop and the direction of propagation of the impinging radiation. The sensitivity pattern (radiation pattern) of a small loop is a torus (doughnut) oriented the same as the loop. See Figure 3a. This was the type of pattern assumed at the beginning of the study. Early experiments with simple loops of 7.5 cm radius showed that there was no null zone on the axis, as had been expected, for 100 MHz short-pulse vertically-polarized radiation.

It is well-known[4] that a small loop in combination with an electric dipole can yield a cardioid radiation pattern similar to that shown in Figure 3b. Such a pattern would be ideal for our purposes. The actual patterns obtained, with representative front/back ratios of the order of 5/4, were believed to be caused by this effect with improper phasing. Efforts were made to eliminate the supposed electric dipole by balancing the loop via an air-cored balun feed transformer, and by Faraday-shielding the loop. For the latter purpose, the loop was formed from coaxial cable, with a shield gap opposite the feed point (balun). These efforts did not improve the radiation pattern.

At the same time, efforts were made to improve loop efficiency by tuning. It had been noticed that many loops produced weak 400 MHz signals, primarily. See Figure 2, top. The feed point of each antenna (generally a BNC connector on which

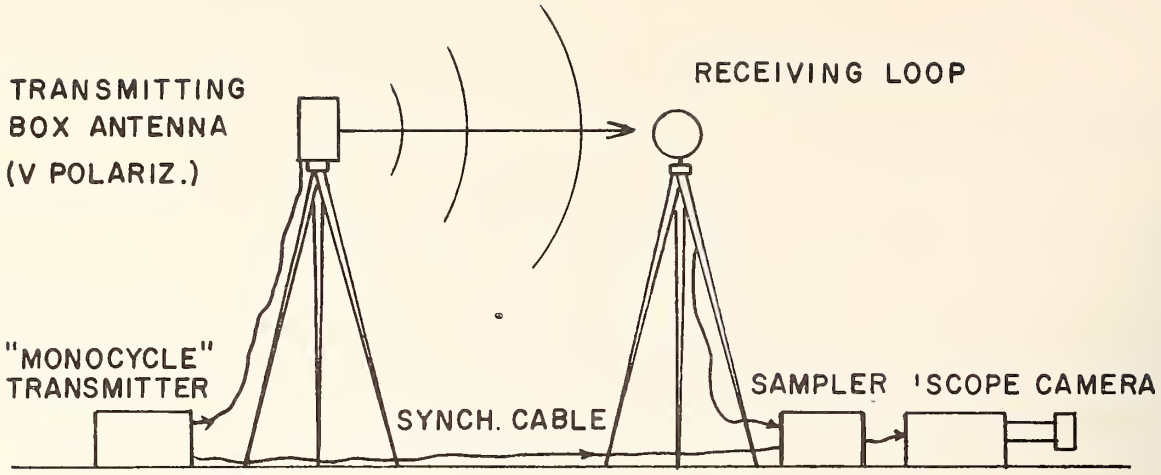

Figure 1. General test arrangement: air medium, spacing > ½ wavelength.

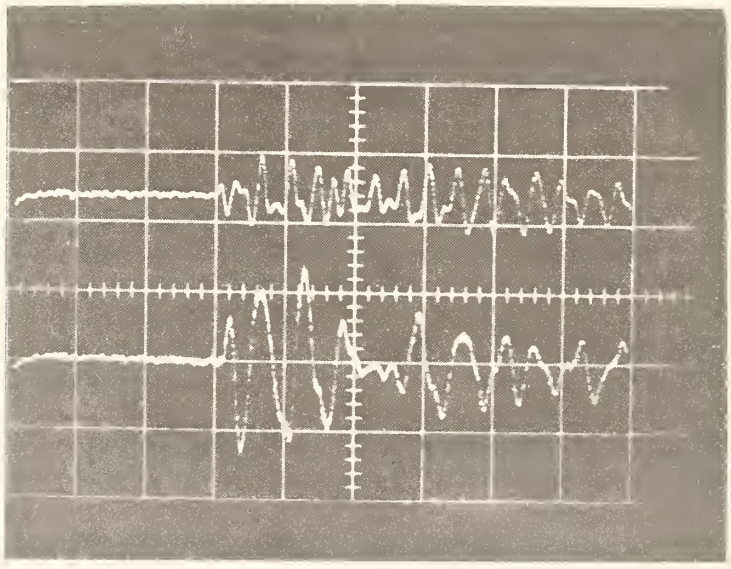

Figure 2. Typical received waveforms. Top: using 8 cm. radius shielded loop; Bottom: using A-R box antenna standard. Scales: vertical 1 volt/cm, horzontal 10 nsec/cm.

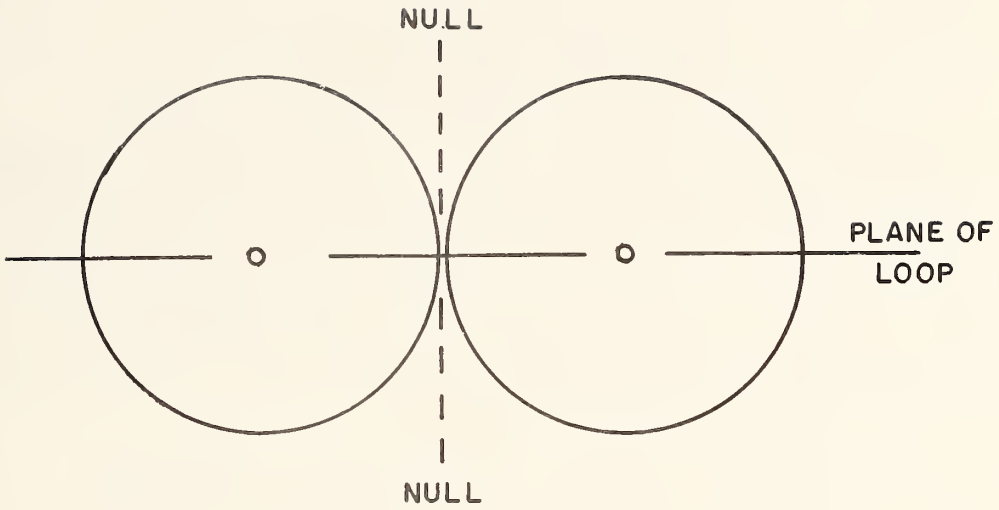

Figure 3a. Expected radiation (sensitivity) pattern for small loops. (in the plane containing the loop axis.)

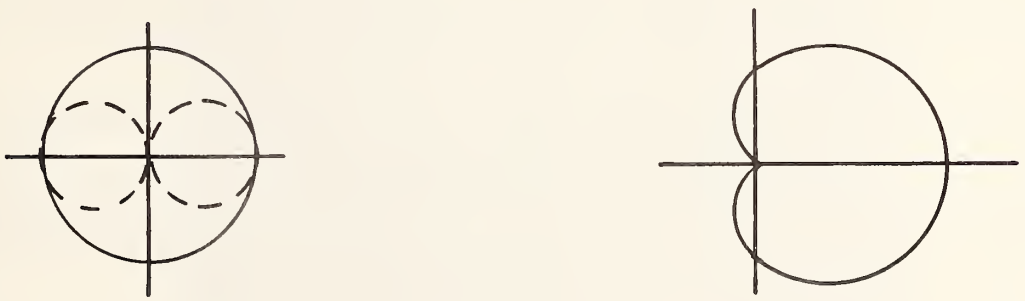

Figure 3b. Small-loop and dipole radiation patterns in plane of loop. Left: loop patterns (solid) and coplanar electric dipole pattern (dashed). Right: pattern for both combined.

(From Jasik[4])

the balanced 2-turn secondary of the balun was mounted) was connected to a Hewlett-Packard type 4815A, RF impedance bridge, which was tuned for an indicated impedance maximum in conjunction with a phase angle of zero (the antenna was then niether inductive nor capacitive). It was found that loops of 7.5 to 15 cm radius could be resonated at about 100 MHz by cutting the top of the loop and inserting a 3 to 5 pfd. capacitor in series. Some broad-banding could be accomplished by shunting the capacitor with 3000 to 30,000 ohms. A typical impedance curve is shown in Figure 4. The 11x35 cm rectangular antenna producing this curve had the best radiation pattern of about six "electrically small" antennas that were tested. Figure 5 shows the broadside (top) and edgewise (center) waveforms produced. There is a 2:1 ratio of amplitudes in the first-arriving (directly-propagated) cycle. The predominant frequency is 210 MHz. Figure 6 shows a partial radiation-pattern plot for the second peak (the first downward peak) of Figure 5. This pattern was made by turning the loop about a vertical axis in 15-degree increments as shown on a cardboard protractor, and manually displacing the oscilloscope spot to the right for each camera exposure, with the spot "frozen in time" on the downward peak by means of the manual sweep knob on the type 1S1 Tektronix sampler unit. It can be seen that this antenna shows no sign of a sharp pattern null.

B. Ferrite Cored Loops:

The use of ferrite cores to improve loop efficiency had been considered from the beginning of the work. Bars of seven types of ferrite already on hand were tested for suitability by measuring their r.f. loss at 100 MHz. Each was inserted into a small 1-turn coil mounted on the impedance bridge, and the departure of the phase angle from 90° (pure inductance) was noted. Two types were found very lossy. Two were found to have negligible permeability (they affected the impedance very little). Three were found reasonably good. The best, a rod 18 cm long and 2.4 cm in diameter, was wound with a double, balanced, 3-3 turn winding mounted on a BNC connector, and was shielded with a Faraday cage. Figure 5 (bottom) shows the signal pattern received by it, which is not a desirable one, since it was not properly tuned. It exhibited no noticeable directionality in its sensitivity pattern.

The rod-type core used in this test was the ideal shape, which could not be used in a borehole antenna unless it were very short, because it should be transverse to the axis of the hole to provide assymmetry in the plane normal to the hole. Generally, we would expect that a large rod core will be constrained to be parallel to the hole, and a rectangular coil would be wound on it end-over-end.

The effectiveness of the core with such unfavorable geometry should not be great. Wait[5] has derived curves for the low-frequency case which bear out this expectation. A spheroidal core wound with a lengthwise (elliptical) coil, three times as long as it is wide, will give an improvement in signal voltage of only x2, for any core material with a permeability greater than 10.

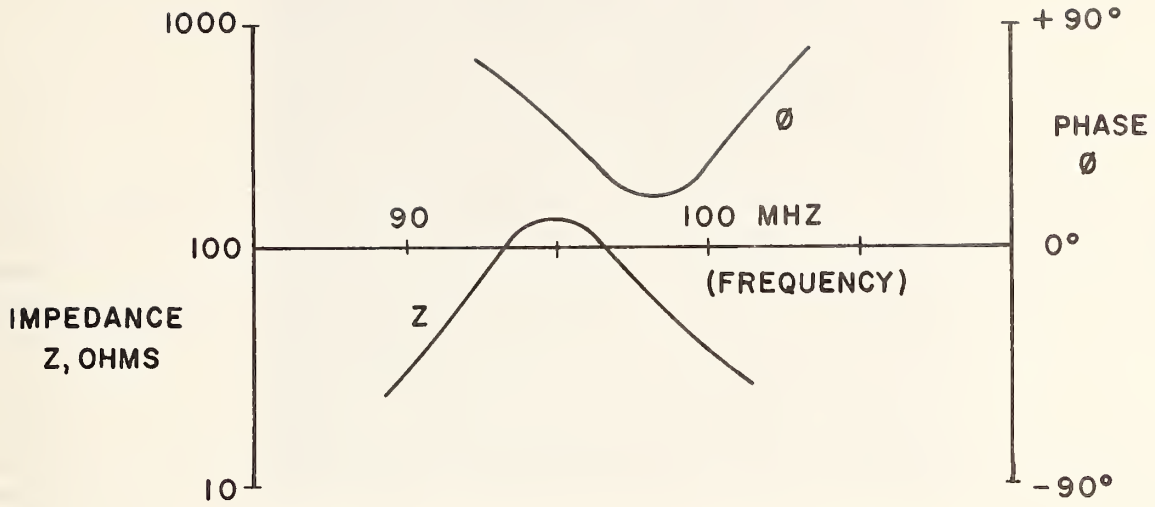

Figure 4. Impedance vs. frequency for a damped, capacitor - tuned, rectangular open loop 4 in. x 14 in.

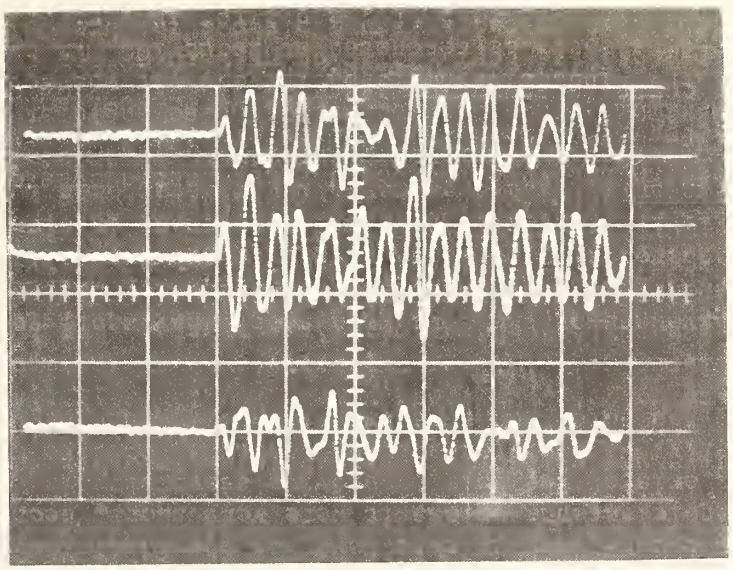

Figure 5. Oscillograms showing first-arriving cycle.
Top: 4 x 14 in. loop, broadside. Middle: same, edgewise.
Bottom: 1 x 7 in. ferrite rod with 4 turns, end to xmtr.
Scales: Vertical 1 volt/ cm, horizontal 10 nsec./ cm.

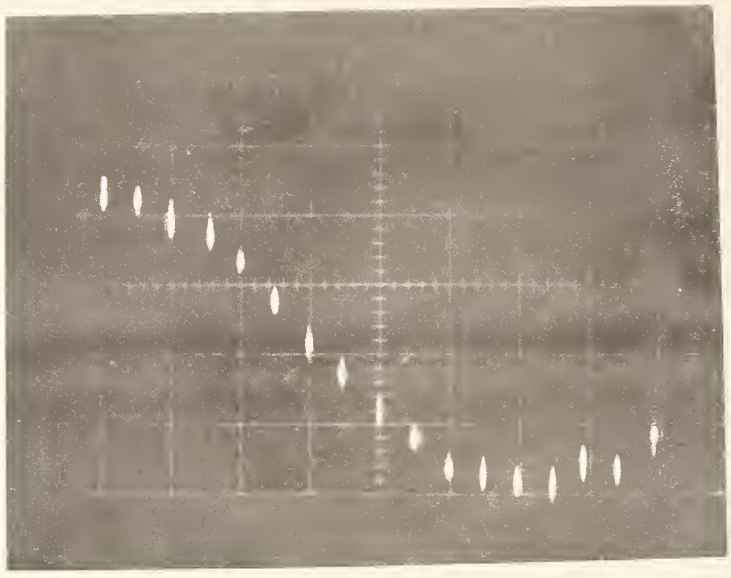

Figure 6. Partial radiation pattern plot, 4 x 14 in. loop; first neg. peak. From-15° (left) to+225° in 15° increments. 0° is in-line. Verticle scale: 0.2 volt/ cm.

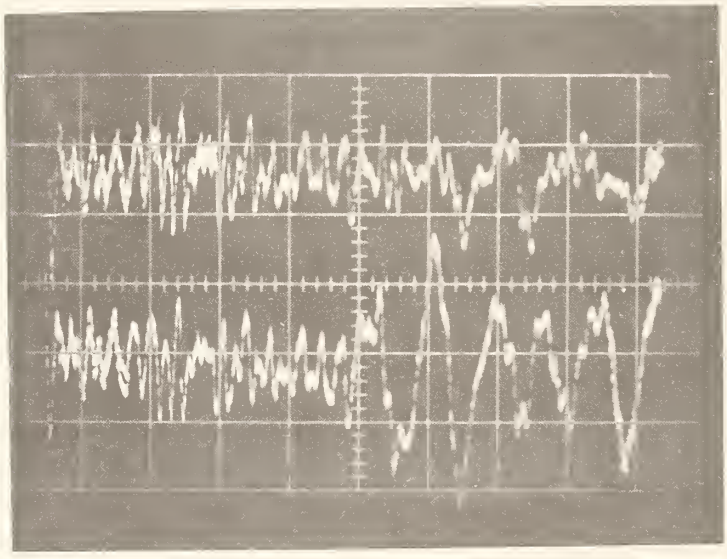

Figure 7. Oscillograms for most directive loop: 0.08 λ perimeter, shielded, balanced, showing first - arriving cycle. Top: broadside, bottom: edgewise to xmtr. Scales: vert. 0.1 v/cm, hor. 5 nec/cm.

A catalog search produced two makers of high-frequency ferrites. One estimated a price of over $1000 for a test core. The other gave a modest price, but could not deliver within the work period allocated to this research. Typical permeabilities at 100 MHz were 5 to 10. In view of the small signal gain expected from a core (unless it could be made small enough to be used transverse to the borehole), further consideration of ferrite-cored antennas was deferred.

C. Loop Directionality at UHF

The research described up to now had given no clue as to the reasons for the observed lack of directionality in the several experimental antennas tested. Something more fundamental than tuning, broadbanding, balancing or shielding was evidently involved. Hence a literature study was performed, starting with the meager references listed in a recent antenna textbook[3]. It was found that loop antenna research at UHF was begun by radio amateurs in the 1930's, and that most publications were made in the 1940's as the broadcasting industry moved into F-M and television. In the UHF region, even single-turn loops were found to behave peculiarly because of variations of the current amplitude and phase along the loop. The existence of nulls in the radiation pattern evidently requires considerable symmetry in the antenna geometry and current distribution.

Most of the seven mathematical papers on UHF loops that were reviewed are flawed by oversimplified assumptions about current distribution and phase. Most writers were chiefly concerned with obtaining a uniform radiation pattern in the plane of the loop, for broadcasting purposes. There are, however, a few calculations showing nulls in the radiation patterns, and some mention of square and rectangular loops. On the basis of published designs, some special rectangular loops were built, mainly of aluminum foil strips, and tested:

1. Twin parallel loops one foot square and three inches apart, coupled at a loading capacitor opposite the feed point, after the design of Marchand[6].

2. An elongated version of (1), one-half wavelength in loop perimeter, on the surface of a four-inch by two-foot cardboard cylinder.

3. A one-wavelength-perimeter simple coil as recommended by Sherman[7], shaped to fit the surface of a three-inch by five-foot cardboard cylinder.

4. The twin-feed, split symmetric loop design of Alford and Kandoian[8], deformed to fit on the surface of a two-inch diameter, 22 inch long cylinder.

5. A half-wavelength loop inductively loaded opposite the feed point, as suggested by Williams[9], distorted into a rectangle 3 x 32 inches, fed at the center of one long side.

All of these large loops provided good signal voltages at reasonably low frequencies, but did not initially provide the hoped-for radiation pattern nulls.

The paper by Williams[9] provides the clearest summary of UHF loop properties:

1. "Electrically small" loops must have a perimeter not exceeding 0.08 wavelength.

2. Loops with perimeters between 0.08 and 0.25 wavelength have all current segments in phase, but current distribution depends upon loop size and shape.

3. Loops with perimeters exceeding 0.25 λ have complicated current distributions and phase relations that depend upon loop size, shape, and conductor size. Such loops "radiate in all directions". Many such loops have front/back assymmetry ratios up to 1.3, which can be increased by inductive front loading.

Williams' statements regarding type (3) UHF loops certainly agree with the present experiments.

D. First Successes

To test the validity of his 0.08λ perimeter limit for "simple" type 1 loops, a shielded, balanced loop of 4 cm radius was made and tested. It exhibited broadside "nulls" where signal amplitude was less than 1/8 that in the edgewise orientation. Figure 7 shows these two signals. Weakness of the signal relative to coherent system noise, as a result of the small loop area, made accurate measurements in the null impossible. However, the presence of broadside nulls for even a short-pulse UHF signal for a sufficiently small loop has been verified.

In an attempt to obtain a "small" loop of greater sensitivity, two small ferrite-cored coils were tuned to about 100 MHz on the RF bridge by removing turns. It was intended that these cores would be used transverse to the borehole to give the needed directionality. Some characteristics are as follows.

A. Ferrite bar 1" diameter, 7" long. Four-turn split, balanced winding resonated at 54.5 MHz (1320 ohms). Two-turn split, balanced winding resonated at estimated frequency of 117 MHz.

B. Ferrite bar 7/16" x 1/2" x 2". Four turns of #14 solid wire resonated at 41.3 MHz, three turns resonated at 56 MHz, two at 86 MHz, and one turn at 115 MHz (estimated), under 100 ohms.

Both showed some directivity in one-way pulse propagation tests both indoors and outdoors. Table 1 summarizes measured peak-to-peak amplitudes of the first-arriving r.f. cycle for several antennas.

Table 1. Antenna Performance Comparisons

Antenna	Indoors, 1.5 m spacing max. sig.	Indoors, 1.5 m spacing min. sig.	Outdoors, 4 m spacing max. sig.	Outdoors, 4 m spacing min. sig.
1. Terradar box	---	---	0.8 v.	---
2. Slim borehole	4. v.	---	1.2 v.	---
3. 1"x7" core, 2 t.	0.35 v.	0.2 v.	0.10 v.	< 0.025 v.
4. 2" core, 2 t.	0.30 v.	0.20 v.	0.10 v.	0.05 v.
2" core, 1 t.	0.22 v.	0.12 v.		
5. 60"x3" λ loop	2. v.	1. v.		
6. 25"x4" folded loop	1.5 v.	1. v.		
7. 35"x3" center-fed, $\lambda/2$ loaded loop	3. v.	1.4 v.		
8. 22"x2" double open-end loop	2.2 v.	1.4 v.		
9. 4 cm. radius shielded loop	0.5 v.	0.05 v.		

For all these antennas, the received first wave had a cycle length between 4 and 8 nanoseconds, which was considered satisfactory. System noise level was 0.05 to 0.10 volt, peak-to-peak.

The improved directivity of the short-core antennas in the outdoor tests demonstrated that the preliminary indoor tests cannot be considered final with respect to directivity. This is no doubt because of secondary radiation from a metal book-case and a metal window frame within one-half wavelength of the transmitting and receiving antennas, respectively. It may be that some of the larger loop designs, which give good signal strengths (half or more those from the electrostatic antennas 1 and 2), will yet prove sufficiently directive for our purpose, although they are considerably distorted from their customary shape, so as to fit in a borehole.

At this point, the pulse tests had to be discontinued, because of more and more frequently-recurring failure in the Tektronix type 1S1 sampler unit. Trouble-shooting and repair by Tektronix promised to be lengthy and expensive. Without it, further tests could not be considered reliable. As it was, the signal levels listed

in Table 2 were noticeably lower than are customarily obtained with the equipment, and the system noise amplitude was 100 times as high as normal; the listed values are useful only for intercomparison.

E. Continuous-wave Tests.

At the suggestion of L.A. Rubin, the pulse tests described above were supplemented with a few C.W. directivity tests of various antennas in the very-far-field of an f.m. broadcast station. The transmitter of WRR-FM is about 10 miles distant (Southwest) over flat terrain, and radiates 100 kW vertically-polarized and 100 kW horizontally-polarized at 101.1 MHz, which is suitable for all the antennas.

An Allied type 2684 four-band, battery-powered receiver was altered by attaching a small capacitor tap-off to the collector of the final I.F. amplifier. The I.F. carrier level at this point was found to be responsive to antenna length and relatively unaffected by the frequency modulation. After fruitless attempts to obtain a d.c. signal by diode rectification of the carrier at the low voltage levels present, a Tektronix type 214 battery-powered miniature oscilloscope was attached at the tap as an a.c. signal indicator. The f.m. whip antenna was disconnected and the f.m. input leads were paired, twisted and brought out to a BNC connector to which the external antennas were connected. Unfortunately, it was found that the input circuit was unbalanced; touching the connector shell or attaching a 5 ft. coaxial cable markedly increased the signal. It is not known whether the I.F. carrier level is proportional to input signal level; since some limiting is frequently designed into all the I.F. stages of a transistorized f.m. receiver, a nonlinear relationship would be suspected. Hence, the equipment used was not the best for antenna comparisons.

Nevertheless, measurements of several antennas were made on an abandoned airport, one-half mile or more from any buildings or other obstructions. The antennas were held about 5 feet high, with the equipment and observer on the ground directly below to minimize reflected fields. Table 2 summarizes the observations.

Table 2 - C.W. Antenna Comparisons

Antenna	max. sig.	min. sig.	Remarks
2. Slim borehole	40 mv.	10 mv.	max. vert.; min. horiz. NW
4. 2" core, 1 t.	50 mv.	50 mv.	no clear null
5. 60"x3" λ loop	80 mv.	20 mv.	odd orientations
6. 25"x4" folded loop	80 mv.	60 mv.	no clear min.
9. 4 cm. radius shielded loop	50 mv.	50 mv.	no min.
10. 26"x3" loop, double loaded	20 mv.	5 mv.	min. broadside

These tests were not clearly successful because of the residual signal from the 5 foot cable sheath and also because of multiple arrival directions of the signal at this distance. Either effect would explain the 10 mv residual signal in the null position for antenna (2), and its incorrect orientation. Time will not permit re-doing the experiment after eliminating these effects.

Nevertheless, promising directivity was indicated for some of the antennas, particularly No. 5 and No. 10, which were adaptations of the designs of Sherman[7] and of Williams[9] to the slim borehole shape. Antenna No. 10 was made similar to the particular design shown in figure 2-85 of the ARRL Handbook (for 1948). The two inductors, calculated to be 360 ohms each at 100 MHz, that is, 0.57 microhenry each had three 2-inch diameter turns of #12 insulated wire. This antenna showed considerable apparent directivity, although its minimum signal direction was not as expected, in common with the other antennas.

CONCLUSIONS

The objectives have all been achieved, as described in the following:

1. A magnetic dipole antenna has been found (Table 1, No. 9) which is capable of being used in a 4-inch diameter borehole, which receives 100 to 200 MHz "monocycle" radar pulses without serious distortion at acceptable sensitivity, and has broadside "null" zones of at least 20 dB lower sensitivity than the edgewise maximum zones. Other borehole loop designs also show promising directivity and higher sensitivity.

2. The width of the null zones of this same antenna is of the order of 10 degrees. The direction of a "point" source or specular reflector could be determined to within 5 degrees, or better.

3. The 180° ambiguity expected seldom occurs in practice. One radiation lobe is generally stronger than the other. Some antennas (No. 10, Table 2) have only one maximum and one minimum.

This work has been confined to the exploration of feasibilities. Directional borehole antennas are almost certainly possible. Practical engineering designs for such antennas will require additional development work.

* * * * *

REFERENCES

1. Cook, J.C., 1975, "Radar Transparencies of Mine and Tunnel Rocks", Geophysics, v. 40, p. 865-885.

2. Jasik, H. (ed.), 1961, Antenna Engineering Handbook, McGraw-Hill, New York, p. 2-51.

3. Ibid., p. 6-2.

4. Ibid., p. 2-8.

5. Wait, J.R., 1953, "Receiving properties of a Wire Loop with Spheroidal Core", Can. Jour. Technol., Jan., p. 9-24.

6. Marchand, N., 1947, "Loop Antennas for F-M Broadcasting", Communications, April, p. 34.

7. Sherman, J.B., 1944, "Circular Loop Antennas at UHF", Proc. IRE, September, p. 534-537.

8. Alford, A. and Kandoian, A.G., 1940, "UHF Loop Antennas", AIEE Trans., v. 59, p. 843-848.

9. Williams, E.M., 1940, "Radiating Characteristics of Short-Wave Loop Aerials", Proc. IRE, October, p. 480-484.

APPENDIX M

SUBSURFACE EXPERIMENTS WITH RADAR

TABLE OF CONTENTS

BACKGROUND STATEMENT

During the conduct of the feasibility study (Task A) of this project, it was painfully obvious that a number of nagging questions could be best answered by a limited objective field experiment. Since such an experiment would have far-reaching significance to the entire subsurface/excavation community, it was decided to seek more general support. Thus, it was that ENSCO proposed, and NSF (RANN) supported by a grant, the study entitled, "Subsurface Site Investigation by Electromagnetic Radar--Phase I, Feasibility."

The final report of this project is available from NTIS at a nominal charge. A short summary is included as this appendix.

SUBSURFACE EXPERIMENTS WITH RADAR

ABSTRACT

This appendix is a summary of a report which covers Phase I (Feasibility of Subsurface Site Investigation by Electromagnetic Radar) of a projected five-phase program to develop new techniques for subsurface investigation by remote sensors in boreholes and tunnels. The objective of the overall program is to determine the benefits of use of advanced computer-based geophysical techniques, as a supplement to other pre-excavation investigation methods. Investigation to date indicates significant promise in that direction.

This project conclusively demonstrated that, with electromagnetic ground-probing radar, geologic structures of interest to subsurface planners will produce detectable signals at ranges greater than 25 feet (7.6 m). It was also shown that it is possible to enhance the interpretation of the information in the raw signals through computer signal processing.

In addition to meeting the expressed goals of the project, there were a number of technical advances made, including: 1) the first application of continuous traversing, long used on the ground surface, to detailed exploration of an underground tunnel surface; 2) the first use of a digital computer and existing seismic software and data-handling methods to enhance and improve radar data; 3) the first extensive radar exploration in metamorphic rock; 4) the first identification and plotting of radar echo signals from gouge-filled joints as thin as a fraction of an inch; and 5) improved techniques for radar operation under high-humidity, dripping-water conditions.

SUBSURFACE EXPERIMENTS WITH RADAR

1. INTRODUCTION

This project addresses an acute need for economical and greatly improved real-time predictive techniques for the investigation, interpretation, and definition of geological conditions prior to subsurface excavation projects. Loss of life, equipment damage, excavation damage, cost overruns, schedule slippages, and unachieved corporate and national goals are the price accompanying the lack of adequate predictive techniques.

A commercially available electromagnetic radar was used plus advanced signal processing techniques to provide geologic information in support of subsurface excavation technology. A crown drift of one of the future stations of the Washington, D.C. Metro system provided the test location. The research identified the degree of success associated with advanced signal processing, analysis, and interpretation, and the appropriate avenues for future research.

2. OBJECTIVE

The major objective of the proposed research was to investigate the utility of electromagnetic (EM) radar as a potentially viable and valuable adjunct to other means of obtaining geological and geophysical data.

3. GOALS

The following goals had to be achieved to accomplish the above stated objectives:

- o Evaluate the operational utility and immediate applicability of electromagnetic (EM) radar for application to subsurface excavation technology.

- o Define developments, requirements, and procedures for enhancement of the utility of electromagnetic radar for subsurface applications.

- o Test the concept and feasibility of the combined use of electromagnetic (EM) radar and digital data enhancement.

- o Provide verifiable design data for subsequent specific applications.

- o Correlate theoretical and laboratory-derived data with verifiable field data from this research.

- o Advance the state of knowledge by investigation of cause-and-effect relationships, and measurements of in-situ velocities of electromagnetic propagation.

4. BACKGROUND

Probing the earth for anomalous geologic conditions with short-pulse UHF electromagnetic radar is a new art. Some development has proceeded intermittently since 1960. This was accomplished through occasional private programs at some half-dozen U. S. institutions, supplemented by a few small government contracts aimed at a variety of different problems. Some of the problems toward which short-pulse UHF radar research has been directed are the following:

1. Measurement of the proximity of salt mine workings to the salt/shale contact at the flanks and roof of a salt dome.

2. Measurement of the thickness of floating ice sheets and glaciers, especially from the air.

3. Detection of clay barriers, abandoned flooded workings, and oil/gas wells in advance of coal mining.

4. Detection of concealed military tunnels and buried land mines at shallow depths in soil.

5. Location of utility lines beneath paving.

6. Delineation of ice and permafrost masses in deep arctic soils.

7. Detection of suspected massive metallic ore-bodies outside of existing mine workings.

8. Measurement of roof coal or gypsum thickness remaining as mining proceeds.

In addition, the use of ground-probing radar to detect geologic hazards in advance of tunneling and heavy excavation has been proposed many times, but has not yet been reduced to practice. The Washington, D.C. Metro experiments are an important step in laying a foundation for this use of the short-pulse UHF radar-probing tool.

5. RESULTS OF FIELD TESTS

The tests conducted under this research, in the crown drift of the Zoological Park Station of the Washington, D. C. Metro system, have shown that even minor hard-rock joints are clearly detectable and traceable to ranges of six to eight feet (2 to 3 m). These tests and the subsequent computer processing of the first data have demonstrated that:

- Major joint intersections can be traced to ranges of 40 to 50 feet (12 to 15 m) in medium-to-hard rock (schist).

- The tunnel for the rail is detectable from the crown drift in one polarization from 25 feet (7.6 m) away.

- Transillumination tests with the transmitter in a rail tunnel and the receiver antenna in the pilot tunnel 25 feet (7.6 m) away proved the capability of EM radar to penetrate hard rock with median transmission characteristics to significant depths.

- Processing of the field data at ENSCO's computer center by special processing software has shown that the signal returns from features of interest can indeed be enhanced, thus making the subsequent geological interpretations more valuable.

- Two major planes intersecting the pilot tunnel were mapped quite accurately.

6. ACCOMPLISHMENTS

The contributions this project has made to subsurface-site investigation technology include: (a) verification of the ability of electromagnetic (EM) radar to penetrate natural subsurface masses, (b) the use of digital-signal processing as a means of enhancing the value of subsurface radar capabilities, (c) multidiscipline-group interpretations of data from optimized analog displays, (d) evidence of resolution power of electromagnetic radar with advanced processing to discern ground discontinuities, and (e) increased user awareness and confidence in utility and viability of ground-probing electromagnetic radar, (f) collection of in-situ data as a basis for future improvements in the radar and applicable processing techniques.

The Metro radar experiments were planned with the participation of Technical Evaluation Group (TEG) members. This group includes: consultants to the government, experts in electromagnetic techniques, and tunneling and heavy excavation experts. The program was directed toward demonstrating the capabilities of ground-probing radar to those best able to foster the needed development work. Thus, it will insure timely application of the tool to important problems in the tunneling and excavation field. It has been apparent for some time that such a demonstration program was essential to the acceptance of this new tool by practical excavation people.

7. SIGNIFICANCE

The significance of the research is that for the first time interpretation of radar returns, transmitted and received in a hard-rock pilot tunnel, combined with advanced computer processing, has resulted in positive detection of the important known subsurface features. This in turn provides great hope for similar results from small boreholes. In some cases, this could provide a cost-effective alternative to pilot tunnels.

Technical advances accomplished under the grant have included the following:

- The first application of continuous traversing, commonly used on the surface of the ground, to detailed exploration of an underground tunnel surface.
- The first use of a digital computer and existing seismic software and data-handling methods to enhance and improve EM radar data.
- The first extensive EM explorations in metamorphic rock.
- The first identification and plotting of EM echo signals from gouge-filled joints as thin as a fraction of an inch.
- Improved techniques for radar operation under high-humidity, dripping-water conditions.
- Collection of needed data upon which to base future improvements.

On the basis of these achievements, it should be clear that this project is an important milestone in the evolution of rock-probing radar from a scientific curiosity into a practical engineering tool. The pioneering already done under this program should now be followed with steps to obtain sufficient additional field experience and to improve equipment to consolidate the progress made. These steps are needed to build a secure technology on the basis of this existing foundation of knowledge.

8. FUTURE PLANS

The next phase of this work will provide for an acoustic probing of the same site along with a higher-power, lower-frequency radar. A borehole radar will be assembled and tested in NX (3-inch [76-mm]) boreholes.

It is anticipated that this effort will further the development of a new family of tools for subsurface investigations and definition of geological conditions in advance of subsurface excavation operations. Because the project utilizes several well-developed disciplines within the present state-of-the-art, the economic payoff could be almost immediate. Data from this project are expected to be of great interest to a wide range of potential users, including both federal and private agencies. It is anticipated that the Technical Evaluation Group of Government and industry representatives would continue to assist the NSF Program Manager and ENSCO in guiding the project and in promoting the concept.

APPENDIX N

COMPARATIVE STUDY OF PROBABILITIES OF SUCCESS OF CANDIDATE SYSTEM DESIGN CONCEPTS

TABLE OF CONTENTS

BACKGROUND STATEMENT

At the conclusion of the preliminary system design, it was obvious that any system which attempted to meet the program requirements as stated would have an excessively high developmental risk.

Individually, the developments and advances of the state-of-the-art needed for the system to function were reasonable. However, the cumulative effect of requiring them all to occur together in a total functioning system was such that there was a very low probability of success.

The modular approach was proposed wherein the prototype system would be designed to meet more modest goals, and would also be designed to grow to meet the full capability required.

This paper was written to define in objective terms a condition which was intuitively obvious, but very difficult to present in concise written form.

COMPARATIVE STUDY OF PROBABILITIES OF SUCCESS OF CANDIDATE SYSTEM DESIGN CONCEPTS

ABSTRACT

A probabilistic approach can be used to help analyze the risks involved in system development. Although the probabilities used are subjective, they are assigned upon the basis of word descriptors. These are objective statements of engineering judgment as to the relative probability of success of various approaches. Although the actual numbers derived have no true relationship to probabilities, their rank and relative values are valid. They provide a sound basis for evaluating alternative approaches and the relative risk associated with respect to each other.

COMPARATIVE STUDY OF PROBABILITIES OF SUCCESS OF CANDIDATE SYSTEM DESIGN CONCEPTS

The developer of an advanced system design is faced with many difficult alternative choices.

If the technological decisions which govern the outcome of the program are too conservative, the eventual tool will be sterile. It will have a capability equivalent to that which would have evolved naturally through privately funded development. Conversely, if these decisions individually push the state-of-the-art, the cumulative result can be a system which has a low probability of achieving rapid field operability. Such a program stands a high risk of cancellation. Even though the eventual tool would be a major step forward, it may never have a chance to prove itself. Since either extreme is unacceptable, the purpose of this section is to present the mathematically simple but powerful laws which govern the outcome of the program based upon the choice of intermediate technological alternatives.

Consider a fairly simple system which requires the resolution of only four independent major technological problems for its success. The probability that the system will be successful is a product of the individual probabilities of success.

$$P_s = \left(P_{s1}\right)\left(P_{s2}\right)\left(P_{s3}\right)\left(P_{s4}\right)$$

where

P_s = Probability of success

P_{s1} --- P_{s4} = The probability of success of each individual problem (known or assumed to be independent of each other)

If the individual probabilities are very high, say .95, the resultant probability of success will be:

$$P_s = (.95)^4 = .81 \text{ (good)}$$

If they are not high but still very good, say .85:

$$P_s = (.85)^4 = .52 \text{ (marginal)}$$

If they are good but not high, say .75:

$$P_s = (.75)^4 = .32 \text{ (very poor, two systems will fail for each one that succeeds)}$$

This illustration represents a very simple system with only four unknowns. However, the margin between program success or failure rests in the ability to predict individual success probabilities of untried approaches to within 25 percentage points of perfection. Even this is a difficult management job. The problem is compounded by the fact that if the risks are kept too low, the resultant system will not advance the state-of-the-art to a sufficient degree.

The answer rests in structuring the program and equipment so that alternative options can be retained. Assume that this same program had available two alternative approaches for each of the four problem areas. If the program retains the ability to exploit either approach in each problem area, then:

$$P_s = (1-P_{f1})(1-P_{f2})(1-P_{f3})(1-P_{f4})$$

where:

$$P_{f1} \begin{cases} = (1-P_{s11})(1-P_{s12}) \\ = \text{The probability of failure of problem area 1} \end{cases}$$

P_{s11} = Probability of success of the first alternative

P_{s12} = Probability of success of the second alternative.

etc.

If we consider the same cases as before and let:

$$P_{s1}=P_{s2}=P_{s3}=P_{s4}=P_{sn}$$

assume that without options:

P_{sn} = .95 and P_s = .81 results in a sterile system, it does not advance the state-of-the-art sufficiently. It will not be considered further.

P_{sn} = .85 and P_s = .52 results in a significant but not spectacular advance in the state-of-the-art, but only marginal probability of success.

P_{sn} = .75 and P_s = .32 results in a major step forward, but with a high probabilty of failure.

By retaining options:

For:

P_{sn} = .85

$P_s = [1-(.15)^2]^4 = .91$ a high probability of success

For:

P_{sn} = .75

$P_s = [1-(.25)^2]^4 = .77$ a reasonably good probability of success.

Thus, the mere ability to retain options throughout the program results in raising a marginal program to a superior

program, or an unsatisfactory program to a fairly safe program.

It should be emphasized that the identification of these options alone is not sufficient. The program must be managed, structured, and the equipment designed in the anticipation of being able to incorporate the alternatives. The system must be modular so that it will be possible to incorporate an option in one area, with, at most, a minor impact on the other problem areas. Otherwise, the probabilities involved are not independent and the advantage of the approach is diluted.

A further advantage of the modular approach rests in the fact that, by keeping the modules thus isolated, there is nothing to prevent incorporating the higher capability, but higher risk approaches as they become available. Conversely, should all else fail, there is nothing to preclude falling back to the lower risk, lower capability approach in any area as a backup. This enables the manager to push closer to the high risk, high payoff areas than prudence would otherwise allow.

PROBABILITY OF SUCCESS OF MODULAR SYSTEM

Unless one has been working with verifiable probabilities in a certain area, a number itself has little intuitive meaning. Word descriptions are more subjective than true probabilities. However, they are more objective than arbitrarily assigned numbers.

The procedure used in this study is to assign partially arbitrary probability numbers to descriptors. Although the magnitudes assigned to these probabilities are uncertain, their ranking is not. This assignment is listed in Table 1 and the rationale of assignment is discussed in the following paragraphs.

Table 1

DESCRIPTOR	ASSOCIATED PROBABILITY
Certain	1.
Almost Certain	.99
Very High	.95
High	.9
Very Good	.85
Good	.8
Fair	.7
Marginal	.5
Poor	.3

It will be noted that the descriptors are ranked in much finer detail in the higher probabilities. This is characteristic of the nature of probability analysis. Actually, nothing is certain and there are probabilities associated with every component. If any function has so obviously low a risk that it doesn't warrant comment, it will be considered a certainty. However, if, even though it is almost certain, if it warrants mention at all it is assigned a value of .99. Any function with a high probability of success should be achievable nine times out of ten, thus, the .95 for very high and .9 for high. Below this, the assignment becomes much more arbitrary. However, any program that had less than a 50% chance of success would be a poor developmental risk.

Approach

The system under consideration has been broken down to nine major areas. These areas are then considered individually from the standpoint of feasible solutions. The probability of success is defined on the basis of descriptors and then converted to numbers for computation. Success probabilities are assigned to all alternatives and the safest (most conservative) approach, as well as the approach which seems to best ensure meeting all system requirements, is then selected for each area. The areas are then combined probabilistically to define the probability of success for three approaches:

- The conservative approach is to package the system with the least technological risk possible. This would be on the assumption that there is no single system today which will accomplish even the basic goals of this system. Thus, even the most rudimentary capability would be a significant step forward.

- The approach implied in the contract requires that the system strive to meet all program goals within realistically achievable individual advances of the state-of-the-art.

- The modular approach defines a system probably slightly more advanced than the conservative system. It incorporates only techniques available within the state-of-the-art, or at most a slight advance. However, it is designed in such a manner as to not preclude the meeting of all requirements by modular additions or changes. It works against carefully designed interfaces. Thus, it is unlike the other two approaches, which are assumed to be truly integrated systems. It retains unique functional capabilities within modules. These are connected at pre-thought-out interfaces which can accommodate alternative approaches by module changes rather than by major system design. In that its assembly is inherently more complex, it pays a probabilistic penalty in the assembly and packaging areas. However, in that it is of modular design, it can exploit the probabilistic gains of having alternatives available in most areas. Thus, it can accept higher individual subsystem development risks without suffering the full probabilistic penalty of these risks.

There are nine major areas evaluated in this study. This is believed to be near optimum. A smaller selection of areas would miss factors of importance and would force lumping statistically independent categories together. A larger selection would require a much more refined and validated probabilistic base of data to really contribute additional information.

The nine areas covered include six equipment and three functional considerations, all of which present isolated uncertainties which must be solved independently from the rest.

- The electromagnetic radar
- The acoustic radar
- The resistivity probe
- The propulsion unit
- The penetrator
- The field data control center
- Variable hole size
- Assembly and packaging
- Data processing

Table 2 presents an evaluation matrix of the results. The extremely low resulting probabilities of success are not truly significant. They are, rather, a result of the wide spread of numbers allocated to the descriptors. Table 2 leads to the following conclusions:

- The geometric mean of the set of probabilities indicates that, where there is a large number of independent uncertainties in a program, the difference between probable success and probable failure of the system rests within a very narrow range of probabilities of success of individual functions or subsystems. There is insufficient data to establish a realistic success estimate within two or three times the spread of these geometric means.

- The modular approach, by being designed to exploit alternatives without major system impact, holds the promise of meeting the full capability of the system presently being designed, at a risk only slightly higher than the most conservative, limited capability approach.

Table 2. Evaluation Matrix.

FUNCTION	CONSERVATIVE	ADVANCED CONCEPT	ALTERNATIVES 1	2	3	4	MODULAR*
EM Radar	.95	.85	.75	.7			.99
Acoustic Radar	.9	.8	.75	.6			.98
Resistivity	.99	.9	.8	--			.98
Propulsion	.99	.9	.7	.6			.98
Penetrator	.99	.85	.7	.6			.97
Field Data Control Center	.95	.9	.7	.7			.99
Variable Hole Size	.95	.6	.5	.5	.5		.95
Assembly and Packaging	.95	.85	N/A				.75
Data Processing	.95	.8	.75	.75	.6	.6	.99
Probability of Success	.68	.17					.61
=Geometric Mean	$\bar{x}$= .96	$\bar{x}$= .87					$\bar{x}$= .95

$$\bar{x} \begin{cases} = \text{Geometric Mean} \\ = (P_s)^{(1/9)} = \left[\Pi_i P_{si}\right]^{1/9} \end{cases}$$

*The numerical values of probabilities assigned here are subjective and might be subject to challenge. More important, however, their ranking for each function can be assigned reasonably objectively, and this ranking is more important than the numerical values (see p. A-4).

APPENDIX O

ECONOMIC ANALYSIS OF FULL-CAPABILITY SYSTEM

TABLE OF CONTENTS

BACKGROUND STATEMENT

The contract required that under Task A (Feasibility Study) an economic analysis was to be prepared covering the sensing techniques and dimensions of the sensing device. This study was prepared and included in the Task A report.

Another contract requirement was to update the economic analysis each time technical alternatives were presented. This appendix represents the final alternative candidate presented which would meet the full-capability requirement.

ECONOMIC ANALYSIS OF FULL-CAPABILITY SYSTEM

ABSTRACT

This appendix provides an updated estimate of the development and operating costs of the proposed system. The system development costs presented encompass all identified costs in the development cycle of the system.

The total development cost of the proposed system, including interest at 10%, will be on the order of $1.9 million. Even at this cost, the system will be cost effective if the system is properly used. The optimum use of the system will probably be in a reconnaissance mode where far more data are taken than ever completely processed. The estimated base operating cost of the system will be on order of $2.50 per foot ($8.20/m) with additional data processing costs as much as $1.51 per foot ($4.95/m).

Data processing costs can be held to a minimum by making efficient use of a quick-look display and making maximum use of the processing capability of the field control center, thus leaving only a small part to be processed on off-site computers.

ECONOMIC ANALYSIS OF THE FULL-CAPABILITY SYSTEM

1. DEVELOPMENT AND OPERATING COSTS

The purpose of this appendix is to provide updated estimates of the development and operating costs of the proposed system. The estimates will be revised and modified as the system performance specifications and design are developed during the next months. However, preliminary cost estimates of the system and subsystems serve to identify relative costs, indicate areas where further analyses are needed, and provide valuable guidelines for selection of the more cost-effective alternatives during system design.

Estimates of the system development costs and its operating costs are presented separately. The procedures and assumptions employed in arriving at the cost estimates for each are discussed.

2. SYSTEM DEVELOPMENT COSTS

The system development costs presented encompass all identified costs in the development cycle of the system. The development cycle is conveniently separated into the following phases:

- Phase I - Feasibility analysis and design;
- Phase II - Prototype fabrication and test;
- Phase III - Field test and evaluation; and
- Phase IV - Fabrication and acceptance testing of an operational model.

The feasibility analysis and design phase is being done under the present contract by ENSCO, Inc. Hence, the associated costs are known to be $250,000. The cost estimates for the remaining phases in the system development cycle are discussed separately.

2.1 PROTOTYPE FABRICATION

The majority of the components and subsystems of the proposed system will be newly-developed items and items which require modifications or repackaging. Hence, in general, hardware does not exist from which the prototype development costs can be obtained directly. Therefore, a large amount of subjective judgment based on past experiences must be used. Where possible, spot checks must be applied to see if costs are reasonable.

The costs for this system were first determined for the Task A Interim Report submitted in July 1975. For this report, two estimators working independently arrived at a cost for development of a prototype. The results of this estimation are shown in Table 1 under Estimator 1 and 2. For a complete discussion of the methods used and the checks performed, see Section 6 of the Task A Report.

In his estimation scheme, Estimator 2 based his cost estimate on the extremes of high and low costs which evolved when various alternate methods were selected. These high and low costs were individually summed and the average of the two taken as the prototype costs. The two independent estimates agreed to within about 10%.

Estimate 3 was performing during March 1976. This estimate is based on new information which was not available at the time of the first two estimates. The experience of the last few months has shown that the high estimates used by Estimator 2 are more nearly correct. Therefore, with three exceptions, these are the estimates used by Estimator 3. The three exceptions were made where specific costs have become available.

The first major exception is the EM Radar Sensor. This cost

Table 1. Independent prototype cost estimates.

FUNCTION	Estimator #1-1975	Estimator #2-1975	Estimator #3-1976
DOWNHOLE PACKAGE	150,000	142,125	282,000
Forward Section			
Penetrator		5,000	7,000
Guidance		3,500	5,000
Power & Controls		3,500	5,000
Internal Telemetry		1,375	2,000
Packaging Forward Section		1,500	2,000
Sensors			
Resistivity		7,500	10,000
EM Radar		35,000	70,000
Acoustic Radar		40,000	120,000
Interface & Packaging		7,500	10,000
Aft Section			
Power Conversion		2,750	5,000
Propulsion		8,500	12,000
Cooling		4,000	7,000
Telemetry and Control		9,500	12,000
Interface and Packaging		12,500	15,000
UMBILICAL	50,000	51,500	63,000
10,000 ft. (3.048 km)		42,500	60,000
Interfaces		9,000	3,000
SURFACE SUPPORT SYSTEM	50,000	40,375	53,500
Logging Truck		20,000	25,000
Drawworks		7,500	10,000
Packaging		6,500	10,000
Power		5,500	7,500
Air Conditioning & Heat		875	1,000

FUNCTION	Estimator #1-1975	Estimator #2-1975	Estimator #3-1976
FDCC	50,000	61,875	175,000
FTO Console		12,500	
Tape Recorder		18,750	
Hard Copy Display		5,000	
Signal Conditioning		2,500	
A/D Conversion		1,250	
D/A Conversion		500	
Status System		3,750	
Downhole Controls		3,750	
Navigational Data		375	
Drawworks		1,000	
Assembly and Packaging		12,500	
DICC	70,000	61,250	76,500
A/D Conversion		1,250	1,500
Software		42,500	50,000
Hardware		17,500	25,000
TOTAL PROTOTYPE	370,000	357,000	650,000
PREVIOUS FUNDING	250,000	250,000	250,000
	620,000	607,000	900,000

was previously estimated at $35,000; the new cost is $70,000. It was anticipated that the state-of-the-art for these devices would be such that only antenna modifications would be necessary to accomplish the goals of the project. However, this has not been the case and in order to meet the goals of the project, major modifications will be necessary. This being the case, the estimate of $70,000 will be more nearly correct.

The second change is in the acoustic device. This was raised from $30,000 to $120,000. The latter price is based on information we have obtained from Southwest Research Institute, who could market such a device.

The final change is in the field data control center. This cost was raised from $50,000 to $175,000. After a study of the potentially immense amounts of data coming from the sensors (see page 12), it was recognized that the best way to get this data into a format suitable for recording was to use a minicomputer processing system. This system would provide the quick-look capability needed to perform on-the-spot analysis and would also exercise the control functions necessary to operate the remote sensor packages. This system would be comparable to those currently being used by the seismic exploration personnel for field processing. There are several of these available today:

- The Command System from Petty-Ray;
- The Phoenix System from Seismograph Service Corporation;
- The CFS system from Texas Instruments, Inc.

The cost of the basic system for each is in the neighborhood of $175,000. In addition to performing the operational control and quick-look functions described above, this system

would also be capable of performing almost all of the in-depth processing desired. This could be accomplished during the time when the borehole probe is not in use. This will enable a large cut in the data processing costs during the operational phase of the system.

The three changes in the cost estimate are significant and would raise the cost from $620,000 to $900,000. However, it is felt that, with the state-of-the-art as it is today, this latter figure is a more realistic one for the first two phases of the contract.

2.2 FIELD TEST AND EVALUATION

Following the development of the prototype system, there is a logical period of field testing and evaluation. This should have two sequential goals:

- The first goal would be to evaluate how well the equipment functions. Up to this point in the program, the system probably will not have been operated inside a borehole. All design and fabrication will probably have been done on the basis of theory and laboratory testing. The functional interplay between subsystems must be evaluated in the actual borehole environment.
- Following proof that the subsystems are functioning correctly, the ability of the overall system to perform its mission should be evaluated. This is the signature acquisition phase. The system should be tested against known targets and classes of targets. Signatures must be identified, codified, and stored. It would also be desirable in this phase to verify the signature by actual drilling into known anomalous areas.

It is assumed that the test and evaluation phase will be about 60% of the original effort of feasibility study and design. (This assumption is based on experience in development of other systems of comparable complexity.) Thus, the test and evaluation costs are estimated to be 0.60 x $250,000 = $150,000.

2.3 OPERATIONAL MODEL COSTS

The prototype system should be converted to an operational model for maximum utilization of the hardware and software developed. This conversion would logically occur after the prototype field test and evaluation. This conversion will almost surely involve physical modification in hardware elements, with attendant costs, as a result of improvements identified during field test and evaluation. Rehabilitation costs to correct wear and damage are also anticipated.

Portions of the operational model costs will also be due to restructuring the software. The original programs will have been written from theoretical considerations and by adapting existing seismological types of programs to an apriori model of the borehole and surrounding environments. The degree of computer processing, the types of processing, and the earlier conceived physical and mathematical models will probably change as a result of the prototype field test and evaluation.

Another cost item is fabrication of a second downhole package identical to the final version of the converted prototype. This is an important consideration. It is assumed that at least once in the life cycle of the system the downhole package will be lost. For example, a hole may collapse to the point that reopening it would be cost prohibitive.

Even without the consideration of loss, the downhole package will be operating in an extremely hostile environment. The availability of a spare unit will allow operations to continue while maintenance is being performed.

The following assumptions are made for purposes of estimating the cost of fabricating an operational model.

- A second down hole package will be required at a presumed cost of 50% of the cost of the first package - $141,000.

- Approximately 25% of the prototype system cost is presumed to be required for redesign and rehabilitation - $150,000
- Major software restructure - $50,000
- 10% inflation allowance - $34,000
- Total cost - $375,000

2.4 TOTAL PROJECTED SYSTEM DEVELOPMENT COSTS

The total development costs estimated above are summarized as:

Phase I - Feasibility Study and Design----------	$250K
Phase II- Prototype Fabrication and Test--------	650K
Phase III-Field Test and Evaluation-------------	150K
Phase IV- Fabrication of Operational Model------	375K
TOTAL ----	$1,425K

These costs will be distributed over a number of years required in the development cycle. During this time, the associated costs may bear interest. In estimating the interest charges, it is assumed that the interest rate will be 10%, compounded annually. The estimated development schedule is shown in Figure 1 with the development phases, their duration and costs identified. In computing the interest charges, it is assumed that the development costs for each are uniformly distributed over that phase and that interest is compounded at the end of each 12-month period.

The development costs will also be distributed over a 20-year period in an analysis that includes operating and system implementation costs to illustrate the potential cost benefits of the system. The 20-year period (twice the expected operational life of one system) is assumed to allow a long period for amortizing development cost.

3. SYSTEM OPERATING COSTS

The operating costs of the proposed system will depend on a number of factors. These include system utilization, direct

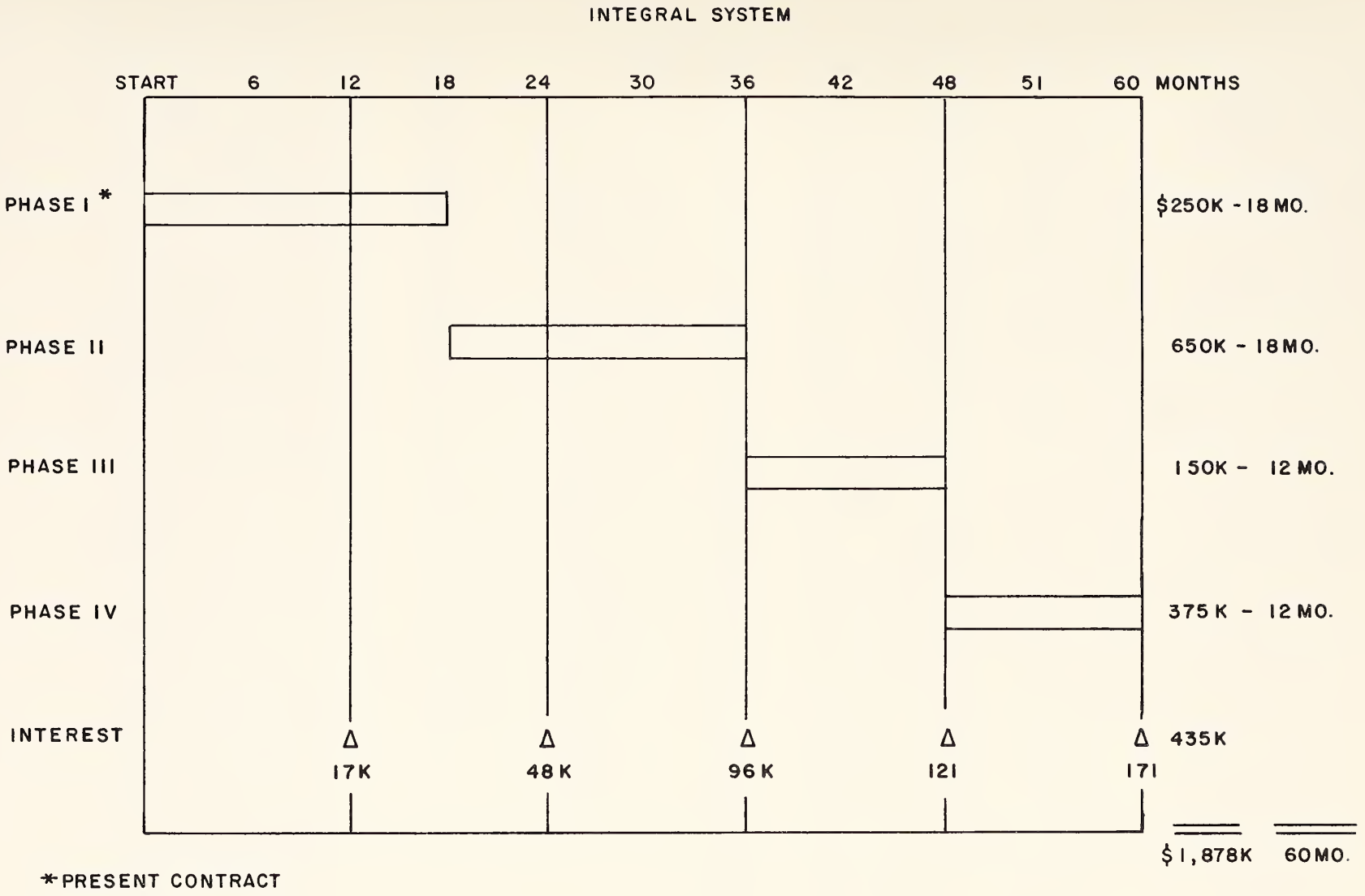

Figure 1. Projected schedule and summary of estimated costs for development of proposed system.

labor requirements, amortization of development costs, system reliability, computer processing, the value of the data to users, and others. There are no operational data for the system from which to extract operating costs. Hence, assumptions as to the operational procedures and system utility are required.

In the following analysis, the operating costs are categorized in terms of 1) amortization of development costs, 2) labor costs for operations and maintenance and 3) data processing. A set of assumptions regarding the operational requirements and procedures are made for each category. Efforts are made to maintain consistency in the assumptions throughout and implications of the assumptions are discussed. The costs are presented in terms of dollars per unit distance of borehole investigated.

3.1 AMORTIZATION OF DEVELOPMENTAL COSTS

In estimating the amortization costs, the following are assumed:

- A 10-year operational life
- A 50% utilization factor
- Three traverses per hole
- An average traverse speed of 10 feet/min (3.05m/min)
- A 40-hour week.

These assumptions lead to a useful operational life of the system of approximately 2 million linear feet (609.6000 km) of hole. Thus, the development costs (excluding interest changes) of approximately $1.5M can be amortized at $.75 per foot ($2.46/m). Higher utilization, extended work days, or more shifts would lower this figure.

3.2 SYSTEM OPERATIONS AND MAINTENANCE COSTS (O&M)

During the collection of data, two shifts of operators should be considered so that the system can be fully utilized. Labor and other costs associated with their support are estimated as:

- 4 operators - 6 hours per day on operations plus 2 hours on support work for 2 48 hour week ---------- = 192 hrs/wk

  At $8 per hour plus 30% average indirect costs ---------- = $2000/wk

  Assuming 2 weeks to complete work for three traversals in a 10000 ft. (3.0480 km) borehole, direct labor would cost $\frac{\$2000 \times 2}{10{,}000 \text{ ft.}}$ ---------- = $0.40/ft. ($1.31/m)

- Housing and subsistence - 4x7x$40/day avg--- = $1120/wk ($0.22/ft.) ($0.72/m)

- Field Engineering Support ---------- = $0.10/ft. ($0.33/m)

- Other operational costs: (Excluding highly variable support costs related to site locations) utilities, communications, security and consummables totaling $500/wk ---------- = $0.10/ft ($.33/m)

- Home office overhead at about 40% of direct labor costs ---------- = $0.16/ft ($.52/m)

The operational model of the system and its components will have a total replacement cost of approximately $250,000. Some components, such as the generator, recorders, and test vehicle, will be highly reliable and will not require excessive maintenance. Other components such as the downhole propulsion unit and interface equipment can be expected to have relatively large maintenance and repair requirements. The labor costs for operators

and other direct costs for their support will continue while the system is down for relatively small repairs and/or replacements. Accordingly, annual maintenance costs are assumed to be 20% of replacement costs. Thus,

- Annual maintenance = $250,000 x 20% = $50,000/yr. This will be averaged over 20 boreholes at 10,000 ft. (3,048 km) each. Hence, annual maintenance in cost per foot are:

  $50,000/200,000 ft.------ = $0.25/ft. ($0.82/m)

Total O&M costs would then total approximately $1.23 per foot ($4.03/m) of borehole.

3.3 DATA PROCESSING COSTS

The term data processing as used here pertains to the nonreal-time in-depth computer processing performed for the analysis and display. The extent of computer processing will depend on the amount of data recorded and the value, or quality, of the data to the users in terms of final results. The value of the data may, in turn, strongly influence the amount of data to be recorded and processed. For example, if a high degree of spatial resolution can be obtained and used to define critical anomalies at the expense of increased data processing, the increased processing costs required to obtain that quality may be fully warranted. In this regard, it may be assumed that the quality, or value, of the data will be a function of the number of data bits per foot that are processed. With this assumption, a data quality factor may be defined on the basis of resolving power or other measures of quality in terms of data bits per foot that are processed, and employed in adjusting the cost per foot of borehole exploration. This is discussed further, but first it is necessary to estimate the amount of data that may be involved in achieving the ultimate in data quality, or system performance. This will represent the maximum amount of data that may be usefully obtained from a borehole by the system.

3.3.1 Estimate of Number of Bits Per Hole for EM and Acoustic

- 2000_4 samples/recorded signal x 10 bits/sample = $2x10^4$ bits/recorded signal
- 4x324 recorded signals/station x 10,000/0.5 stations/borehole = $26x10^6$ recorded signals/borehole.
- Therefore, $2x10^4$ bits/signal x $26x10^6$ signals/borehole = $5.2x10^4$ bits/borehole.

In estimating this limit, the following operational and performance criteria were assumed for both the acoustic and electromagnetic radars.

- A maximum analog bandwidth of one million Hertz is a reasonable goal for a long coaxial cable.
- A circumferential resolving power of 5 degrees, range resolution of 0.5 ft (0.152 m) and longitudinal resolution along the borehole axis of 0.5 ft (0.152 m).
- A circumferential resolution of 90 degrees without data processing. This is a realistic beamwidth for the wavelengths and borehole diameters involved.
- A signal amplitude resolution of 0.1%, or ten binary bits. This is a reasonable upper limit for digitizing the analog data.
- The acoustic and electromagnetic radars perform separate traversals.
- A 100-ft (30.5 m) detection range.
- A 10,000-ft (3.05 km) borehole length.

A five degree circumferential resolving power divides the circle into 72 segments. However, with a 90-degree true beamwidth, the data redundancy required to reduce the effective bandwith to five degrees is about 324 [i.e., improvement is approximately the square of the beamwidth reduction factor, or $(90/5)^2 = 324$].

The maximum number of data bits that would be obtained from the borehole for either the acoustic or electromagnetic radar systems

is thus 9.3×10^{11} bits. It is assumed that the resistivity system would require about 10% of the number of data bits for either of these, or about 0.9×10^{11} bits. This gives an upper limit of about 1.96×10^{12} data bits from the borehole, which represents the system operating at its ultimate capability over the full length of the borehole. It seems very unlikely that the system would be so operated and especially over the full length of the borehole. This is because the amount of time and associated costs would be large and because critical areas requiring such highly detailed examination are not likely to occur over the full extent of the borehole environment. However, the assumed operating and performance criteria and the resultant upper limit of data establishes a useful reference value. In terms of unit distance, this upper limit in data may be expressed as 1.96×10^{12} bits/10,000 ft = 1.96×10^{2} mega-bits/ft. (6.43×10^{2} mega-bits/m). With this limiting value, a data quality factor Q in units of mega-bits/unit distance, where $Q \leq 1.96 \times 10^{2}$ mega-bits/ft (6.43×10^{2} mega-bits/m) may be defined. The cost of data processing can then conveniently be related to the data quality if the cost of processing is known in terms of cost per data bit.

The cost of in-depth computer processing of the data, based on previous experience in computer processing of acoustical data, is estimated to be $2.50/mega-bit. This is exclusive of the costs of data acquisition or for realtime processing and display performed in the field to provide a quick-look capability for the operators. The costs associated with data acquisition and quick-look capabilities are included in previous cost estimates.

The cost of in-depth data processing may now be estimated as

$$\text{data processing costs} = (\$2.50/\text{mega-bit})(Q \text{ mega-bit/unit distance})$$

In order to arrive at an estimate for Q and hence the final data processing costs, an operational scenario is developed and discussed.

Assume that during a survey or logging operation, one run is made with each sensor. The runs are made at the logging speed of 10 feet/minute (3 m/min.). A 10,000 ft (3.05 km) hole could be surveyed at the rate of approximately two days per sensor. The data would be recorded and observed by the field operator on the operator display, but not yet subjected to in-depth computer processing. The cost of performing the field operation would be the costs of amortization of the system development (see page 10), O&M costs (see page 11), and a contingency cost of approximately 20% of the amortization and O&M costs. In summary, this gives:

• Amortization of Development Costs	$.75/ft. ($2.46/m)
• O&M Costs	$1.23/ft ($4.03/m)
Subtotal	$1.98/ft. ($6.50/m)
• Contingency (storm damage and delay, retrieval, etc.) at 20%	$.40/ft. ($1.31/m)
Total	$2.38/ft. ($7.80/m)

Hence, it would cost $2.38/ft ($7.80/m) to survey, or log, the borehole and acquire data for later in-depth analysis.

A speed of 10 ft/minute (3m/minute) would require 6 seconds per foot (20.0 sec/m). The system would acquire and store approximately 93 mega-bits/ft (305 mega-bits/m) of data for the run with the acoustic radar and an equal amount for the electromagnetic radar. For the resistivity probe, it is again assumed that only 10% of the amount of data for either the acoustic or electromagnetic radar are required, or 9.3 mega-bits/ft. (30.5 mega-bits/m). Hence, the amount of data acquired from the borehole is 19.6 mega-bits/ft (64.3 mega-bits/m). It is unlikely that all the

data will require in-depth computer processing. It is assumed that the field operator, on the basis of the realtime processing and display identifies areas requiring subsequent in-depth processing which total 5% of the hole length. Hence, the number of data bits to be processed in detail are 9.8 mega-bits/ft, (32.2 mega-bits/m) of borehole. This detailed processing can be performed in two phases. The first part will be done on the field system itself during the off hours. This could account for 95% of the in-depth processing and the cost for this processing with the exception of the personnel is included in the system development costs.

Using the previous figures, assume that two operators work eight hours a day five days a week processing the data from the probe.

- 2 operators - 8 hours, 5 days = 80 hrs/wk, at $8 per hour plus 30% average indirect costs = $850/wk.
- Housing and subsistance 2 x 7 x $40/day = 560/wk.
- Assume 2 weeks to complete work for 10,000 ft. (3.048 km) borehole, direct costs = $\frac{1410x2}{10,000}$ = $0.28/ft ($.93 m)

The off-site processing will be mainly for display and permanent records. This processing is assumed to be 5% of the total. Thus, A is now 5% of 9.8 mega-bits/ft.

• On-site processing	$0.28/ft. ($0.93/m)
• Remote processing = $2.50 x Q or $2.50 x (.49 mega-bits/ft)	= $1.23/ft ($4.02/m)
TOTAL	$1.51/ft. ($4.95/m)

3.4 SUMMARY OF OPERATING COSTS

The total operating costs may be summarized as:

- Amortization of Development Costs ---------- $0.75/ft. ($2.46/m)
- O&M Costs ---------- $1.23/ft ($4.03/m)
- Contingency Costs ---------- $0.40/ft ($1.31/m)
- Data Processing Costs ---------- $1.51/ft. ($4.95/m)

Total----- $3.89/ft. ($12.76/m)

4. POTENTIAL COST BENEFITS

The system development and operating costs estimated above are used in this section in conjunction with estimates of overall tunnel construction costs, to arrive at potential cost benefits of the system.

The system development costs, excluding interest charges, were estimated above to be about $1.5M (see page 8). Based on a $1.5M, 20-year loan at a 10% interest rate, the annual payments for retiring this loan are approximately $176K. Operational and replacement costs must be included to arrive at overall costs of using the system.

The operating costs were estimated as $3.89/ft ($12.76/m). This included runs with the three sensors over the complete 10,000 ft (3.05 km) length of each borehole with in-depth data processing performed for 5% of this length. Amortization of development costs and O&M costs were included. However, amortization of the development costs ($0.75/ft = $2.46/m) was based on a 10-year

life cycle with a total of 2 million feet (610 km) of borehole investigated (see page 10). In amortizing the system development costs over 20 years (or 4 million feet = 1220 km of borehole), the amortizing cost becomes $0.38/ft ($1.23/m). Thus, the operating costs become $3.88/ft - $0.38/ft = $3.50/ft ($11.50/m).

Assuming a ten-year useful life for the system, one replacement will be needed during the 20 years. Replacement cost was estimated above to be $250K (see page 11). Averaged over the 20 year period, this gives $12.5K per year for replacement costs. To summarize:

- Loan for System development (20-year loan, 10% interest)---------- $176K/yr.
- Operating costs (system amortization, O&M, data processing)---------- $718K/yr.
- Replacement costs ---------- $ 13K/yr.

Total --- $907K/yr.

A reasonable estimate of highway tunneling activity appears to be $160M per year the next decade or so. The cost of developing and utilizing the proposed system for the pre-excavation investigations is thus about 0.57% of the total tunneling costs on an annual basis. A significant cost of tunnel construction is attributable to risk factors resulting from lack of knowledge of the subsurface conditions prior to excavation. If the risk factor is assumed to be 10% of the total construction costs, then it would appear that the proposed system would become cost effective if it reduced the risk factor by 6%. It is conceivable that if the system could provide reliable knowledge of only the major subsurface discontinuities along the tunnel route that would preclude unexpected major rock falls and water inflows, that it would

accomplish this degree of risk reduction. The system, of course, is expected to provide much greater capability.

No attempt is made here to estimate the cost benefits further. However, once the system has been proven and gains user acceptance, it should contribute significantly to faster, more efficient, and safer tunnel construction with attendant reduction in construction costs. Also, it is noted that the major cost factor in using the system is the operating costs. It is conceivable that as the system is tested and operated, system improvements will be made with these improvements, and the experience gained in signal processing and analysis, the operating costs can be significantly reduced.

5. CONCLUSIONS

The following conclusions can be drawn from this analysis.

- The total development cost of the proposed system, including interest at 10%, will be in the order of $1.9 million.
- If the system is used effectively, it has the capability of being an extremely cost-effective tool.
- The efficient use of the system will depend upon an interplay and learning process between the geotechnical personnel and the data processing personnel.
- The optimum use of the system will probably be in a reconnaissance mode where far more data are taken than ever completely processed.
- The estimated base operating cost of the system will be in the order of $2.50 per foot ($8.20/m) of borehole, plus data reduction costs.
- Data processing costs will be a major factor in the ultimate operational costs $1.51/ft ($4.95/m).

- Data processing costs can be held to a minimum by making efficient use of a quick-look display and making maximum use of the processing capability of the field control center, thus leaving only a small part to be processed on off-site computers.

APPENDIX P

COSTS OF PILOT TUNNELS

TABLE OF CONTENTS

BACKGROUND STATEMENT

The original study was completed by Dr. E. L. Foster, Head of the Underground Technology Division of Foster-Miller Associates, Inc., in June 1975. The study was prepared as an appendix to the Task A Report. It was made to provide factual information on costs in support of discussions and conclusions on the merits of boreholes for the collection of data on subsurface materials and their conditions.

The study has been supplemented with information on the costs of pilot tunnels excavated in the metropolitan area of Washington, D.C. Some additional information from Foster-Miller reports prepared for the Federal Highway Administration in October 1975 has also been added in the supplement attached to the study.

COST OF PILOT TUNNELS

ABSTRACT

A horizontal borehole is an alternative to a pilot tunnel for use in the collection of data on subsurface materials and their conditions. Construction cost is an important factor in considering its use.

Since relatively few pilot tunnels have been excavated in the United States, comparisons were made to the costs of excavation and primary support only for 17 lined tunnels in the same size range as pilot tunnels, built from 1956 to 1973. The costs were updated to a 1974 construction cost base. Pilot tunnel costs per foot (m) were estimated to average $225 ($738/m) for easy ground conditions; $356 ($1168/m) for normal conditions and $877 ($2877/m) for difficult conditions.

Estimates for long horizontal boreholes from a study by Fenix and Scisson show costs as low as $13 to $14 per foot ($43 to $46/m) on the average for lengths to 1000 feet (304.8 m), with estimates rising to from $17 to $40 per foot ($56 to $131/m) for holes 5000 feet (1524 m) long.

It is concluded that exploratory excavation costs can be reduced by an order of magnitude, if boreholes can be used instead of pilot tunnels.

The study has been supplemented with information on the costs of pilot tunnels in the Washington, D. C. area and information on estimating borehole costs. In 1975 an 8' (2.4 m) x 8.5' (2.6 m) pilot tunnel 653' (199 m) long was bid at $450 per foot (1476/m) and two 6' (1.8 m) x 8' (2.4 m) tunnels 715' (218 m) and 775' (326 m) long were bid at $400 per foot ($1312/m).

A sample 5000-foot (1524 m) borehole, 2.36-inch (6.0 cm) size, in average rock ranging from soft to hard was estimated at

$314,000 or $61 per foot ($200 m) using diamond wireline core drilling techniques. This estimate could rise to $95 per foot ($312 m) with the use of other drilling techniques. The estimated costs per foot were considerably lower for shorter boreholes.

A PRELIMINARY APPRAISAL OF THE RELATIVE CONSTRUCTION COSTS OF PILOT TUNNELS vs. LONG HORIZONTAL BORE HOLES

by

Dr. Eugene L. Foster

June 30, 1975

Underground Technology Division
Foster-Miller Associates, Inc.
Alexandria, Virginia

1. INTRODUCTION AND BACKGROUND DISCUSSION

It is generally agreed among the professionals of the tunneling community that one key to reduced construction costs is improved knowledge of subsurface conditions. There is some conjecture about the relative value of improved instrumentation vis a vis better interpretation of the outputs of today's instruments, and a strong case can be made for more knowledgeable use of the current state-of-the-art. However, one important fact remains; even when this is done, optimization of subsurface investigation will be improved by obtaining the "biggest bang for the buck." As the cost of geotechnical measurements is reduced, the opportunities to obtain adequate subsurface information will be enhanced.

Ideally, a contractor who is bidding a job would like to have a "feel" for the condition he will encounter during construction. The present generation of contractors is most comfortable when this is obtained by a walk-through inspection along the alignment, e.g. a pilot tunnel. This is believed to "tell it like it is" and, to some extent, it does. The pilot tunnel offers the advantage of first-hand observation, and in addition provides some indication of ground behavior during excavation. The latter must be carefully interpreted, however, since there are size and time effects which must be taken into account. A pilot tunnel as presently used has some disadvantages, as well. An observer in the tunnel cannot "see" into the surrounding material. At best, he can only infer what lies beyond the tunnel boundaries, using information from boreholes, the general geological maps of the region, and other sources. Pilot tunnels also cost money, a great deal of money, and they require a relatively long time to build. Both of these factors may cause problems, and often lead to a decision not to construct the pilot tunnel.

One alternative to the pilot tunnel is the long horizontal borehole. Because of its small diameter (of the order of one foot), both cost and construction time are greatly reduced. While its small size prevents personal observation, it does not in fact have as big a handicap in this respect as might at first be expected. Core samples can be obtained at any point along the path of the borehole. In addition, new concepts in instrumentation suggest that TV scan techniques would provide a view of the borehole surface and that electromagnetic and acoustic radiation could be used to detect geologic features up to 10'-100' (3.05-30.5 m) range beyond that surface. Since direct human participation at the sensor level is no longer required, safety precautions to protect the sensor package are minimized.

For all of the above reasons, a careful comparison needs to be made between the pilot tunnel and the horizontal borehole as alternate means of obtaining subsurface information. The present study addresses one factor in that comparison, construction costs. In it, we shall make cost predictions based on past experience and on the developing state-of-the-art for both types of cavities. The methods employed and the results obtained are described in the following sections.

2. METHOD OF APPROACH

Despite their usefulness, relatively few pilot tunnels have been employed in the U.S. Of these, only a small fraction have had their construction costs documented in a manner which allows reliable conclusions to be drawn about their original cost. This suggests that if one wishes to obtain representative costs for a reasonable number of tunnels in order to provide a basis for prediction, another approach will be necessary.

The alternative chosen for the present study was to select a sample of tunnels made for other purposes and for which footage costs were known. These tunnels were in size ranges considered to be comparable to those of typical pilot tunnels.

In order to ascertain what fraction of their total quoted costs would have been attributable to making a comparable pilot tunnel, the following procedure was used. The assumption was made that a pilot tunnel would have the same excavation and primary support requirements as any other tunnel. Analyses were made of four recent tunnel cost estimates made by Foster-Miller for their contractor-clients to determine the percentage of total per footage costs attributable to excavation and primary support. Portals, intermediate shafts and other appurtenances were not included. The average of the four examples was 50%, and the spread about that average ±10%. On this basis, we concluded that per-footage costs equal to 50% of those given for the lined tunnels were a good first approximation to the cost of a pilot tunnel of equivalent excavated dimension constructed under similar geographical and geotechnical conditions.

One other adjustment was necessary. The tunnels for which cost information was available were built during the time frame 1956-1973. Their costs had to be adjusted to a common time base, chosen arbitrarily to be 1974. The adjustment was made in the following way.

The Engineering New Record Construction Cost Index, Figure 1, provides a composite measure of the relative cost of wages and materials on a yearly basis. Using 1913 as the original base, (1913=100) index numbers for other years may be ratioed to obtain a cost adjustment factor between any two. For example, the wages and materials for a pilot tunnel constructed in 1956 when the ENR CCI was 700 would be expected to cost 2099/700=3 times as much in 1974 when the CCI was 2099.

One other correction factor must be applied, the productivity adjustment factor. Increases in productivity reduce overall costs from the values obtained based on wage and material escalations alone. The tunneling industry has had relatively modest gains in productivity over the past two decades. Dr. Lloyd Money of the US Department of Transportation estimates average values during the past five years to have been of the order of 1-2%. The prior gains for drill and blast tunneling, which is the principal method used on the tunnels studied in this report, are probably comparable.(1)

(1) Dr. Lloyd Money, personal communication.

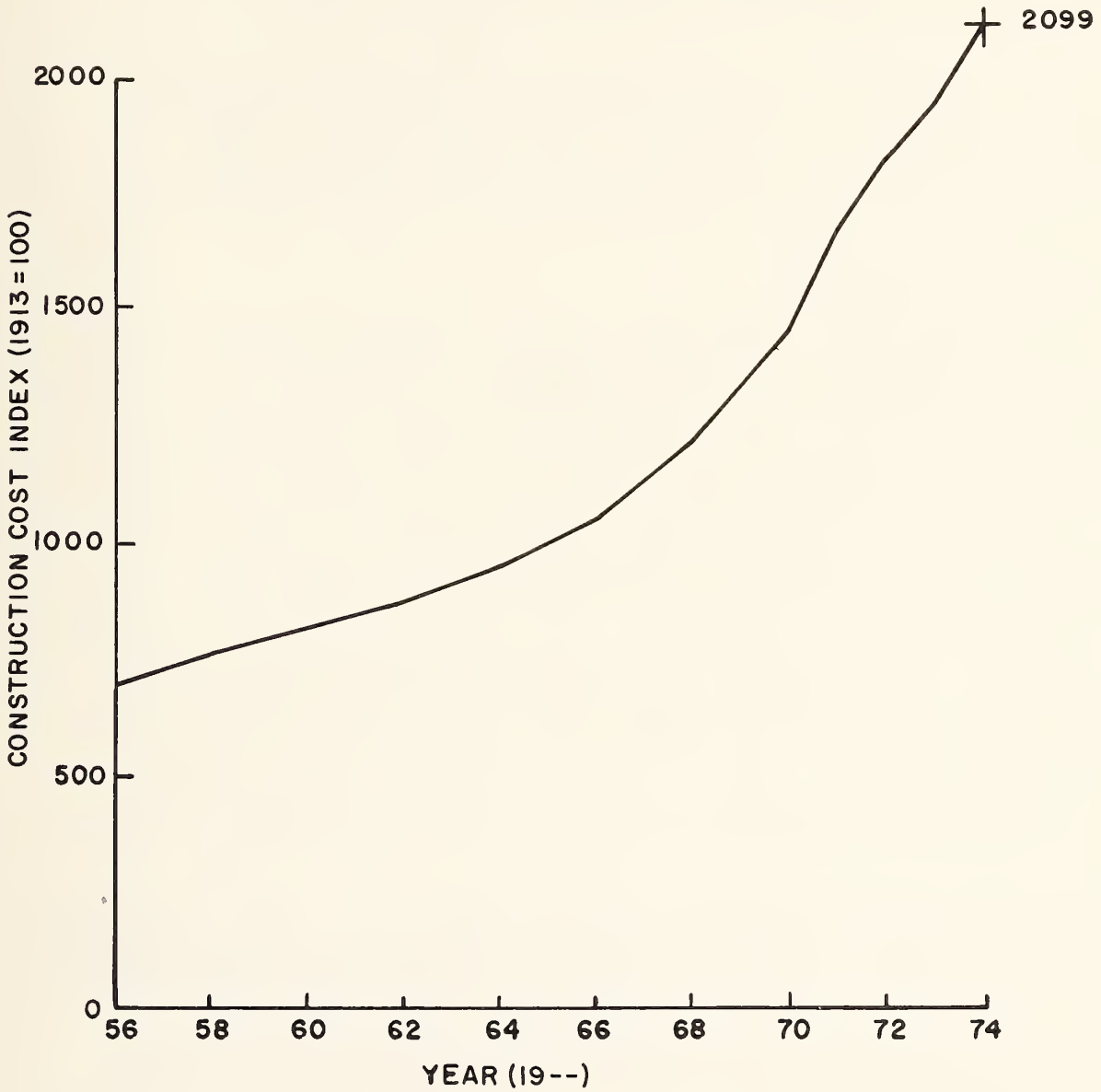

Figure 1. Construction cost index 1956-1974. (Engineering News Record).

Considering that labor costs comprise approximately 50% of total pilot tunneling costs, an adjustment of 1% per year for increased productivity is considered to be reasonable. A curve of the productivity factor is given in Figure 2. As in the cost adjustment, productivity factor adjustments are made by taking the ratio of factors for the two years under consideration. For example, the cost factor of 3 between 1956 and 1974 developed in our earlier example would be reduced to 1-1/2 x 3=2.5 due to the increase in productivity for 1974 compared with 1956.

A group of 17 tunnels for which cost data is available[1] is given in Table I. In this table, original costs and year(s) of construction are given, together with a brief description of each tunnel and the conditions under which it was driven. The estimated costs in 1974 shown in Table I were developed by adjusting original costs for both the construction cost index and changes in productivity as described above.

3. DISCUSSION OF RESULTS

The adjusted tunnel costs shown in Table I range from $294/Ft ($965/m) to $1734/Ft ($5689/m). If these are converted to cost per cubic yard of excavation and then applied to a standard pilot tunnel of 8' x 10' (2.4 x 3.05 m) horseshoe cross section, the results shown in Table II are obtained. In compiling Table II, it was noted from descriptions of the geological conditions encountered that costs could be grouped as shown in the table under three main categories of ground conditions, difficult, normal and easy. The available data contained only one exception to these classifications, the 8432' (2570 m) long Snettisham (Alaska) power tunnel, where excavation costs were $38/cubic yard ($50/m^3). This tunnel differs from most of the others in two respects. First, it is much longer, and second, it may not fit our cost model since an unspecified fraction of its length was unlined. It was also made in a formation for which minimum information is known. If 90% of its length were unlined, the excavation costs would rise to $72/cubic yard ($94/m^3) and it would fit very well into the "easy ground" category. For the above reasons, it is not considered prudent to assume that $38/cubic yard ($50/m^3) represents a readily attainable value in the excavation of pilot tunnels based on present experience.

Fenix and Scisson have studied the costs of drilling long horizontal holes, and have published the data given in Figure 3[2]. Backup information for Figure 3 is given in Table 3. The Fenix and Scisson report was published in 1974. However, it is not known whether the costs have been calculated in 1974 dollars. Regardless, the values given are generally more than an order of magnitude lower than our projected costs for pilot tunnels. On that basis, and assuming that reasonably priced instrumentation packages can be developed, it appears that horizontal borehole technology development has considerable potential for reducing the cost of subsurface investigation. If this can be done, more thorough investigation should become routine, and there should be a reduction in the risk and hence in the cost of tunneling.

[1] Engineering and Design, Tunnels and Shafts in Rock. EM 1110-2-2901 Draft, December 1973, Appendix I. Office of the Chief of Engineers, U.S. Army.

[2] Improved Subsurface Investigation for Highway Tunnel Design and Construction, Vol. 1, by J. L. Ash, et al, Fenix and Scisson, Tulsa, OK.

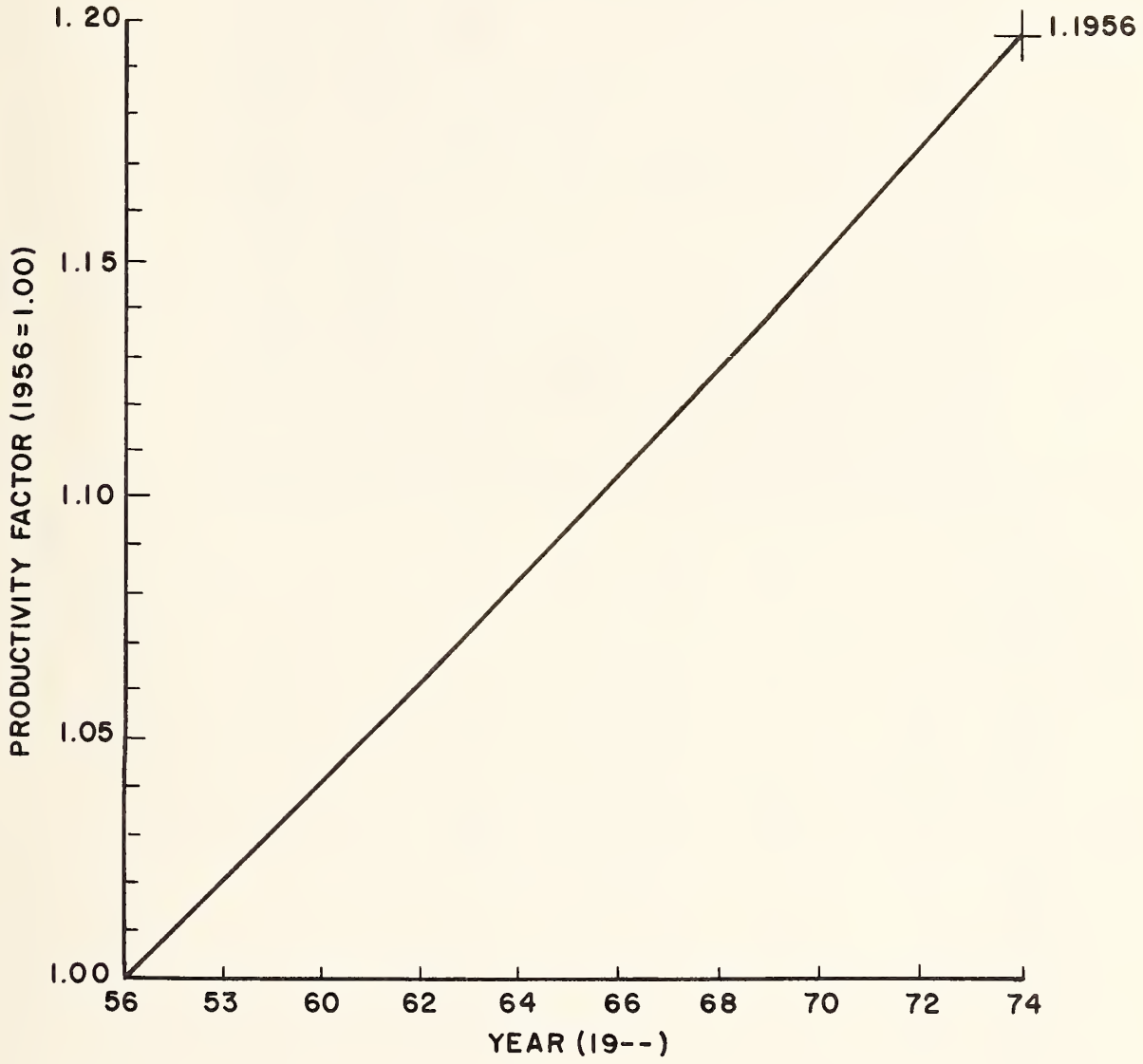

Figure 2. Productivity factor (based on 1% per annum growth).

Table 1. Summary of tunnel information.

LOCATION	CONSTRUCTION DATE 19-	LENGTH FT (m)	EXCAVATED DIAMETER FT (m)	SHAPE	ESTIMATED COST ORIGINAL $/Ft. ($/m)	ESTIMATED COST CORRECTED TO 1974 $/Ft. ($/m)	REMARKS
Oahe, S. Dakota	50-59	2050 (624.8)	9 (2.7)	Circ.	340 (1115)	774 (2539)	Pierre Formation, U. Cret., clay-shale, montmorillonitic, soft to firm (average compressive strength 400 psi [2.75 MPa]). Highly faulted and slickensided. Closely spaced bentonite seams from fraction of inch to several inches in thickness. Numerous joints whose orientation, spacing and extent varies between bentonite beds. Difficulties in tunneling occurred where concentration and intersections of rock defects were encountered, i.e., joints, faults, slickensides and bentonite seams. Degree of success of the 4 different tunneling machines used was largely dependent on how close to heading ringbeams could be erected. This distance varied from 3 ft. (0.91 m) to 11.5 ft. (3.5 m). Consequently, when shale fallouts occurred the machine with its ringbeam erection jig located closest to heading experienced much less difficulty in passing through reaches of heavy ground. No water problems. The shale slacked rapidly due to loss of moisture which required adding water to air for humidity control or protective coating like shotcrete.
N. Fork Pound, VA	63-64	641 (195)	10.8 (3.29)	Horse-shoe	213 (699)	1404 (428)	Lee, Wise and Gladesville Formations, PA. Shale hard, dense, sandy. Conventional drill and blast. Steel ribs with blocking and/or rock bolts as required. No significant water.
Wilson Kansas	63	998 (304)	16 (4.9)	Circ.	393 (1289)	817 (2680)	Dakota Formation, U. Cret. Shale, soft, massive, occasionally laminated by lenses of soft siltstone and sandstone. Support by CWF 15.5 ring beams spaced from 3 ft. (0.9 m) to 4 ft. (1.2 m).
Snettisham Alaska	72	8432 (2570)	15.5 (4.72)	Horse-shoe	259 (850)	294 (9656)	No fm. given. Cretaceous (?). Quartz diorite and granite gneiss associated with the Coast Range batholith. Three minor faults were crossed in the power tunnel with no particular problem. Relatively thin (up to 10 ft. [3m]), vertical basalt dikes with closely spaced jts. were encountered and required installation of tunnel lining. No significant water encountered. Tunnels excavated full face, powerhouse excavated by top heading and bench. Rock of excellent quality.
Snettisham Alasks	72	1200 (365.8)	10.5 (3.20)	Circ.	827 (2713)	941 (2999)	
General Edgar-Iadwin Dam, PA.	58	548 (167)	11 (3.4)	Circ.	155 (509)	315 (1033)	Catskill fm. (Red beds). Penn. Dev., siltstone, sandstone and shale. 10-15,000 psi (69-103.4 MPa) comp. strength flat lying beds, wide jt. spacing, no water problem. Drill-blast, rockbolted.

Table 1 (continued)

LOCATION	CONSTRUCTION DATE 19-	LENGTH FT (m)	EXCAVATED DIAMETER FT (m)	SHAPE	ESTIMATED COST ORIGINAL $/Ft. ($/m)	ESTIMATED COST CORRECTED TO 1974 $/Ft. ($/m)	REMARKS
Gillham, Arkansas	73	627 (191)	13 (4.0)	Circular	383 (1257)	409 (1342)	Stanley Shale Fm., Miss.-Penn. Quarzitic sandstones interbedded shales. Excavation encountered minor fault (healed) which gave no problem and numerous joints and fractures open to filled with secondary minerals.
Ervin R. Bush, Penn.	62	768 (234)	16 (4.9)	Horseshoe	240 (787)	514 (1686)	Catskill Fm., (Redbeds), Penn. Dev., Siltstone, sandstone, shale comp. strg. 10-15,000 psi (69-103.4 MPa), mod. jointing, no water, rock failure at one portal, excavate by drill-blast, steel sets.
Abiquiy Dam Rio Chama New Mexico	56	2078 (633)	15 (4.6)	Circular	360 (1180)	902 (2959)	Abo Fm., Upper Permian. Mudstone, silty, blocky to massive, no open joints. Unconfined compressive strength 1,900 psi (13.1 MPa). Dry density 147 lbs/ft^3 (2355 kg/m^3). Drill and blast. No significant water.
Pomme de Terre, Missouri	59	514 (157)	14 (4.3)	Circular	304 (997)	695 (2280)	Jefferson City Formation. Dolomite, hard, dense to finely xin. Thin to thick bedded, some fine fractures and healed faults. No water problems. Drill and blast. Support - none required.
Mills Creek, Oregon	62	667 (203)	15 (4.6)	Circular	810 (2657)	1734 (5689)	Tuff Breccia, massive, faulted. One prominent vertical fault zone about 10 feet (3 m) wide paralleled with tunnel crown for much of its length. Rockbolts, mine ties, steel sets where required. No water. Drill and blast.
Littlefield Westfield River, Vermont	65	285 (87)	10.5 (3.20)	Horseshoe	185 (607)	326 (1070)	Schist, containing quartz stringers, biotite and garnet. Coarse grained, moderately hard. Slight water flows. Support by steel sets where required. Foliation planes in schist dip from 45° to 70° causing rough overbreak in crown and one rib. Convention drill and blast.
North Springfield, Vermont	60	600 (183)	15.9 (4.85)	Horseshoe	255 (837)	567 (1860)	Cavendish Schist, U. Cambrian. Schist and gneiss, highly folded and faulted with steeply dipping foliation planes. Several shear zones required lagging, otherwise, rockbolts and steel sets used. Insignificant water flows. Drill and blast - lined drilled where required to prevent opening joints and foliation planes. No significant water.
Hall Mt. West River, Vermont	61	865 (264)	16 (4.9)	Circular	244 (801)	533 (1749)	Schist (sericitic, chloritic, garnetiferous) with numerous granitized zones. Foliation dips 30° to 40° downstream. Several joint sets, some slickensided. Drill and blast. Insignificant water. Suppoer, partial steel sets, few rockbolts.

Table 1 (continued)

LOCATION	CONSTRUCTION DATE 19-	LENGTH FT (m)	EXCAVATED DIAMETER FT (m)	SHAPE	ESTIMATED COST ORIGINAL $/Ft. ($/m)	ESTIMATED COST CORRECTED TO 1974 $/Ft. ($/m)	REMARKS
Cougar, Oregon	64	1043 (317.9)	16 (4.9)	Horse-shoe	364 (1194)	735 (2411)	Tertiary Volcanic Rocks. Basalt, fine grained, xin, bedded tuffs and hard brittle tuff. Gouge zones up to 3" (7.6 cm). One fault zone 25' wide (7.6 m), but no problems. No large water inflow. Support, 3/4" (19 mm) hi-strength rockbolts, 5' (1.5 m) o.c. 6'-8" (2.0 m) long, set radically in arch. Mesh and bolts in brittle tuff reach of tunnel. Drilling and blasting. Several joint sets.
Straight Creek, Colorado	64	9000 (2743)	10 (3.0)	Horse-shoe	166 (545)	335 (1099)	Located near the eastern flank of the Rocky Mtns. at 11,050' (3368 m) elev. Bedrock was 75% granite & 25% metasedimentary gneiss & schist that occurred as migmatite inclusions w/numerous shear zones, faults & joints. Over 3,600' (1097 m) of tunnel was thru squeezing ground. Little water encountered except near portals during spring thaw. Drill and blast.
Hawaii	71	5200 (1585)	13x18 (4.0x5.5)	Horse-shoe	615 (2018)	736 (2415)	This tunnel included six chambers 50'x27'x200' (15x8.2x61.0 m) prepared for full instrumentation. Cost is based on engineer's estimate.

Table 2. Projected costs for pilot tunnels.

Category of Ground Conditions	EXCAVATION COSTS	
	$/Cub. Yd. ($/m^3) Base Year: 1974	$/Ft ($/m), 8'x10' (2x3m) tunnel. Base Year: 1974
Difficult	$296 ($387 ±10%	$877 ($2877) avg.
Normal	$120 ($157) ±15%	$356 ($1168) avg.
Easy	$76 ($99) ±20%	$225 ($738) avg.

4. CONCLUSIONS

(a) It is concluded that the cost of subsurface investigation using long horizontal boreholes has the potential for reducing excavation costs by more than an order of magnitude compared with pilot tunnels.

(b) In order to translate these savings into savings in tunnel construction costs, it will be necessary to develop horizontal borehole instrumentation and techniques to a state-of-the-art where the information obtained is as credible to the construction community as as the methods presently employed with pilot tunnels.

Table 3. Drilling data for drilled horizontal long holes. (Source: Fenix and Scisson, Inc.)

HOLE SIZE AND LOCATION	DRILLING TECHNIQUE USED	DEPTH (FEET) (m)	MATERIAL HARDNESS (PSI)		TIME REQUIRED TO DRILL (Feet per day, three shifts) (m/day)	COST PER FOOT ($) (Cost per m ($))	REMARKS
			0 to 10,000 (68.9 MPa)	10,000-50,000 (344.7 MPa)			
3 inch (7.6 cm) Mercury, Nevada	wireline diamond core	3,700 (1,128) deepest 2,000 (610)	2000-5000 (13.79 - 34.47)		100 for 3,000 ft. (914 m) hole. 120 for up to 1,000+ (305) feet.	30 (98) overall average for 3,000 to 3,500 feet.	Includes survey and wedging.
3 inch, (7.6 cm) U. S. A. Estimator #1	wireline diamond core	to 5,000 (1524)	yes	yes	1000 (305)-75 (23) 2000 (610)-60 (18) 3000 (914)-51 (16) 4000 (1219)-36(11) 5000 (1524)-24 (7) (conservative)	30+ (98) overall for 4,000' (1219) hole. Est. 40 (131) for everything.	Cost per foot is basic cost; does not include such items as mud, survey, directional control, mobilization, bad ground, grouting. etc.
3 inch, (7.6 cm) U. S. A. Estimate #2	wireline diamond core	to 5,000 (1524)	yes	yes		1,000' = 6 (20) to 10 (33) 3,000' = 6.50 (21) to 12 (39) 5,000' = 15 (49) to 20 (66)	Would not include mud, survey, directional control, mobilization, etc.
3 inch, (7.6 cm) U. S. A. Estimator #3	wireline diamond core	to 5,000 (1524)	yes	yes	Estimated time to drill 5,000'(1524) hole = 100 days or 2,400 hours.	0-1,000', NX=14 (46), BX=13 (43) 1,000'-2,000', NX=16 (52), BX=14 (46) 2,000'-3,000', NX=18 (59), BX=15 (49) 3,000'-4,000', NX=21 (69), BX=18 (59) 4,000'-5,000', NX=26 (85), BX=21 (69)	Estimated drilling costs; does not include time for extensive survey or directional work.
3-1/2 inch, Ohio	rotary w/ 3-cone roller bit	1,100 (335)	600 (4.14) to 2,000 (13.79)		600± (183)	2.50 (8.20) to 4.50 (14.76)	Drilling 1,000 ft. (305 m) horizontal holes to coal seam.
3 inch, Pennsyl.	1-3/4" (4.5 cm) Dyna-Drill and diamond plug bit-curved hole from surface	1,730 (527)	yes		30± overall average. Est. 40'(12) per day, under good conditions	30 (98) to 35 (115)	This estimate includes a lot of downtime, several days without drilling.

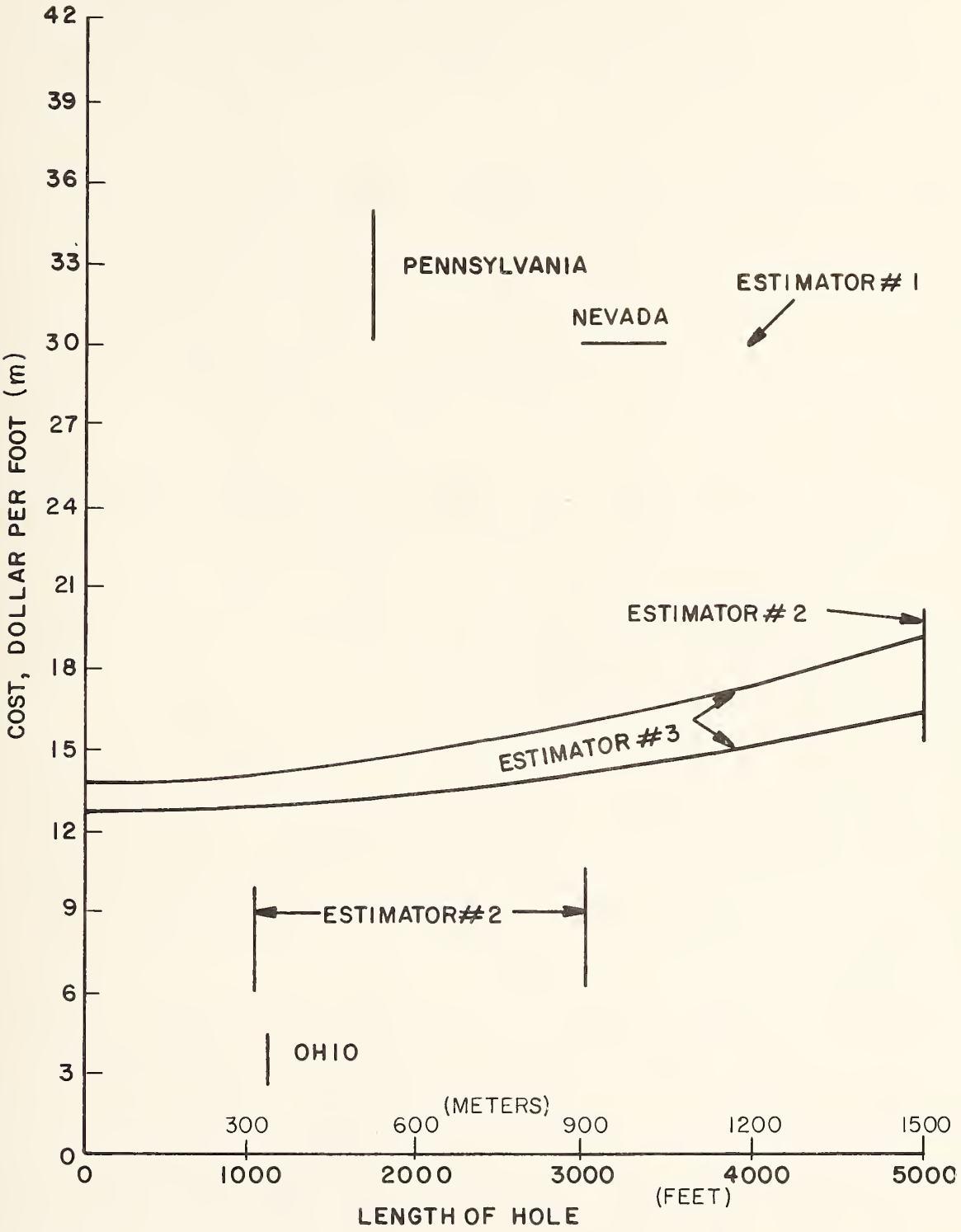

Figure 3. Representative drilling costs for horizontal holes. (Source: Fenix and Scisson, Inc.)

SUPPLEMENT NUMBER 1
CONSTRUCTION COSTS OF
PILOT TUNNELS VERSUS BOREHOLES

The limited cost data available on pilot tunnels built in the United States indicates that their costs have been rising at about the same rate as general construction costs. Data from the Engineering News Record Construction Cost Index shows that this rate rose to a recent high of 15% per year for the year 1971 and fell to 8% for the year 1974 then rose again to 9.6% for 1975.

The general construction cost trend for the years 1966 through 1975 is shown by the curve plotted in Figure 4.

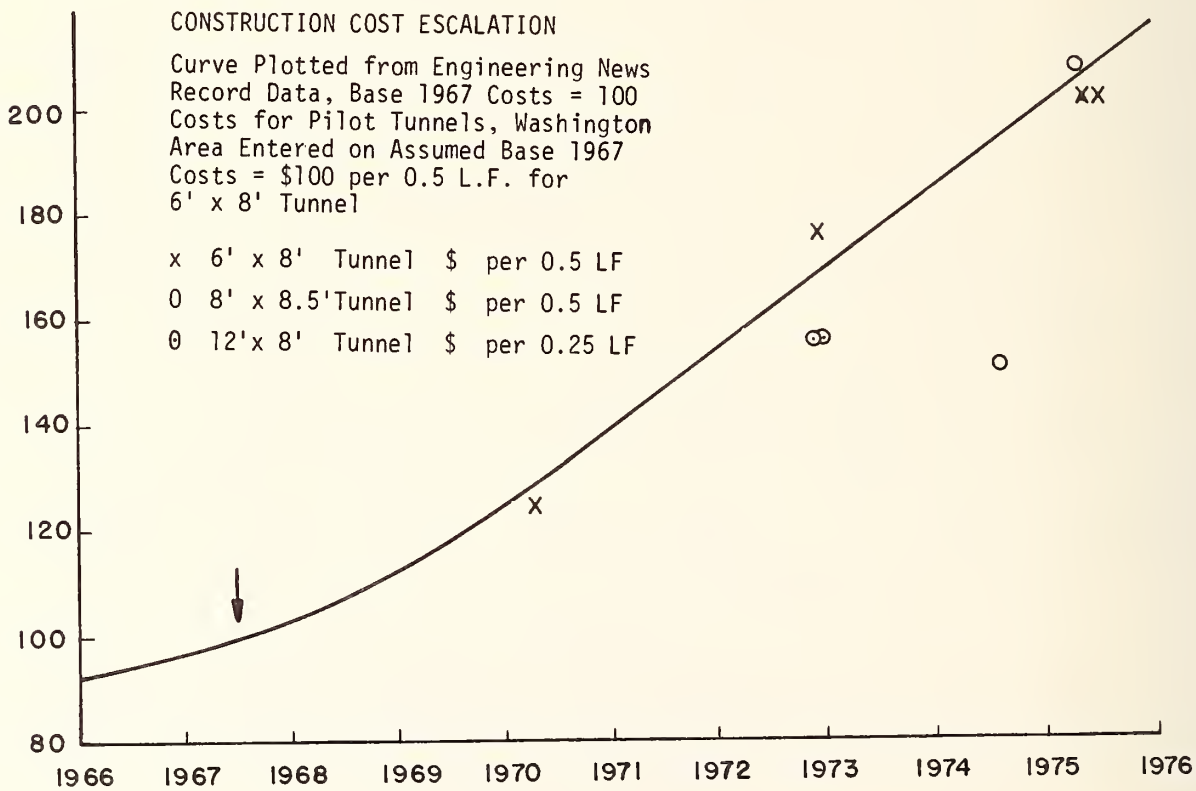

Figure 4. Construction cost trend.

The costs of pilot tunnels in the Washington metropolitan area have also been plotted on Figure 4 with the assumption that the average cost for a 6 x 8 foot (1.8 x 2.4 m) pilot tunnel would have been $200 per lineal foot ($656/m) about 1967.

This assumption placed the cost per 0.5-foot (0.15 m) unit of pilot tunnel on the curve plotted for the cost of a unit of construction at midyear, 1967, and permitted the examination of the escalation of tunnel construction costs in relation to other construction costs. The costs per 0.5 foot (0.15 m) for other 6 x 8 foot (1.8 x 2.4 m) tunnels and an 8 x 8.5 foot (2.4 x 2.6 m) tunnel were then plotted on Figure 4 at the dates they were bid. The costs for two 12 x 8 foot (3.7 x 2.4 m) pilot tunnels were also plotted on Figure 4, but in these cases the costs per 0.25 foot (0.08 m) were plotted, as these tunnels were twice the size of the 6 x 8 foot tunnels (1.8 x 2.4 m). The adjustment may have been too great, as both tunnel costs fell well below the general construction cost curve.

The data plotted on Figure 4 indicate that the trend of pilot construction costs generally follows the trend of construction costs, although there is considerable scatter among the tunnel cost data. This is understandable, because costs are greatly affected by many location dependent factors which are not averaged when data are plotted for individual projects.

The cost of a typical 6 x 8 foot (1.8 x 2.4 m) pilot tunnel in the Washington area has risen from approximately $250 per lineal foot ($820/m) in 1970 to $400 ($1312/m) in 1975. It can be expected to increase approximately 30% by mid 1979 to over $500 per lineal foot ($1640/m).

Improvements in working conditions made to comply with health and safety regulations have the short-term effect of reducing productivity and increasing costs. Recently the changes have been made more severe in tunnel construction projects than they

have in general construction projects. However, over long periods the adverse effects that improvements in working conditions have on costs seem to be balanced by improvements in equipment and methods and by reductions in the costs of injuries and lost time.

In recent years through 1974, the dominant factors in the escalation of construction costs were wages and benefits. In the future rising energy costs can be expected to continue to dominate.

A recent assessment of the state-of-the-art of drilling long bore holes in rock and in gouge (3) was accompanied by the development of a model for estimating time and cost (4). Procedures for applying the estimating model are illustrated by examples of cost estimates made for the same hole.

The requirements set for the horizontal borehole are:

- A 5,000 foot (1524 m) long horizontal hole.
- BX, approximately 2.36 inches (6.0 cm) diameter minimum size.
- Maintain the hole within a ±1% deviation.
- A five foot (1.52 m) core sample is required at least every 60 feet (18.3 m).

An average rock profile (11% soft, 59% medium and 30% hard) was assumed; and assumptions were made on the need for changes: in hole direction, hole surveys, fishing, hole stabilization, drill rod extraction and return velocity, and job efficiency to approximate average conditions.

Estimates were made for four drilling methods with costs as follows:

Diamond wireline core	$302,900 total or $61/ft. ($200/m)
Rotary	$427,500 total or $86/ft. ($282/m).

Down-Hole Motor	$476,500 total or $95/ft. ($312/m)
Down-Hole Percussion	$406,100 total or $81/ft. ($266/m)

While these estimated costs for boreholes are much higher than the estimates referred to in the basic study, they are only small fractions of the costs estimated for pilot tunnels. The costs per foot for shorter boreholes would be considerably lower as detailed in Appendix A of reference (4).

---

(3) Harding, J. C., Rubin, L. A., and Still, W. L., "Drilling and Preparation of Reusable, Long Range, Horizontal Bore Holes in Rock and in Gouge, Vol. 1, State-of-the-Art Assessment," Report to the Federal Highway Administration, Report No. FHWA-RD-75-95, October 1975.

(4) Mack, W. M., Jr., Tracy, N., and Wickham, G. E., "Drilling and Preparation of Reusable, Long Range, Horizontal Bore Holes in Rock and in Gouge, Vol. II, Estimating Manual for Time and Cost Requirements," Report to the Federal Highway Administration, Report No. FHWA-RD-75-96, October 1975.

APPENDIX Q

ANALYSIS OF SENSING COST-BENEFIT RATIOS AS A FUNCTION OF BOREHOLE SIZE

TABLE OF CONTENTS

BACKGROUND STATEMENT

A contractual requirement was to determine the most cost-effective minimum borehole diameter for the subsurface sensing system. This study was performed to meet this requirement. It was one of the first contract deliverables but it has been updated several times during the course of the contract as better data has become available.

ANALYSIS OF SENSING COST-BENEFIT RATIOS AS A FUNCTION OF BOREHOLE SIZE

ABSTRACT

Unless the cost of drilling and the time frame in which long horizontal holes can be drilled are considered, there are few technical factors in the sensing system that would limit it to smaller borehole diameters. In general, the larger the borehole the better the data. Qualitatively, it is obvious that as the hole gets larger, the propulsion system, acoustic couplers, and the system will become less mobile and more expensive. In addition, a greater degree of sophistication in data processing and computer programming will have to be incorporated to exploit the inherent increased capability achievable from the larger hole. Obviously, there is an optimum size where the added benefits do not justify increasing the hole diameter. Unfortunately, the quantitative data and the experience factors necessary to establish a truly objective optimum are lacking. Annex A of this appendix establishes the trend of this value/cost ratio. It takes into account the value to be gained by enhanced sensor range against the increase in borehole and system costs, with increasing borehole diameters.

The minimum usable borehole diameter is shown to be 6-3/4 inches (17.1 cm) with a broad optimum in the vicinity of 9 inches (22.9 cm). The 6-3/4 inch (17.1 cm) borehole was selected on the basis of many factors involving technical, economic, and pragmatic engineering judgment considerations.

ANALYSIS OF SENSING COST-BENEFIT RATIOS AS FUNCTIONS OF BOREHOLE SIZE

1. INTRODUCTION

Conceptually, it would seem that the smaller the diameter of the value of the information derivable from the hole. Consequently, one task of the program was to determine the minimum size for the horizontal borehole sensing system. This study analyzes the many factors inherent in the problem. The following discussion involves both technical and economic risk considerations.

2. FACTORS AFFECTING BOREHOLE DIAMETER

2.1 GENERAL CONSIDERATIONS

Unless the cost of drilling and the time frame in which long horizontal holes can be drilled are considered, there are few technical factors in the sensing system that would limit it to smaller borehole diameters. In general, the larger the borehole the better the data. Qualitatively, it is obvious that as the hole gets larger, the propulsion system, acoustic couplers, and the system will become less mobile and more expensive. In addition, a greater degree of sophistication in data processing and computer programming will have to be incorporated to exploit the inherent increased capability achievable from the larger hole. Obviously, there is an optimum size where the added benefits do not justify increasing the hole diameter. Unfortunately, the quantitative data and the experience factors necessary to establish a truly objective optimum are lacking. Annex A to appendix establishes the trend of this value/cost ratio. It takes into account the value to be gained by enhanced sensor range against the increase in borehole and system costs, with increasing borehole diameters.

Annex A establishes an optimum based on the statistical mean of a wide range of parametric variables. This leads to a borehole diameter of 6.5 ± 3 inches (16.5 ± 7.6 cm). There is little in this portion of the study to justify a specific choice within these bounds.

Past work on the horizontal borehole study under Contract No. DOT-FH-11-8486 plus work on Task A of this contract indicates the undesirability of smaller diameters[1]. The following portion of the study will present and discuss these trends.

2.2 SIZE OF AVAILABLE COMPONENTS

There seems to be little difficulty in miniaturizing electronic and sensing components so that their impact on the borehole size is negligible. However, in the area of supporting power and mechanical components, there seems to be a break in the vicinity of 4 to 6 inch (10 to 15 cm) diameter packages. Actually, as package diameters drop below 8 inches (20 cm), it becomes more and more difficult to find standard components which will fit into the package. Initially, the impact is not too serious as it must be expected that a certain percentage of the larger components will become custom-made. The problem becomes especially critical in electric motors with usable powers and hydraulic pumps with acceptable flow rates. These are available in aircraft and milspec quality as well as on special orders. The costs and lead times, however, are disproportionately higher.

As an example, the smallest electrohydraulic power package we have found suitable for the propulsion unit, with minimal modification, will require a 4-1/2 inch to 5 inch (11 to 13 cm) package. When a half-inch (1.3 cm) clearance between package and borehole is allowed, this places the hole size in the 6 to 6-1/2 inch (15.2 to 16.5 cm) range. To go below this range will raise the component costs by factors of two to five.

2.3 RADAR DIRECTIVITY

There will be a minimum borehole diameter below which it will

---

[1] References are listed at end of Annex A, p. A16.

be impossible to get both azimuthal directivity and effective penetration. However, it should be pointed out that even the best directivity obtainable from a borehole of realistic size will do little more than locate the quadrant of a signal return.

Figure 1 is an extract from the Antenna Engineering Handbook by Jasik [2]. This is probably the most universally accepted reference on broadband antenna configurations. The patterns shown in Figure 1 are representative of what can be designed into borehole-size spacing by standard procedures. They in effect define the needed borehole size in terms of radar wavelengths.

The spacings given in wavelengths are reasonable approximations of the borehole diameters required to achieve these patterns. A quarter wavelength, $\frac{\lambda}{4}$, is required to form a basic pattern. This deteriorates rapidly for smaller diameters.

Figure 2 is an extract from Cook's paper [3] showing the radar probing distances for various rock types. It can be seen that frequencies in the order of 100 to 200 megahertz are required to probe to 100 feet (30.5/m).

The equation relating wavelength (λ) to a borehole diameter, where $D=\frac{\lambda}{4}$ is

$$D = \frac{C}{4f\sqrt{K}} \qquad (1)$$

where, in any consistent set of units,

- D = Minimum hole diameter
- f = Frequency
- K = Dielectric constant of the medium at the frequency of interest, and
- C = Velocity of light.

For D in inches and f in megahertz, (1) becomes

$$D = \frac{2.95 \times 10^3}{f\sqrt{K}}$$

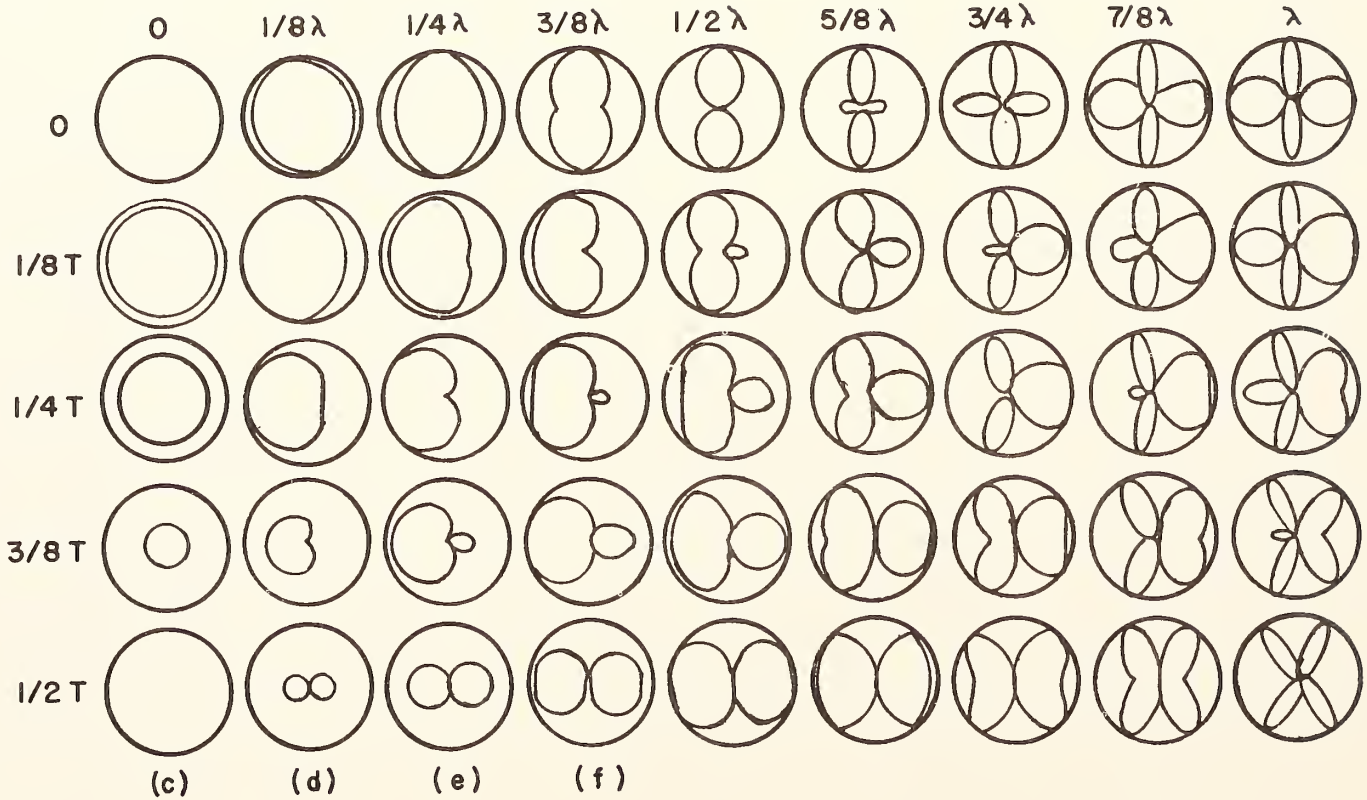

Figure 1. Directive amplitude diagrams for an array of two antennas driven by currents of equal amplitude. Separation in wavelengths (λ) along the top. Phase difference in periods (T) at left.

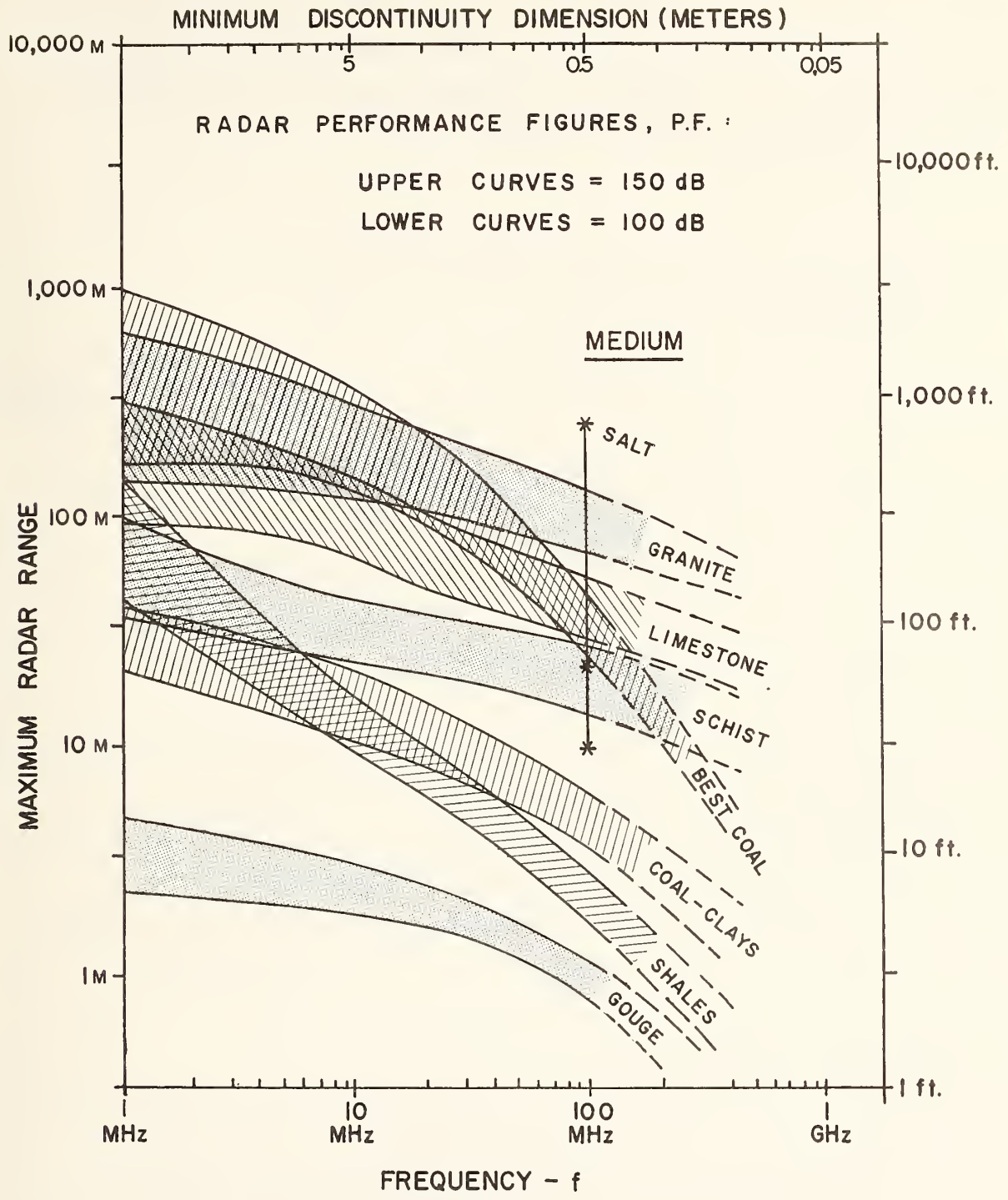

Figure 2. Radar probing distances through some typical "rocks".

Typical values of the dielectric constant for these frequencies are 4 to 8. Using these ranges, we have summarized the results in Table 1 for the minimum hole diameter, which will support a one-quarter wavelength radar antenna.

Table 1. Hole diameter for $\lambda/4$ antenna,

	f megahertz	
K	100	200
4	14.8	7.38
8	10.4	5.21

Diameter in inches

(multiply by 2.54 for cm)

Examination of Figure 2 will show that variations of frequency in the vicinity of 200 megahertz will have little effect on the penetration distance. Table 1 shows that it will have a major effect on hole diameter. Thus, contrary to original expectation, rather large variations of hole diameter in the vicinity of 6 inches (15 cm) will have minimal effect on either radar range or resolution.

2.4 FORMATION PRESSURE

Figure 3 is a curve showing the hydraulic pressure on the formation while drilling a 10,000 foot (3.048 km) hole of various diameters. This curve was extracted from work in support of the horizontal borehole study [1]. In this case, the drill string size was optimized for minimum hydraulic horsepower loss through the system. As hole size decreases, there is a rapid rise in the curve in the vicinity of a 7 inch (18 cm) borehole diameter. The pressure required to generate sufficient fluid velocity to

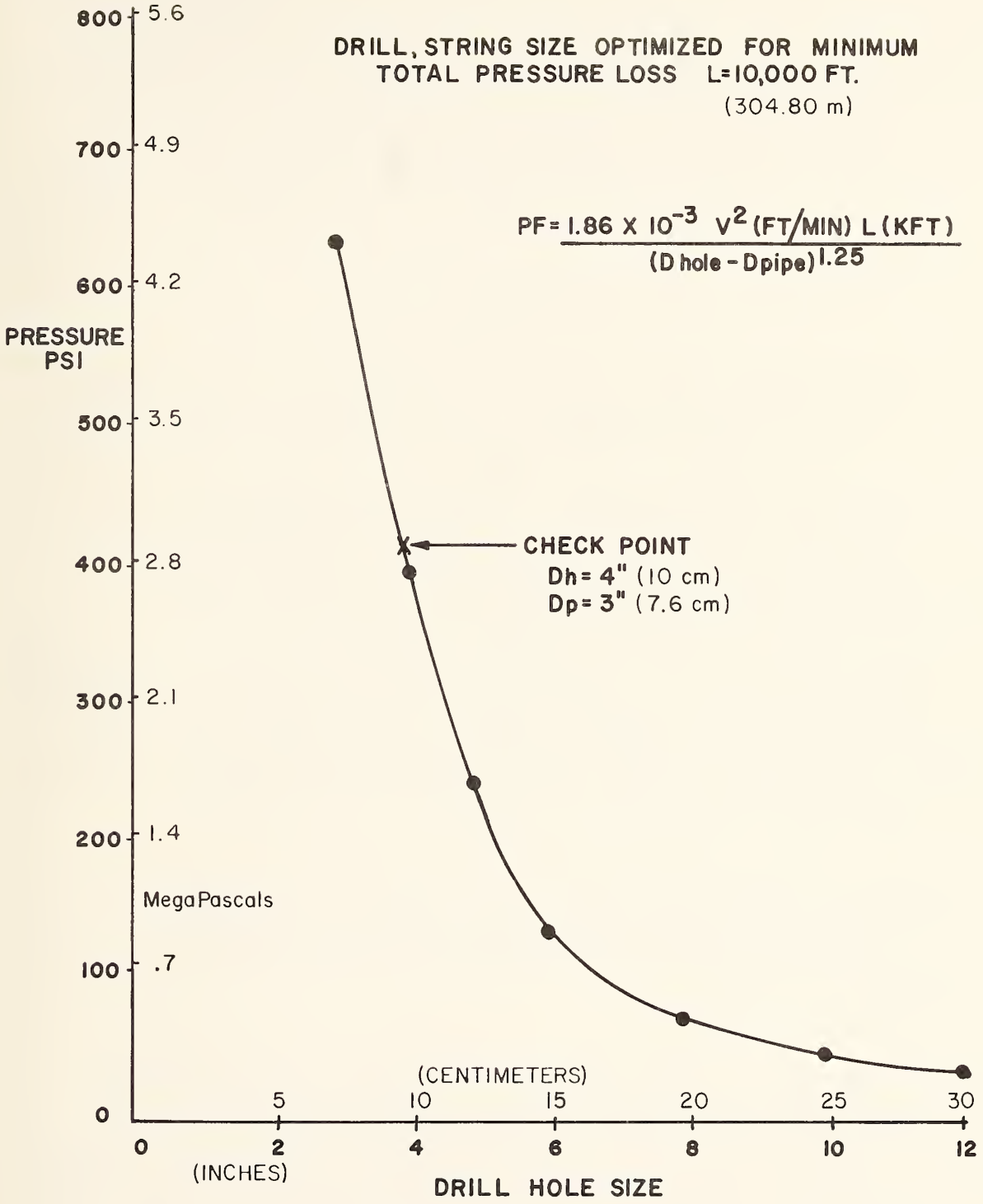

Figure 3. Formation pressure to maintain 150 ft/min. (0.763 m/s) return flow.

carry out the cuttings rises rapidly below this diameter. This pressure can rapidly become great enough to exceed the formation pressure, resulting in destruction of the hole and the jamming of the drill string. Based on this consideration, it seems that aside from the purely sensing considerations, the physical achievability of a horizontal borehole to an appreciable depth may be limited to a hole 6 to 7 inches (15 to 18 cm) or larger in diameter.

2.5 AVAILABILITY OF DRILLING EQUIPMENT

Currently, horizontal holes can be drilled in NX (diameters of 3" [7.6 cm]) and less, to distances in the order of 1,000 feet (304.8 m). Between 4-3/4 (12 cm) and 6-3/4 inches (17 cm) [1], there is a gap in the normally available equipment and bits. Drilling in hard rock will require either a diamond bit or a roller cone cutter of some type. Diamond drilling in the larger sizes is uneconomical except for coring or drilling in the hardest rock. As hole sizes get smaller, roller cones become less reliable because the available bearing area becomes marginal. In fact, many reports of 4-3/4 inch (12 cm) roller cone bits in hard rock indicate a bit life in the order of inches or a few feet at most.

Six and three-quarter inches (17 cm) seems to be the smallest size where a wide range of roller cone bits is available. Thus, in all probability, this would be the most economical minimum hole diameter to choose.

There is additional effort anticipated under NSF Grant APR76-03300, "Research in Subsurface Site Investigation by Radar: Phase II", which will cover smaller borehole diameters, probably NS (3" [7.6 cm]). Annex A of this report indicates little value advantage to larger diameter holes, at short (under 2,000 ft. [609.6 m]). Thus, it seems that a 6-3/4 inch (17 cm) hole is the logical target diameter for the prototype system.

3. CONCLUSIONS

- There seems to be a general trend in a number of areas which would place the minimum acceptable hole diameter in the general range of 6 to 7 inches (15 to 18 cm). There is no clear reason to specify a specific minimum within this range on purely technical grounds.

- The availability of drilling hardware and the fact that all the trends present a lesser penalty for overspecifying than underspecifying the hole size tend to make the upper limit of the above range preferable.

- It is recommended that the minimum acceptable hole diameter for a 10,000 foot (3.048 km) hole be set at 6-3/4 inches (17 cm).

- On the basis of purely technical considerations, a larger hole than the above minimum would be preferable. A nine-inch (23 cm) hole seems to be the maximum needed for full utilization of the foreseeable techniques. Thus, the recommended size for a 10,000 foot (3.048 km) hole is in the vicinity of 9 inches (23 cm).

- One fact that has become apparent in the conduct of this study is that, if the borehole lengths were considerably shorter than 10,000 feet (3.048 km), possibly 1,000 (304.8 m) or 2,000 feet (609.6 m), the minimum borehole size could be less than that specified above.

- The 6-3/4 inch (17 cm) hole seems near optimum for the shorter holes, using currently available, state-of-the-art radar and acoustic sensors.

ANNEX A

COST/BENEFIT STUDY

BENEFIT

Typically, a plot of the benefit derived from an advance in the state-of-the-art versus the added capability achieved by that advance follows the general pattern of exponential saturation. The rate of increase in benefits diminishes as the tool approaches its full capability. A nominal advance achieved in the early developmental stages may provide a 100% increase in capability. A similar advance when the tool is mature would probably provide only a 3 to 5% increase in capability.

The evaluation of the benefits to be accrued from the use of borehole sensors is subjective. This study makes the assumption that, at a certain range of penetration, at least 50% of the system goals can be obtained. Added range would accrue added benefits but at a lower payoff per unit of range. Thus, while it might not be possible to obtain a consensus on the total benefits, a reasonable consensus should be achievable for the 50 percentile range.

The form of the benefit function is assumed to be

$$V = 100\left[1 - \exp\left(-\frac{0.693r}{r_{(50)}}\right)\right] = 100\left[1-e^{-\frac{0.693r}{r_{(50)}}}\right] \qquad \text{(A-1)}$$

where:

V = Percentage of potential value of the system achieved at the specified range

e = Natural log base, 2.718

r = Range of sensor penetration

$r_{(50)}$ = Range at which consensus agrees that 50% of the potential value can be achieved.

The value starts at zero for zero detection range and increases in accordance with the above equation. At some point, the

consensus will agree that, if the system can work as desired to a specified detection range, at least 50 percent of the total potential value of the system can be achieved.

DEFINITION OF 50 PERCENTILE RANGE

This study examines three sets of alternative assumptions for defining the 50 percentile range. Added value would accrue beyond this point to infinite range but at a decreasing rate of payoff.

ALTERNATIVE 1

The most important range is out to the tunnel diameter. It is believed that few civil engineers would accept a shorter range than this as an acceptable goal for the 50% value. A tunnel diameter of 50 feet (15 m) is assumed. This would place $r_{(50)}$ at 25 feet (7.6 m).

ALTERNATIVE 2

Considerable value could be attached to probing beyond the eventual tunnel diameter. The second level explored, places the 50% value at exploring an additional tunnel radius beyond the tunnel alignment for an $r_{(50)}$ of 50 feet (15 m).

ALTERNATIVE 3

The contract specifies a maximum range of 100 feet (30.5 m). Although it would be unrealistic to place $r_{(50)}$ this far out, it is included to bracket the range of sensitivities.

CORRELATION BETWEEN RANGE AND HOLE DIAMETER

In order for equation (1) to be of value in determining the optimum hole diameter, a functional relationship must exist between range and hole diameter. Figure A1 shows a logarithmic curve derived from data on the Birdwell 3-D Acoustic Log.

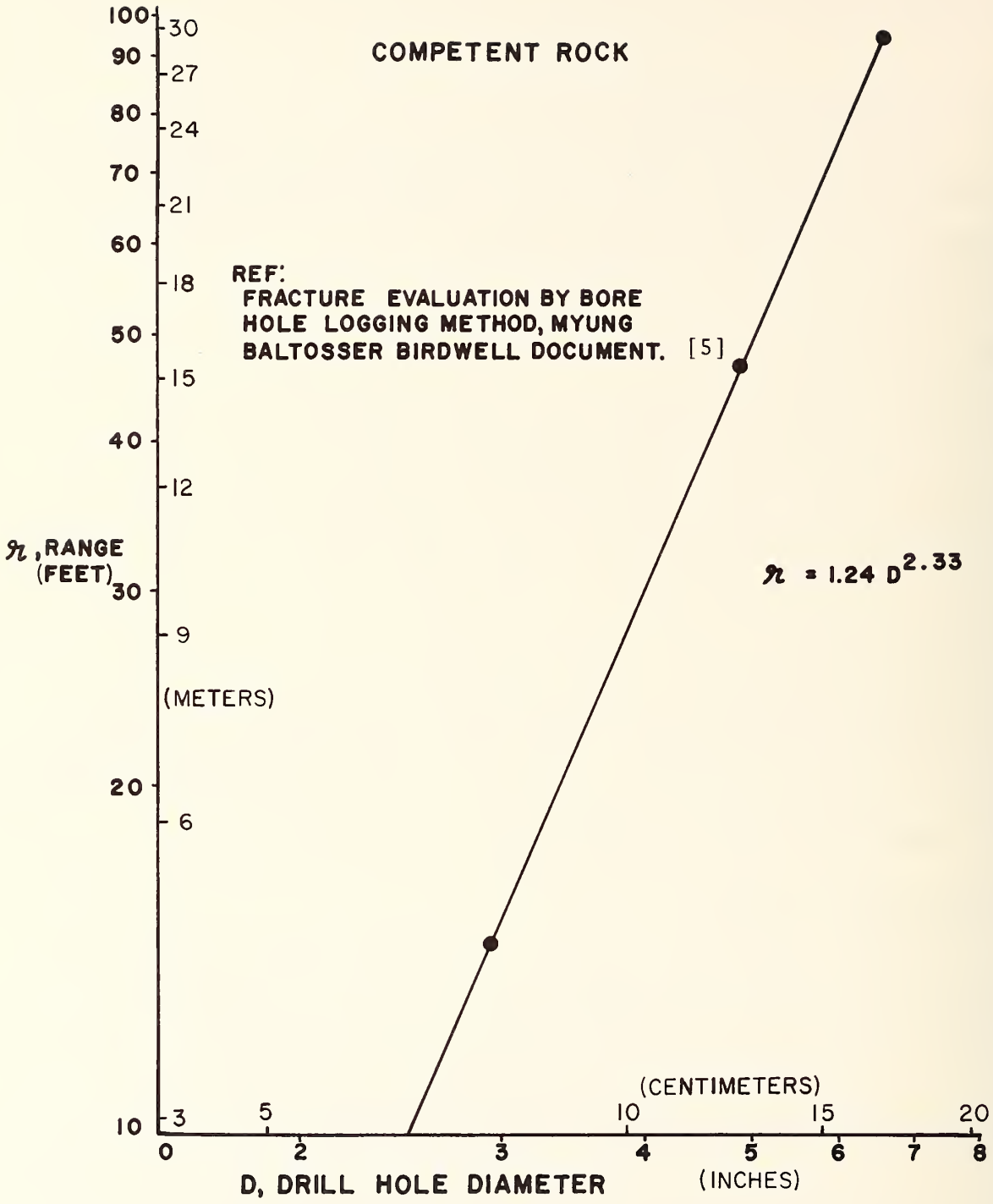

Figure A1. Expected range vs hole diameter for Birdwell 3-D Velocity Log.

Although only three data points are available, it can be seen that they fit the following empirical curve quite well:

$$r = 1.24D^{2.33} \text{ feet} \qquad \text{(A-2)}$$

where

r = Range of sensor penetration in feet

D = Hole diameter in inches.

Other functional relationships exist for other sensors between range and hole size. Acoustics has been chosen because it presents the most severe case. While none of the other relationships can be as neatly defined, none is as sensitive to variations in diameter as the $D^{2.33}$ term of equation (2). For example, it was shown in the body of this report that electromagnetic radar was rather insensitive to variations in the hole size. Thus, by optimizing for the most severe parametric variable, we are assured that the other variables are within bounds.

Combining equations 1 and 2 gives

$$V = 100 \left[1-\exp\left(-\frac{.86D^{2.33}}{r(50)}\right)\right]. \qquad \text{(A-3)}$$

DRILL HOLE COSTS

The other half of the value/cost ratio is the parametric variation of the drill hole cost with hole diameter. Figure A2 is a logarithmic curve showing the results of one model of the projected drill hole costs. This was derived early in the horizontal drilling study[1] on the basis of incomplete data. It shows the costs increasing as $D^{1.88}$. Later data indicates that the sensitivity of drilling costs to hole size will probably be much lower than those assumed. Although the results of these refined cost studies are not yet available, early indications are that the costs will probably come

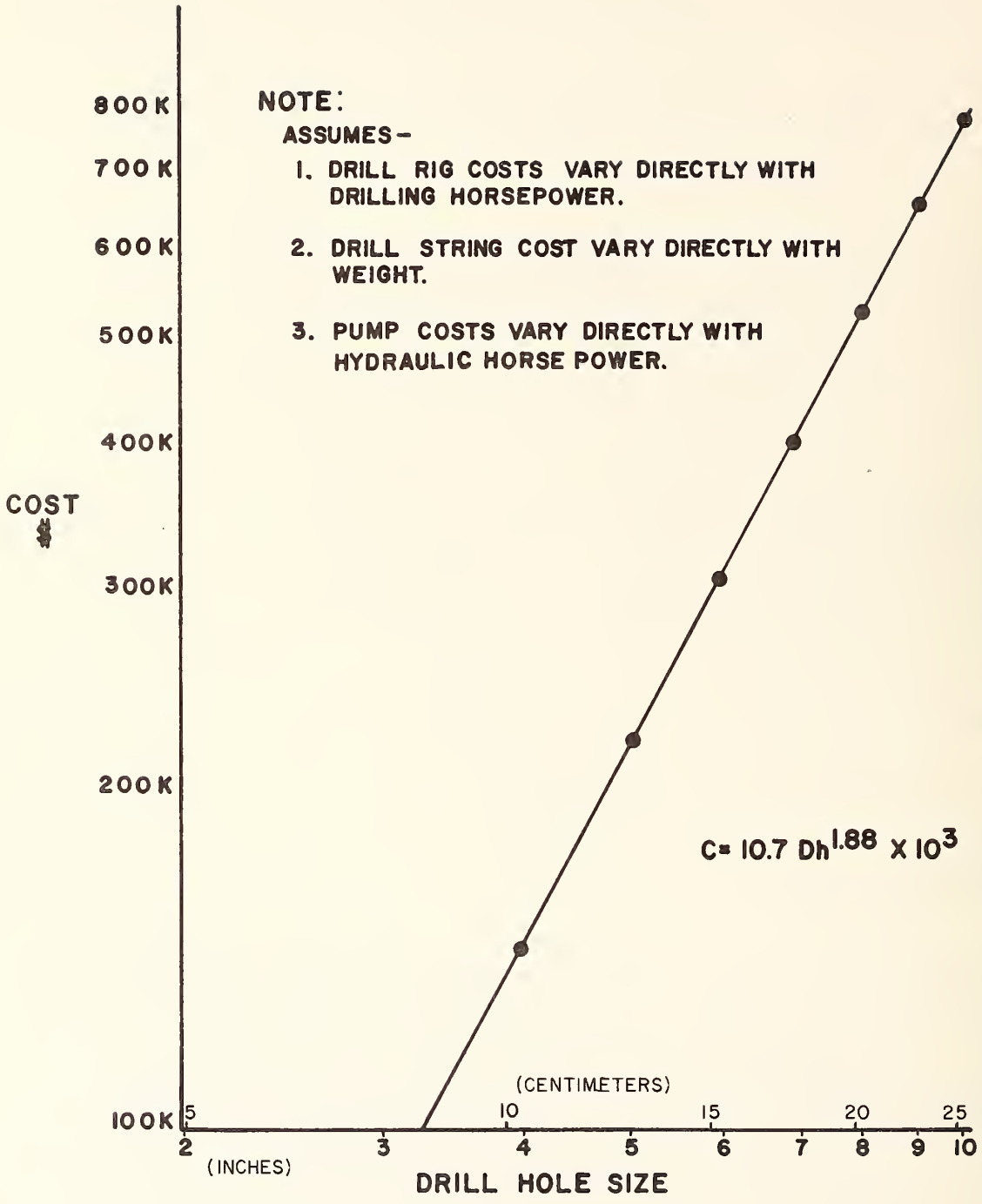

Figure A2. Major equipment cost vs drill hole size for 15,000 foot (4.57 km) hole.

closer to varying directly with the diameter. In addition, it is possible that, when account is taken of the increased penetration rates which can be achieved at the larger diameters, the costs may only vary as a fractional power of the diameter.

Three empirical relations are assumed in this study:

- Drill hole costs vary as D^2
- Drill hole costs vary as D
- Drill hole costs vary as $D^{1/2}$.

Since the first submission of this report, additional data has become available in the form of a FHWA report dealing with cost and time estimating for horizontal drilling[4]. Although it contains much valuable information, this report does not adequately cover the parametric variations in costs as a function of hole diameter. However, it contains several detailed costing examples in which hole diameter is one factor.

Reference [4] in Tables A-18 and A-20, pages A-25 and A-27, presents the projected drilling costs in 1,000-foot (304.8 m) increments for wire line coring in an NX (3" [7.6 cm]) hole, and for rotary drilling in a 6-3/4 (17 cm) inch hole.

Table A1 presents the ratio of drilling costs per foot for these two studies. It has been found in the past that this type of data usually lends itself quite well to power law types of approximation in the general form of

$$C = KD^n \qquad \text{(A-4)}$$

where:

C = Cost in $/ft.

K = A conversion constant in appropriate units

D = Hole diameter in inches

n = An empirical exponent.

Thus, for the cost ratio in Table A1.

$$\frac{C_1}{C_2} = \left(\frac{D_1}{D_2}\right)^n = R_c - R = R_d{}^n$$

and

$$n = \frac{\log R_c}{\log R_d}$$

where

R_c = The ratio of the costs involved

R_d = The ratio of the hole diameters

For this case $R_d = 2.25$.

Table A1. Relative drill costs for $R_d = 2.25$

Hole Length ft. (m)	NX (3") (7.6 cm)	6-3/4" (17 cm)	R_c	n
1000 (304.8)	$32.16	$54.80	1.93	.66
2000 (609.6)	$37.45	$59.88	1.60	.58
3000 (914.4)	$45.10	$67.24	1.49	.49
4000 (1219)	$52.90	$76.78	1.45	.46
5000 (1524)	$60.59	$85.50	1.41	.42

It can be seen that for D^n, n varies in the vicinity of .5, and becomes less severe as hole length increases. It is believed that when all factors are considered the costing examples will tend to be optimistic for the larger hole diameters. However, the final variation will probably be less severe than the $D^{1.88}$ first developed.

Since this report already covers this range of parametric variations, its conclusions are still valid.

VALUE/COST RATIO

For purposes of this study, the value/cost ratio is defined as:

$$\frac{V}{C} = \frac{100\left(1-e^{-\frac{.86D^{2.33}}{r(50)}}\right)}{D^{n}(V/C)_{max}} \qquad \text{(A-5)}$$

where

$(V/C)_{max}$ is a normalizing function applied to remove the magnitude variation and is the value of V/C at

$$\frac{\partial(V/C)}{\partial D} = 0, \text{ and}$$

n defines the exponent chosen for the variation of drill hole costs with hole diameter.

Equation (A-5) has been normalized, as only the relative shapes and maxima of the curves are significant. Unless actual value and cost dollars are available, the magnitudes would be meaningless.

Figures A3, A4, and A5 present the nine curves derived in this study.

Figure A6 is a cross plot of the maxima of the above nine curves. The centroid of these data places the mean at a hole diameter of 6.4 inches (16.3 cm), with a standard deviation of $\pm$3.1 inches (7.9 cm). This would place the range for 50% value at 62 feet (19 m) and a probable cost per inch of diameter varying at slightly less than D, possibly $D^{0.7}$.

NOTE:

1. Assumes that the consensus places 50% value on data between 0 to 25 ft. (7.6 m) from drill hole.
2. C = Cost variation of drill hole with diameter.

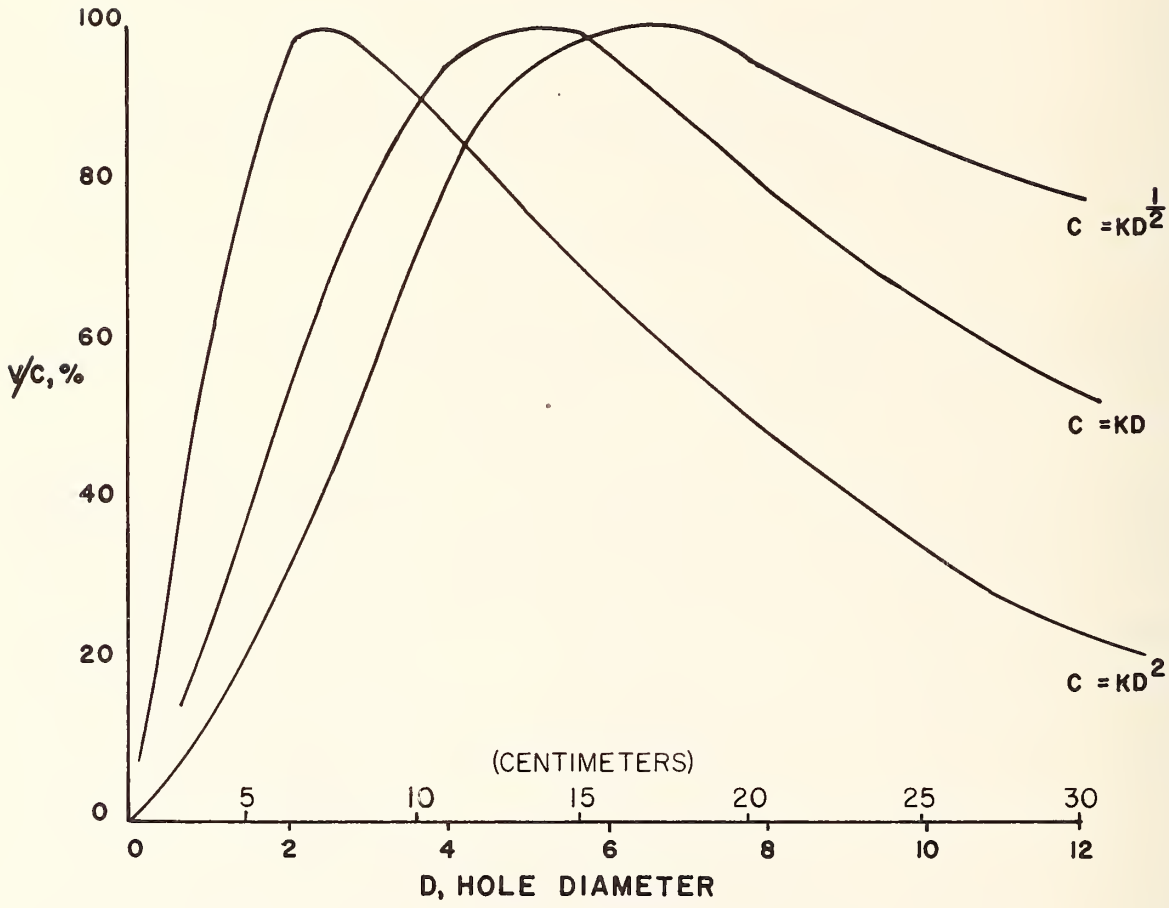

Figure A3. Normalized ratio of value to cost of drill hole.

NOTE:

1. Assumes that the consensus places 50% value on data between 0 to 50 ft. (0-15 m) from drill hole.
2. C = Cost variation of drill hole with diameter.

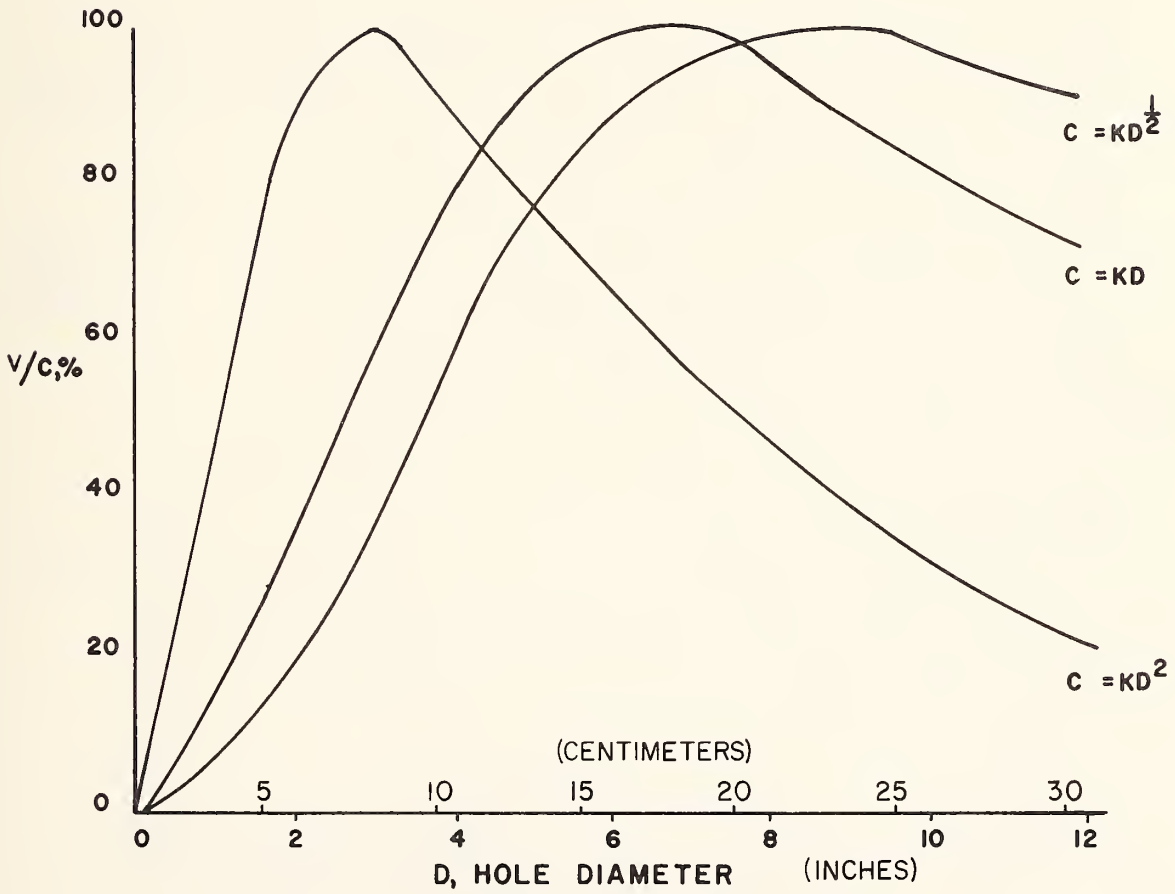

Figure A4. Normalized ratio of value to cost of drill hole.

NOTE:

1. Assumes that the consensus places 50% value on data between 0 to 100 ft. (0-30.5 m) from drill hole.
2. C = Cost variation of drill hole with diameter.

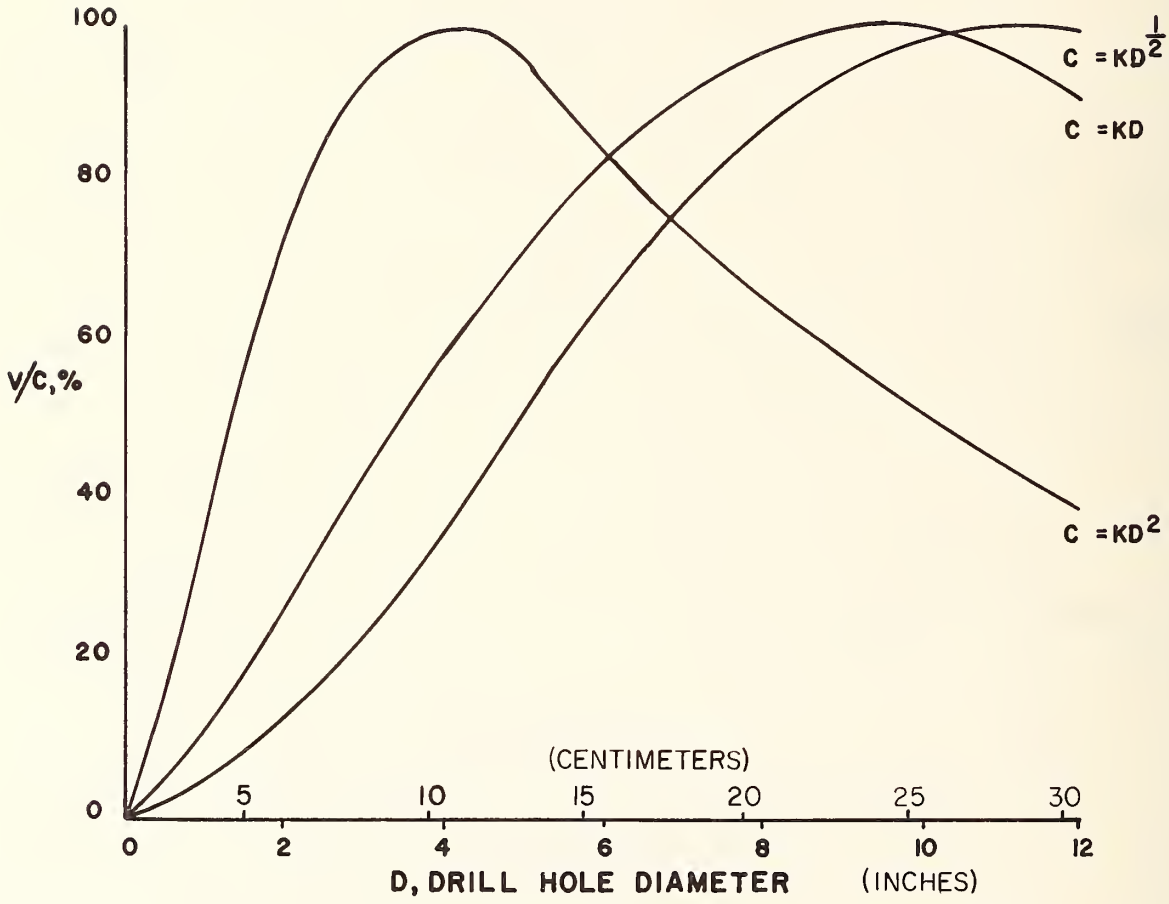

Figure A5. Normalized ratio of value to cost of drill hole.

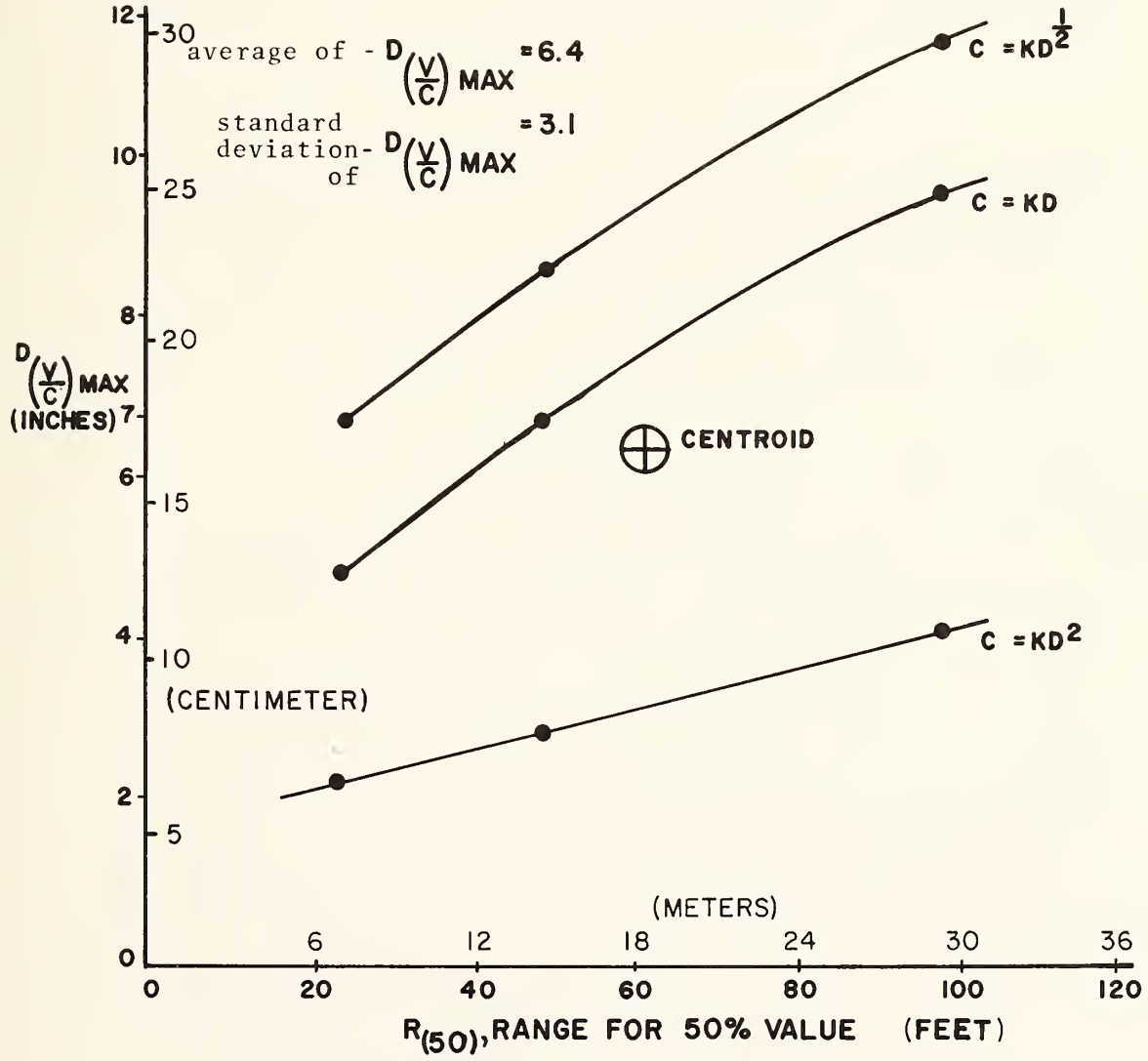

Figure A6. Optimum hole diameters vs assumed penetration range for 50% informational value.

Table C-A1 presents a trend of decreasing cost advantage of a small borehole over a larger hole, as the length of the hole increases. This trend appears valid. For a small diameter hole, a major cost advantage rests in the smaller invested capital and lower setup costs. As the hole length increases, the major cost factors are operating costs. The drilling rate will increase with hole diameter, as will bit life. Thus, the operating costs per foot will tend to decrease with respect to those for diamond-core drilling with wire line recovery of all core.

Although it is risky to extrapolate data to this degree, the general trends are probably valid. Figure A7 presents the optimum (greatest value to cost ratio) hole diameters as a function of hole length. These curves were obtained using the maximum values from equation (5) for the values of n from Table 1, of the main body.

The trends of Figure A7 are extremely interesting. The limited capability prototype which we are proposing would probably have a 50 percentile range of between 25 and 50 feet (7.6 and 15 m). The recommended minimum hole size is already 6-3/4 inches (17 cm) based on other factors. Figure A7 indicates that this is near optimum for the prototype in short (1000-2000 foot [304.8-609.6 m]) holes. As the system capability grows, through modular improvement, and as horizontal drilling capability increases to greater depths, the optimum hole size will also increase. However, in this time frame, better cost and requirement data would be available. Thus, the added expenses would be easier to justify on a value-added basis.

These values all seem to be realistic from a practical viewpoint and thus the problem has been reasonably well bracketed. There are other factors and considerations not covered here, which rule against the smaller diameters. Thus, we accept

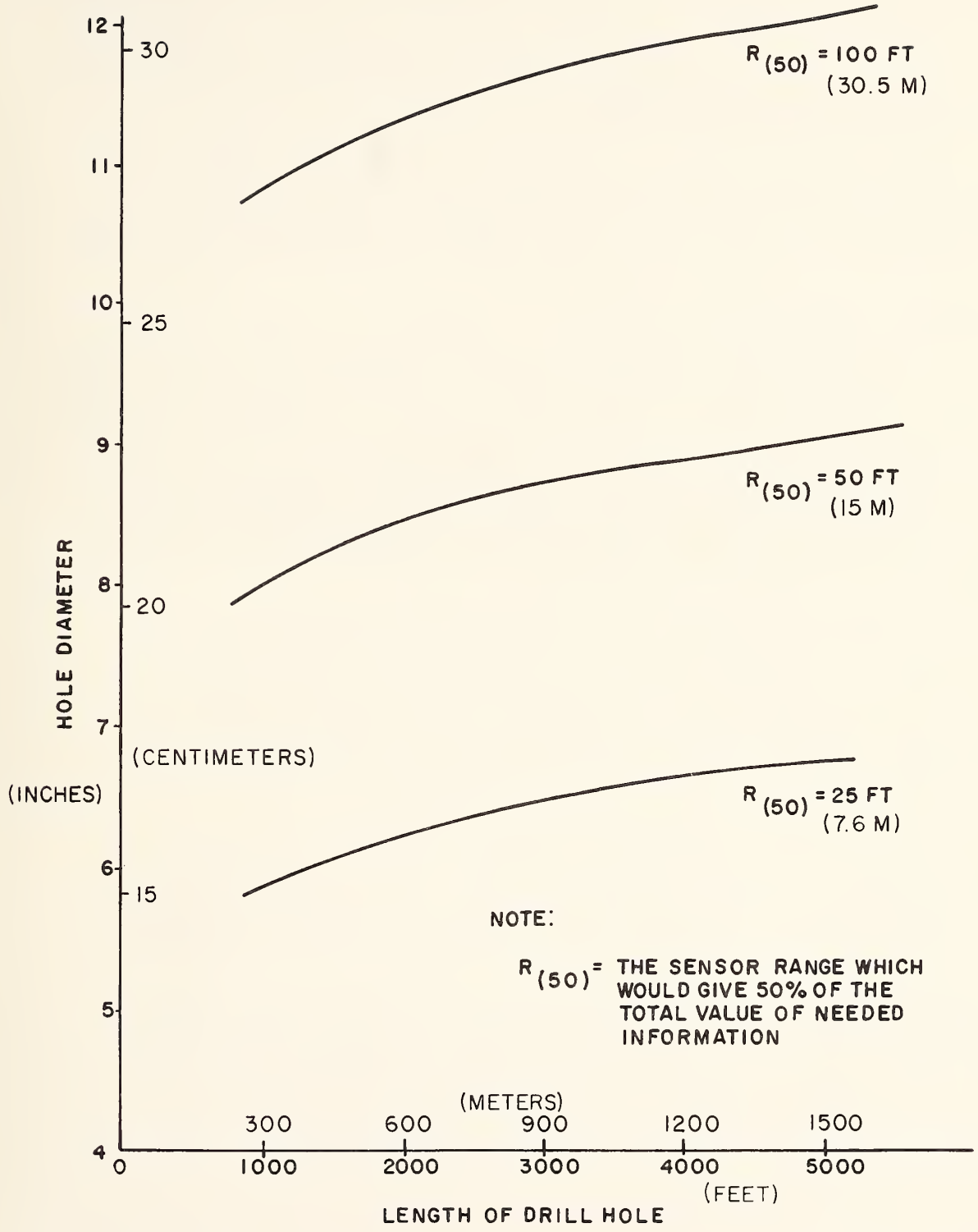

Figure A7. Length of drill hole

the mean value as a reasonable lower limit, and the mean plus-one standard deviation as a reasonable upper limit for borehole size.

SPECIFICATION OF BOREHOLE SIZE

The closest borehole size to the mean which is standard for drilling is 6-3/4 inches (17 cm). Thus, this is selected for the initial target borehole diameter.

SUMMARY OF APPROACH AND RESULTS

The approach used in this study involved the selection of the one parameter which is most sensitive to borehole size. This is the range achievable by a pulsed acoustic system. It is then used to define an exponential value function.

A set of ranges at which a 50% of total informational value can be obtained and another set of power law cost variations with borehole diameters are assumed. The span of these variables is explored to cover the reasonable extremes of probable values, and a value-to-cost ratio is established.

Since actual dollar values are unknown, the value/cost curves are normalized to their optimum values. The mean of the results of this spectrum of parametric variations is then established.

The central limit theorem of statistics states that, lacking other data, this mean would be the best estimate of borehole size. The value obtained, and the centroid of parametric variables, are tested against engineering judgment. They seem reasonable and consistent.

Therefore, the results are accepted as a major valid input to establishing the minimum acceptable borehole diameter.

REFERENCES

1. Harding, J. C., L. A. Rubin, and W. L. Still, "Drilling and Preparation of Reusable, Long Range, Horizontal Bore Holes in Rock and in Gouge, Volume I, State-of-the-Art Assessment," FHWA RD-75-95, October, 1975.

2. Jasik, Henry, Antenna Engineering Handbook, McGraw-Hill Book Company, p. 5-4.

3. Cook, John C., Radar Transparencies of Mine and Tunnel Rock. Presented at the 44th Annual Meeting, SEG, Dallas, 12 November 1974.

4. Mack, W.M., Jr., N. Tracey, and G. B. Wickham, "Drilling and Preparation of Reusable, Long Range, Horizontal Bore Holes in Rock and in Gouge, Volume II, Estimating Manual for Time and Cost Requirements," FHWA-RD-75-96, October, 1975.

5. Myung, J. I., and R. W. Baltosser, "Fracture Evaluation by the Borehole Logging Method," published by Birdwell Division of Seismograph Service Corp., Tulsa, Oklahoma, August 30, 1971, p. 25.

APPENDIX R

COST-EFFECTIVENESS CONSIDERATIONS FOR PROPULSION AND PENETRATION

TABLE OF CONTENTS

BACKGROUND STATEMENT

One of the decisions defining the final configuration of the system was to eliminate the development of an in-the-hole thrust device for penetration. The concept was to use the drill which produced the borehole to push the survey package. A companion study (Appendix 9) indicates that this is a feasible approach, provided the hole length is less than a few thousand feet.

This short study was performed to examine the relative cost effectivity between using the heavy drill rig which drilled the hole and using a lightweight dedicated drill rig purchased as part of the system.

COST-EFFECTIVENESS CONSIDERATIONS FOR PROPULSION AND PENETRATION

ABSTRACT

An alternative to the development of a propulsion and penetration unit is to conduct the hole survey immediately after the hole is drilled. The drill rig could remain on site and be used to propel the package into the hole. In addition, it would be available to clean out any blockages. This approach is attractive on the basis of low initial investment. However, it will be costly from the standpoint of prolonged operational costs. A second alternative is to supply a light-duty dedicated drill rig as part of the survey system. The two alternatives have been compared, and the light-duty drill rig has a considerable cost advantage.

COST-EFFECTIVENESS CONSIDERATIONS FOR PROPULSION AND PENETRATION

An alternative to the development of a propulsion and penetration unit is to conduct the geophysical survey immediately after the hole is drilled. The drill rig could remain on site and be used to propel the package into the hole. In addition, it would be available to clean out any blockages. This approach is attractive on the basis of low initial investment. However, it will be costly from the standpoint of prolonged operational costs.

The drilling equipment to drill a 6-3/4 inch (17 cm) horizontal hole to depths of 1000 to 2500 feet (304.8 to 762 m) will be massive. The standby charges will be high. Table 1 is derived from a recent borehole cost study [1]. It indicates that the standby charges on a drill rig and crew will run on the order of $1,750 per day.

The main advantage of this approach rests in the savings of developmental costs. However, it is doubtful if, once the sensor system has proven its value, this approach will prove to be cost effective. It has several major disadvantages.

- It is estimated that the complete survey of a 2500 foot (762 m) hole will take from three to five days. Even if one assumes perfect coordination between the drilling crews, the time of day that the hole will bottom out will be difficult to schedule in advance. This will almost certainly lead to added standby costs for either the survey crew and equipment or for the drilling crew and equipment. This would provide an added survey cost factor of approximately $3.50 per foot ($11.48/m).

[1] FHWA Report, FHWA-RD-75-96 (see p. 2).

Table 1. Standby cost for 6-3/4 (17 cm) horizontal drill and crew.

*Equipment Costs @ $35.97/hr. x 24 hrs.		$863.28
Selected Material Costs		
-Drill Rod @$6.53/hr.		
-Miscellaneous $1.30/hr Subtotal $7.83 x 24 hrs.		187.92
Standby Crew @ $36/hr x 8		288.00
	SUBTOTAL	1,339.20
OVERHEAD at 15%		200.88
	SUBTOTAL	1,540.08
PROFIT at 15%		231.01
	TOTAL	$1,771.09

THEREFORE, USE $1,750/DAY FOR USE OR RIG

*Source of Data:

Tables A-3 and A-5, PPA-6, A-7
FHWA-RD-75-96 Report
Drilling and Preparation of Reusable
Horizontal Bore Holes in Rock and Gouge
Volume II, October, 1975.

- The approach will lack flexibility. It will preclude resurveys of the hole, to follow up on information derived as a result of the data processing or to explore in greater detail zones of interest to geotechnical personnel. One of the attractive features of the self-propelled system is its capability to reenter the hole, after geotechnical personnel have evaluated all available data and look for specific features.

A second alternative would be to purchase a light-duty, dedcated drill rig to go with the prototype system as part of its normal support equipment. This rig could provide the propulsion and light-duty clean up of minor blockages of the hole.

Several drill rig manufacturers have been contacted, including Longyear, Acker and GeoSpace. Their price estimates and equipment are very similar. A representative estimate is given in Table 2.

Table 2

Light duty drill rig (Longyear-24 or Acker "ACE")	$ 7,800
Gardner-Denver Compressor WCQ-204	2,000
1000 ft. (304.8 m) ACQ drill rod @ 4.20/ft ($13.78/m)	4,200
Thin wall core bit, Acker 20227-33	415
Trailer for rig and rod transport	2,300
Misc.: Junk basket, hose, couplings, tools, etc.	1,000
	$17,715

This would be a light-duty rig; the survey crew could be trained to set it up and operate it; thus, the operational costs would not increase significantly. It would probably add about a day to the survey time to set it up and tear it down.

This would imply that the system would reach a breakeven point with respect to the drill rig standby after 10 days of operation. This approach would not only be cost-effective, but it would also add to the system flexibility. It would enable the system to operate as a functional entity, without the necessity of coordination with the drilling contractor, and the associated management problems and delays.

A comparison study (Appendix J) indicates that neither the heavy drill rig used to bore the hole, nor the light duty rig recommended in this study, will be completely satisfactory. However, for shallow hole depths, the use of the light-duty drill rig will enable valuable operational survey data to be gathered to prove the value of the sensor concept. Thus, the drill rig should be considered as an interim propulsion system, which enables the deferral of the development of an in-hole thruster.

*U.S. GOVERNMENT PRINTING OFFICE : 1977 0-731-789/131